Sustainable Methods for Oxidative Transformations via Immobilized Organocatalyst in Flow

Dissertation

Submitted in partial fulfillment of the requirements for the degree of
Dr. rer. nat.

Prepared at the Faculty of Mathematics and Natural Sciences

of the University of Wuppertal

Michael Tapera

March 2026

This page intentionally left blank

This work was carried out under the supervision of Prof. Stefan F. Kirsch at the Institute of Organic Chemistry, University of Wuppertal, between September 2022 and February 2026.

[†] Denotes equal contribution.

Parts of this work have been published in the following articles:

[1] **M. Tapera**, A. Savvidis, C. Meysing, A. Gómez-Suárez, S. F. Kirsch, *Org. Lett.,* **2026**, *28*, 681-685.

[2] **M. Tapera**, [†] M. Chotia, [†] J. L. Mayer-Figge, A. Gómez-Suárez, S. F. Kirsch, *Green Chem.,* **2024**, *26*, 10058-10063.

[3] **M. Tapera**, F. Borghi, J. L. Mayer-Figge, F. Mittendorf, I.-E. Çelik, A. Gómez-Suárez, S. F. Kirsch, *Molecules*, **2024**, 29, 3710.

Acknowledgements

I am deeply grateful to all who have supported me throughout this doctoral work. First and foremost, I would like to express my sincere gratitude to my advisor, Prof. Stefan F. Kirsch, for his continuous enthusiasm and dedication throughout my doctoral studies. His curiosity-driven approach to research and passion for science have been a constant source of inspiration. Stefan provides his students with a remarkable degree of academic freedom, enabling them to explore their scientific interests while developing independence and critical thinking. I am profoundly thankful for his mentorship, advice, and trust, which guided me through every stage of my PhD. The knowledge, skills, and scientific mindset I have gained under his supervision will be invaluable for my future career.

My sincere appreciation goes to the Senior Academic Advisors of the Kirsch research group, Dr. Adrián Gómez-Suárez, Dr. Markus Roggel, Dr. Andreas F. Kothaus, and Dr. Hülya Aldemir, for their insightful discussions and valuable scientific guidance. Their expertise and thoughtful input significantly contributed to the development of this research and strengthened my interest in organic chemistry. I would also like to thank the technical staff, Ilka Polanz, Boris Ihmenkamp, and Andreas Siebert, for their essential support in analytical data collection, which was critical to the completion of this work.

I am deeply thankful to the current and former doctoral students of the Kirsch research group for making my time in the laboratory both enjoyable and memorable. I greatly value the collaborative atmosphere, stimulating discussions, and mutual support during challenging moments. In particular, I would like to acknowledge my lab colleagues Srashti Chaudhary and Hauke Junghans for their friendship and encouragement throughout this journey. I would also like to thank Mohit Chotia, Timo Zschau, Nau Jan, Cedric Meysing, Malavika Krishnan, Dr. Venkadesh Balakrishnan, Dr. Bincy Chindan, Antonia Gres, Ibrahim Çelik, Fabia Mittendorf, Athanasios Savvidis, Kathrin Bensberg, Anastasiia Krupka, Kevin Kunz, and Bastian Springer for their collaboration and for fostering a motivating and collegial research environment.

I am also grateful to Tanja Lohr and former administrative assistant Christine Schneidereit for their invaluable assistance with organizational and administrative matters, which greatly facilitated the smooth progress of my doctoral work.

Finally, I wish to express my heartfelt gratitude to my family for their unwavering support, patience, and understanding throughout this journey. My parents, in particular, have supported me in every possible way and taught me the importance of perseverance,

responsibility, and selflessness. Their belief in me and guidance have been essential to the successful completion of this thesis.

Table of Contents

Chapter 1
General Introduction

1.1 Oxidative transformations

Oxidative transformations are widely employed in organic synthesis in both academic research and industrial chemical production.[1] They enable the conversion of relatively simple functional groups into more highly functionalized motifs, providing access to a broad range of fine and specialty chemicals, including pharmaceuticals, agrochemicals, and their key intermediates.[2] Through controlled changes in oxidation state, these reactions allow the strategic introduction of oxygen-containing functionalities. These include alcohols, aldehydes, ketones, and carboxylic acids, which are frequently encountered functional groups in relevant compounds, such as biologically active molecules and fine chemicals.[3] Beyond direct functionalization, oxidation steps often create reactive intermediates that can be exploited in subsequent bond-forming or bond-cleaving transformations, making them integral to the construction and modification of complex molecular frameworks.[4–6]

As a result, oxidative transformations are routinely incorporated into multistep synthetic sequences, where the timing and selectivity of oxidation reactions can strongly influence overall route design and efficiency.[6] In addition to their established role in fine chemical and pharmaceutical synthesis, oxidation reactions have gained renewed attention in the context of sustainable chemistry, particularly for the selective conversion of renewable feedstocks into value-added chemicals and functional materials.[7,8] These emerging applications highlight the continued relevance of oxidative transformations across both traditional and evolving areas of organic synthesis.

1.2 Oxidation Methods and Sustainability Challenges

Although oxidative transformations are widely applied, traditional oxidation chemistry has historically relied heavily on metal-based catalysts and stoichiometric oxidants, including chromium(VI) species, permanganates, and a variety of transition-metal complexes.[9] These reagents have demonstrated broad applicability and often exhibit high chemo-, regio-, and stereoselectivity across diverse transformations.[10]

Despite their synthetic utility, conventional oxidation methods raise several practical and environmental concerns. Many widely used oxidants are toxic, environmentally persistent, or generate large quantities of hazardous waste. Chromium(VI) reagents, for example, are effective oxidants but are associated with severe health and disposal issues.[11] In addition, metal-based oxidation systems frequently require harsh reaction conditions or extensive purification steps, which can increase solvent consumption and process complexity. These factors become particularly problematic when reactions are scaled beyond laboratory settings.[11,12]

In response to these limitations, increasing attention has been directed toward the development of more sustainable oxidation strategies. Approaches that reduce or eliminate toxic metals, improve atom economy, and operate under milder conditions are now widely sought. While no single solution has emerged as universally applicable, these efforts reflect a broader shift toward oxidation methods that are better aligned with contemporary sustainability and regulatory expectations.[10,13,14]

1.3 Organocatalysis for Oxidative Transformations

Efforts to address the limitations of traditional metal-based oxidation methods have led to increased interest in organocatalysis. In this approach, small organic molecules are used to promote chemical transformations without the involvement of metals. Organocatalytic systems have been explored for a range of oxidative reactions, offering alternative pathways that may reduce toxicity and simplify waste handling.[15]

One of the main attractions of organocatalysts is their compatibility with mild reaction conditions. Many operate in the presence of air or moisture and do not require strictly controlled environments. This feature can be advantageous in oxidative chemistry, where sensitivity to reaction conditions often limits practicality. In addition, the absence of metals reduces the risk of contamination, which is particularly relevant in pharmaceutical synthesis. For these reasons, organocatalytic oxidation methods have attracted sustained attention in both academic and applied research.[16,17]

At the same time, organocatalysis is not without limitations. Compared with transition-metal catalysts, organocatalysts may display lower intrinsic activity or narrower substrate scope, which can necessitate higher catalyst loadings. Reaction rates can also be sensitive to subtle changes in substrate structure or reaction conditions.[18] These considerations suggest that, while organocatalysis offers clear benefits from a sustainability perspective, further development is often required to achieve levels of efficiency and robustness comparable to established metal-based systems.[19]

1.4 Immobilized Organocatalysts: Addressing Practical Limitations

While organocatalysis offers several advantages, practical challenges remain, particularly with respect to catalyst recovery and reuse. Most organocatalysts are employed in homogeneous form, which can complicate separation from reaction mixtures and limit their application in large-scale or continuous processes. In addition, the need for relatively high catalyst loadings can reduce process efficiency and increase cost.[20]

Immobilization provides a practical strategy to address these issues by anchoring organocatalysts onto solid supports. When successfully implemented, immobilization allows catalysts to be retained within the reaction system while maintaining catalytic activity and selectivity.[21] Solid-supported organocatalysts can be readily separated from reaction mixtures, enabling reuse and improving operational simplicity. An overview of the underlying concept is presented in Figure 1.1 and in some cases, immobilization may also enhance catalyst stability or reduce degradation under oxidative conditions.[22]

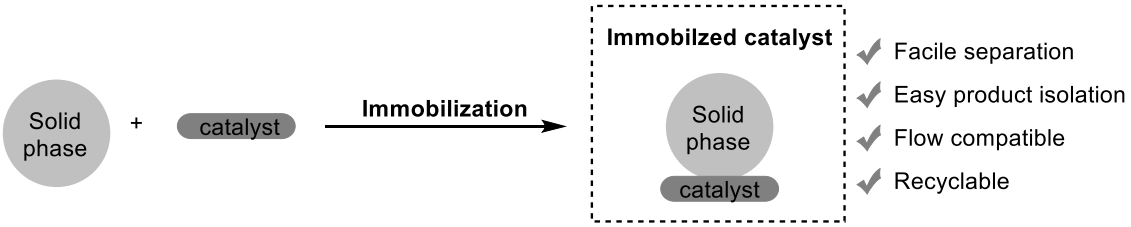

Figure 1.1 Schematic representation of organocatalyst immobilization and its associated benefits.

The performance of immobilized organocatalysts depends strongly on both the nature of the catalyst and the properties of the support. Factors such as linker length, support porosity, and surface functionality can influence accessibility to active sites and overall catalytic behaviour.[21] As a result, immobilization is not merely a technical modification but a design parameter that requires careful optimization for specific oxidative transformations. When appropriately tailored, immobilized organocatalysts offer a promising route toward more sustainable and scalable oxidation processes.[23]

1.5 Continuous Flow Chemistry for Oxidative Transformations

Continuous flow chemistry has become an increasingly used approach for conducting chemical reactions, particularly where precise control over reaction conditions is required. In flow systems, reagents are introduced into reactors as continuously moving streams, allowing reaction parameters such as temperature, residence time, and concentration to be tightly regulated.[24] These features can be advantageous for oxidation reactions, which are often sensitive to local concentration effects or heat release.[25]

One practical benefit of flow reaction is improved heat and mass transfer compared with conventional batch reaction. This can be especially relevant for exothermic oxidative transformations, where inefficient heat dissipation may lead to side reactions or safety concerns.[26] Flow systems also allow reactive oxidants to be handled in small, controlled quantities, which may reduce risks associated with scale-up. As a result, reactions that

are difficult to manage in batch can often be performed more safely under flow conditions.[27]

When combined with immobilized organocatalysts, continuous flow operation enables sustained catalytic activity over extended periods.[28] Catalysts can be retained within packed-bed or fixed-bed reactors, minimizing leaching and simplifying product separation. This configuration allows reactions to be run continuously with consistent performance, while also facilitating catalyst reuse.[29] Taken together, the integration of immobilized organocatalysts with flow chemistry provides a practical framework for developing oxidation processes that are efficient, controllable, and better suited to sustainable chemical production.

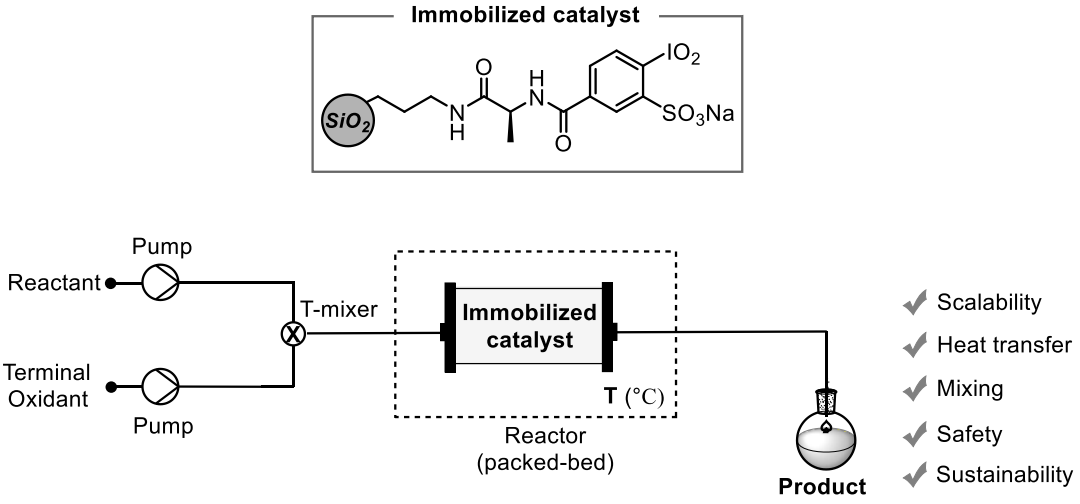

Figure 1.2 Continuous flow setup with immobilized organocatalysts in a packed-bed reactor, illustrating the advantages of flow.

1.6 Aims of the Thesis

Oxidative transformations are central to modern organic synthesis but are often limited by challenges related to sustainability, operational safety, and scalability. Traditional methods frequently rely on metal-based catalysts or stoichiometric oxidants, which can generate hazardous waste and complicate process development. Organocatalysis provides a promising alternative, particularly for metal-free operation and functional group tolerance. However, practical implementation is often hindered by difficulties in catalyst recovery, recyclability, and long-term operational stability.

This thesis aims to develop sustainable methods for oxidative transformations using immobilized organocatalytic reactions, with particular emphasis on mild, metal-free protocols that are amenable to scale-up. These strategies seek to enhance catalytic

activity, selectivity, and operational stability while improving catalyst recyclability and long-term performance under continuous-flow conditions. Collectively, the work provides a framework for efficient, scalable, and sustainable oxidation methodologies.

Chapter 2 focuses on hypervalent iodine(V) organocatalysts immobilized on solid supports, evaluating their activity, selectivity, and durability in oxidative cleavage reaction under continuous-flow conditions. Chapter 3 describes an immobilizable oxaziridine catalyst for selective hydroxylation reactions and its potential for recyclable, metal-free operation. Chapter 4 presents a metal- and catalyst-free protocol for *anti*-dihydroxylation of olefins, highlighting mild conditions, functional group tolerance, and flow compatibility. Chapter 5 reports an independent side project: a modular, stereocontrolled approach to the formal synthesis of (+)-hannokinol, using a chiral Horner–Wittig reagent to install the 1,3-diol motif and allowing variation of aromatic substitution patterns.

Overall, the dissertation explores key challenges in organocatalytic oxidation, demonstrating how immobilization, operational robustness, and mild reaction conditions can be combined to develop sustainable methodologies, while also including a side project that illustrates broader applications of stereocontrolled synthesis of diarylheptanoids.

Chapter 2

Immobilization of Hypervalent Iodine(V) Catalysts and their Application in Flow

2.1 Introduction

Background and Significance of Hypervalent Iodine(V) Reagents

Hypervalent iodine compounds have been extensively investigated in organic synthesis over the past several decades and have emerged as powerful reagents for a wide range of oxidative transformations. In particular, iodine(V) species play a central role in oxidation chemistry, displaying reactivity patterns that are often comparable to those of transition metal-based oxidants.[30–33] Despite these similarities, hypervalent iodine(V) reagents offer several significant advantages, including high selectivity, mild reaction conditions, low toxicity relative to heavy-metal oxidants, operational simplicity, and comparatively low cost.[34–36] These attributes render hypervalent iodine(V) compounds attractive alternatives to traditional metal-based oxidants and position them as promising organocatalysts for sustainable oxidative transformations.

The first hypervalent iodine(V) compound to gain widespread attention was *o*-iodoxybenzoic acid (IBX), originally reported in 1893 by Hartmann and Meyer as a product of the oxidation of 2-iodobenzoic acid using potassium permanganate in presence of sodium hydroxide.[37] Subsequently, several alternative synthetic routes for IBX were developed, including methods employing chlorine and aqueous sodium hypochlorite,[38] and aqueous sodium periodate as oxidants.[39] Among these, the procedure reported by Greenbaum, which utilizes potassium bromate in aqueous sulfuric acid, became one of the most commonly used methods for IBX preparation (Scheme 2.1).[40]

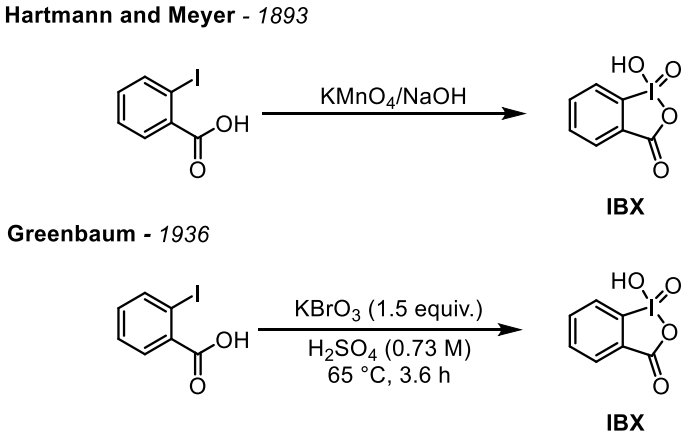

Scheme 2.1 Early methods for the synthesis of IBX.

2.2 Limitations of Early IBX Chemistry and Sustainable Advances

Despite its high oxidative efficiency, the practical use of IBX as a replacement for metal-based oxidants was initially limited. This was largely due to its poor solubility in most

organic solvents, with appreciable solubility observed only in DMSO.[41] The use of DMSO introduces additional challenges, including difficult solvent removal and increased purification costs. Furthermore, early synthetic methods, such as the potassium bromate-based procedure by Greenbaum (Scheme 2.1), were suspected to generate IBX contaminated with bromate impurities, raising safety and explosion harzards.[42,43]

Renewed interest in IBX emerged following the pioneering work of Santagostino and co-workers, who reported a milder and more sustainable synthesis of IBX from *o*-iodobenzoic acid using Oxone® in aqueous media.[44] This method employs water as the solvent, avoids the use of toxic reagents, generates minimal hazardous waste, and is amenable to large-scale synthesis. As a result of this advance, IBX has become a benchmark organoiodine(V) oxidant and a widely used representative for metal-free oxidative transformations.[45–49]

Santagostino and Frigerio - *1999*

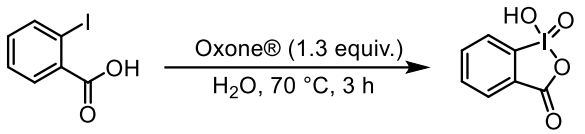

IBX

Scheme 2.2 Improved synthesis of IBX using mild oxidant in aqueous medium.

To address the solubility limitations of IBX, numerous analogues were subsequently developed either by making similar benziodoxole heterocyclic system or through functionalization of the aromatic core. These structural modifications improved solubility, reactivity, and stability, leading to a family of iodine(V) reagents that expanded the scope and practicality of hypervalent iodine chemistry (Scheme 2.3).[50–56]

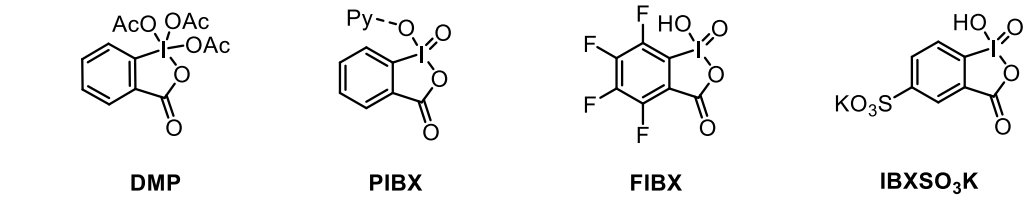

DMP **PIBX** **FIBX** **IBXSO$_3$K**

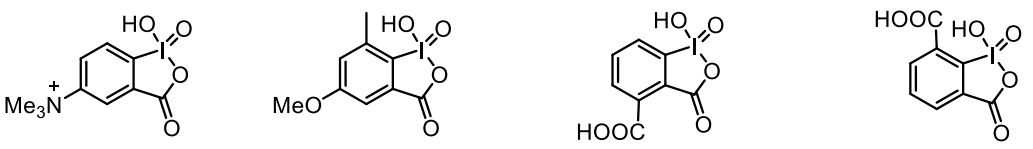

AIBX **Me-IBX** ***m*IBXI** ***m*IBXII**

Figure 2.1 Structurally modified IBX derivatives designed to address limitations.

2.3 Sustainability Challenges and Catalytic Use of Hypervalent Iodine(V)

Despite these advances, significant sustainability challenges remain associated with hypervalent iodine reagents. Most commonly, they are employed in stoichiometric or super-stoichiometric amounts, resulting in the formation of non-recyclable aryl iodide byproducts. This leads to poor atom economy and increased waste generation. In addition, many hypervalent iodine reagents are thermally unstable and sensitive to light and mechanical stress, which can result in rapid decomposition and pose safety concerns, particularly in large-scale applications.[43,57–59]

In accordance with the principles of green chemistry, sustainable oxidation methodologies should minimize waste generation, reduce hazards to human health and the environment, and ideally employ catalytic rather than stoichiometric quantities of reagents.[8,60–62] A key breakthrough toward this goal was reported by Vinod and co-workers, who demonstrated the catalytic use of IBX in alcohol oxidations. In this system, primary and secondary alcohols were oxidized to carboxylic acids and ketones using *o*-iodobenzoic acid in catalytic amounts in combination with Oxone® as a terminal oxidant in aqueous acetonitrile at elevated temperature (Scheme 2.3).[63]

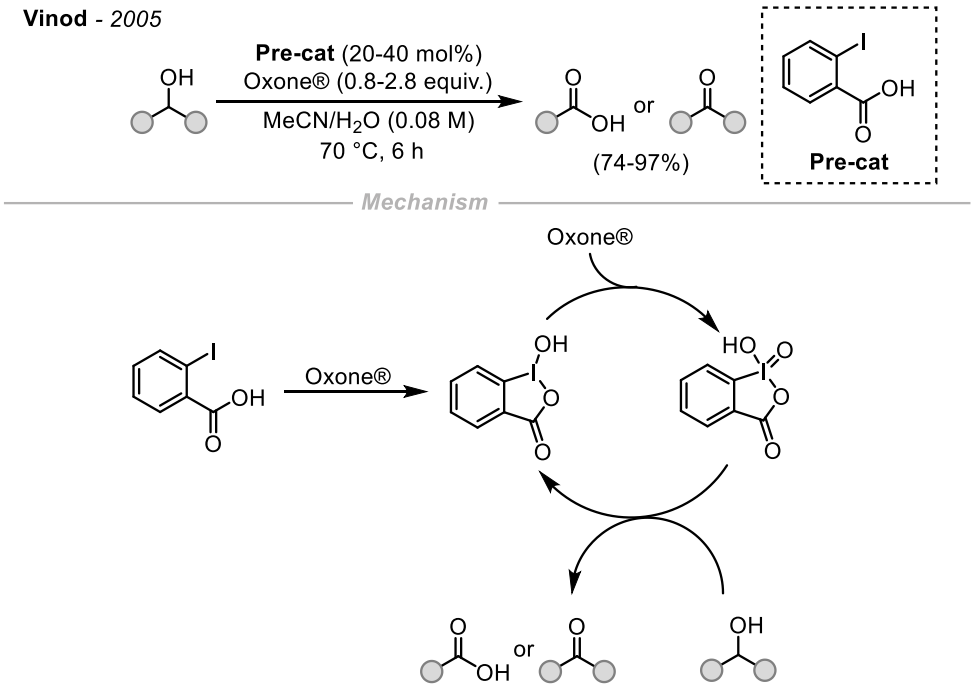

Scheme 2.3 *In situ* generation of hypervalent iodine(V) reagent (IBX) for a catalytic oxidation of alcohols.

Following this discovery, numerous catalytic hypervalent iodine-mediated oxidation protocols were reported by several groups, including Moorthy, Page, and Zhdankin.[64–69] A 2013significant advancement was achieved by Ishihara and co-workers, who identified

sodium *ortho*-iodobenzenesulfonate as an effective precatalyst for the *in situ* generation of 2-iodoxybenzenesulfonic acid. This system enabled alcohol oxidations to proceed with catalyst loadings as low as 1 mol%, affording products in high yields (80–96%) (Scheme 2.4).[70]

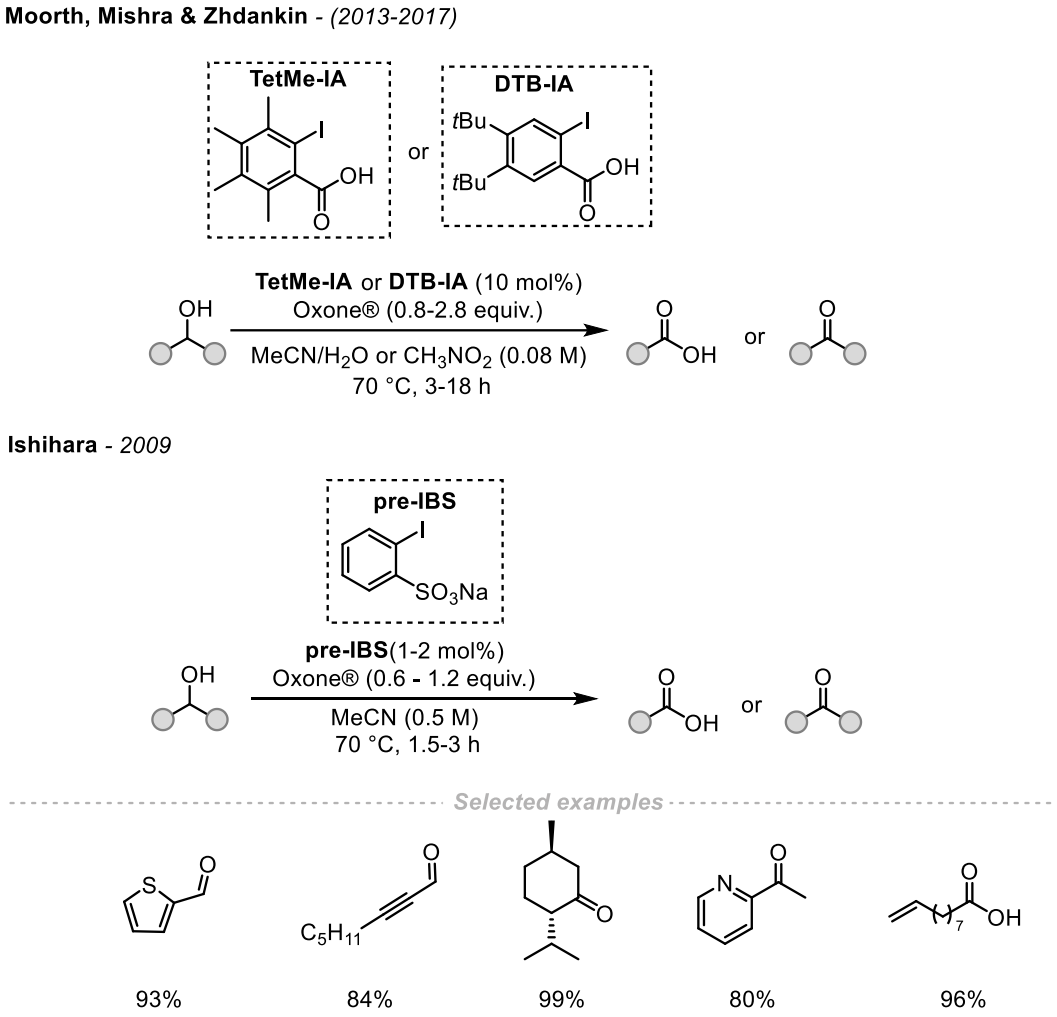

Scheme 2.4 Catalytic oxidative transformations enabled by *in situ* generation of hypervalent iodine(V) species.

2.4 Immobilization as a Strategy for Catalyst Recycling and Flow Chemistry

While catalytic hypervalent iodine systems represent a major step toward sustainability, recyclability remains a critical requirement for truly green processes. One effective strategy to address this limitation is the immobilization of hypervalent iodine precatalysts onto solid supports. Immobilization enables facile separation of the catalyst from the reaction mixture, allows reuse over multiple cycles, reduces waste generation, and improves operational simplicity. Moreover, solid-supported catalysts are particularly well

suited for implementation in continuous-flow systems, especially in packed-bed reactors.[26,71,72]

Immobilization can also enhance the stability and safety profile of hypervalent iodine reagents, which are otherwise prone to decomposition under thermal or photochemical stress.[58] By anchoring the active species onto a solid matrix, exposure to external stimuli can be mitigated, thereby reducing explosion hazards and improving process safety under oxidative conditions.[21,23,73]

2.5 Development of Solid-Supported Hypervalent Iodine(V) Catalysts

The first reports on the immobilization of hypervalent iodine reagents were published independently by Giannis and Rademann.[74,75] Both approaches employed 5-hydroxy-2-iodobenzoic acid as a key precursor. The hydroxy substituent at the C5 position enabled covalent attachment of the iodine precursor either to aminopropyl-functionalized silica gel or to merrifield resin. Subsequent oxidation with Oxone® afforded the corresponding immobilized iodine(V) species **SP-IBX I** and II. These solid-supported oxidants were successfully applied to oxidation reactions, retaining the high reactivity and selectivity characteristic of hypervalent iodine chemistry while offering improved handling, recyclability, and reduced environmental impact (Scheme 2.5).

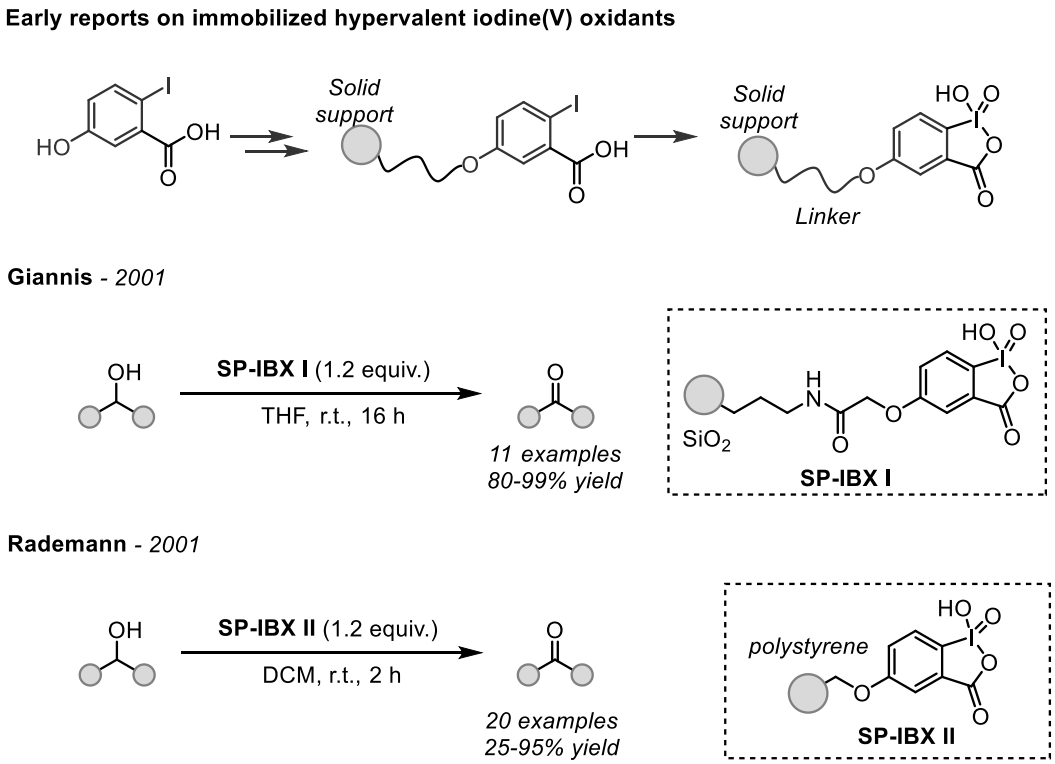

Scheme 2.5 Representative strategies for the immobilization of hypervalent iodine(V) reagents on solid supports.

Subsequently, a variety of solid supports have been explored for immobilization of hypervalent iodine(V) reagents, including microporous polystyrene resins,[76] graphene oxide,[77,78] and porous organic polymers. While effective, most of these systems were employed in stoichiometric amounts and were not adapted for continuous-flow applications.

A significant advance was reported in 2019 by Kirsch and co-workers, who developed polystyrene-supported IBX and IBS catalysts (**PS-IBX III** and **PS-IBS I**) using a peptide-coupling strategy that enabled automated solid-phase peptide synthesis (SPPS) (Scheme 2.6).[79] These catalysts exhibited high activity in the oxidation of secondary alcohols to ketones using as little as 5 mol% catalyst loading in the presence of Oxone® as a co-oxidant. Importantly, this work was further extended to continuous-flow oxidation using a packed-bed reactor containing **PS-IBS I**. The flow protocol dramatically reduced reaction times from 18 hours in batch to approximately 20 minutes, while maintaining high yields and selectivity, and expanded the scope to include primary alcohol oxidations.[80]

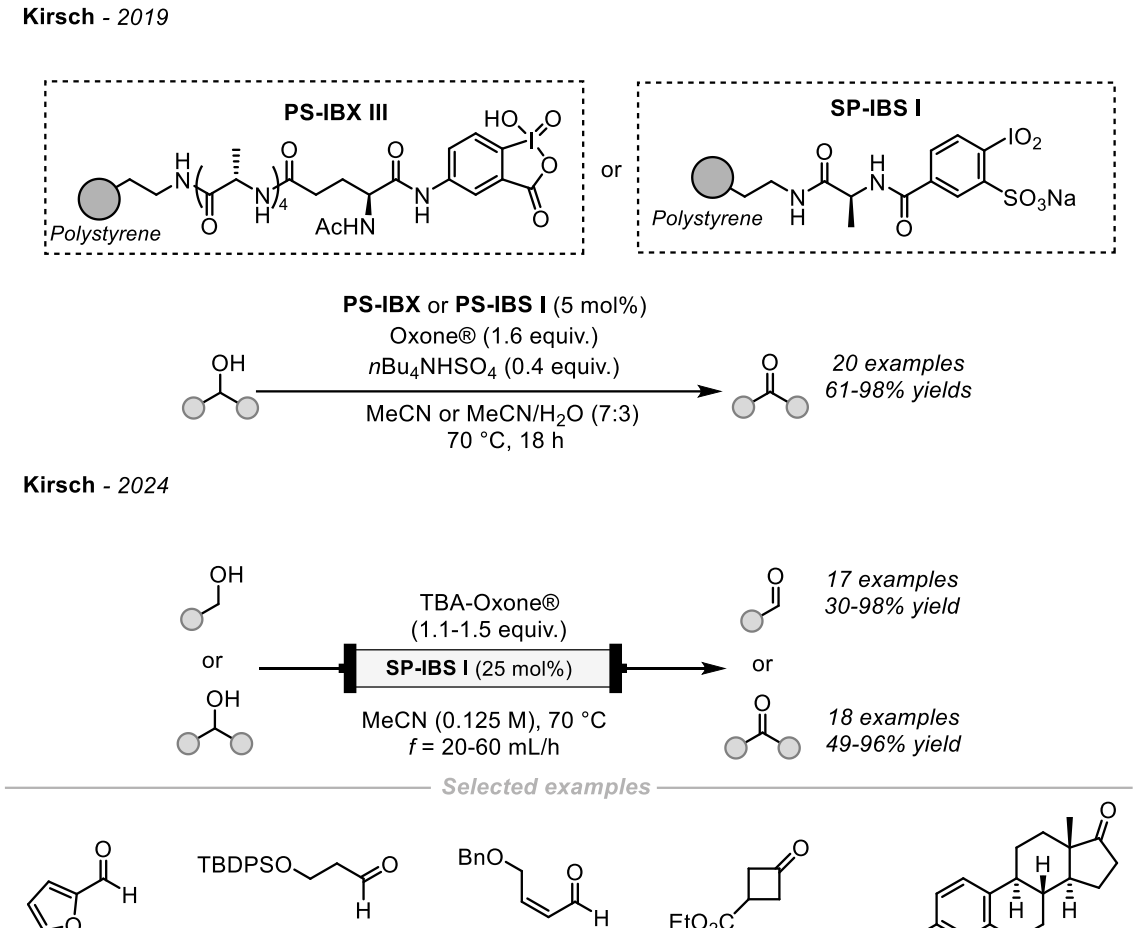

Scheme 2.6 Peptide-based immobilization strategy and catalytic alcohol oxidation using solid-supported hypervalent iodine(V) catalysts.

2.6 Oxidative Cleavage of β-Substituted Primary Alcohols

The oxidative cleavage of carbon-carbon bonds has emerged as a powerful and versatile transformation in synthetic organic chemistry, enabling the efficient construction of complex molecular architectures from simple and readily accessible precursors.[81–83] Owing to the inherent thermodynamic stability of C-C bonds, traditional approaches to oxidative C-C bond cleavage have typically relied on strained or activated substrates, or on transition-metal-mediated processes capable of facilitating oxidative addition or β-carbon fragmentation.[84–86] As a result, the development of mild, selective, and sustainable methodologies for C-C bond cleavage remains a significant challenge.

Within this context, the oxidative cleavage of β-substituted primary alcohols represents a particularly attractive strategy, as it enables direct access to structurally simplified yet highly valuable molecular motifs through selective C-C bond scission. Among the products accessible via this transformation, γ-butyrolactone (GBL) occupies a prominent

position as a versatile C4 building block of considerable industrial relevance. γ GBL is widely employed as a precursor in the synthesis of pharmaceuticals,[87,88] agrochemicals,[89,90] and fine chemicals,[91–93] and also finds application as a biodegradable and environmentally benign solvent (Figure 2.2). Despite its importance, the majority of established synthetic routes to GBL rely on petrochemical feedstocks, highlighting the need for alternative, renewable approaches (Scheme 2.9).[94,95]

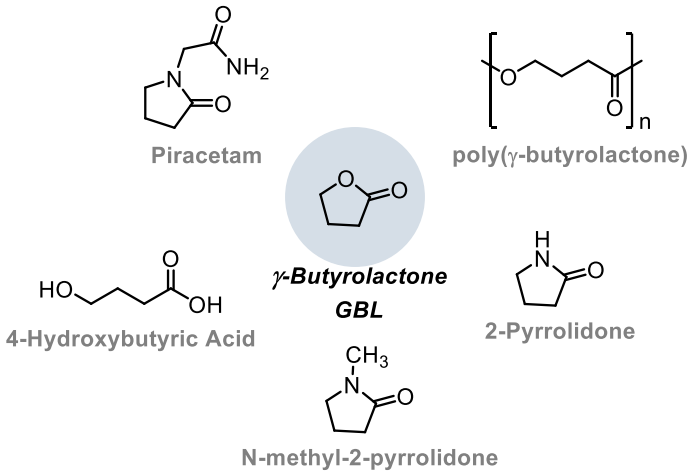

Figure 2.2 Application of GBL in various industries.

Biomass-derived substrates offer an attractive solution to this challenge. In particular, tetrahydrofuran-2-methanol (THF-M), which can be readily obtained from furfural, represents a renewable and structurally well-suited precursor for the synthesis of GBL via oxidative cleavage (Scheme 2.7).[96–99] The valorization of such biomass-derived alcohols through oxidative cleavage reactions aligns closely with the principles of sustainable chemistry and provides a direct pathway for converting renewable carbon sources into high-value platform chemicals.

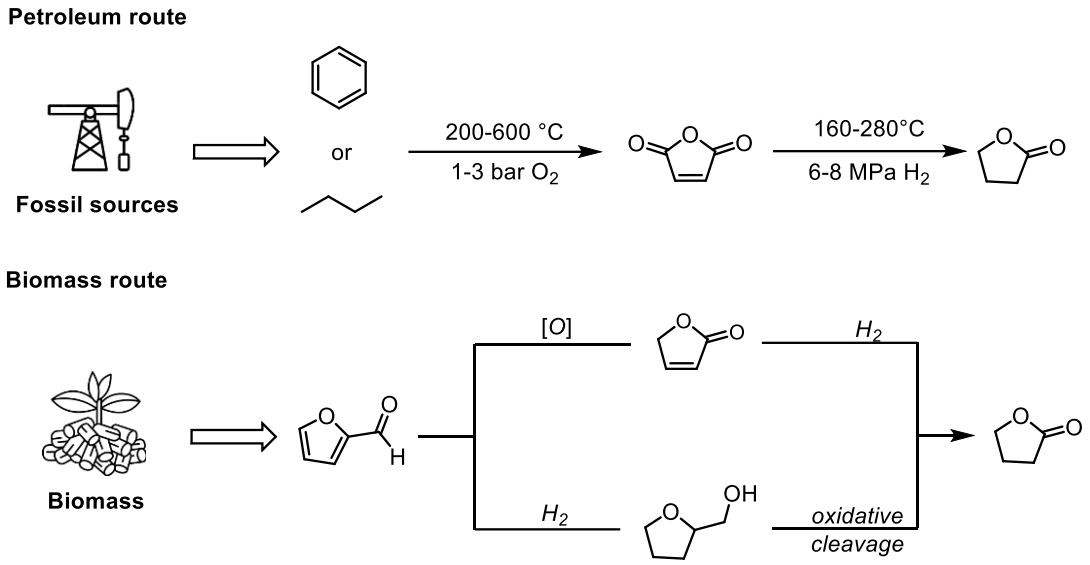

Scheme 2.7 Representative synthetic routes to GBL from petrochemical feedstocks and from biomass-derived precursors.

Several methods for the oxidative cleavage of primary alcohols to γ-lactones have been reported. However, many of these approaches rely on harsh or environmentally problematic oxidants, such as pyridinium chlorochromate (PCC)[100] or pyridinium dichromate (PDC),[101] or require multistep sequences involving initial oxidation to aldehydes followed by Baeyer–Villiger oxidation using peracids such as *m*-chloroperbenzoic acid (Scheme 2.8).[102–104] These methods often suffer from drawbacks including poor atom economy, the generation of toxic waste, limited functional group tolerance, and challenges associated with scalability and operational safety.

Hypervalent iodine reagents have emerged as promising metal-free alternatives for oxidative transformations, combining high oxidative efficiency with milder and safer reaction conditions. Notably, Yakura and co-workers reported the oxidative cleavage of THF-M and pyrrolidine-2-methanols to the corresponding γ-lactones and γ-lactams using a hypervalent iodine(V) catalyst in combination with Oxone® as a terminal oxidant (Scheme 2.8).[105,106] This approach enabled the direct conversion of β-substituted alcohols into cleaved products in a single operational step. Despite its conceptual significance, this approach is limited by practical considerations, including the use of hazardous solvents such as DMF and nitromethane, prolonged reaction times ranging from 5 to 40 hours, and restricted scalability due to safety concerns associated with handling hypervalent iodine(V) species under batch conditions.

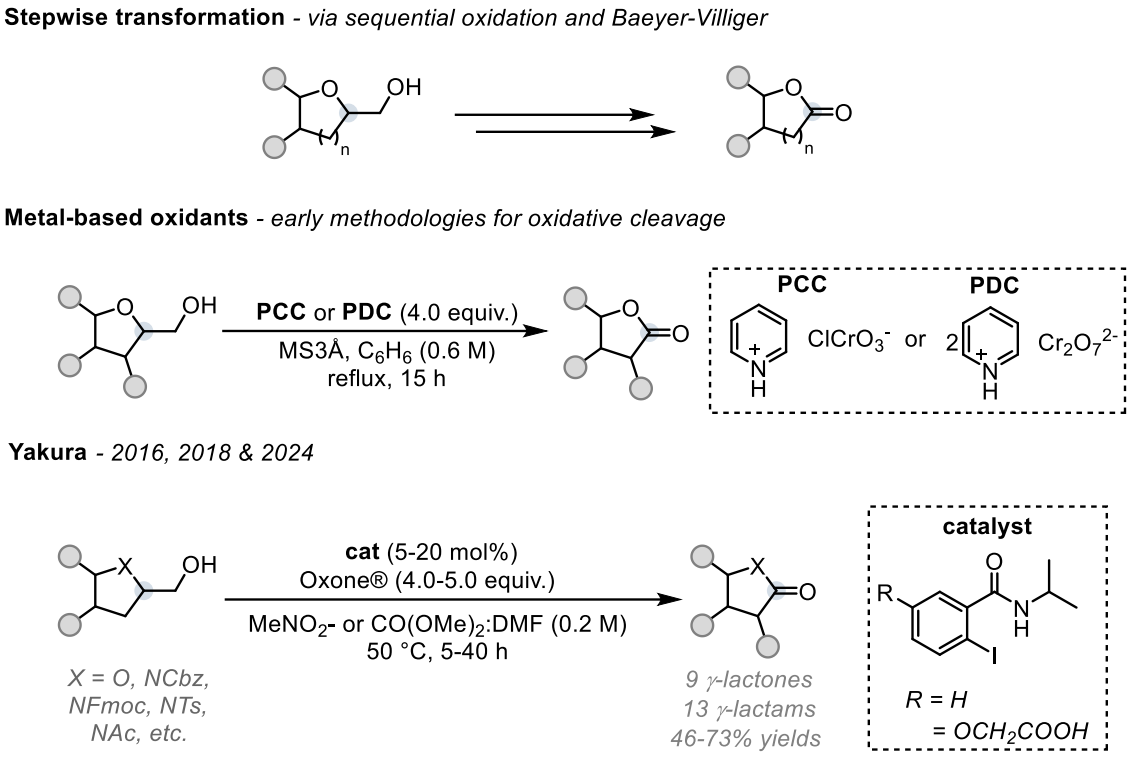

Scheme 2.8 Current advances in the oxidative C-C Cleavage of β-substituted primary alcohols.

Consequently, there remains a clear need for the development of safer, more efficient, and scalable methodologies for the oxidative cleavage of β-substituted alcohols. In particular, the combination of metal-free hypervalent iodine(V) catalysis with immobilization strategies and continuous-flow processing represents an attractive yet largely unexplored approach for enabling sustainable access to γ-lactones, γ-lactams, and related dehomologated products from renewable feedstocks.

2.7 Project Aim

Despite significant advances in the development of hypervalent iodine(V) reagents for oxidative transformations, several challenges remain that limit their broader application in sustainable and scalable chemical processes. Although the use of hypervalent iodine(V) species in catalytic amounts has been demonstrated, the catalytic application of solid-supported hypervalent iodine(V) reagents reported to date has been largely restricted to polystyrene-based supports, which are inherently susceptible to oxidative degradation, swelling, and limited long-term stability under strongly oxidative conditions. These shortcomings significantly compromise catalyst durability and reproducibility, particularly under continuous-flow operation.

While immobilization strategies have improved catalyst handling and recyclability, their use under continuous-flow conditions remains limited, and the scope of transformations

explored has largely been confined to benchmark alcohol oxidations. The development of more robust solid supports capable of withstanding prolonged exposure to oxidative conditions is therefore essential to unlock the full potential of hypervalent iodine(V) catalysis for sustainable and scalable applications.

In light of these challenges, the aim of this project is to develop a robust and recyclable silica-supported hypervalent iodine(V) catalyst and to evaluate its performance in sustainable oxidative transformations under continuous-flow conditions. This work focuses on enhancing catalyst durability by employing a chemically and mechanically robust silica support, as well as on evaluating the catalytic performance of the resulting system in oxidative transformations. Particular emphasis is placed on the oxidative dehomologation of β-substituted alcohols to afford dehomologated products such as γ-lactones, γ-lactams, and carbamates under mild, metal-free conditions, thereby demonstrating the potential of silica-supported hypervalent iodine(V) catalysts for sustainable and scalable oxidation processes.

2.8 Results and Discussion

2.8.1 Polystyrene-Supported Iodine(V) Catalyst

As a starting point for the development of a robust solid-supported hypervalent iodine(V) catalyst, the synthesis of a polystyrene-supported iodine(V) catalyst was initially synthesized based on previously reported procedures by Dr. Frederic Ballaschk.[79] In the synthesis, amino-functionalized polystyrene was used as the solid support. The iodine(V) precatalyst was synthesized from aminosulfonic acid, which was transformed into the iodinated intermediate via a Sandmeyer-type reaction, affording iodine(I) derivative **2.1** in moderate yield of 52%. Oxidation of the benzylic methyl group with potassium permanganate then produced the carboxyl-functionalized precatalyst **2.2** in excellent yield of 94%, making it suitable for immobilization onto the polystyrene support. The precatalyst was covalently attached to the solid support (amino-functionalized polystyrene) by means of standard SPPS. Following immobilization, the residual unreacted amino groups (ethyleneamine residues) were end-capped to prevent their potential interference in subsequent oxidative transformations catalyzed by the immobilized system. Finally, the immobilized precatalyst was subjected to oxidation in presence of methanesulfonic acid (MSA), affording the active hypervalent iodine(V) species **SP-IBS I** (Scheme 2.9).

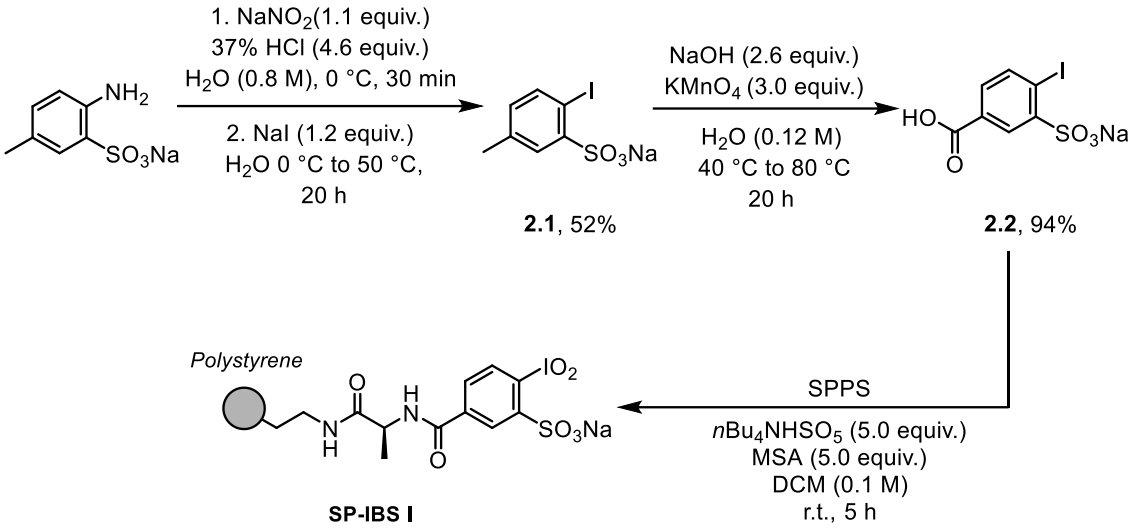

Scheme 2.9 Synthesis of the iodine precatalyst and its immobilization on the solid support.

The loading of the active hypervalent iodine(V) species on the solid support was determined through a combination of theoretical calculation and experimental evaluation. The theoretical loading was first calculated using Equation 1, as described in the experimental Section. Resulting in a value of 0.75 mmol/g. To assess the actual loading, the secondary alcohol L-(–)-borneol was treated with 30 mol% of the immobilized iodine(V) catalyst, as depicted in (Scheme 2.10). The conversion of the reaction was quantified by GC-FID analysis of the crude product and found to be 21%, corresponding to approximately seven-tenths of the maximum achievable conversion. From this data, the actual active iodine(V) loading was calculated to be 0.53 mmol/g. This methodology thus provides a direct correlation to the amount of active iodine(V) species present on the polystyrene.

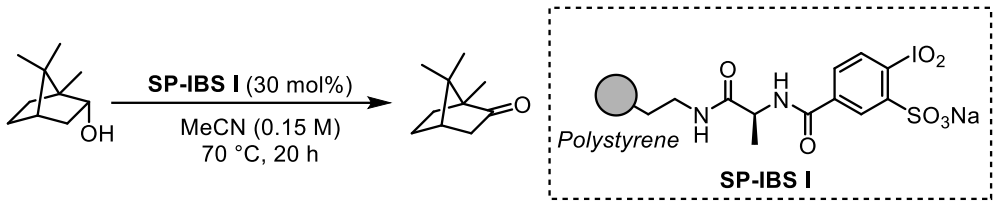

Scheme 2.10 Loading determination of solid-supported hypervalent iodine(V) catalyst.

This methodology provided a robust foundation for the development of solid-supported iodine(V) catalysts capable of promoting oxidative transformations under heterogeneous conditions. The application of solid-supported iodine(V) catalysts **SP-IBS I** for the oxidation of alcohols was investigated as described earlier (Scheme 2.6), wherein TBA Oxone® was employed as a terminal oxidant to reoxidize the catalyst *in situ*. While this catalytic system demonstrated notable advantages over stoichiometric methodologies, it

failed to fully satisfy the criteria of a sustainable oxidation protocol. The recyclability of the supported catalyst was restricted to reactions conducted under shaking conditions, necessitating the use of non-standard laboratory equipment. Conventional stirring with magnetic bars resulted in mechanical degradation of the resin matrix, thereby limiting catalyst reuse. Furthermore, a significant synthetic drawback of the system was its inability to afford isolated aldehyde products. This limitation was attributed to undesirable side reactions of the aldehydes with the aminofunctionalized polystyrene support, which ultimately diminished the synthetic utility of the method.

To address the aforementioned limitations, the oxidation protocol was transferred to a continuous-flow system by incorporating the solid-supported catalyst into a packed-bed reactor by Dr. Kathrin Bensberg. In this system, two inlet streams, comprising the substrate solution and the oxidant, were combined at a T-mixer. The mixed reaction stream was subsequently introduced into a heated fixed-bed reactor containing the immobilized iodine(V) species, where the oxidation proceeded under controlled flow conditions. The outflowing reaction mixture was collected in a cooled vessel to quench the reaction and facilitate product handling. For the laboratory implementation, a two-channel syringe pump was employed to deliver the respective reagent solutions at defined flow rates (Scheme 2.11).

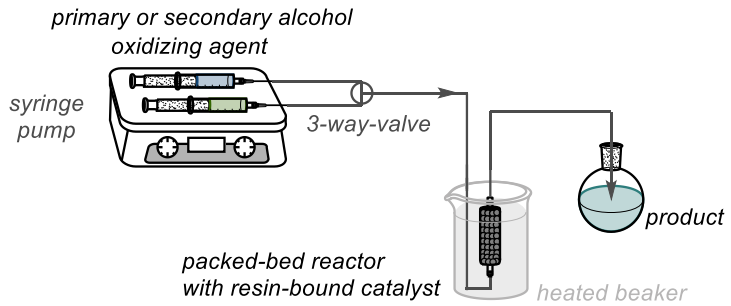

Scheme 2.11 Schematic representation of the continuous-flow system employing an immobilized iodine(V) catalyst for alcohol oxidation.

2.8.2 Catalytic evaluation in GBL synthesis

Building on the previous development of the catalyst system in continuous-flow processes, its application was extended to the oxidative cleavage of β-substituted primary alcohols to afford dehomologated products. Part of the preliminary work in this area was conducted in collaboration with Dr. Athanasios Savvidis.

The initial catalytic evaluation employed the previously reported polystyrene-supported iodine(V) catalyst (**SP-IBS I**, 0.53 mmol/g) under continuous-flow conditions. Using TBA Oxone® (1.9 equiv.) as the oxidant in acetonitrile (0.125 M), at 70 °C and a flow rate of

20 mL/h, GBL was obtained in 25% yield as determined by GC-FID analysis (Table 2.1, entry 1). In an effort to improve the yield, the quantity of terminal oxidant was increased, since multiple sequential oxidation steps are required for complete oxidative cleavage. Increasing the oxidant to 3.5 equiv. enhanced the yield to 41% (Table 2.1, entry 2). However, lowering the substrate concentration under otherwise identical conditions resulted in a reduced yield of 26% (Table 2.1, entry 3). Further optimization by extending the residence time to 27.7 mins led to a significant improvement, affording GBL in yields of up to 82% (Table 2.1, entries 4 and 5).

Table 2.1 Optimization studies for oxidative cleavage of β-substituted alcohols.

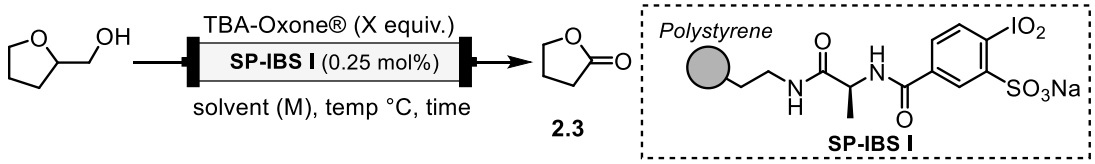

Entry	TBA Oxone® (equiv.)	MeCN (M)	*f* (mL/h)	t_R (mins)	Yield[a] (%)
1	1.9	0.125	20	10.9	25
2	3.5	0.125	20	10.9	41
3	3.5	0.083	20	10.9	26
4	3.5	0.083	10	21.2	68
5	3.5	0.083	7.5	27.7	82

Reactions were carried out at 1.0 mmol scale. [a] The yields of the reactions were determined by GC-FID analysis, using methyl laurate as an internal standard. (These studies were performed in collaboration with Dr. Athanasios Savvidis)

2.8.3 Recyclability and Limitations

Following the establishment of the optimal reaction conditions, an important objective was to evaluate the potential for catalyst recovery and reuse, as recyclability is a key aspect of developing a sustainable catalytic process. Accordingly, the polystyrene-supported iodine(V) catalyst (**SP-IBS I**) was systematically tested under the optimized continuous-flow conditions for the oxidative cleavage of THF-M to GBL.

Evidence of inconsistency in catalytic performance was apparent from the outset of the recycling experiments. The first run of the recyclability study afforded a yield of 75%, which was notably lower than the 82% yield obtained under the optimized conditions. This initial deviation suggested a degree of instability or variability within the catalyst bed even before multiple reuses. Such fluctuations are most likely associated with the intrinsic swelling behavior of the polystyrene support, which affects the accessibility of

the catalytically active sites. Variations in the extent of swelling between runs can influence substrate diffusion and local microenvironments around the active iodine(V) centers, leading to inconsistent reaction outcomes.

Although the catalyst maintained moderate activity throughout the early cycles, a gradual decrease in performance was observed after the seventh cycle, with the median yield stabilizing around 75.5% after 20 consecutive runs (Figure 2.1). This trend indicates that prolonged exposure to oxidizing conditions may compromise the structural and mechanical stability of the polymeric support, thereby reducing catalytic efficiency over time.

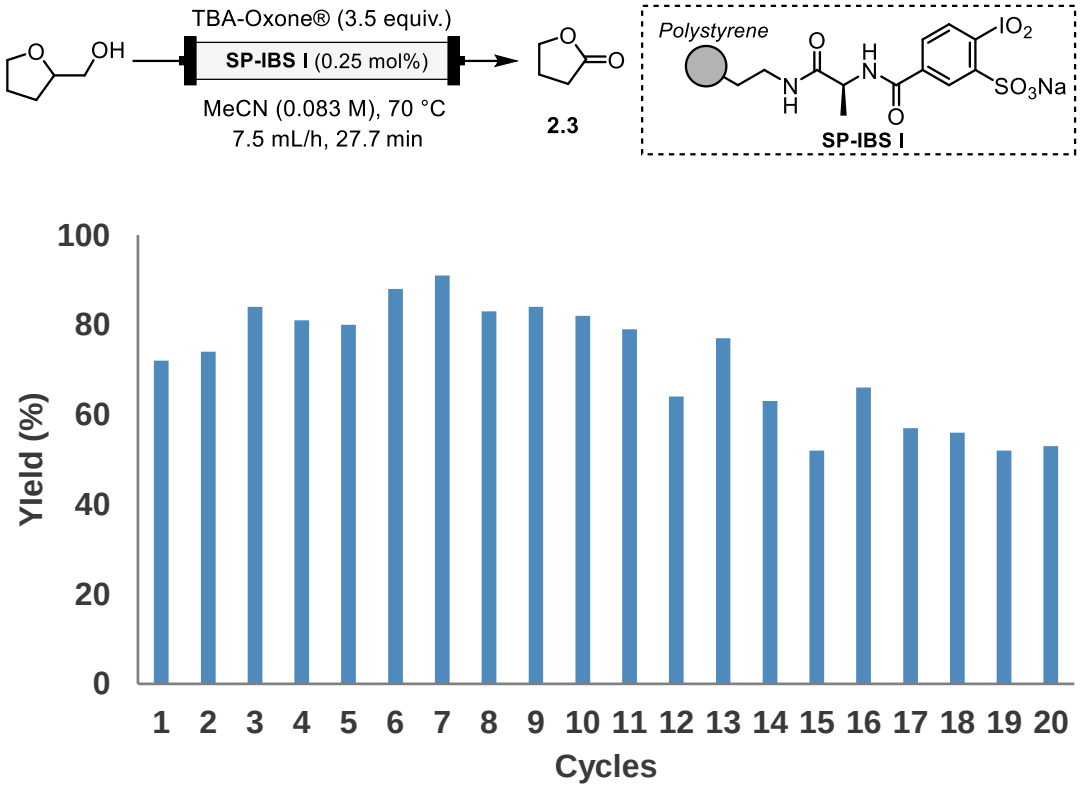

Figure 2.3 Recycling results of the silica-supported iodine(V) catalyst (**SP IBS I**) for the oxidative cleavage reaction under continuous-flow conditions.

In summary, while the **SP-IBS I** catalyst demonstrated reasonable activity and partial recyclability, its operational stability under continuous-flow conditions was hindered by the swelling and oxidative degradation of the polystyrene matrix. These findings underscore the inherent limitations of polymer-based supports for sustained oxidative transformations. The observed decline in catalytic efficiency and yield reproducibility highlights the need for a more chemically and mechanically resilient support capable of maintaining its stability under oxidative flow conditions.

To address these shortcomings, the subsequent stage of this research focused on the development of a robust solid supported iodine(V) catalyst, with intention to overcome the drawbacks of the polystyrene supported system.

2.8.4 Silica-Supported Iodine(V) Catalyst

The limitations observed with the polystyrene-supported iodine(V) catalyst **SP-IBS I**, including swelling-induced variations and partial oxidative degradation, highlighted the need for a more robust support material capable of sustaining prolonged catalytic activity under continuous-flow conditions. To address these challenges, a commercially available 3-aminopropyl functionalized silica was selected due to its superior mechanical strength, thermal stability, and oxidative robustness. The high surface area of silica facilitates efficient mass transfer and uniform dispersion of the immobilized catalytic species, ensuring consistent access of substrates to the active sites.[107–109] The silica-supported iodine(V) catalyst was synthesized by attaching the iodine(V) precursor **SP-IBS II** to the 3-aminopropyl functionalized silica via standard solid-phase peptide coupling (Scheme 2.12). Following immobilization, the residual unreacted amino groups (ethyleneamine residues) were end-capped to prevent their potential interference in subsequent oxidative transformations catalyzed by the immobilized system. The immobilized precatalyst was then subjected to oxidation, affording the active hypervalent iodine(V) species **SP-IBS II**. The loading of the active species on the solid support was determined to be 0.38 mmol/g through a combination of theoretical calculation and experimental evaluation, analogous to the method employed for the polystyrene-supported iodine(V) catalyst. This design was intended to enable reproducible catalytic performance, extended operational lifetime, and effective recyclability under continuous-flow conditions.

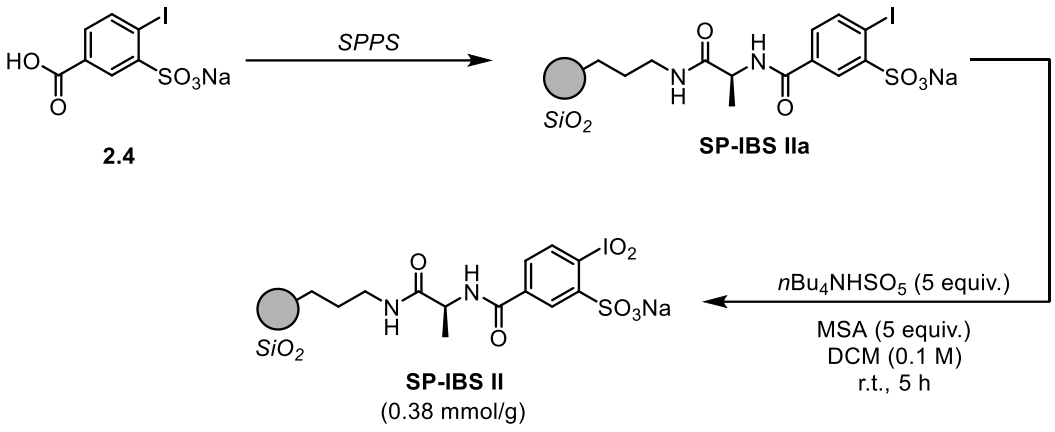

Scheme 2.12 Synthesis of the silica-supported iodine(V) catalyst.

2.8.5 Catalytic Evaluation in GBL Synthesis

The following sections describe the catalytic evaluation of the silica-supported catalyst, with particular emphasis on its application to the oxidative cleavage of β-substituted primary alcohols. Prior to continuous-flow evaluation, preliminary optimization of the oxidative cleavage of THF-M was conducted in batch to establish optimal reaction conditions. To identify optimal parameters, several solvents were examined based on their ability to solubilize the reaction reagents (educt and oxidant), as solvent selection was critical to ensure complete dissolution and prevent clogging issues during flow operation. The results of solvent screening are summarized in Table 2.2. Acetone and tetrahydrofuran (THF) were excluded as solvents, as literature reports indicate that acetone can undergo *in situ* formation of reactive oxidizing species such as dioxiranes, while THF may lead to the formation of γ-butyrolactone under oxidative conditions.[110] The oxidant TBA-Oxone® exhibited good solubility in DCM, DMF, water, acetic acid, and nitromethane; hence, these solvents were investigated for the oxidative cleavage of THF-methanols to GBL using the precatalyst (30 mol%) and 5 equivalents of oxidant. Among these, acetic acid afforded the best performance, providing a 58% yield of GBL after 18 hours (Table 2.2, entry 4). Although nitromethane gave a comparable yield of 58% after 24 hours, acetic acid was chosen for subsequent studies due to its greener profile, lower toxicity, and reduced explosion risk.

Next, the effect of temperature on the reaction outcome was examined. Increasing the temperature to 50 °C resulted in a significant improvement, yielding 85% of GBL within 2 hours (Table 2.2, entry 10). However, further elevation to 70 °C led to a decrease in yield 53% (Table 2.2, entry 11), likely due to thermal instability or side reactions at higher temperatures. To facilitate smooth handling of the reaction under continuous flow conditions, the substrate concentration was reduced from 0.3 M to 0.1 M. The optimized batch conditions thus provided a robust foundation for continuous-flow evaluation, enabling systematic assessment of the activity, reproducibility, and recyclability of the silica-supported iodine(V) catalyst.

Table 2.2 Solvent and temperature optimization for the oxidative cleavage of β-substituted primary alcohols.

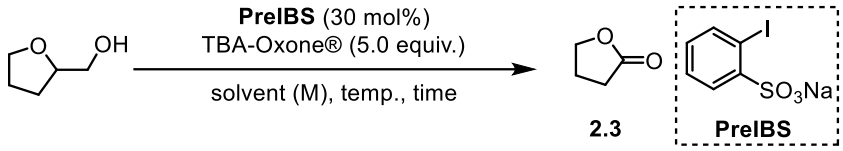

2.3 PreIBS

Entry	Solvent	Temp (°C)	Time(h)	Conversion (%)	Yield (%)
1	DCM	rt	18	15	7
2	DMF	rt	18	40	14
3	H_2O	rt	18	<5	--[a]
4	AcOH	rt	18	100	58
5	$MeNO_2$	rt	24	100	58
6	MeCN	rt	24	98	23
7[a]	MeCN:H_2O (1:1)	rt	18	28	<1
8	MeCN:HFIP(1:1)	rt	24	100	76
9	AcOH	30	2	81	73
10	AcOH	50	2	100	85
11	AcOH	70	2	100	53
12	MeCN	50	2	100	67
13	MeCN:AcOH (1:1)	50	2	100	82
14[b]	AcOH	50	2	65	54
15	AcOH (0.1M)	50	2	100	86

Reactions were carried out at 0.3 mmol scale. The reaction conversion and yields determined by GC-FID analysis, using methyl laurate as an internal standard. The reaction was carried out using TBA-Oxone® (5 equiv.). [a] Trace amounts of product formation was observed.

With the optimized conditions in hand, the reaction was subsequently evaluated in a batch setup at the reduced concentration to facilitate reagent handling under continuous-flow conditions. Gratifyingly, the reaction efficiency was largely retained, affording the desired product in 86% yield. The optimized batch protocol was then translated to continuous-flow reaction, where further optimization efforts focused primarily on the residence time, defined as the average duration that the reaction mixture (substrate and oxidant) remains within the reactor.

Initial experiments conducted with a residence time of 4 minutes resulted in incomplete conversion, providing GBL in 76% yield (Table 2.3, entry 1). To achieve full conversion, the residence time was extended to 7.5 min, which led to complete substrate

consumption and afforded GBL in 97% yield (Table 2.3, entry 2). Further increasing the residence time to 14.4 min resulted in a quantitative yield of GBL. However, when the reaction was carried out at a higher substrate concentration of 0.2 M with a shorter residence time of 2 min, incomplete conversion was again observed, affording GBL in 81% yield.

These findings collectively highlight the critical influence of residence time and reaction concentration on conversion efficiency under continuous-flow conditions, underscoring the importance of balancing throughput and reactivity in achieving optimal reactor performance.

Table 2.3 Optimization of reaction concentration and residence time for the continuous-flow oxidation of THF-M to GBL.

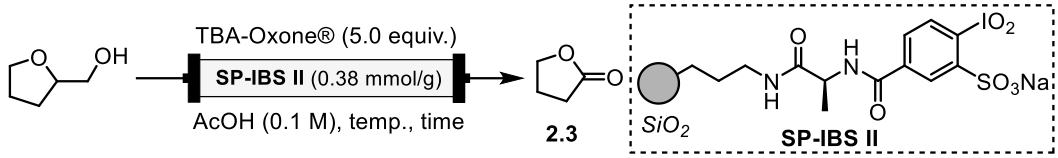

Entry	*f* (mL/h)	t_R (mins)	GC Conversion (%)	GC Yield of GBL (%)
1	15	4.8	81	76
2	10	7.5	100	97
3	5	14.4	100	99
4[b]	5	2	80	81

Reactions were carried out at 1.0 mmol scale. The reaction conversion and yields determined by GC-FID analysis, using methyl laurate as an internal standard. [b]Total reaction concentration was 0.2 M.

After establishing the optimal reaction conditions, the silica-supported catalyst was subsequently evaluated for its recyclability, which represents an important factor in the development of sustainable catalytic systems. The silica-supported iodine(V) catalyst **SP-IBS II** was systematically tested under the optimized continuous-flow conditions for the oxidative cleavage of THF-methanol to γ-butyrolactone (GBL) without catalyst reactivation between reaction cycles. The catalyst demonstrated excellent recyclability, maintaining a median yield of approximately 93% over 20 consecutive reaction runs, as presented in Figure 2.4.

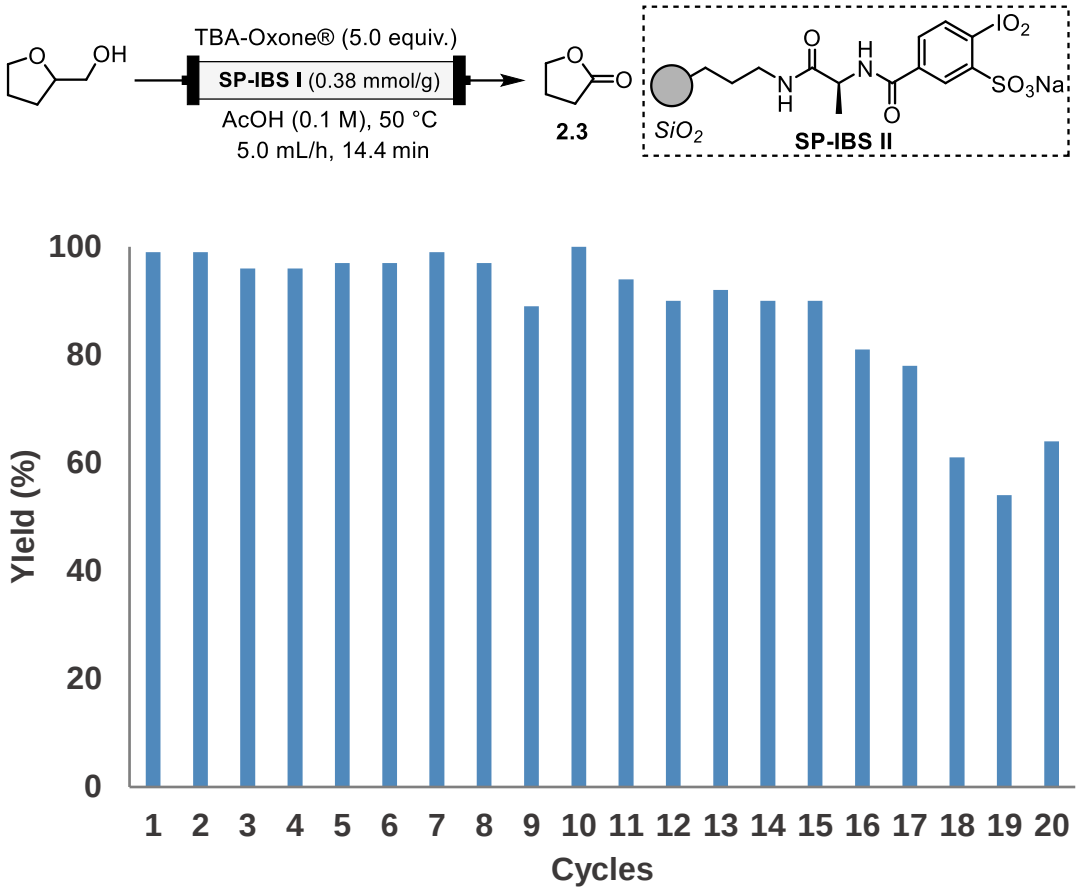

Figure 2.4 Recycling results of the silica-supported iodine(V) catalyst (**SP IBS II**) for the oxidative cleavage reaction under continuous-flow conditions.

To evaluate the scalability and robustness of the developed continuous-flow process, a 20 mmol reaction was performed over an extended operating period of about 21 hours. Periodic monitoring through aliquot analysis showed consistently high conversion of THF-M to γ-butyrolactone **2.3**, ranging from 96% to 99% throughout the run. During the first 8 hours, product was collected in hourly fractions, resulting in eight separate samples, while the remaining product from hour 8 to 21 was collected as a single combined fraction. Considering the reactor volume of 1.2 mL, this corresponds to a space–time yield (STY) of 800 mmol/L/h. These results demonstrate the operational stability and scalability of the continuous-flow system, highlighting its potential as a practical and sustainable method for the synthesis of γ-butyrolactone from furfural-derived biomass feedstocks.

Table 2.4 Long-term continuous-flow synthesis of γ-butyrolactone (GBL) **2.3** from tetrahydrofurfuryl alcohol (1) over 21 hours.

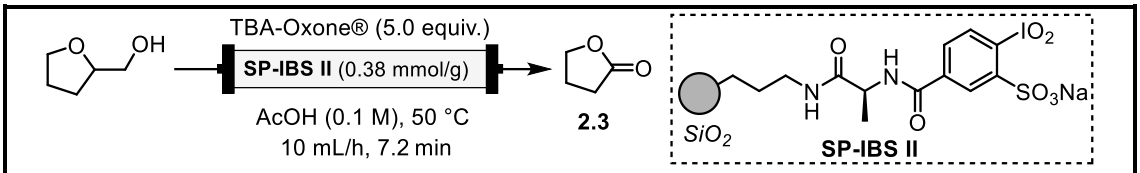

Hour	**1**	**2**	**3**	**4**	**5**	**6**	**7**	**8**	**9-21**
Conversion (%)	100	100	100	100	100	100	100	100	100
Yield (%)	99	98	96	99	97	98	97	99	99

The reaction conversion and yields determined by GC-FID analysis.

2.8.6 Scope and Limitations

With the optimized reaction conditions established, the scope and limitations of the developed methodology were subsequently investigated. Initially, the applicability of the protocol toward the synthesis of C4-substituted lactones from C5-substituted tetrahydrofuran-2-methanols was tested. A range of C5-substituted tetrahydrofuran-2-methanols bearing various *O*-protecting groups such as phenyl **2.5**, benzyl **2.6**, benzoyl **2.7**, acyl **2.8**, tosyl **2.9**, and TBDPS **2.10** were efficiently transformed into the corresponding lactones in good to excellent yields (61–90%).

The reaction displayed a broad functional group tolerance, accommodating substrates containing azides **2.11**, phthalimides **2.13**, chlorides **2.12**, and alkynes **2.14**, which furnished the desired C4-substituted lactones in high yields (66–79%). These functionalities are of particular interest as they provide useful handles for further synthetic elaboration, enabling the synthesis of more complex molecular architectures. On the other hand, substrates containing alkenes **2.15** or nitriles **2.16** resulted in diminished yields (33–38%), likely due to competitive side reactions such as epoxide formation.

Given the well-documented neuropharmacological activity of alkyl-substituted γ-butyrolactones,[111,112] considerable research effort has been directed toward the synthesis of these structural motifs, which often necessitates multiple synthetic transformations. Using this method, a simple aliphatic γ-lactone **2.17** was obtained in excellent yield (86%), highlighting the efficiency and synthetic utility of this approach.

Phenyl-substituted substrates bearing either electron-donating **2.18** or electron-withdrawing **2.19** groups were also well tolerated, affording the corresponding C4-substituted lactones in moderate to good yields (70–73%). While the thiazole-substituted derivative **2.20** provided the corresponding lactone in low yield 22%, basic heterocycles

such as triazoles **2.21** and oxadiazoles **2.22** proved compatible under the reaction conditions, delivering the desired products in 62–72% yields (Scheme 2.13).

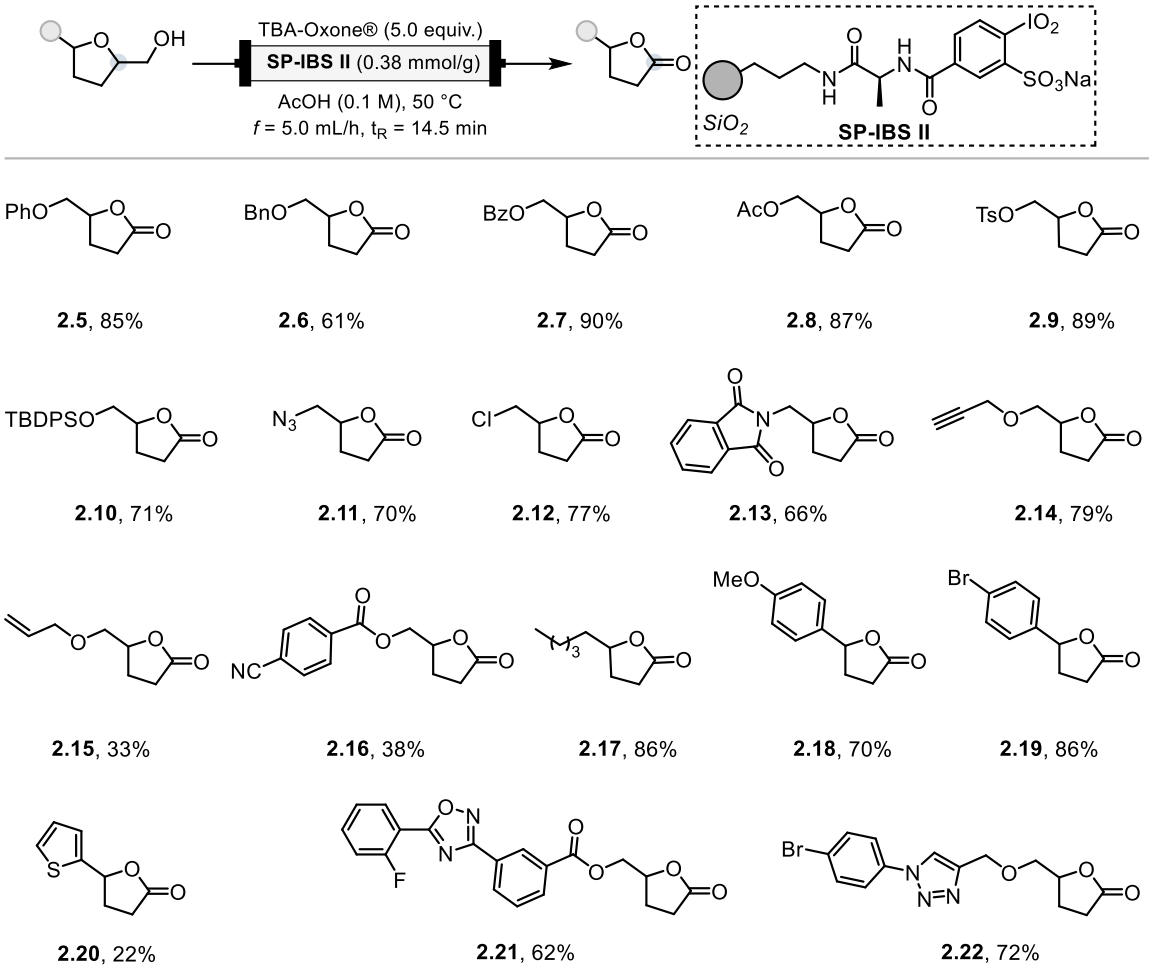

Scheme 2.13 Oxidative cleavage of C5-substituted THF-M to γ-lactones using silica-supported hypervalent iodine(V) catalyst (**SP-IBS II**).

The applicability of the developed protocol toward the synthesis of C3-substituted lactones from C4-substituted THF-M was subsequently examined. Initially, a series of C4-aryl-substituted THF-M bearing various substituents on the aromatic ring and encompassing a range of electronic properties were investigated. These substrates **2.23-2.27** were well tolerated under the optimized reaction conditions and afforded the corresponding lactones in good to excellent yields (61–88%), with minimal electronic influence observed from the aryl substituents.

To further demonstrate the versatility of the transformation, the methodology was extended to the synthesis of C3-substituted gammalactones possessing more complex molecular architectures. Given the well-recognized significance of spirolactones in medicinal chemistry,[113,114] the formation of spirocyclic lactones incorporating

tetrahydropyran **2.28** and Cbz-protected piperidine **2.29** frameworks was explored. In both cases, the desired spirolactones were obtained in good yields (51–68%), thereby underscoring the synthetic potential of this strategy for the synthesis of structurally complex lactone motifs (Scheme 2.14).

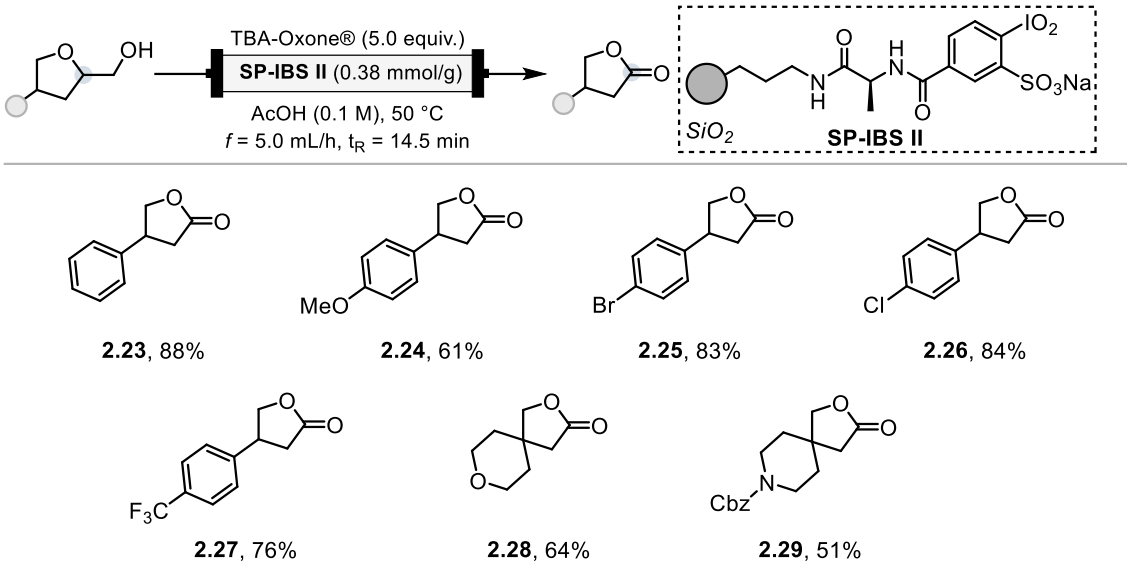

Scheme 2.14 Oxidative cleavage of C4-substituted THF-M to γ-lactones using silica-supported hypervalent iodine(V) catalyst (**SP-IBS II**).

Encouraged by the promising results obtained in the earlier substrate scopes, next the applicability of the method toward more challenging transformations was explored. Particular attention was directed toward substrates that could potentially undergo difficult cleavage steps leading to the formation of C3-phenyl-substituted lactones, C5- and C4-substituted lactones, as well as structures extending beyond γ-butyrolactone derivatives, including protected β-amino acid analogues. The method proved sufficiently robust to accommodate these challenging substrates. Notably, the synthesis of the C3-phenyl-substituted lactone **2.30** was achieved in good yield (70%). This transformation is especially significant given the sterically demanding nature of the substrate, as the phenyl substituent is positioned in close proximity to the reactive site, potentially hindering the oxidation process. Nevertheless, the reaction proceeded smoothly, affording the desired lactone without notable loss in efficiency.

Furthermore, a fused bicyclic lactone **2.31** was successfully prepared in moderate yield of 59%, demonstrating the tolerance of the system toward conformationally constrained frameworks. Both six-membered cyclic substrates and their acyclic analogues were also compatible under the reaction conditions, delivering the corresponding δ-lactone **2.32** and benzyl ester **2.33** in 45% and 28% yield, respectively.

Finally, the versatility of the methodology was further demonstrated through its application to β-amino alcohols. Both Cbz- and Fmoc-protected prolinols were smoothly converted into the corresponding γ-lactams (**2.34-2.35**) in 43% and 80% yield, respectively. In addition, the carmate **2.36** was obtained in 39% yield highlighting the method's potential utility (Scheme 2.15).

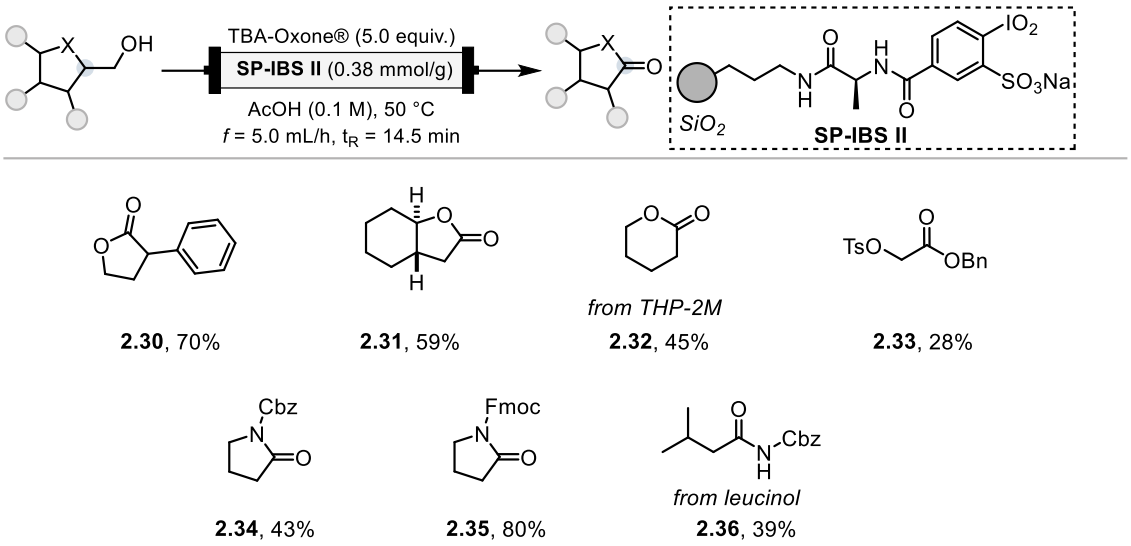

Scheme 2.15 Oxidative cleavage of β-substituted alcohols derivatives using silica-supported hypervalent iodine(V) catalyst (**SP-IBS II**).

Several substrates that were anticipated to perform well under the optimized reaction conditions failed to furnish the desired lactone products. Although the methodology successfully delivered lactones bearing benzylic substitution in other cases, certain substrates featuring similar structural motifs did not provide the expected products, suggesting that subtle steric or electronic effects at the benzylic position may inhibit the key oxidation step.

The TBS-protected derivative also proved unreactive under the standard conditions, and no formation of the corresponding lactone **3.37** was observed. This lack of reactivity is most likely attributable to cleavage of the silyl ether moiety under the acidic reaction environment, leading to substrate decomposition prior to cyclization. Similarly, the pyridine-containing substrate did not afford the corresponding product, which is presumed to arise from the instability of the heteroaromatic system under the acidic and oxidative conditions employed,[115] or possible deactivation of the catalytic species through coordination to the pyridine nitrogen (Scheme 2.16).

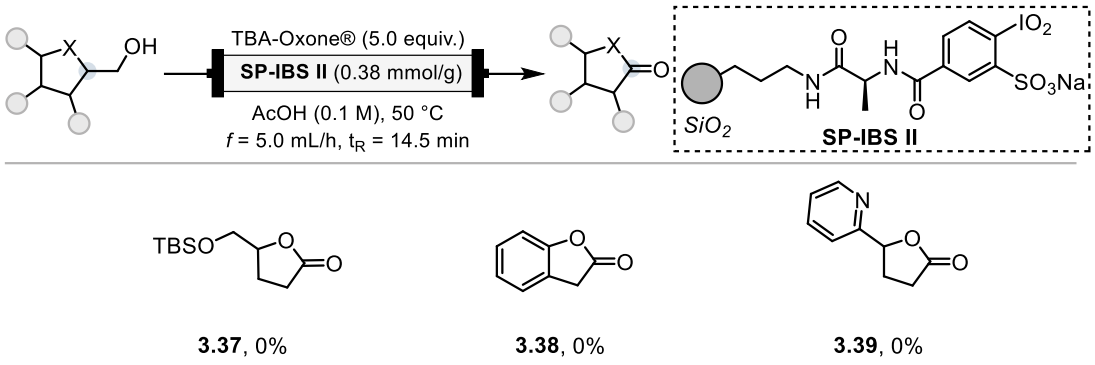

Scheme 2.16 Unssuccessful substrate

2.8.7 Mechanism

Based on the mechanism previously proposed by Yakura et al.,[105,106] the oxidative cleavage is believed to proceed via an initial oxidation of the primary alcohol by the immobilized hypervalent iodine(V) species (**SP-IBS II**), yielding the corresponding aldehyde intermediate **2.40**. This is followed by a TBA-Oxone®-mediated Baeyer–Villiger oxidation, generating the acetal intermediate **2.41**. Under the acidic reaction conditions, this acetal species undergoes rapid hydrolysis to form the hemiacetal **2.42**, which is subsequently oxidized, either by **SP-IBS II** or TBA-Oxone®, to afford the final γ-butyrolactone product **2.3** (Scheme 2.17).

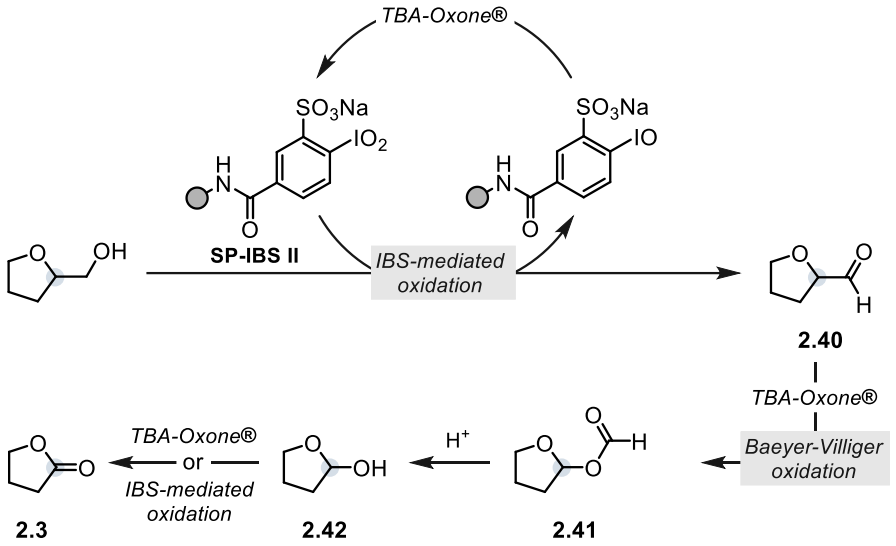

Scheme 2.17 Proposed mechanism for the oxidative cleavage.

To verify that this mechanistic pathway remains operative under continuous-flow conditions and to exclude any potential influence of the solid support, a series of control experiments were performed. In the first experiment, the reaction was conducted using oxidant (TBA-Oxone®) in a packed-bed reactor containing end-capped, catalyst-free

silica. Under these conditions, the aldehyde intermediate **2.40** was obtained in only 9% yield (Scheme 2.18), indicating very low catalytic activity from the support itself.

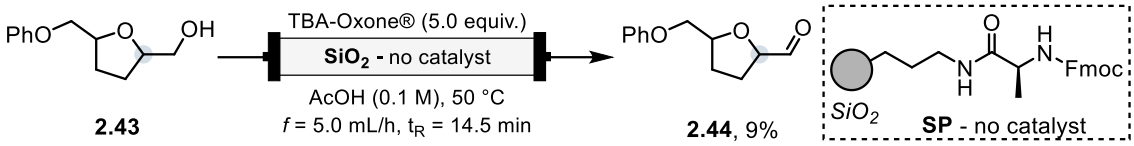

Scheme 2.18 Control reaction in absence of the silica-supported hypervalent iodine(V) catalyst.

In contrast, oxidation of the THF-M derivative **2.43** using the immobilized iodine(V) **SP-IBS II** under flow conditions afforded the corresponding aldehyde in 86% yield, confirming that **SP-IBS II** efficiently catalyzes the initial alcohol oxidation step (Scheme 2.19).

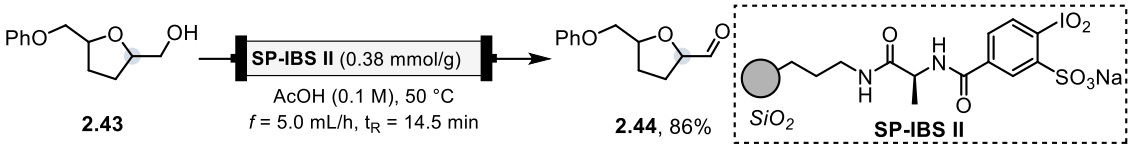

Scheme 2.19 Oxidation of **2.43** to aldehyde **2.44** using silica solid supported hypervalent iodine(V) oxidant **SP-IBS II**.

Subsequently, the conversion of the aldehyde intermediate **2.44** to the corresponding formate species was investigated. In this case, TBA-Oxone® promoted the formation of the γ-butyrolactone **2.5** in 91% yield, whereas **SP-IBS II** alone afforded only 8% of the product (Scheme 2.20). These results indicate that the Baeyer–Villiger oxidation step is primarily mediated by TBA-Oxone®, while the initial alcohol oxidation is facilitated by the immobilized iodine(V) catalyst.

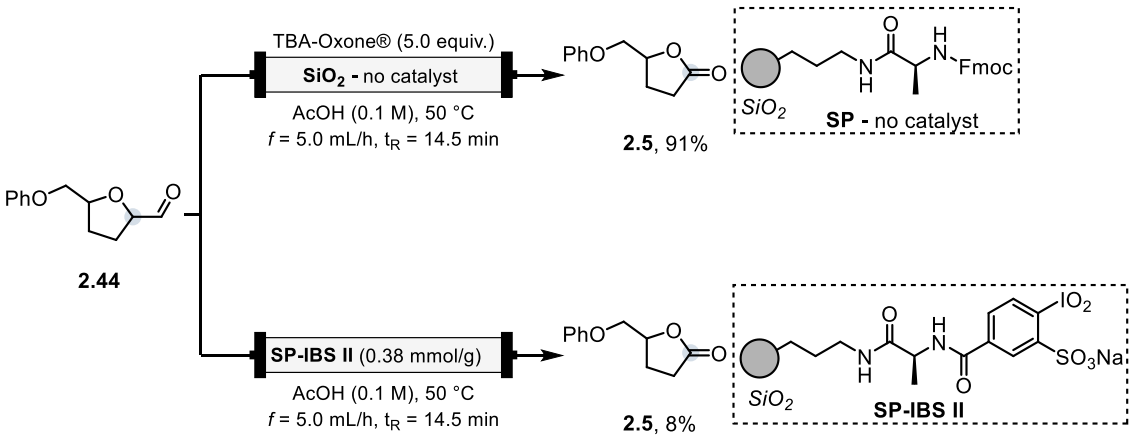

Scheme 2.20 Oxidative cleavage of aldehyde **2.44** to γ-butyrolactone derivative **2.5** using TBA-Oxone® and using hypervalent iodine(V) oxidant **SP-IBS II**.

2.9 Conclusion

In conclusion, a robust and recyclable silica-supported hypervalent iodine(V) catalyst was successfully developed and applied to oxidative transformations under continuous-flow conditions. Substitution of polystyrene with a silica support markedly enhanced the chemical and mechanical stability of the catalyst, overcoming limitations such as swelling and oxidative degradation observed in previous solid-supported systems. The catalyst exhibited excellent activity in the oxidative dehomologation of β-substituted alcohols, efficiently delivering γ-lactones, γ-lactams, and carbamates under mild, metal-free conditions. Its operational durability and effectiveness in continuous-flow highlight the potential of immobilized organocatalysts to enable sustainable, scalable, and practical oxidative processes. This study demonstrates the value of solid-supported hypervalent iodine(V) species in improving catalyst stability, recyclability, and applicability, contributing to the advancement of greener methodologies in oxidative chemistry.

Chapter 3
Development of an Immobilized Oxaziridine-Based Organocatalyst

3.1 Oxaziridines

Oxaziridines represent a distinctive class of versatile organic oxidants characterized by a strained three-membered ring containing two electronegative heteroatoms, nitrogen and oxygen. This structural feature endows them with high potential for atom-transfer reactions while maintaining notable thermal and chemical stability.[116–118] Comparable small heterocyclic oxidants include dioxiranes and diaziridines, all of which have been widely explored for a range of oxidative transformations (Figure 3.1).[110,119,120]

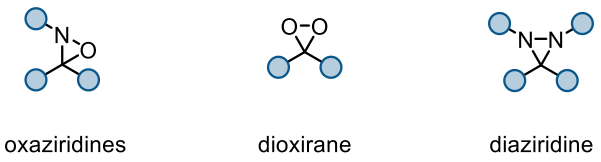

Figure 3.1 Representative oxidizing three-membered heterocycles containing two electrophilic heteroatoms.

The first report of oxaziridines, was reported by Emmons in 1957**,** describing their formation via the oxidation of imines with peracetic acid (Scheme 3.1).[121] These early examples established the foundation of oxaziridine compounds, demonstrating that such compounds could be isolated as stable crystalline solids without requiring distillation. Their stability facilitates purification by simple chromatography and long-term storage under ambient conditions. Although this stability often correlates with reduced intrinsic reactivity, oxaziridines can still effectively participate in O- and N-atom transfer reactions**,** depending on their substitution pattern.[120,122–124]

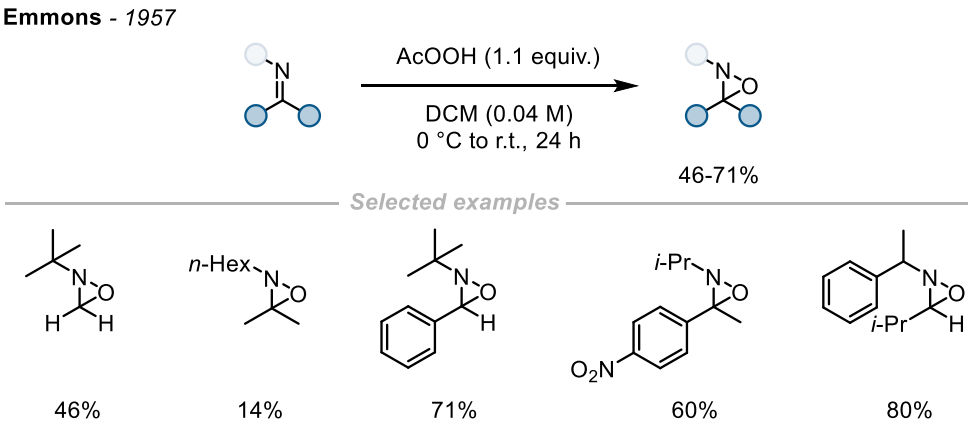

Scheme 3.1 Oxaziridines synthesis via oxidation of imines with peracetic acid.

3.1 Reactivity and Substituent Effects

The unique reactivity of oxaziridines arises from the polarized N-O bond, enabling both O-atom and N-atom transfer.[120] The chemoselectivity of these reactions is primarily

dictated by the nature of the N-substituent.[125–127] Oxaziridines bearing hydrogen, *tert*-butyloxycarbonyl (Boc), or silyl groups at nitrogen typically favor N-atom transfer, whereas those with sterically demanding or electron-withdrawing groups (EWGs) preferentially undergo O-atom transfer.[128–130] Consequently, oxaziridines can be systematically categorized according to their N-substituent, which determines both their atom-transfer pathway and the scope of compatible substrates (Figure 3.2).[131–133]

Figure 3.2 Reactivity patterns of oxaziridines exhibiting N- or O-atom transfer, dictated by the characteristics of the N-substituent.

The earliest and most widely studied class of oxaziridines are the N-alkyl-substituted derivatives which was first synthesized by Davis.[118] These compounds, prepared through oxidation of N-benzylidene sulfonamides, were reported to oxidize phosphines to phosphine oxides, marking one of the first demonstrations of their oxidative capability. Subsequent studies expanded their scope to the oxidation of sulfides, amines, and phosphines, capitalizing on their ease of preparation and long-term stability.[134,135]

3.2 Development of Oxaziridine-Mediated Oxidations

By the early 1980s, oxaziridines had emerged as practical reagents for various oxidative transformations. In 1981, the first oxaziridine-mediated epoxidation of alkenes was reported, affording a range of epoxides in moderate to good yields (Scheme 3.2). Although these reactions often required stoichiometric amounts of the oxidant and elevated temperatures (~60 °C), they showcased the utility of oxaziridines as metal-free epoxidizing agents.[136]

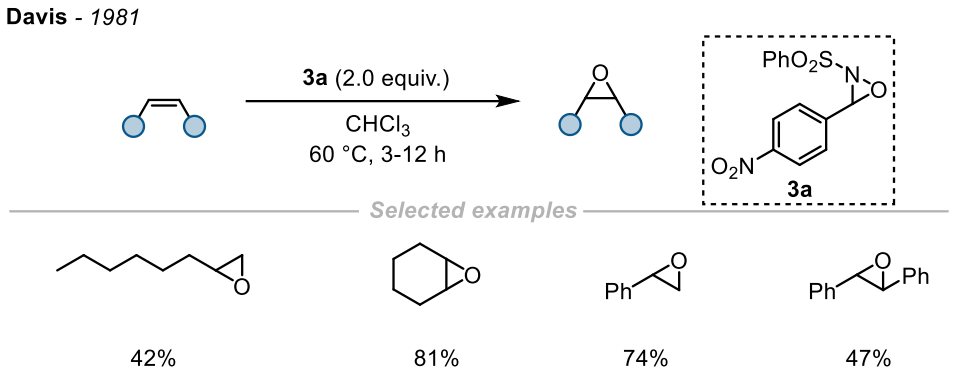

Scheme 3.2 First reported oxaziridine-mediated epoxidation of alkenes, demonstrating the utility of oxaziridines as metal-free oxidants.

Subsequent refinements allowed the synthesis of acid-labile epoxides, by oxidation of substrates such as α-silyl-substituted alkenes, under milder conditions using 1.0 equivalent of oxaziridine oxidant (Scheme 3.3).[117]

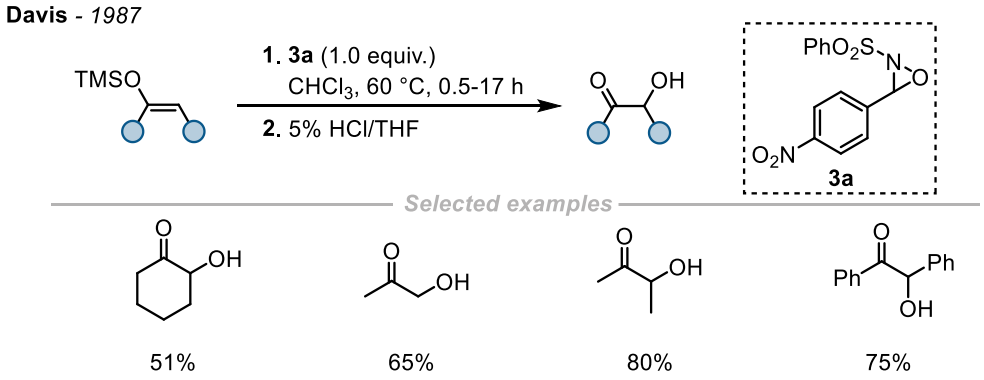

Scheme 3.3 Oxaziridine-mediated oxidation of acid-labile alkenes under mild conditions.

3.3 Highly Reactive and Fluorinated Oxaziridines

Further advancements by Resnati and co-workers revealed that polyfluorinated oxaziridines exhibit markedly enhanced reactivity due to their electron-deficient nature.[137–140] These derivatives have been applied across a broad range of oxidative transformations, including the oxidation of sulfides to sulfoxides and sulfones,[141] amine oxidation to N-oxides,[142,143] and epoxidation of alkenes.[144] Notably, these highly electron-deficient oxaziridines were also shown to effect direct C-H hydroxylation,[145,146] achieving reaction scopes similar to those of dioxiranes,[147] thereby establishing oxaziridines as powerful electrophilic oxygen-transfer reagents. For example, oxidation of a single tertiary C-H bond proceeds with a high degree of stereochemical fidelity to give the product with net retention of configuration (Scheme 3.4).[148]

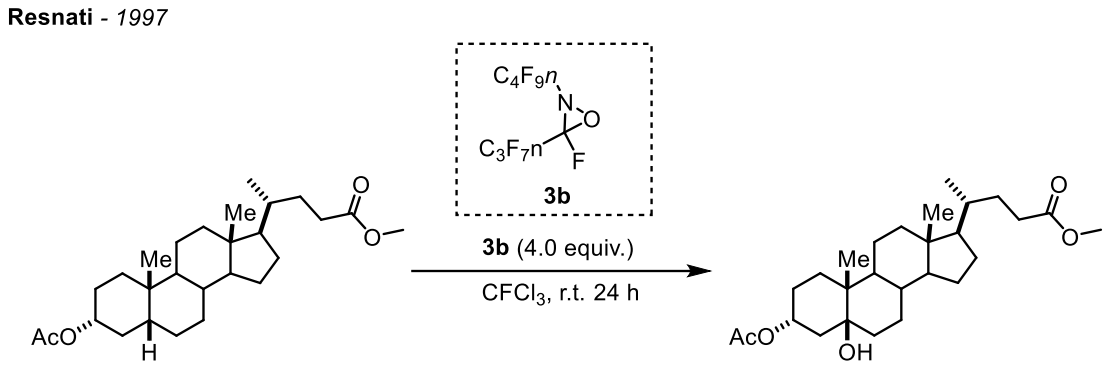

Scheme 3.4 Hydroxylation of C-H bonds facilitated by a polyfluorinated oxaziridine.

3.4 Emergence of Catalytic Oxaziridine Systems

A significant advancement in the field was achieved by Davis and co-workers, who developed the first catalytic oxidation method mediated by oxaziridines. Using N-(4-nitrobenzylidene)benzenesulfonamide as a precatalyst, sulfides were oxidized to sulfoxides in yields up to 90% within 20 minutes (Scheme 3.5). Reactions conducted under biphasic conditions minimized overoxidation to sulfones and enabled efficient substrate conversion, representing an important step toward more sustainable catalytic oxidations.[149,150]

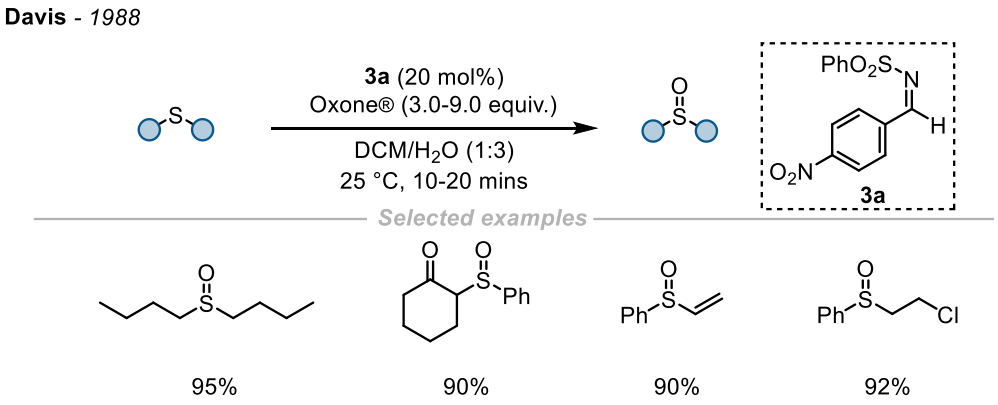

Scheme 3.5 First example of oxaziridine-facilitated catalytic sulfide oxidation.

Building upon these earlier developments, Du Bois and Brodsky reported a dual-catalytic oxaziridine system capable of promoting both olefin epoxidation and unactivated C–H hydroxylation reactions. Using 10–20 mol% of an electron-deficient 1,2,3-benzoxathiazine-2,2-dioxide catalyst in combination with 1.0 mol% of a diaryldiselenide co-catalyst, the system enabled near-quantitative epoxidation of electron-poor alkenes and achieved C–H hydroxylation of cis-decalin in yields of up to 63%, demonstrating high efficiency and notable chemoselectivity. Mechanistically, the benzoxathiazine-based catalyst functioned as the oxygen-transfer agent, while the diselenide co-catalyst

facilitated catalyst turnover through reoxidation of the reduced species by hydrogen peroxide. In this context, urea–hydrogen peroxide (UHP) was employed as a bench-stable solid oxidant, generating perseleninic acid *in situ*, which served to regenerate the active oxaziridine intermediate and sustain catalytic activity (Scheme 3.6).[151] (*For clarity, 1,2,3-benzoxathiazine-2,2-dioxide heterocycles are going to be referred to as benzoxathiazines throughout this thesis*)

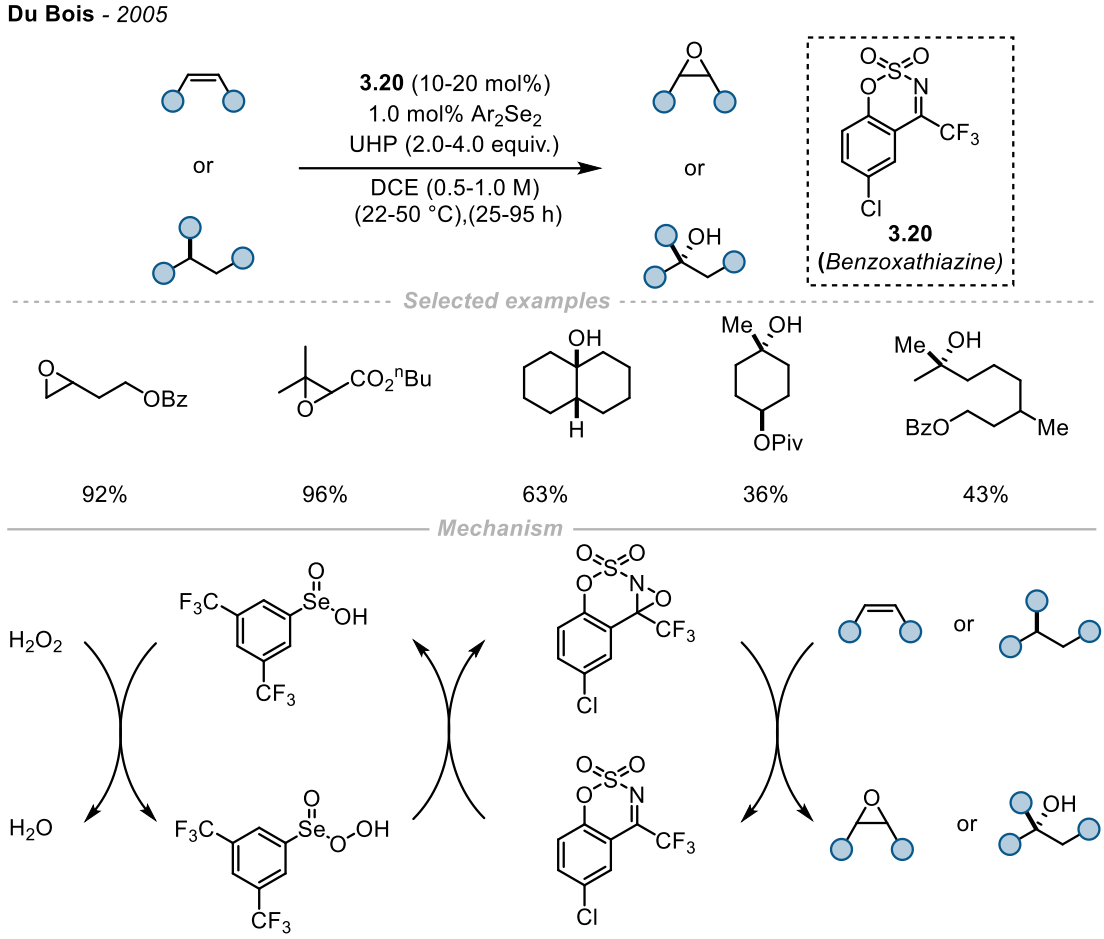

Scheme 3.6 Oxaziridine catalysed olefin epoxidation and C–H hydroxylation.

Further developments of the benzoxathiazine-based oxaziridine catalysts, guided by density functional theory (DFT) calculations led to the rational design of improved catalyst scaffolds. These investigations revealed that introducing electron-withdrawing substituents at the C6 position of the benzoxathiazine ring, particularly para to the phenolic oxygen, effectively lowers the activation barrier for O-atom transfer during oxidation. This modification was shown to enhance both the rate and selectivity of the catalytic process. For instance, a newly designed catalyst incorporating an additional pentafluorophenyl substituent at this position exhibited markedly improved reactivity, confirming the beneficial electronic effects predicted by DFT analysis.[152]

In parallel, reaction medium effects were also examined to further optimize catalytic performance. It was observed that polar solvents and hydrogen-bond donor additives could stabilize the key reaction intermediate, thereby facilitating more efficient oxygen transfer. Consequently, changing the solvent from 1,2-dichloroethane (DCE) to a more polar and protic aqueous acetic acid medium significantly enhanced the efficiency of C-H hydroxylation reactions. Under these conditions, the system operated via a similar catalytic cycle to that previously described: peracetic acid, generated *in situ* from the reaction between acetic acid and hydrogen peroxide, acted as the oxidant responsible for regenerating the active oxaziridine species, which then mediated selective C–H oxidation.[152]

However, while oxidation reactions catalyzed by benzoxathiazine were successful for a limited range of substrates, several drawbacks were noted. The acidity of the aqueous acetic acid medium, the limited solubility of many organic substrates under these conditions, and the prolonged reaction times (typically around 96 hours) collectively led to product racemization, particularly in substrates bearing stereogenic tertiary C–H bonds, as well as inconsistent reaction performance across different substrate classes (Scheme 3.7).

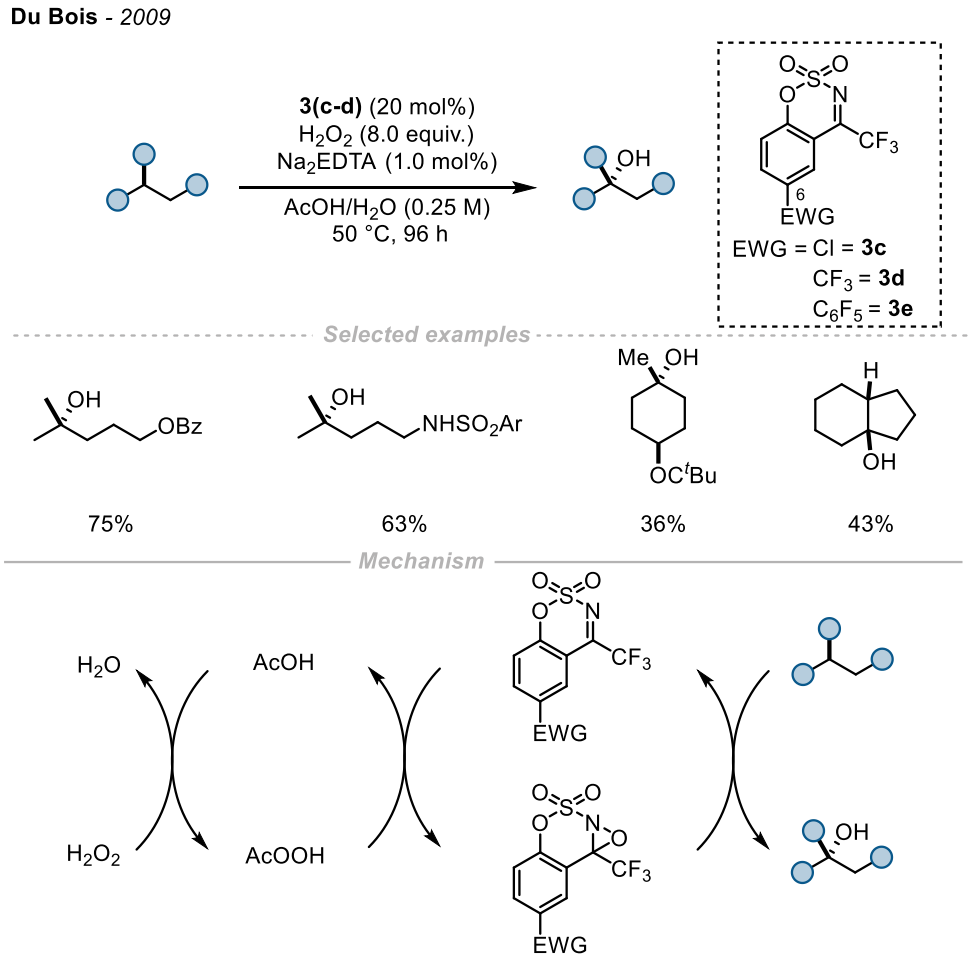

Scheme 3.7 Further improvements on oxaziridine catalysed C–H hydroxylation system in terms of oxidant and catalyst.

Subsequent studies by Du Bois and co-workers addressed these limitations by identifying that both water and tertiary alcohols (susbrates) promote oxaziridine decomposition, thereby reducing catalytic efficiency. To solve this, they introduced fluoroalcohol solvent mixtures, which shielded the oxaziridine intermediate from polar reactants such as water and oxidants (Oxone®). This modification enabled efficient C-H hydroxylation using a non-metal-based catalyst (benzoxathiazines) with Oxone® as the terminal oxidant. The optimized system demonstrated enhanced substrate scope, shorter reaction times, and improved overall efficiency, underscoring the importance of solvent microenvironments in stabilizing reactive intermediates during organocatalytic oxidation (Scheme 3.8).[153]

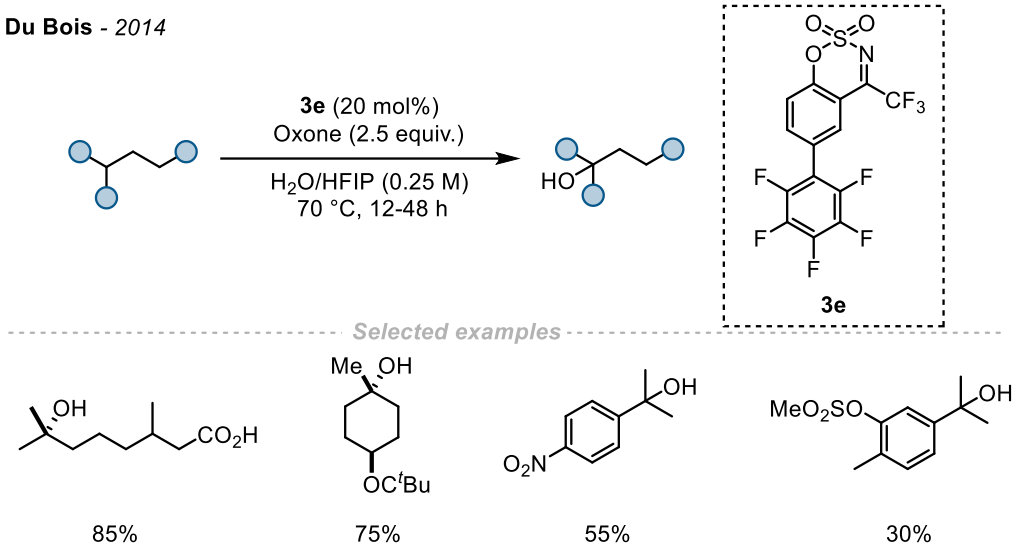

Scheme 3.8 Advancements in the oxaziridine-catalyzed C–H hydroxylation system.

3.5 Challenges in Catalyst Recovery and Reuse

Despite the remarkable oxidative potential of oxaziridines, particularly their efficiency in facilitating C–H oxidation reactions such as olefin epoxidation and C–H hydroxylation with notable site selectivity toward tertiary (3°) C–H bonds, their recovery and reuse remain a significant challenge. In most reported systems, both the oxaziridines and the corresponding imine byproducts formed upon oxidation are recovered with great effort if at all. Consequently, these compounds are generally discarded after a single use, thereby restricting their broader practical applicability and hindering their adoption in sustainable catalytic processes.

As originally noted by Davis in early applications of this catalyst class, the imine by-product formed upon oxygen atom transfer is prone to hydrolysis during purification, yielding a mixture of the corresponding nonpolar aldehyde and polar sulfonamide.[154,155] This decomposition complicates product isolation and prevents reliable re-isolation or regeneration of the imine derivative (precatalyst responsible for forming active species oxaziridines). Consequently, developing strategies that enable efficient recovery and reuse has been a major research focus aimed at improving both the atom economy and environmental footprint of these oxidation systems.

One of the earliest notable efforts in this direction was reported by Yulin Lam and co-workers, who synthesized a soluble polymer-bound 2-phenylsulfonyloxaziridine **3f**, a tethered analogue of the classical Davis reagent by radical copolymerization with styrene and 4-vinylbenzaldehyde (Scheme 3.9).[156] This polymer-supported oxaziridine was applied successfully to the oxidation of sulfides, selenides, amines, phosphines, and

enolates, delivering high product yields with straightforward workup. The immobilization of the oxaziridine moiety onto a polymeric backbone simplified catalyst recovery through precipitation or filtration, representing an important step toward recyclable oxidants.

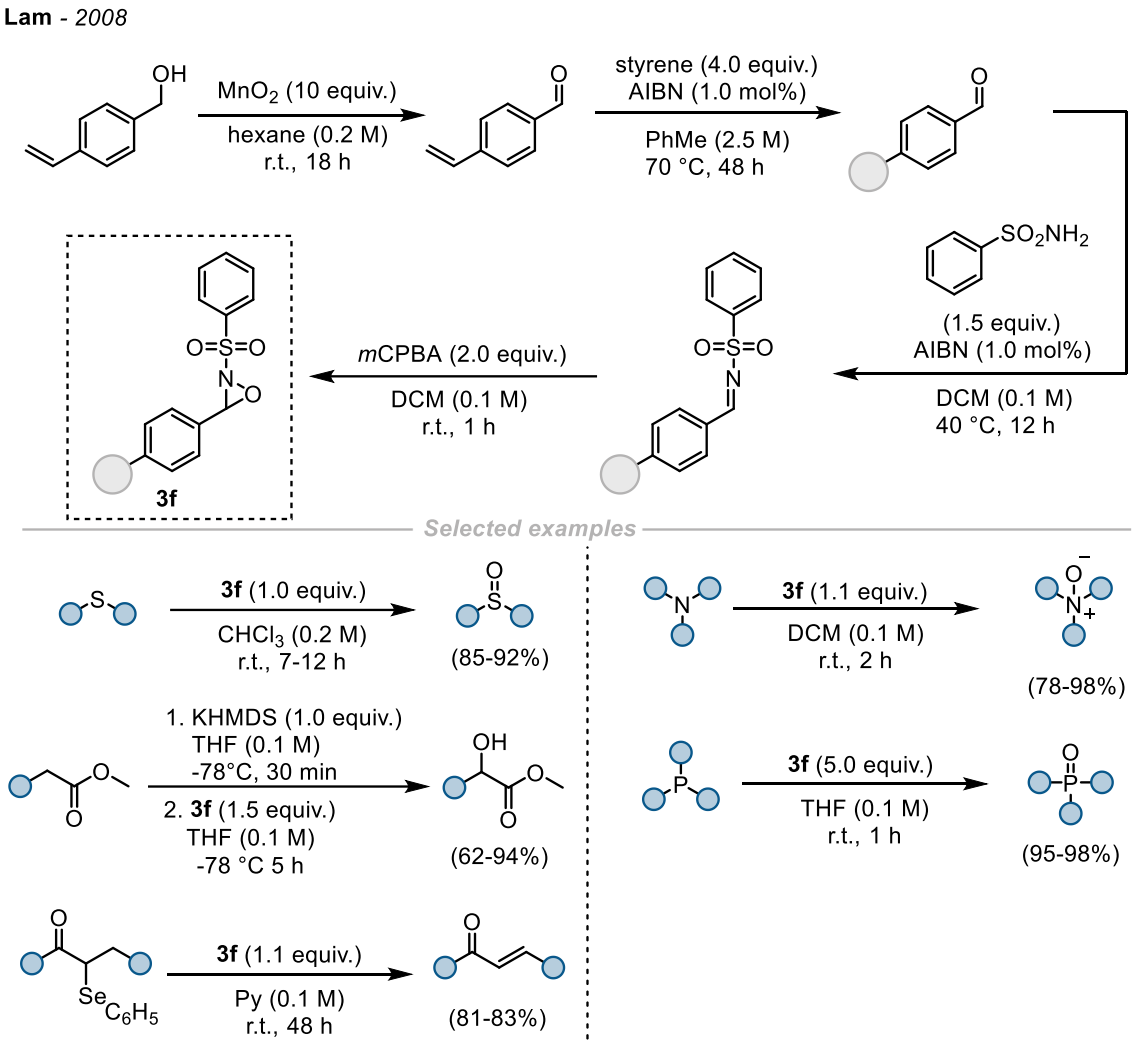

Scheme 3.9 Soluble polymer-supported 2-phenylsulfonyloxaziridine for oxidative transformations.

However, despite these advantages, the thermal stability and operational longevity of the polymer-bound **3f** reagent were limited. The catalyst progressively lost activity after approximately four to five oxidation cycles, likely due to degradation of the polymer matrix.[157] Furthermore, the 2-phenylsulfonyloxaziridine framework (Davis oxaziridine framework),[122] although well-studied and synthetically accessible, is intrinsically less reactive than the benzoxathiazine-derived oxaziridines developed later by Du Bois and co-workers,[151] which exhibit superior reactivity and can be employed catalytically with higher turnover in both C–H hydroxylation and olefin epoxidation reactions. As a result, while this polymer-supported approach demonstrated the feasibility of oxaziridine

immobilization, its performance and robustness were insufficient for practical, sustainable oxidation and remained limited to batch reactions.

These limitations have sparked considerable interest in the development of solid-supported oxaziridine-based catalysts. However, for such an approach to be feasible, the oxaziridine framework must retain high intrinsic activity. In this context, the benzoxathiazine-derived catalysts developed by Du Bois and co-workers have demonstrated enhanced reactivity and superior catalytic efficiency compared to earlier oxaziridine systems, rendering them particularly attractive candidates for immobilization. Covalent attachment of these catalysts to inert solid supports offers a means of preserving the well-defined molecular active site and its associated selectivity while addressing challenges associated with catalyst recovery and reuse. Thus, the catalyst retains its molecular identity while gaining the practical advantages of a solid-supported system. As discussed in Chapter 1, heterogeneous catalysis provides distinct advantages for sustainable oxidation chemistry, including facile catalyst separation, improved operational stability, and compatibility with continuous-flow processings. The immobilization of benzoxathiazine-derived oxaziridines onto a solid-supported, heterogeneous format therefore aligns directly with the central aims of this thesis, which is development of sustainable oxidative transformations using immobilized organocatalysts.

In later sections, the discussion outlines the rationale for designing an immobilizable oxaziridine catalyst, describes the proposed synthetic strategy, summarizes preliminary batch reactivity studies, and examines the challenges, limitations, and outlook for translating this system into a heterogeneously catalyzed, flow-compatible format.

3.6 Catalyst Design Rationale

Building on the insights from previous studies of oxaziridine-mediated oxidations discussed in earlier sections, particularly the electron-deficient benzoxathiazine frameworks developed by Du Bois and co-workers, the design of an immobilizable oxaziridine-based organocatalyst in this work was guided by two principal objectives: (i) to preserve the high catalytic activity characteristic of benzoxathiazine-derived oxaziridines, and (ii) to enable covalent attachment to solid supports for enhanced recyclability and operational stability.

As established in the literature, benzoxathiazine-derived oxaziridines exhibit superior reactivity and selectivity in catalytic C–H oxidative transformations, including both hydroxylation and epoxidation. Their capacity to perform selective oxidations under mild

conditions, employing environmentally benign oxidants such as *in situ* prepared peracetic acid or Oxone®, renders them particularly attractive for the development of sustainable oxidation systems.

Despite these advantages, their homogeneous nature presents inherent challenges, notably difficult catalyst recovery, limited recyclability, and the consequent inefficiency for large-scale or continuous-flow applications. To overcome these limitations, the present work aimed to translate the reactivity of benzoxathiazine-derived oxaziridines into a heterogeneously supported catalyst, combining the molecular precision of homogeneous catalysts with the practical benefits of heterogeneous systems, including facile separation, reusability, and potential compatibility with continuous-flow oxidation processes.

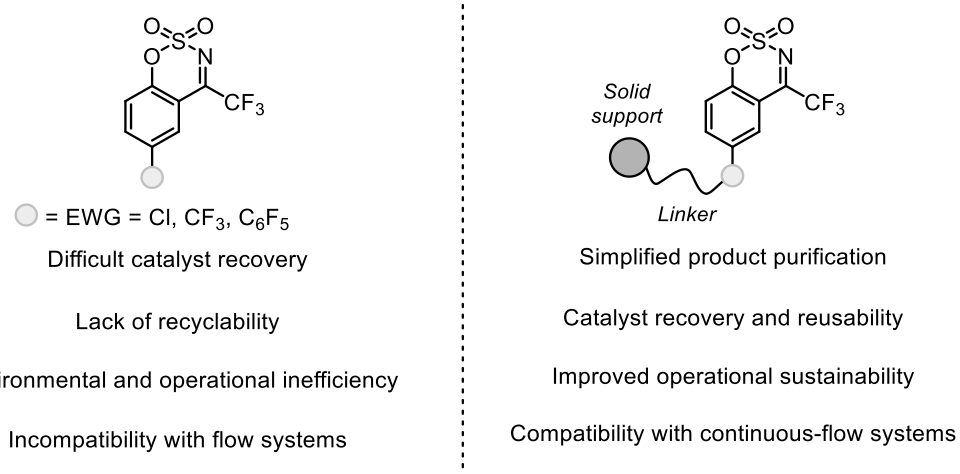

Scheme 3.10 Design strategy for an immobilizable benzoxathiazine-derived oxaziridine catalyst, illustrating limitations of homogeneous systems and the benefits of covalent attachment to a solid support for reuse and flow compatibility.

The design strategy centered on introducing a functional handle to the benzoxathiazine scaffold in a manner that maintains the structural integrity and electronic characteristics essential for oxygen-transfer reactivity. Previous mechanistic and computational studies have shown that the C6 position of the benzoxathiazine core exerts a critical influence on catalytic performance through electron-withdrawing effects, as supported by density functional theory (DFT) calculations. In particular, substitution at this site with strongly electron-withdrawing groups enhances the electrophilicity of the oxaziridine oxygen, thereby increasing its oxidative capability.[151,152]

Guided by this understanding, a new catalyst bearing a pentafluorophenyl substituent at C6 was developed, which demonstrated superior reactivity and compatibility with Oxone® as a terminal oxidant.[153] Specifically, a carboxyl substituent at C6 was selected

3.1 (Scheme 3.9), as it would (i) retain the electron-withdrawing character necessary for maintaining high catalytic activity, and (ii) provide a reactive site for amide bond formation with functionalized solid supports such as aminopropylated silica. Such covalent linkage would ensure robust immobilization, prevent catalyst leaching under oxidative conditions, and facilitate recycling.[23,158,159]

Alternatively, selective functionalization of one of the fluorine atoms in the pentafluorophenyl ring to introduce a suitable immobilization handle was also considered as a complementary approach **3.2** (Scheme 3.11), providing flexibility in optimizing the tethering site. The experimental studies directed toward the development of this strategy were conducted by Mohit Chotia.

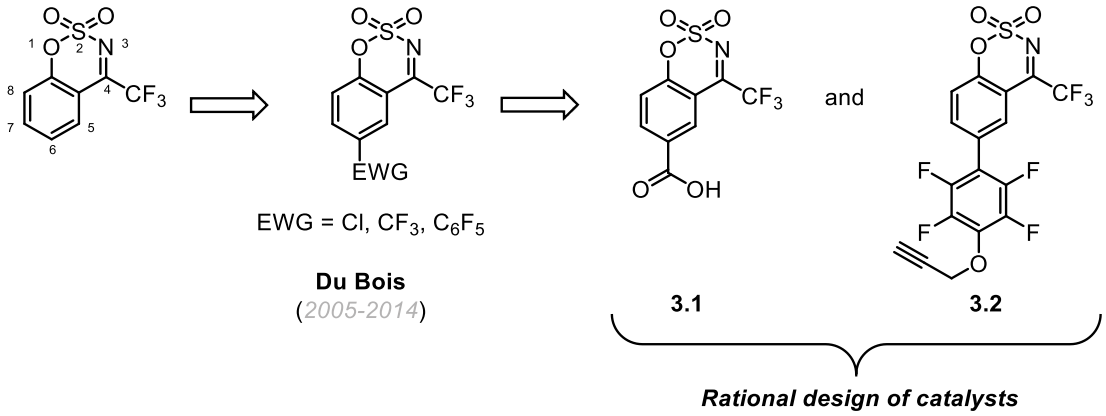

Scheme 3.11 Conceptual design of a solid-supported oxaziridine catalyst.

Overall, this design strategy laid the foundation for developing a heterogenized benzoxathiazine-derived oxaziridine catalyst that preserves the high oxidative performance of the parent system while achieving solid-phase immobilization for sustainable catalytic operation. In the following sections, the synthetic implementation, characterization, and initial reactivity studies of this catalyst **3.1** will be detailed and discussed.

3.7 Synthetic Strategy for the Immobilizable Oxaziridine Catalyst

3.7.1 Retrosynthetic Analysis

The retrosynthetic analysis guiding the synthesis of the target oxaziridine catalyst, 4-(trifluoromethyl)benzo[1,2,3]oxathiazine-6-carboxylate 2,2-dioxide **3.1**, was based on earlier reports describing the preparation of benzoxathiazine scaffolds (Scheme 3.12).[151,160] The target compound **3.1** was anticipated to result from the saponification of benzoxathiazine **3.3**. Benzoxathiazine **3.3** was envisioned to arise sulfamoylation of phenolic trifluoromethyl ketones **3.4**, which in turn could be derived from phenolic

aldehydes **3.5** through sequential trifluoromethylation and oxidation steps. The methyl-protected phenolic aldehyde **3.5** precursor was anticipated to originate from a formylation reaction on commercially available 4-hydroxybenzoic acid **3.6**.

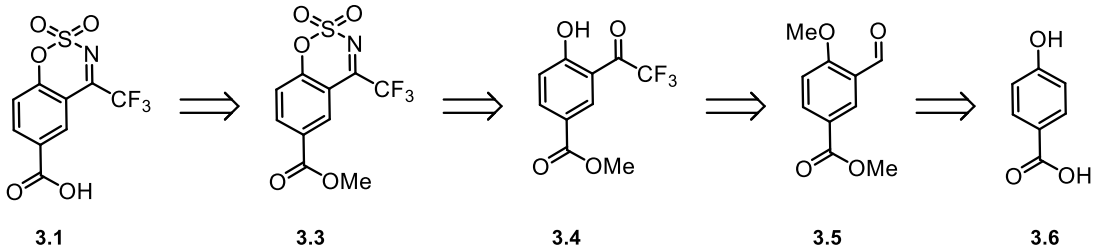

Scheme 3.12 Retrosynthetic analysis of the immobilizable oxaziridine catalyst **3.1**.

Accordingly, the key intermediate methyl 3-formyl-4-methoxybenzoate **3.5** served as the primary synthetic pivot for accessing the oxaziridine catalyst. Two independent formylation methods were evaluated to synthesize this intermediate: Method A, Silver triflate-promoted formylation[161] and Method B, HMTA aromatic formylation (Duff reaction).[162,163] Method A produced a mixture of regioisomers and afforded a low overall yield of 19%. In contrast, Method B proved superior, delivering the desired aldehyde **3.5** in 48% yield with high regioselectivity (Scheme 3.13). Thus, the Duff formylation route was adopted for subsequent transformations.

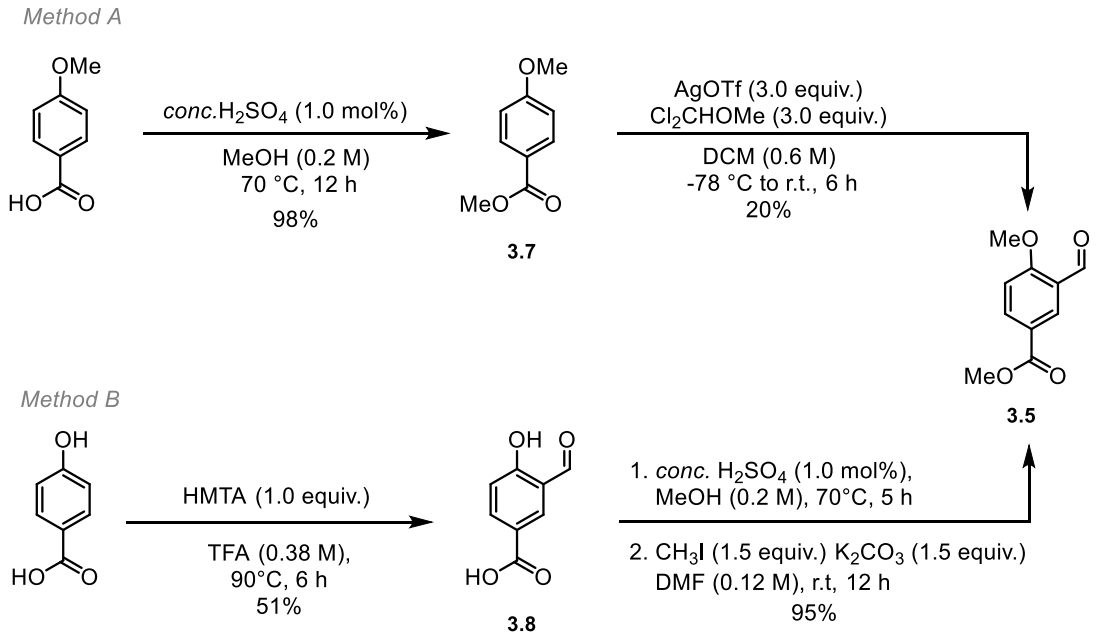

Scheme 3.13 Synthesis of starting material towards benzoxathiazines.

3.7.2 Catalyst Synthesis Route 1

With methyl 3-formyl-4-methoxybenzoate **3.5** in hand, the next step involved installation of the trifluoromethyl group using Ruppert–Prakash reagent ($TMSCF_3$) in the presence of a catalytic amount of tetrabutylammonium fluoride (TBAF) to generate the nucleophilic CF_3 species.[164,165] This transformation yielded methyl 4-methoxy-3-(2,2,2-trifluoro-1-hydroxyethyl)benzoate **3.9** in 84% yield. Subsequent oxidation of the α-trifluoromethyl alcohol with bis(acetoxy)iodobenzene (PIDA) and catalytic TEMPO[166] furnished the corresponding α-trifluoromethyl ketone **3.10** in 89% yield. The demethylation step using boron tribromide exposed both phenolic and carboxylic functionalities, affording intermediate **3.11** in 54% yield. Selective methylation of the carboxyl group under Fischer esterification conditions produced methyl 4-hydroxy-3-(2,2,2-trifluoroacetyl)benzoate **3.12** in 92% yield. Finally, sulfamoylation of the phenolic ketone **3.12** delivered the desired methyl 4-(trifluoromethyl)benzo[1,2,3]oxathiazine-6-carboxylate 2,2-dioxide **3.13** in 32% yield, corresponding to an overall yield of 11.6% across the entire sequence (Scheme 3.14).

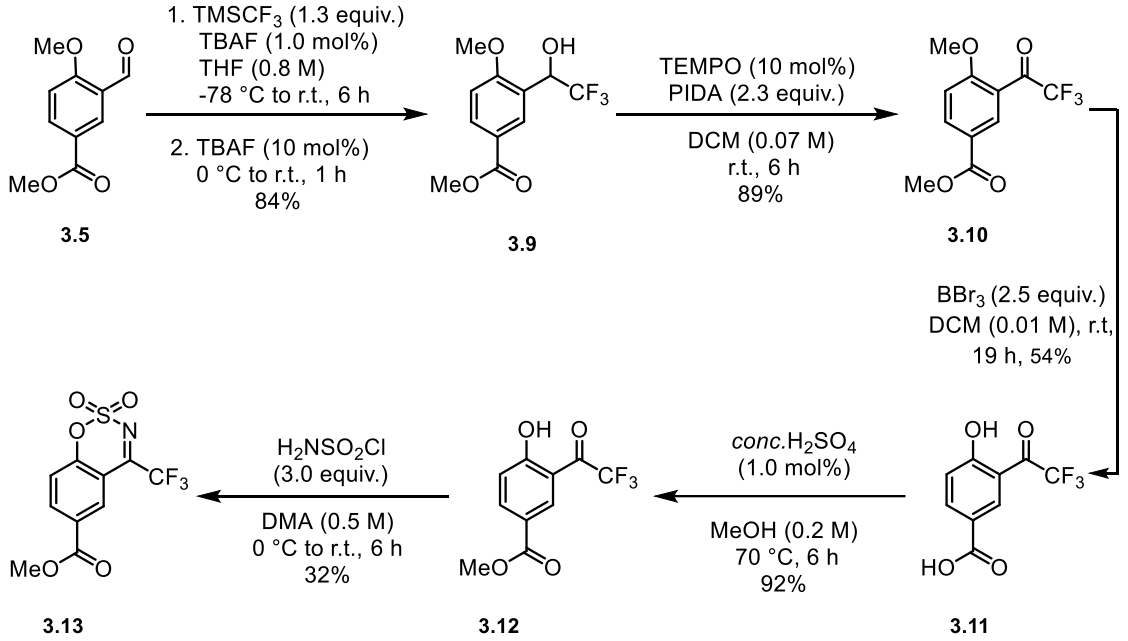

Scheme 3.14 Synthesis of benzoxathiazine (**3.13**) via Route 1.

3.7.3 Catalyst Synthesis Route 2

A complementary synthetic route was also explored, inspired by the work of Ashley Adams et al., which employed a different synthetic sequence (Scheme 3.15).[153] In this approach, sulfamoylation of the hydroxyl aldehyde was first carried out to yield a benzoxathiazine intermediate **3.16** and **3.17**. The trifluoromethyl group was then installed by treating this benzoxathiazine derivative with $TMSCF_3$ to afford methyl 4-

(trifluoromethyl)-3,4-dihydrobenzo[1,2,3]oxathiazine-6-carboxylate 2,2-dioxide **3.18** and 6-chloro-4-(trifluoromethyl)-3,4-dihydrobenzo[e][1,2,3]oxathiazine 2,2-dioxide **3.19**. The structure of **3.18** was confirmed by single-crystal X-ray diffraction, providing clear structural validation of the benzoxathiazine framework. Subsequent oxidation afforded the fully oxidized target catalyst **3.13** and **3.20**, though with a modest overall yield of 9-10%.

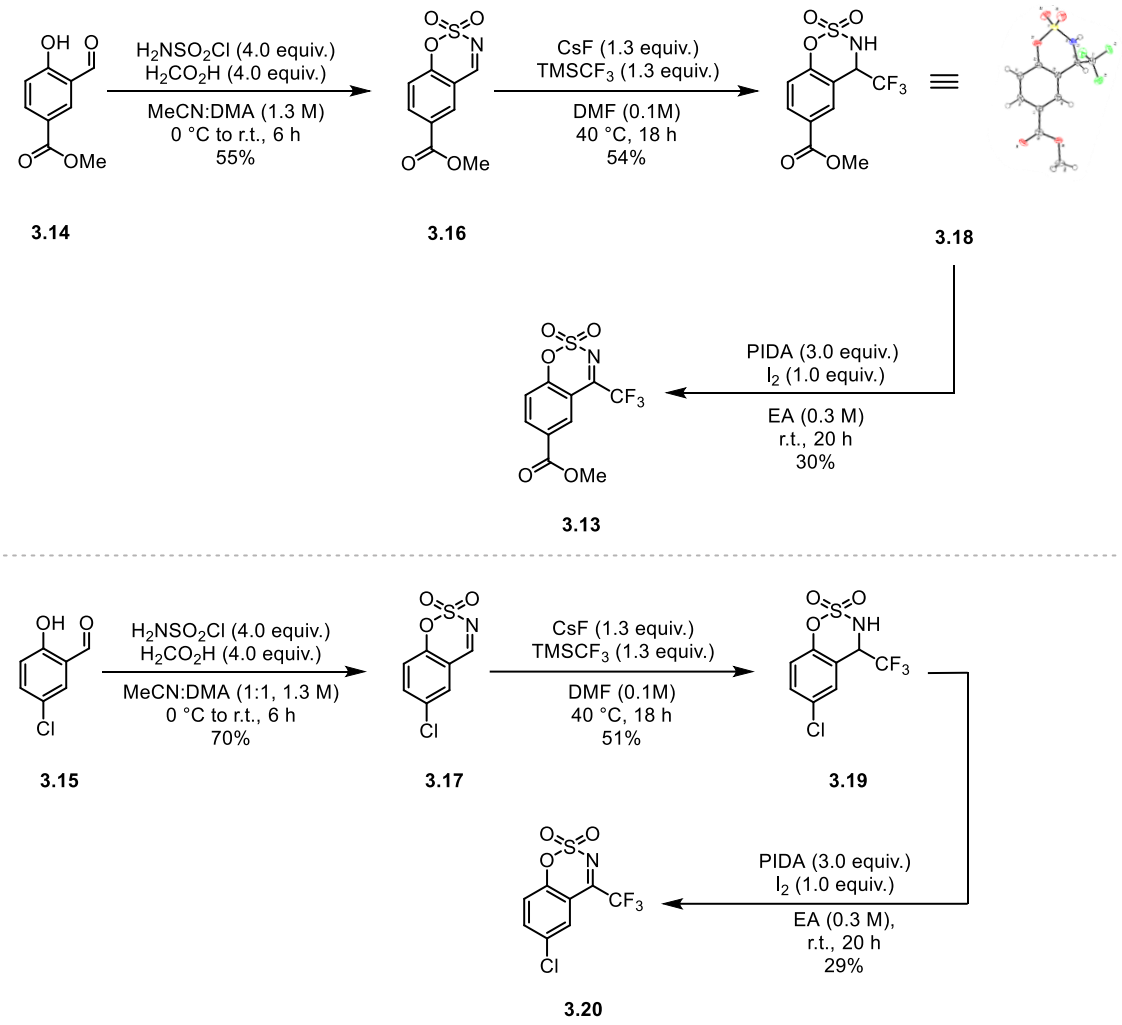

Scheme 3.15 Alternative synthetic route to the target oxaziridine precatalyst via early sulfamoylation and late-stage trifluoromethylation (Route 2).

A comparison of the two synthetic routes reveals clear differences in efficiency. Route 1, although longer and involving multiple functional group deprotection and protection reaction, provided consistently high-yielding intermediates and delivered the target benzoxathiazine catalyst **3.13** in an overall yield of 12%, making it the more reliable and scalable pathway. Route 2, which relied on early sulfamoylation followed by late-stage CF_3 installation, was synthetically more concise but suffered from reduced tolerance of the benzoxathiazine framework to trifluoromethylation conditions, resulting in a lower

overall yield of 9%. Together, these results indicate that Route 1 is the more robust approach for accessing the desired catalyst, while Route 2 remains informative but operationally limited. This comparative assessment establishes the synthetic rationale that underpins the catalyst development presented in the subsequent sections.

3.8 Preliminary Evaluation of Catalytic Activity in C-H Hydroxylation

With the protected derivative of the target catalyst **3.13** in hand, its oxidative reactivity was evaluated to assess its suitability for catalytic oxidation. As an initial validation, the capacity of benzoxathiazine **3.13** to form the corresponding oxaziridine was examined. Oxidation of **3.13** with *meta*-Chloroperoxybenzoic acid (*m*CPBA) proceeded cleanly, affording oxaziridine **3.14** in 77% yield. This result confirms that the modified benzoxathiazine framework remains competent to generate the active oxaziridine species under oxidative conditions.

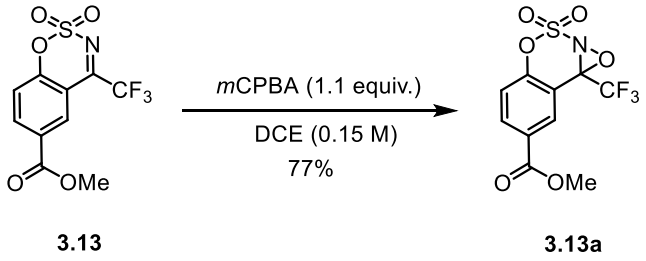

Scheme 3.16 Validation of oxaziridine formation.

The catalytic competence of compound **3.13** was first examined using olefin epoxidation as a model reaction. In line with previously reported protocols,[152] a mixture of acetic acid and hydrogen peroxide was employed with the expectation that *in situ* generated peracetic acid would oxidize benzoxathiazine **3.13a** to the active oxaziridine, which would subsequently transfer oxygen to the olefin substrate. Under these conditions, however, no epoxide was observed. Instead, a vicinal diol **3.16** was obtained (Scheme 3.17). These products could arise either from hydrolysis of an initially formed epoxide or from direct *anti*-dihydroxylation mediated by the acetic acid-hydrogen peroxide system.[167]

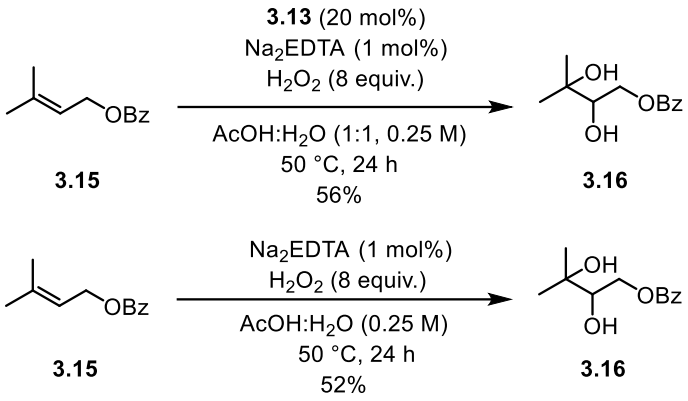

Scheme 3.17 Divergence from expected epoxidation pathway.

To distinguish between these possibilities, a control experiment was conducted in the absence of the catalyst. The same product was observed, indicating that the transformation proceeded independently of the oxaziridine catalyst. This observation led to the identification of a mild, metal-free protocol for *anti*-dihydroxylation of olefins, which is discussed in detail in Chapter 4.

Attention was subsequently redirected toward the targeted C-H hydroxylation of tertiary carbon centers. Compound **3.17** was selected as a model substrate, and an initial background reaction was performed in the absence of catalyst, resulting in no detectable oxidation and recovery of approximately 95% of the starting material. When the reaction was repeated in the presence of the catalyst under otherwise identical conditions, no hydroxylated product was observed. Increasing the reaction temperature and extending the reaction time similarly failed to induce conversion. Given that the active oxidant in this system is generated *in situ* via peracid formation, reactions were also performed using a preformed peracid as the terminal oxidant; however, no C-H oxidation was observed. Variation of the solvent likewise did not result in product formation (Table 3.1).

A change in oxidant and solvent system proved to be critical. When Oxone® was employed as the terminal oxidant along with a solvent system of HFIP and water, formation of the desired hydroxylated product was observed for the first time, albeit in modest yield 25%. Prolonging the reaction time led to an improved yield to 36%. For comparison, the originally reported benzoxathiazine precatalyst **3.20** was evaluated under identical conditions, delivering the hydroxylated product in a higher yield of 55%. This comparison highlights both the feasibility of C-H hydroxylation using the newly designed catalyst framework and the need for further optimization to bridge the reactivity gap relative to established benzoxathiazine catalyst.

Table 3.1 Optimization of reaction conditions for catalytic oxaziridine-mediated C–H hydroxylation.

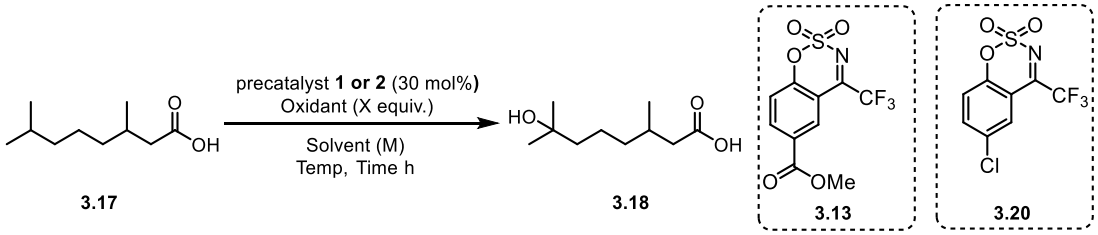

Entry	Precatalyst (20 mol%)	Oxidant (X equiv.)	Solvent (0.3 M)	Temp (°C)	Time (h)	Yields (%)
1	--	H_2O_2 (8 equiv.)	AcOH:H_2O (1:1)	50	68	--[a]
2	1	H_2O_2 (8 equiv.)	AcOH:H_2O (1:1)	50	48	--[b]
3	1	H_2O_2 (8 equiv.)	AcOH:H_2O (1:1)	70	96	--
4	1	CH_3CO_3H (2 equiv.)	AcOH:H_2O (1:1)	70	48	--
5	1	CH_3CO_3H (8 equiv.)	MeCN	50	24	--
6	--	Oxone® (2.5 equiv.)	HFIP: H_2O (1:9)	70	19	--[b]
7	1	Oxone® (2.5 equiv.)	HFIP: H_2O (1:9)	70	19	25
8	1	Oxone® (2.5 equiv.)	HFIP: H_2O (1:9)	70	48	36
9	2	Oxone® (2.5 equiv.)	HFIP: H_2O (1:9)	70	24	55

Reactions were carried out at 0.1 mmol scale. The yields of the reactions were determined by ^{1}H NMR analysis using trichloroethylene as internal standard. [a] 95% of starting material was recovered [b] 89% of starting material was observed.

Overall, these preliminary studies demonstrate that the designed benzoxathiazine-derived oxaziridine catalyst is capable of participating in oxidative C-H hydroxylation under catalytic conditions, but its activity is strongly dependent on the nature of the terminal oxidant and reaction medium. While *in situ* generation of peracid-based system failed to generate productive tertiary carbon oxidation, the use of Oxone® enabled formation of the desired hydroxylated product in moderate yield, confirming that the catalyst framework remains competent for oxygen-transfer chemistry after functionalization. The lower efficiency observed relative to the originally reported homogeneous precatalyst suggests that introduction of the carboxyl functionality and the modified electronic environment influences oxaziridine formation or catalyst turnover. These results establish proof of concept for catalytic activity, while simultaneously highlighting limitations that must be addressed to improve reactivity and robustness.

3.9 Summary and outlook

In summary, this project described the design, synthesis, and preliminary evaluation of a benzoxathiazine-derived oxaziridine catalyst bearing a functional handle for immobilization. An electron-deficient catalyst framework was selected to preserve the high reactivity and selectivity characteristic of Du Bois-type oxaziridines while enabling covalent attachment to solid supports. Two synthetic routes were explored, providing access to the target catalyst and highlighting practical considerations in scaffold construction and late-stage functionalization.

Initial reactivity studies confirmed that the catalyst could be converted to the corresponding oxaziridine and promote oxidative transformations under catalytic conditions. While *in situ* production of peracid-based systems were ineffective, Oxone® enabled productive hydroxylation of unactivated tertiary carbon–hydrogen bonds, albeit with reduced efficiency compared to homogeneous benchmark systems. These results underscore both the potential and current limitations of the catalyst design, particularly regarding oxidant compatibility and catalytic turnover.

Looking forward, further optimization of the catalyst structure and reaction conditions will be required to enhance activity and reproducibility. Incorporation of the catalyst into a solid-supported format represents a critical next step toward efficient recovery, recyclability, and continuous-flow implementation. Addressing these challenges is essential for translating oxaziridine-mediated C–H hydroxylation into a sustainable and practically viable heterogeneous oxidation methodology.

Chapter 4

Metal- and Catalyst-Free *anti*-Dihydroxylation of Olefins in Batch and Flow

4.1 Introduction

The development of sustainable oxidative methodologies remains a central objective within modern synthetic chemistry, driven by the principles of waste minimization, and safer reaction design. While the preceding chapters of this thesis have explored heterogeneous organocatalyst platforms, including immobilized hypervalent iodine(V) reagent Chapter 2 and focus towards immobilized oxaziridine-based oxidants Chapter 3, the broader context of sustainable oxidation also include catalyst-free transformations that exploit benign reagents and thermodynamically favourable equilibria.[168–171] Within this landscape, the direct *anti*-dihydroxylation of alkenes represents a transformation of both fundamental and applied significance. Vicinal 1,2-diols constitute indispensable building blocks in natural product synthesis, pharmaceutical intermediates, carbohydrate chemistry, and polymer science.[172–175] Although the *syn*-dihydroxylation of olefins has been extensively optimized, most notably through osmium-mediated protocols and their catalytic variants,[176–178] the development of operationally simple, scalable, and environmentally benign *anti*-dihydroxylation methodologies has historically lagged behind.[167,179]

Classically, access to *anti*-1,2-diols relies on an initial epoxidation step followed by hydrolytic ring opening. Numerous strategies have been introduced to promote this epoxidation, ranging from transition-metal catalysis using Mn[180,181], Ru[182,183], and Mo-based systems[184,185] to metal-free processes involving organocatalysts,[186–192] photocatalysts,[193,194] electrocatalysts,[195–199] and biocatalysts.[200–202] Despite these advances, many protocols continue to depend on hazardous oxidants, toxic solvents, or precious metals, thereby limiting their suitability for large-scale or industrial use. Moreover, *in situ* generation or isolation of epoxides often introduces additional synthetic operations that negatively impact reaction yields.[203]

A representative illustration of this classical epoxidation and hydrolysis pathway, exemplified by a metal-catalysed system reported by Wang and co-workers in 2018 (Scheme 4.1).[184] In this method, the active oxidizing species is proposed to arise from oxidation of $MoO_2(acac)_2$ by hydrogen peroxide, leading to the formation of an oxoperoxidomolybdenum(VI) intermediate. This high-valent molybdenum species promotes epoxidation of the alkene substrate to generate the corresponding oxirane intermediate. Subsequently, the epoxide is activated through coordination to $MoO_2(acac)_2$, which acts as a Lewis acid, thereby facilitating regioselective nucleophilic ring opening by water to afford the *anti*-1,2-diol. The catalytic cycle is completed by regeneration of the $MoO_2(acac)_2$ species. While this approach effectively demonstrates

access to *anti*-1,2-diols via a two-step sequence, it relies on transition-metal catalysis, underscoring the motivation to develop alternative, more sustainable *anti*-dihydroxylation strategies.[184,204,205]

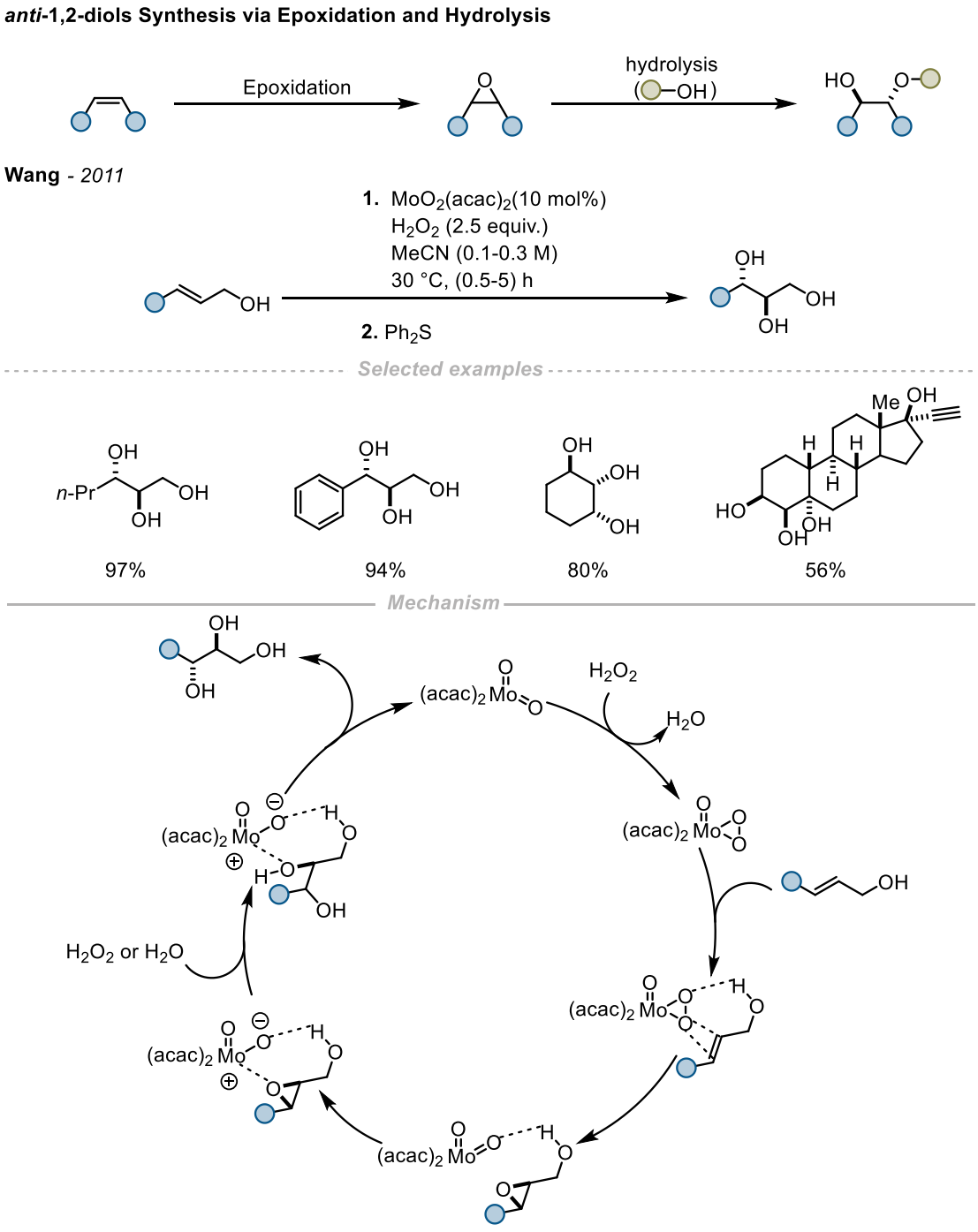

Scheme 4.1 Classical two-step synthesis of *anti*-1,2-diols via epoxidation followed by hydrolytic ring opening.

Alternative approaches circumvent this epoxide pathway entirely by employing dioxygenation agents capable of delivering two oxygen atoms in a single, stereocontrolled process. Hypervalent iodine reagents and peroxide-derived

intermediates, including cyclic diacyl peroxides, have been evaluated within this context.[206,207] Despite their synthetic potential, many of these oxidants exhibit disadvantages such as high cost, thermal sensitivity, demanding handling requirements, or limited substrate scope. A representative example of this mechanistic class is outlined in Scheme 4.2, which illustrates the generally accepted pathway for the Prevost diacetoxylation. In this mechanism, an alkene engages iodine(III) to form an iodonium ion intermediate (I), which undergoes nucleophilic ring-opening by acetate to afford an acetoxonium species (II). Subsequent backside attack by a second acetate nucleophile under strictly anhydrous conditions generates the anti-diacetoxylated product (III) with high stereospecificity.[208]

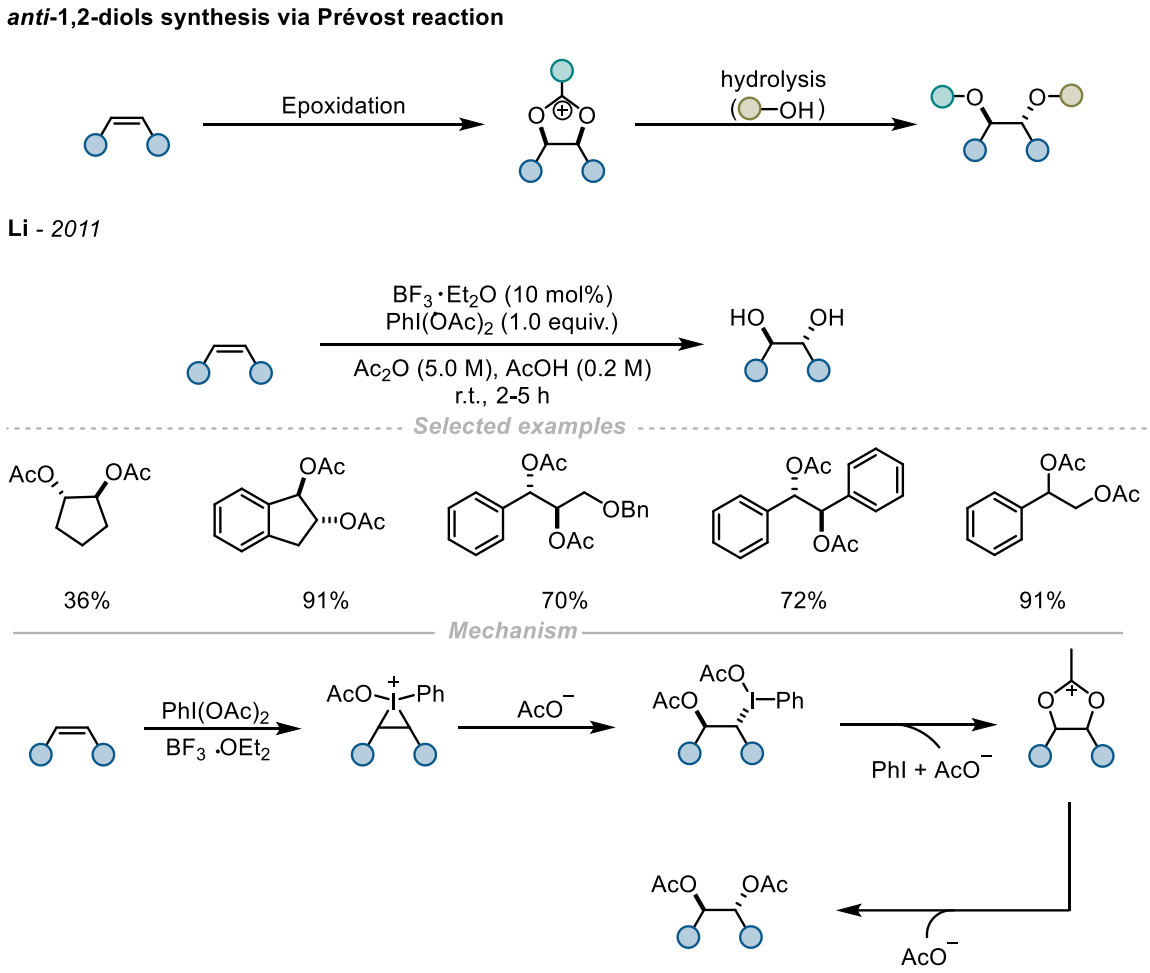

Scheme 4.2 Mechanistic pathway of the Prevost reaction.

In addition to ionic diacetoxylation pathways exemplified by the Prevost mechanism, further diversification of *anti*-dioxygenation strategies has emerged from radical-mediated systems that engage alkenes through O-centred oxidants.[209] Among these, N-hydroxyphthalimide (NHPI)–derived radicals constitute a mechanistically distinct class

capable of initiating dioxygenation without the intermediacy of iodonium or acetoxonium ions. Under appropriate oxidative conditions, NHPI is known to undergo homolytic O–H cleavage to generate the phthalimide-N-oxyl (PINO) radical, an electrophilic O-centred species competent in adding to alkene bond to furnish a carbon-centred radical intermediate. Subsequent interception of this transient radical by a persistent radical trap such as TEMPO results in formal dioxygenation. As illustrated in Scheme 4.3, this pathway enables a stepwise oxidation sequence driven by radical propagation rather than nucleophilic displacement. Importantly, these systems frequently display substrate-dependent diastereoselectivity, performing most efficiently with rigid or conformationally restricted alkenes. Indeed, for substrates such as norbornene and α-methylstyrene, radical addition followed by TEMPO capture afforded dioxygenated products in diastereomerically pure form, underscoring the potential of O-centred radical addition for stereodefined vicinal difunctionalization.[210] Nevertheless, despite these promising outcomes, the broader application of this method remains limited by sensitivity to substrate geometry and competing radical pathways, reinforcing the ongoing need for *anti*-dihydroxylation protocols that combine stereocontrol, operational safety, and environmental compatibility.

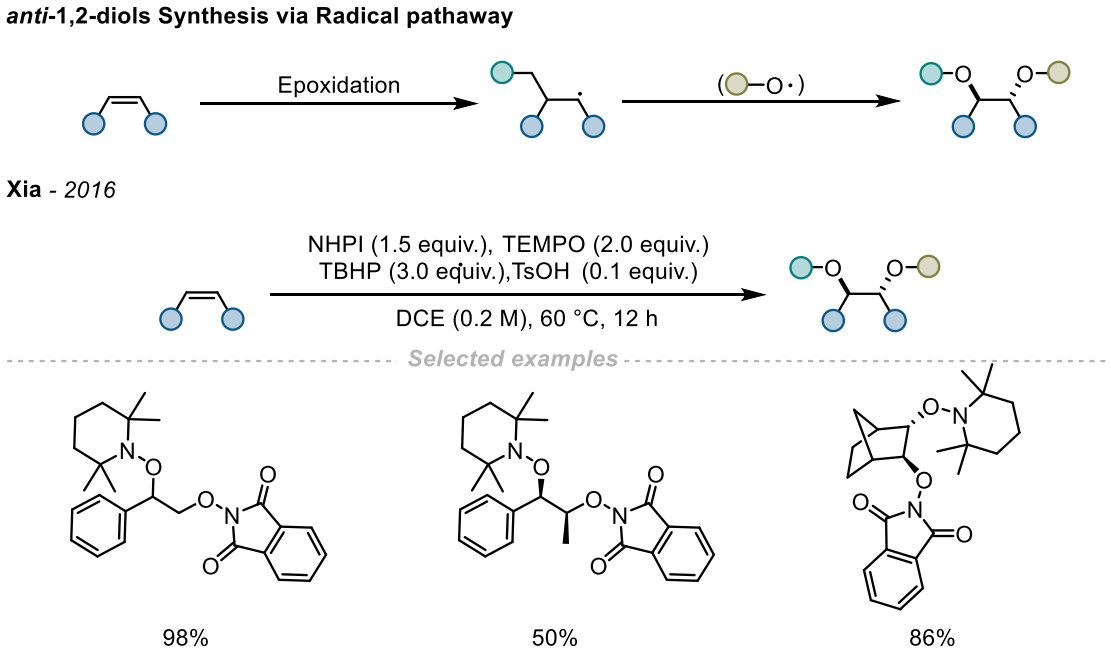

Scheme 4.3 Radical-mediated dioxygenation via NHPI-derived *O*-centred radicals.

Historically, one of the earliest reported catalyst-free *anti*-dihydroxylation methods was described by Hilditch in 1926, who demonstrated that combining hydrogen peroxide with acetic acid generates peracetic acid *in situ*, enabling transformation of oleic and elaidic

acid derivatives to the corresponding *anti*-diols. Although the chemistry was conceptually elegant, employing two inexpensive, readily available, and inherently benign reagents, the reported reaction suffered from extremely slow kinetics at ambient temperature, requiring up to nine days for full conversion. Subsequent studies attributed these limitations to the low equilibrium constant for peracid formation under mild conditions, necessitating large excesses of hydrogen peroxide to drive the process forward (Scheme 4.4).[211,212]

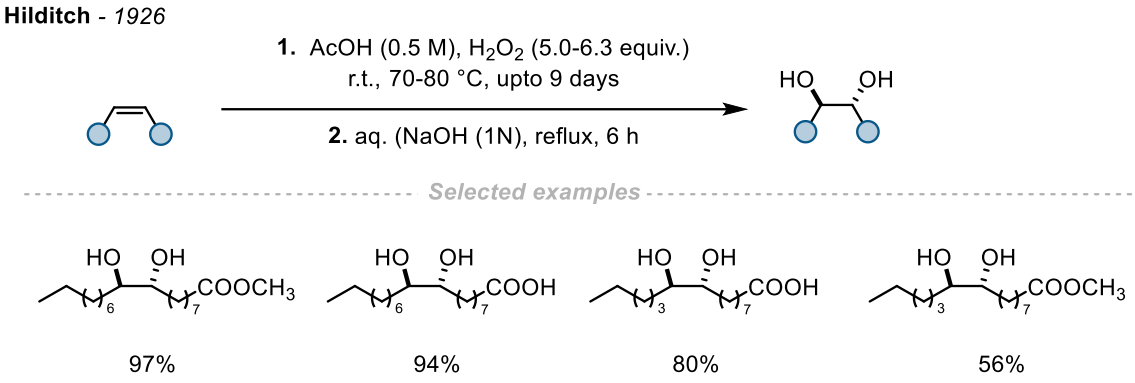

Scheme 4.4 Early demonstration of peracetic acid-mediated *anti*-dihydroxylation.

Later refinements, including the use of catalytic sulfuric acid or the substitution of acetic acid with formic acid, succeeded in shifting the equilibrium toward more efficient peracid formation, which subsequently reacted with a variety of olefins to furnish the corresponding 1,2-diols in moderate yields (Scheme 4.5). However, despite improved oxidant efficiency, these modifications introduced substantial safety concerns arising from the highly exothermic nature of peracid generation in strongly acidic media.[179,213]

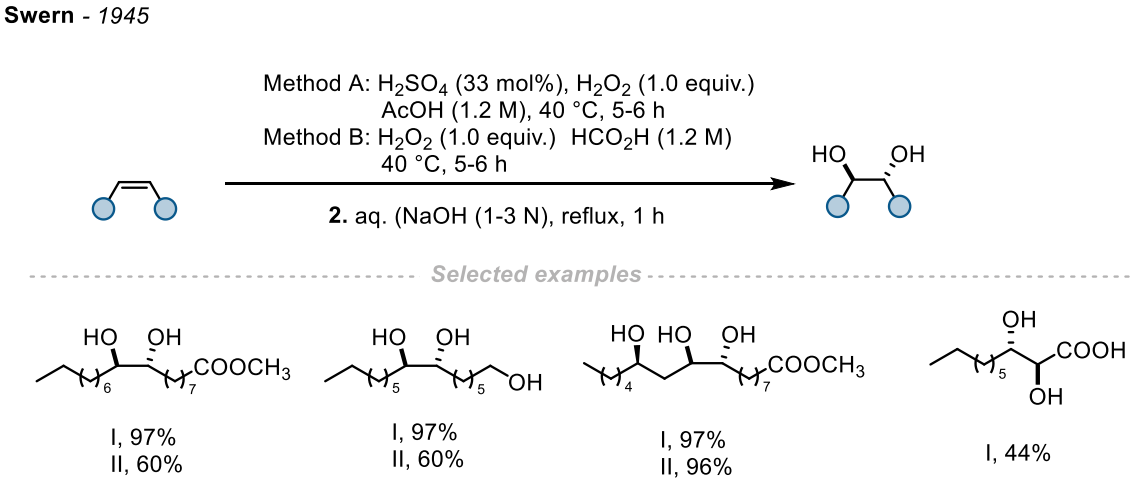

Scheme 4.5 Representative examples of improved peracid-mediated *anti*-dihydroxylation of olefins using catalytic Brønsted acids.

To address these safety limitations, several alternative strategies were developed to enable catalytic, *in situ* formation of the reactive peracid species under milder conditions. One such approach involves the use of sulfonic acids to promote peracid formation catalytically. The first notable report of this type was disclosed by Sato in 2003, who demonstrated that diverse olefins could be converted into the corresponding dihydroxylated products in good to excellent yields using NAFION (a resin-supported sulfonic acid) in combination with hydrogen peroxide (Scheme 4.6). The mechanistic pathway proposed for this transformation proceeds via initial epoxidation of the olefin by hydrogen peroxide, followed by acid-catalyzed hydration of the epoxide to deliver the 1,2-diol, consistent with the classical epoxidation–hydrolysis route previously discussed. Despite its operational simplicity, this protocol is limited by the high cost of NAFION and its requirement for temperatures above ambient conditions to achieve practical reaction rates.[214]

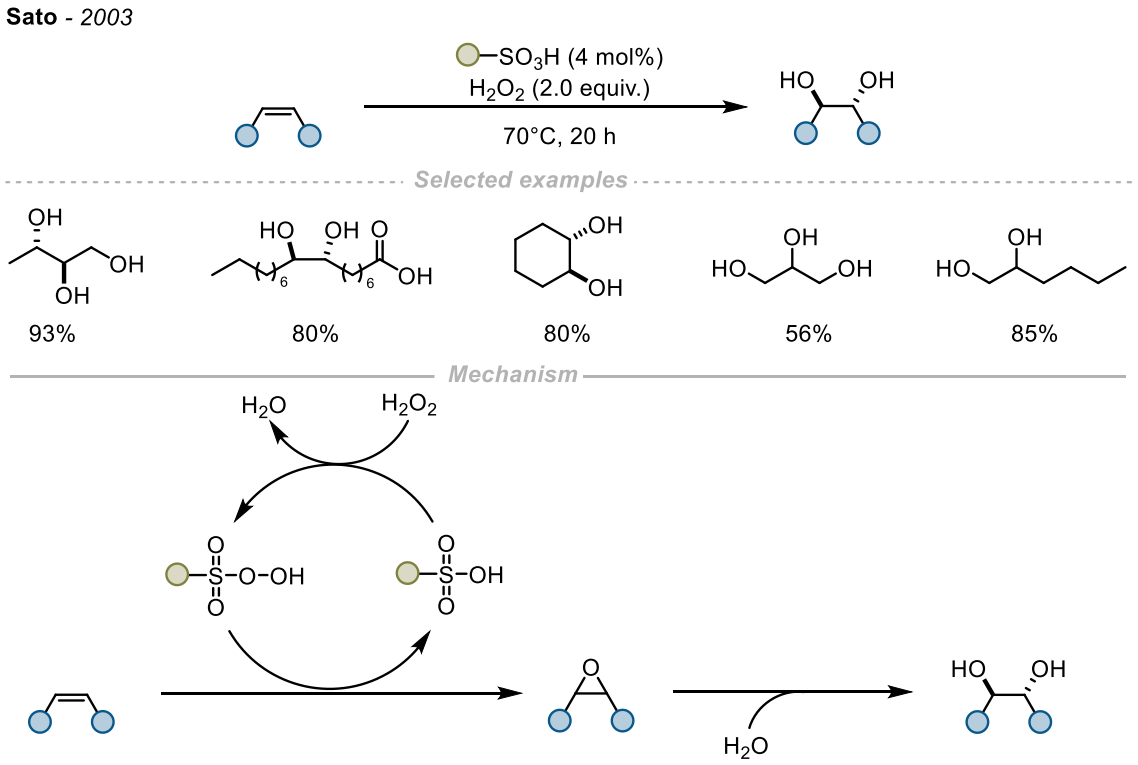

Scheme 4.6 NAFION-catalyzed epoxidation-hydrolysis sequence enabling *anti*-dihydroxylation of olefins.

Nearly a decade later, a conceptually related method employing a more economical sulfonic acid was reported by Afonso in 2011, who developed a catalytic system based on *p*-toluenesulfonic acid (*p*-TsOH) and hydrogen peroxide to achieve *anti*-dihydroxylation across a broad substrate range (Scheme 4.7). The transformation tolerated several functional groups as additives, including Boc, Cbz, benzyl, tosyl, and

ketal. As in Sato's protocol, the reaction mechanism was proposed to involve epoxidation via a peroxysulfonic acid intermediate followed by acid-promoted epoxide ring opening to yield the *anti*-1,2-diol.[215]

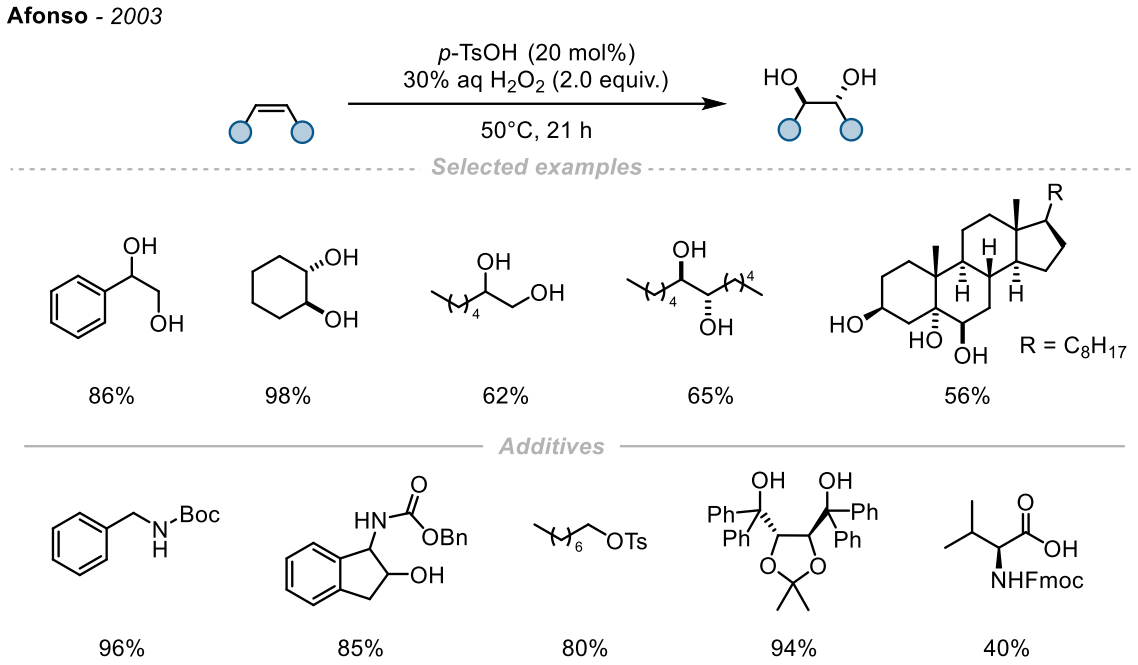

Scheme 4.7 *p*-TsOH-catalyzed hydrogen-peroxide-driven *anti*-dihydroxylation of olefins.

A different strategy to mitigate the hazards associated with peracid generation was introduced by Kraft in 2007, who explored the use of continuous-flow technology to enhance both safety and scalability. In this study, the synthesis of cyclohexane-1,2-diol was compared under conventional batch conditions versus continuous-flow operation. The flow-based process afforded substantial synthetic advantages, including faster reaction rates, enhanced thermal control, and improved product purity, while enabling safer scale-up (Scheme 4.8). [216] These observations are consistent with the general advantages of continuous-flow reactions discussed in Chapter 1, particularly with respect to reaction time, superior thermal management, and enhanced product quality, thereby providing supporting evidence for the suitability of flow chemistry as a safer and more efficient platform for scaling oxidative transformations.

Kraft - *2007*

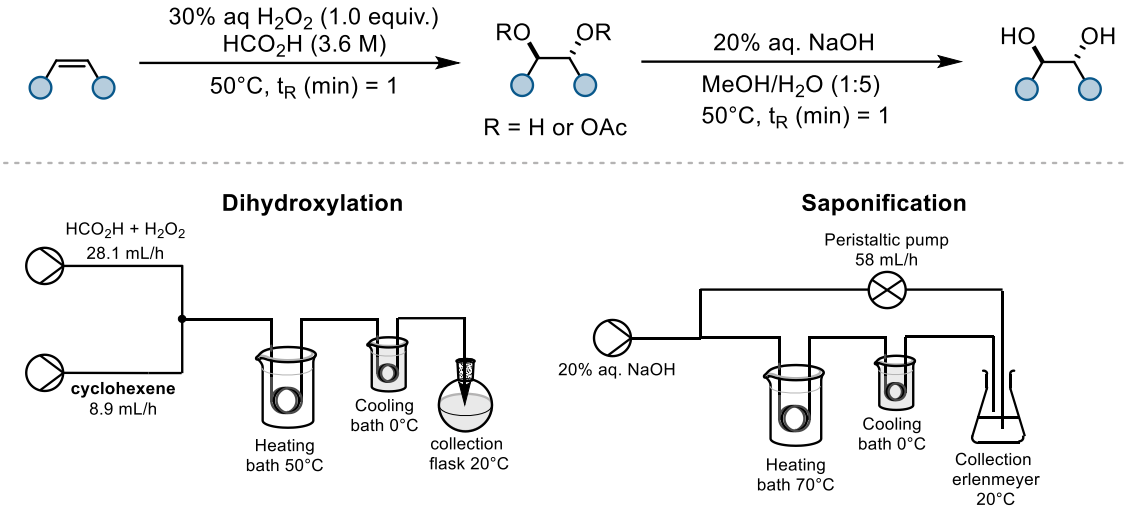

Scheme 4.8 Continuous-flow peracid-mediated *anti*-dihydroxylation enabling improved safety, reaction rate, and product quality.

Despite the long-standing recognition of peracid-mediated *anti*-dihydroxylation as a conceptually simple and atom-economical transformation, its practical implementation has remained surprisingly underdeveloped. Early reports clearly show that *in situ* generated peracids can react with olefins to give *anti*-dioxygenated products using inexpensive and readily available reagents; however, these methods were hindered by slow kinetics, poor efficiency under mild conditions, and significant safety concerns when strong acids were employed to accelerate peracid formation. Subsequent refinements introduced metal catalysts, corrosive acids, and pre-formed oxidants which collectively undermined the inherent simplicity and sustainability of the original approach. Consequently, no general, safe, and scalable protocol has emerged that fully exploits the potential of peracetic acid-based *anti*-dihydroxylation while adhering to modern principles of green chemistry.

In particular, the generation and handling of peracetic acid at scale remains a critical challenge, as its high reactivity and oxidising power pose significant safety hazards. As outlined in Chapter 1, continuous-flow has emerged as an effective strategy for mitigating hazards associated with highly energetic or transient oxidising species through enhanced heat and mass transfer, precise residence time control, and minimized reagent inventories. While continuous-flow approaches have been explored for various oxidative transformations, their application to catalyst-free peracid-mediated dihydroxylation chemistry remains limited. This highlights an opportunity to revisit this classical transformation using a contemporary perspective, integrating systematic reaction optimization, comprehensive substrate scope evaluation, and process intensification

strategies. Thus, this chapter seeks to re-examine peracetic acid–mediated anti-dihydroxylation of alkenes under catalyst-free conditions, with the aim of developing a practical, sustainable, and scalable oxidative methodology.

4.2 Aims and Objectives

The aim of this project is to develop a sustainable and operationally straightforward strategy for the *anti*-dihydroxylation of olefins that complements the immobilized organocatalytic systems discussed in the preceding chapters. Whereas Chapters 2 and 3 focus on immobilization of organocatalysts and their implementation under continuous-flow conditions, the present study demonstrates that carefully designed catalyst-free oxidative transformations can likewise satisfy key criteria of sustainability, safety, and scalability. Specifically, this work revisits and optimizes the peracetic acid-mediated *anti*-dihydroxylation of alkenes using hydrogen peroxide and acetic acid as inexpensive and environmentally benign reagents. The methodology is evaluated in terms of substrate scope, functional group tolerance, and synthetic generality across a range of unactivated and substituted olefins. Furthermore, the scalability of the process is assessed through multi gram-scale batch reactions, followed by translation of the optimized conditions into a continuous-flow platform to enhance operational safety during *in situ* peracid generation. This chapter places catalyst-free *anti*-dihydroxylation within sustainable oxidative chemistry and supports the dissertation's main goal of developing sustainable methods for oxidative transformations.

4.3 Results and Discussion

4.3.1 Reaction optimization

This research project was conducted collaboratively with Mohit Chotia and Jan Lukas Mayer-Figge. Reactions conducted or compounds synthesized by co-workers are indicated in the schemes.

The reaction optimization studies were carried out using cyclohexene as the model substrate due to its simple structural features and extensively reported behaviour in oxidative functionalization. All reactions were performed in deuterated acetic acid, enabling direct monitoring of substrate consumption and product yield by ^{1}H NMR spectroscopy. Initial experiment employed 8.0 equivalents of H_2O_2 at 50 °C, resulting in full conversion after 3 h and formation of *anti*-cyclohexane-1,2-diol **4.1** and the corresponding monoacetylated species **4.2** in 40% and 25% NMR yield, respectively (Table 4.1, Entry 1). This result confirmed that *in situ* generated peracetic acid is sufficiently reactive to promote dioxygenation under catalyst-free conditions.

Next, the oxidant amount was reduced to evaluate its effect on reactivity. Using 2.0 equivalents of H_2O_2 led to an incomplete conversion after 6 h; however, extending the reaction time to 16 h afforded full consumption of cyclohexene and a shift in product yield towards the monoacetylated species (Table 4.1, Entry 3). Further reducing peroxide loading to 1.5–1.25 equivalents resulted in significantly slower reactivity or incomplete conversion even after extended reaction times (Table 4.1, Entries 4–6). These observations indicate that efficient *in situ* peracid formation requires at least two equivalents of hydrogen peroxide under these conditions.

Table 4.1. Optimization studies for the peracetic acid–mediated *anti*-dihydroxylation of cyclohexene.

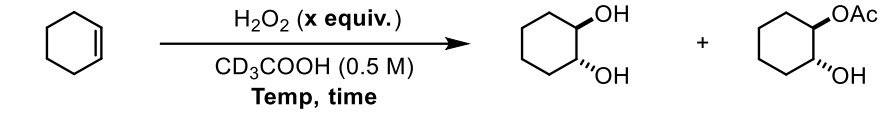

cyclohexene **4.1** **4.2**

Entry	H_2O_2 (equiv.)	Temp. (ºC)	Time (h)	Conversion (%)	Yield 4.1(%)	Yield 4.2(%)
1	8	50	3	100	40	25
2	2	70	2	78	13	44
3	2	50	16	100	15	60
4	2	50	6	100	20	56
5	2	24	24	100	30	54
6	2	50	6	62	12	29
7	2	50	16	100	25	66
8	1.5	50	24	100	23	67
9	1.5	50	16	80	15	49
10	1.25	50	24	75	17	60
11	0	50	24	0	0	0

Reactions were carried out at 0.1 mmol scale. The reaction conversion and yields determined by ^{1}H NMR analysis, using trichloroethylene as an internal standard. Reaction optimization studies were performed in collaboration with Mohit Chotia.

As a result, the condtions of 2.0 equivalents of H_2O_2 at 50 °C for 16 h were selected as the standard reaction conditions for subsequent scope studies. Reaction mixtures containing both the free diol and the monoacetylated intermediate could be processed cleanly by alkaline saponification (5 M NaOH), providing access to pure *trans*-cyclohexane-1,2-diol in high yields. This operationally simple work-up proved broadly applicable and was employed throughout later stages of the study.

4.3.2 Scope and limitation

With the optimized conditions in hand, the substrate scope was explored. In cases where incomplete conversion was observed under the standard conditions (2.0 equiv. H_2O_2, 50 °C,16 h), increasing the oxidant amount to 8.0 equivalents consistently enhanced reaction efficiency, often enabling full conversion within 4 h and leading to higher isolated yields of the corresponding *anti*-1,2-diols.

Unactivated alkenes performed well under these conditions. Cyclic olefins underwent clean *anti*-dihydroxylation to furnish the corresponding vicinal diols **4.4**-**4.8** in moderate to good yields ranging from 36-84%. Notably, the method tolerated nucleophilic and potentially acid-sensitive groups; for example, a substrate bearing a *tosyl*-protected amine provided the targeted diol **4.8** in 36% yield, demonstrating the compatibility of the protocol with sulfonamide motifs.

Non-cyclic internal olefins exhibited lower reactivity when using 2.0 equivalents of oxidant, often leading to diminished diol yields. However, applying 8.0 equivalents of hydrogen peroxide restored high performance across this class of substrates, affording the desired products in yields of up to 86%. The method also proved effective for more structurally complex substrates for example oleic acid, a key compound sourced from renewable feedstocks underwent smooth dihydroxylation to furnish the corresponding *anti*-diol **4.12** in 78% yield, thereby showcasing the applicability of the system to long-chain unsaturated fatty acids.

Terminal olefins likewise displayed excellent reactivity and chemoselectivity. Across the examined substrates, the relevant *anti*-1,2-diols **4.13**-**4.17** were isolated in yields ranging from 74-85%, irrespective of whether 2.0 or 8.0 equivalents of hydrogen peroxide were employed. These findings collectively demonstrate that the optimized peracetic acid–mediated protocol delivers a broadly applicable, operationally straightforward, and functionally tolerant platform for the sustainable *anti*-dihydroxylation of olefins.

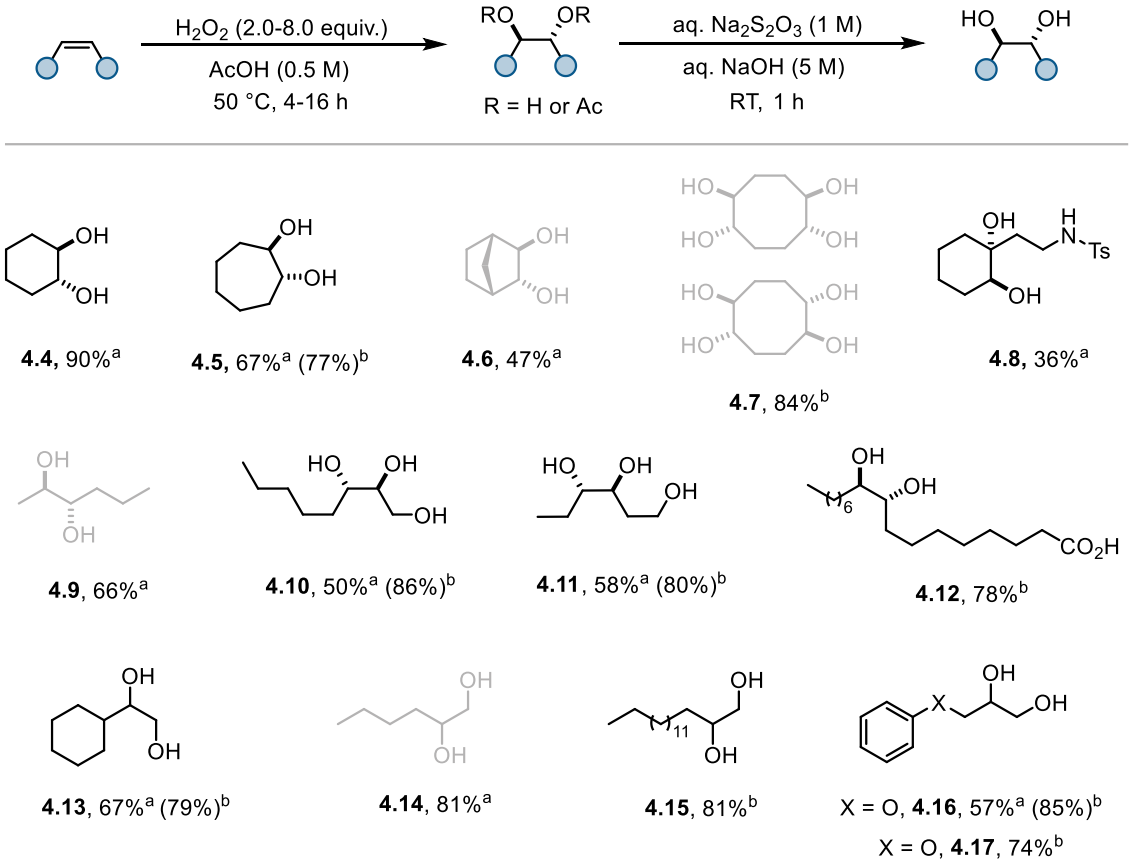

Scheme 4.9 Scope of the unactivated alkenes. [a] alkene (0.5 mmol), H_2O_2 (2.0 equiv.), HOAc (0.5 M), 50 °C, 16 h; 2. aqueous $Na_2S_2O_3$ (1.0 M), aqueous NaOH (5.0 M), RT, 1 h. [b] H_2O_2 (8.0 equiv.), 4 h. Compounds highlighted in grey were synthesized by Mohit Chotia.

The applicability of the optimized conditions was subsequently tested using a representative series of styrene-derived substrates **4.18-4.27**. Under the established reaction conditions, unsubstituted styrene underwent smooth conversion to the corresponding vicinal diol **4.18**, delivering a 68% isolated yield. In contrast, the introduction of electron-withdrawing substituents on the aromatic ring, exemplified by the para-trifluoromethyl group, resulted in attenuated reactivity. Even upon increasing the oxidant amount to 8.0 equivalents of H_2O_2, the formation of diol **4.19** proceeded with a reduced yield of 40%, indicating the sensitivity of the system to electronic effects.

Substrates bearing electron-donating or withdrawing groups at the *ortho* or *meta* positions were tolerated, affording the respective 1,2-diols **4.21** and **4.23** in moderate yields (42–45%). These results suggest that steric perturbation along the aryl framework exerts a less detrimental influence compared to strongly deactivating electronic substituents.

The influence of α-substitution on the styrene backbone was also examined. Both α-phenylstyrene and α-methylstyrene displayed satisfactory reactivity, producing diols **4.26** and **4.26** in 65% and 71% yield, respectively, thereby demonstrating the compatibility of the method with increased steric bulk proximal to the alkene. Finally, dihydroxylation of the more conformationally constrained substrate 1-phenyl-1-cyclohexene proceeded efficiently to furnish the *anti*-configured 1,2-diol **4.27** in 83% yield, further highlighting the robustness of the protocol across diverse structural motifs.

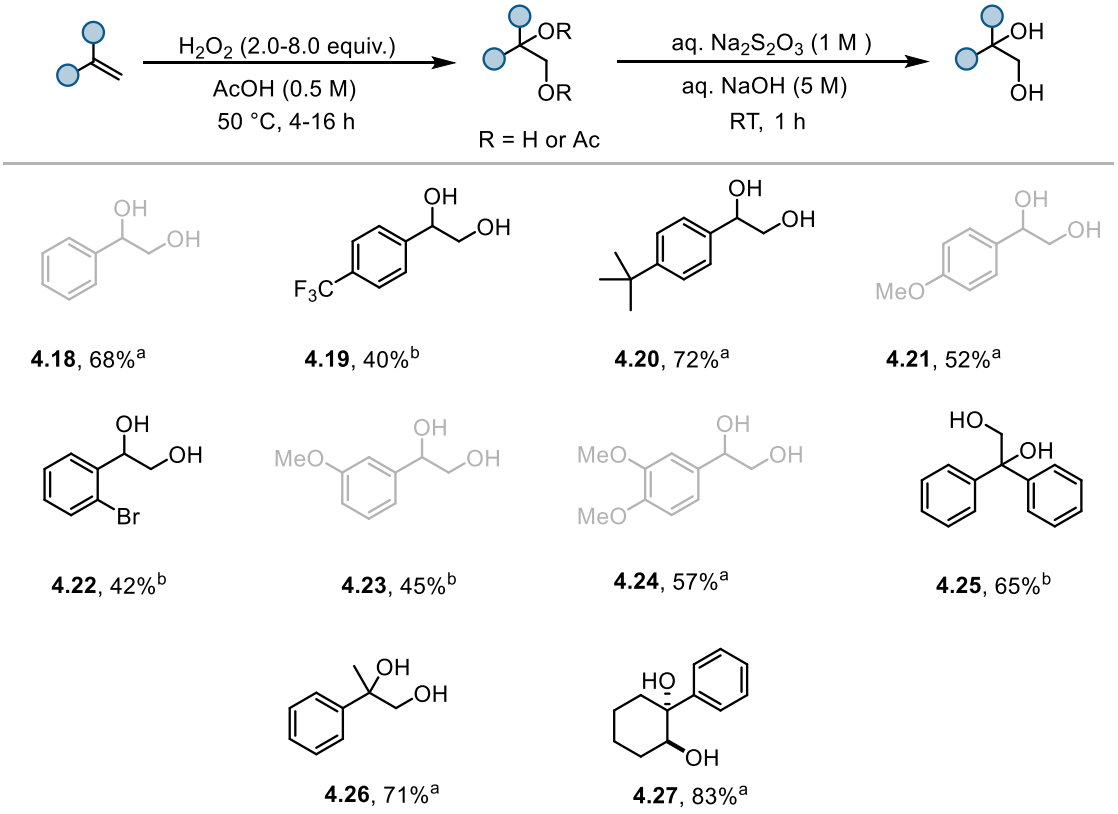

Scheme 4.10 Scope of the styrene derivatives. [a] 1. alkene (0.5 mmol), H_2O_2 (2.0 equiv.), AcOH (0.5 M), 50 °C, 16 h; 2. aqueous $Na_2S_2O_3$ (1.0 M), aqueous NaOH (5.0 M), RT, 1 h. [b] H_2O_2 (8.0 equiv.), 4 h. Compounds highlighted in grey were synthesized by Mohit Chotia and Jan Lukas Mayer-Figge.

4.3.3 Functional group tolerance

To evaluate the functional group compatibility of the developed dihydroxylation protocol, an additive screening study was conducted (Scheme 4.11). Cyclohexene and an equimolar quantity of each additive **A1**-**A16** were subjected to the standard reaction conditions, employing 2.0 equivalents of H_2O_2 at 50 °C in acetic acid (0.5 M). Reaction outcomes were quantified by GC-FID analysis using methyl laurate as the internal standard. The results indicated that free alcohols **A1**, alkyl bromides **A2**, acrylates **A3**, ketones **A4**, nitriles **A5**, alkynes **A8**, phenols **A9**, benzofurans **A10**, benzoyl-protected

anilines **A11**, pyridines **A13**, and thiophenes **A14** were well tolerated, with 78–100% of the additive remaining and only minimal reduction in product yield (82–90% vs. 94% in the absence of additives). Although aldehydes **A6**, acetals **A7**, and Boc-protected pyrroles **A15** exhibited partial decomposition (0–58% remaining), the desired diol could still be obtained in good yields (73–89%). In contrast, unprotected amines **A12** and **A16** fully inhibited product formation. Overall, the additive study demonstrates that the method possesses broad functional group tolerance, maintaining high diol yields while preserving most additives under the reaction conditions.

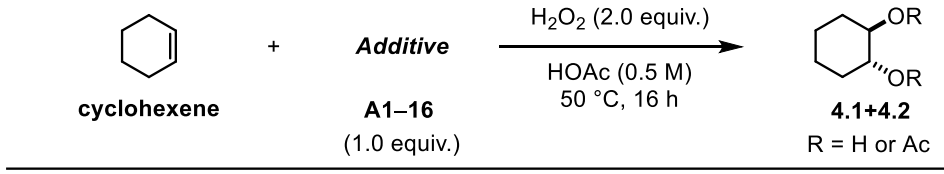

	A1	A2	A3	A4	A5
4.1+4.2	82%	90%	86%	84%	89%
Additive	84%	78%	100%	95%	90%

	A6	A7	A8	A9	A10
4.1+4.2	89%	81%	84%	87%	87%
Additive	39%	0%	100%	100%	92%

	A11	A12	A13	A14	A15	A16
4.1+4.2	81%	0%	83%	83%	73%	20%
Additive	98%	0%	87%	87%	58%	76%

Scheme 4.11 Additive-based evaluation of functional group compatibility under the optimized conditions. (Functional group tolerance studies were performed in collaboration with Mohit Chotia).

4.3.4 Scale up

To fully assess the broader applicability of this *anti*-dihydroxylation protocol as a sustainable oxidative platform, its performance under scalable conditions was next evaluated (Scheme 4.12). Initial scale-up was conducted using cyclohexene on a 10 mmol scale under the standard batch conditions. This experiment proceeded smoothly

and furnished the corresponding *anti*-diol **4.2** in 86% isolated yield (0.99 g), demonstrating that no operational modifications were required to maintain efficiency at this scale. Encouraged by this outcome, the reaction was subsequently performed on a 100 mmol scale, affording diol **4.2** in 78% yield (9.1 g). These findings collectively demonstrate that the method is essentially suitable for gram-scale synthesis.

Despite these promising batch-scale results, the further expansion of this chemistry to larger preparative scales requires careful consideration of safety. The key oxidant generated *in situ*, peracetic acid, is a highly reactive and corrosive species, and high-volume accumulation of this intermediate poses obvious operational harzard. Although the protocol avoids the external handling or storage of peracetic acid, scaling the batch process inevitably increases the instantaneous quantity of oxidant present, thereby elevating the associated hazard profile.

To mitigate the safety hazards associated with the generation of peracetic acid at scale, the feasibility of translating the *anti*-dihydroxylation into a continuous-flow process was investigated. A dedicated flow setup was constructed using a dual syringe pump, allowing independent delivery of two solutions: cyclohexene in acetic acid and hydrogen peroxide in acetic acid. These streams were introduced at controlled and pre-adjusted flow rates and combined via a three-way mixing junction. The resulting reaction mixture was then passed through a residence tubes submerged in a water bath before being collected in a receiving flask (Scheme 4.12).

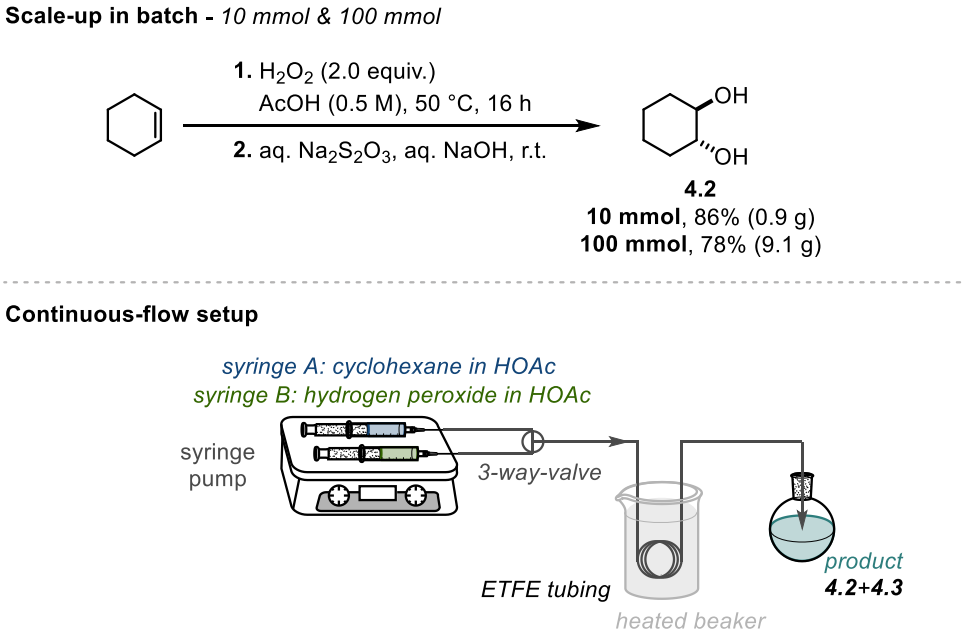

Scheme 4.12 Scale-up studies and schematic representation of the continuous-flow setup.

Initial flow experiments were conducted using 2.0 equivalents of hydrogen peroxide and a residence time of 39 min resulted in partial conversion of 41%, affording the *anti*-diol **4.1** and its monoacetylated derivative **4.2** in 5% yield each (Table 4.2, entry 1). Systematic variation of the reaction parameters revealed that increasing both the hydrogen peroxide amount and the reaction temperature led to a significant enhancement in conversion, reaching up to 99% (Table 4.2, entries 2-10). Under these conditions, the *anti*-diol **4.1** and monoacetate **4.2** were obtained in yields ranging from 12–85% and 16–24%, respectively. Optimal flow conditions were identified using 8.0 equivalents of hydrogen peroxide with a residence time of 39 min, under which the targeted *anti*-1,2-diol was isolated in 85% yield on a 5 mmol scale (Table 4.2, entry 10). Collectively, these results demonstrate the suitability of continuous-flow processing as a safer and more controlled platform for scaling peracetic acid-mediated *anti*-dihydroxylation reactions.

Table 4.2 Optimization studies in a continuous flow.

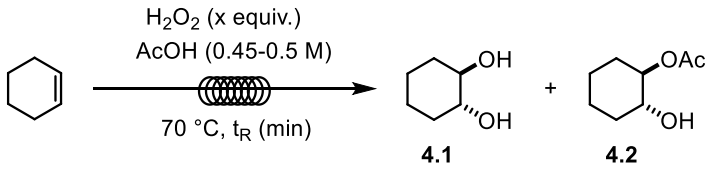

Entry	AcOH (M)	H_2O_2 (equiv.)	Temp. (°C)	Residence time t_R (min)	Conversion (%)	4.1 (%)	4.2 (%)
1	0.5	2	50	39	41	5	5
2	0.5	2	70	39	62	12	16
3	0.5	4	70	39	86	24	18
4	0.5	6	70	39	99	42 (65)	24
5	0.5	5	70	39	95	34	22
6	0.45	8	70	20	-	(67)	-
7	0.5	8	50	39	80	19	4
8	0.5	8	70	25	92	31	10
9	0.5	8	70	29	98	34	11
10	0.45	8	70	39	100	(85)	-

Yields mentioned in parentheses are the isolated yield followed by the saponification step. Reaction optimization studies in flow were performed in collaboration with Mohit Chotia.

4.4 Conclusion

In summary, this project has demonstrated that *anti*-dihydroxylation of alkenes can be achieved efficiently under metal- and catalyst-free conditions through the *in situ* generation of peracetic acid from hydrogen peroxide and acetic acid. Careful optimization of reaction parameters enabled the identification of mild and operationally simple conditions that afford *anti*-1,2-diols in moderate to excellent yields across a broad

substrate scope, consisting of cyclic, acyclic, terminal, internal, and styrene derivatives. Importantly, the method exhibits good functional group compatibility, as evidenced by additive-based screening, underscoring its potential applicability to complex molecular settings.

Beyond scope and efficiency, the scalability of the transformation was validated through successful batch reactions at up to 100 mmol scale without modification of the standard conditions. Recognising the intrinsic safety considerations related with peracids, the methodology was further adapted to a continuous-flow reaction, enabling controlled generation and consumption of reactive oxidising species while maintaining high reaction efficiency. This translation highlights the compatibility of the protocol with modern process intensification strategies and reinforces its potential for safe and sustainable large-scale application.

Overall, the work presented in this chapter revisits and modernises a classical oxidative transformation, demonstrating that peracid-mediated *anti*-dihydroxylation can be rendered practical, scalable, and environmentally responsible. This catalyst-free approach complements the catalyst- and immobilization-based strategies explored in other chapters of this thesis, collectively contributing to a coherent framework for sustainable method for olefin oxidation.

Chapter 5
A Modular Approach to the Formal Total Synthesis of (+)-Hannokinol

5.1 Introduction

(+)-Hannokinol is a representative member of the linear diarylheptanoid family, a structurally diverse class of naturally occurring secondary metabolites characterized by two aryl rings linked through a seven-carbon aliphatic backbone.[217–219] Biosynthetically, diarylheptanoids arise from the convergence of phenylpropanoid and polyketide pathways, resulting in a wide range of structural motifs and oxidation states.[220,221] Depending on the substitution patterns present on the aryl rings, linear diarylheptanoids can be broadly classified into two subclasses: symmetrical linear diarylheptanoids, in which both aromatic rings are identical, and unsymmetrical linear diarylheptanoids, where the two aryl units bear different substituents. The structural diversity within this family is further governed by variations in phenyl substitution, most commonly hydroxyl, methoxy, or glycosyl groups located at the 3′- and 4′-positions of the aromatic rings, as well as by functionalization along the heptane chain, including unsaturation, carbonyl formation, and hydroxylation (Scheme 5.1).[222,223] In certain subclasses, additional complexity is introduced through macrocyclization processes, giving rise to biaryl or diaryl ether frameworks.[224–226]

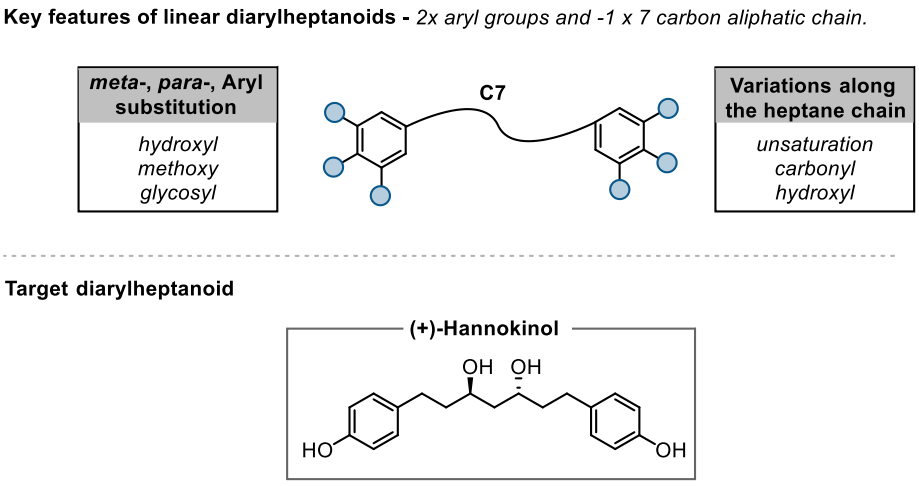

Scheme 5.1 Structural features of linear diarylheptanoids and structure of target compound.

Within this family, (+)-hannokinol is distinguished by a linear diarylheptanoid framework comprising two *para*-hydroxylated phenyl rings connected by a seven-carbon chain bearing a stereodefined *anti*-1,3-diol motif (Scheme 5.1). This architectural combination of multiple stereogenic centers, oxygenated functionalities, and densely substituted ary groups poses a significant synthetic challenge, particularly with respect to stereochemical control and step economy. The precise installation of the 1,3-diol unit within an acyclic system, while maintaining functional group compatibility, renders (+)-hannokinol an attractive and demanding target for synthetic investigation.

Among linear diarylheptanoids, hannokinol has attracted particular attention due to its occurrence in medicinal plants, its broad spectrum of biological activities, and its proposed role as a biosynthetic intermediate in the formation of more structurally complex diarylheptanoids, such as taccachanfurans.[222,227–231] These attributes position hannokinol as a valuable molecular platform for probing structure–activity relationships (SAR), elucidating biosynthetic pathways, and developing new synthetic methodologies. The structural complexity arising from substituted aromatic rings, stereodefined hydroxyl groups on the aliphatic chain, and the potential for further chemical modification makes this molecule an attractive target for synthetic, mechanistic, and biological studies.

5.2 Occurrence

Linear diarylheptanoids are widely distributed in higher plants, particularly among species belonging to the families *Zingiberaceae*, *Betulaceae*, *Juglandaceae*, and *Myricaceae*.[232] (+)-Hannokinol was first isolated in 1995 from the seeds of *Alpinia blepharocalyx*, a member of the *Zingiberaceae* family known for producing polyphenolic secondary metabolites.[233] Subsequently, in 2002, hannokinol was also isolated from the rhizomes of *Tacca chantrieri*, a plant extensively employed in traditional Chinese medicine for the treatment of gastric ulcers, enteritis, hepatitis, and other inflammatory disorders.[227]

The co-occurrence of hannokinol with structurally related diarylheptanoids and lignans suggests its biosynthesis proceeds through conserved phenylpropanoid-derived pathways involving chain elongation, selective oxygenation, and oxidative transformations.[234] Despite their biological relevance, linear diarylheptanoids such as hannokinol are typically present only as minor constituents within complex plant extracts, often alongside a multitude of other polyphenolic compounds.[235] This low natural abundance, coupled with challenges associated with isolation and purification, underscores the importance of developing efficient synthetic routes to access these diarylheptanoids in sufficient quantities for detailed chemical and biological studies.

5.3 Biology activity

Linear diarylheptanoids, and (+)-hannokinol in particular, are associated with a broad range of biologically significant activities that are consistent with their traditional medicinal applications across Asia, Africa, and South America.[224] Reported pharmacological properties include pronounced anti-inflammatory activity, which has been attributed to the inhibition of pro-inflammatory mediators and modulation of key enzymatic pathways such as cyclooxygenase (*COX*) and lipoxygenase (*LOX*).[236] In

addition, these compounds exhibit notable antioxidant activity arising from their phenolic functionalities, which enable efficient radical scavenging and metal chelation.[237,238]

Further biological investigations have demonstrated hepatoprotective effects of diarylheptanoids in both *in vitro* and *in vivo* models of liver injury, as well as anticarcinogenic activity, including cytotoxic effects against a variety of human cancer cell lines such as colorectal, melanoma, renal, breast, and fibrosarcoma.[228,239] Antiviral and antimicrobial activities have also been reported, potentially linked to interference with viral replication or inhibition of microbial growth.[240–242]

The biological profile of (+)-hannokinol is closely correlated with its structural features, particularly the presence of phenolic aromatic rings and a stereodefined 1,3-diol motif embedded within a flexible heptane chain. These characteristics bear structural resemblance to curcumin and related bioactive diarylheptanoids, which similarly display diverse pharmacological activities.[243] The convergence of potent biological activity, structural complexity, and limited natural availability strongly motivates the development of reliable synthetic access to hannokinol and its analogues. Such access is essential for systematic biological evaluation, detailed SAR studies, and the exploration of hannokinol as a versatile scaffold for medicinal chemistry applications.

5.4 Previous Synthetic Strategies toward (+)-Hannokinol

The structural complexity and biological relevance of (+)-hannokinol have sparked several synthetic efforts aimed at accessing this linear diarylheptanoid in enantiomerically enriched form. In particular, the stereodefined *anti*-1,3-diol unit within the linear heptane chain presents a major synthetic challenge, as it requires precise control of stereochemistry while maintaining compatibility with multiple functional groups. To date, only a limited number of total or formal syntheses of (+)-hannokinol have been reported, most notably by Yadav and co-workers and by Babu and co-workers, each employing distinct strategic disconnections and key stereochemical transformations.

Yadav and co-workers reported an enantioselective synthesis of (+)-hannokinol that relies on substrate-controlled stereochemical induction and strategic functional group interconversions (Scheme 5.2).[244] Their approach was initiated from 3-(4-methoxyphenyl)propionaldehyde, which was converted into the corresponding homoallylic alcohol via a Keck-Maruoka allylation.[245,246] Protection of the resulting secondary alcohol as its *tert*-butyldimethylsilyl (TBS) ether was followed by Upjohn dihydroxylation of the terminal alkene,[247] furnishing a vicinal diol. Subsequent oxidative cleavage of the diol afforded an aldehyde, which underwent an aldol reaction with

methoxyacetophenone to provide a β-hydroxy ketone intermediate. Oxidation of the secondary alcohol using DMP yielded a β-diketone, which upon treatment with trifluoroacetic acid in dichloromethane underwent cyclization to form a dihydropyranone intermediate. Ring opening of the tetrahydropyran framework and concurrent reduction of the resulting ketone under hydrogenation conditions delivered the linear diarylheptanoid skeleton. Final deprotection of the aryl methyl ethers furnished (+)-hannokinol. This synthesis highlights the effective use of allylation chemistry, oxidative transformations, and cyclic intermediates to control stereochemical outcomes within an acyclic target.

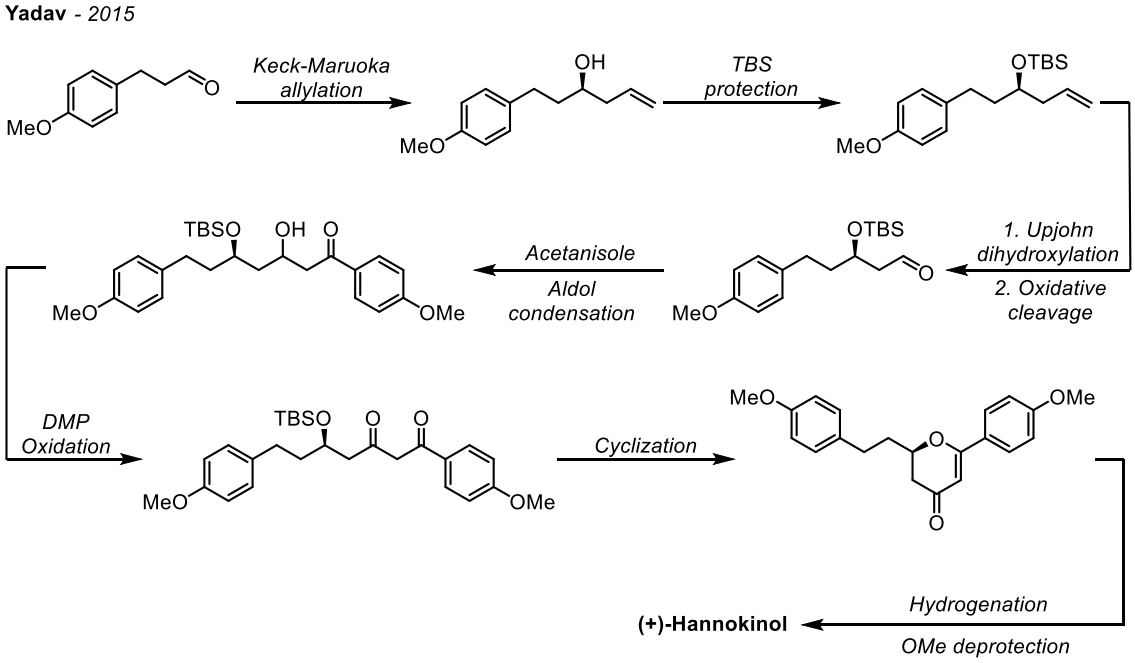

Scheme 5.2 Yadav's synthesis of (+)-hannokinol.

An alternative synthetic strategy was later disclosed by Babu and co-workers, who employed a combination of Brown's allylation and diethylzinc-mediated diastereoselective alkynylation as key bond-forming steps (Scheme 5.3).[248] Their synthesis commenced with the conversion of an aldehyde precursor into an unsaturated ester via a Wittig olefination, followed by sequential reductions to furnish the corresponding aldehyde. Brown's asymmetric allylation of this aldehyde generated a homoallylic alcohol with high stereocontrol,[222] which was subsequently protected as its TBS ether. The terminal alkene was subjected to Upjohn dihydroxylation,[247] and oxidative cleavage of the resulting diol provided an aldehyde intermediate. Diastereoselective alkynylation of this aldehyde with 1-(benzyloxy)-4-ethynylbenzene under diethylzinc conditions afforded a propargylic alcohol derivative. Subsequent

hydrogenation of the alkyne moiety and global deprotection of the silyl protecting groups delivered (+)-hannokinol. This route underscores the utility of asymmetric allylation and alkynylation methodologies for assembling the diarylheptanoid framework.

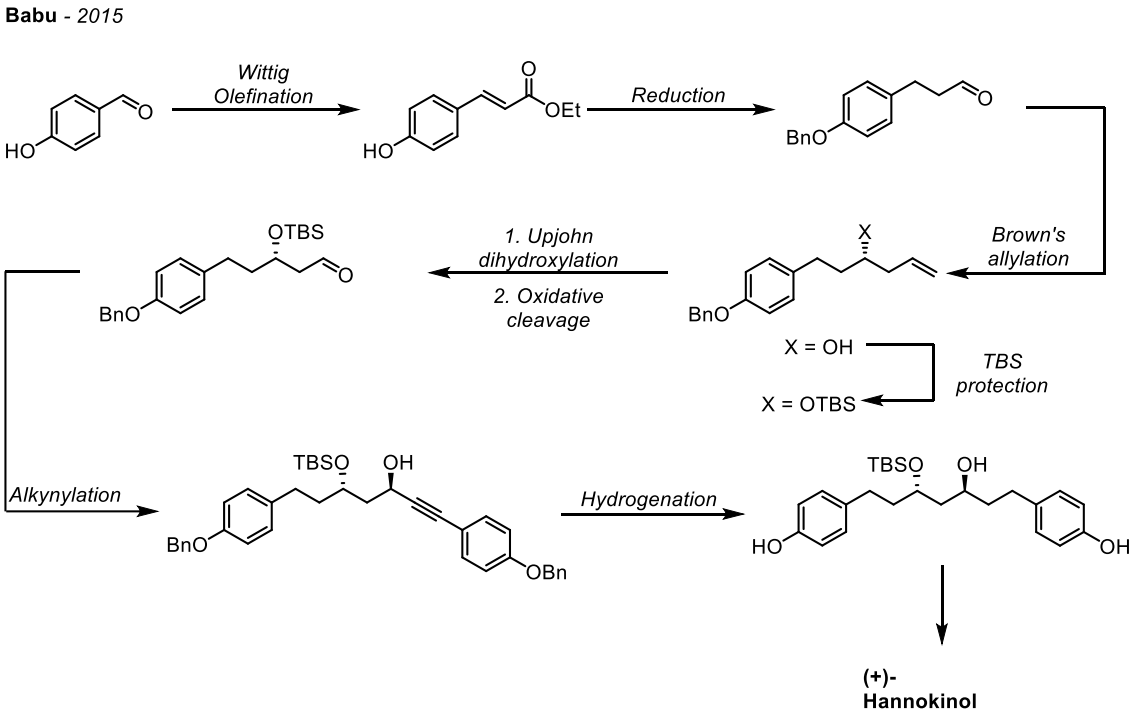

Scheme 5.3 Babu's synthesis of (+)-hannokinol.

5.5 Scope and Objectives

In view of the compelling biological activities of (+)-hannokinol and its potential role as a versatile natural building block, coupled with the persistent synthetic challenges associated with stereocontrolled synthesis of its linear diarylheptanoid framework, the primary objective of this chapter is to develop an efficient and modular synthetic strategy toward (+)-hannokinol. Specifically, this study aims to achieve the assembly of the *anti*-1,3-diol motif embedded within the seven-carbon aliphatic chain using a chiral phosphane oxide-based building block derived from readily available and inexpensive starting materials (Scheme 5.4).[249,250] A further objective is to establish a convergent route that enables efficient carbon–carbon bond formation between the aromatic and aliphatic fragments through robust olefination and cross-coupling methodologies. Emphasis is placed on minimizing non-strategic functional group manipulations while maintaining high levels of stereochemical integrity throughout the synthesis. Ultimately, the successful synthesis of a late-stage intermediate that can be converted into (+)-hannokinol according to previously reported protocols is targeted, thereby accomplishing

a formal total synthesis and providing a flexible platform for future analogue synthesis and SAR studies.

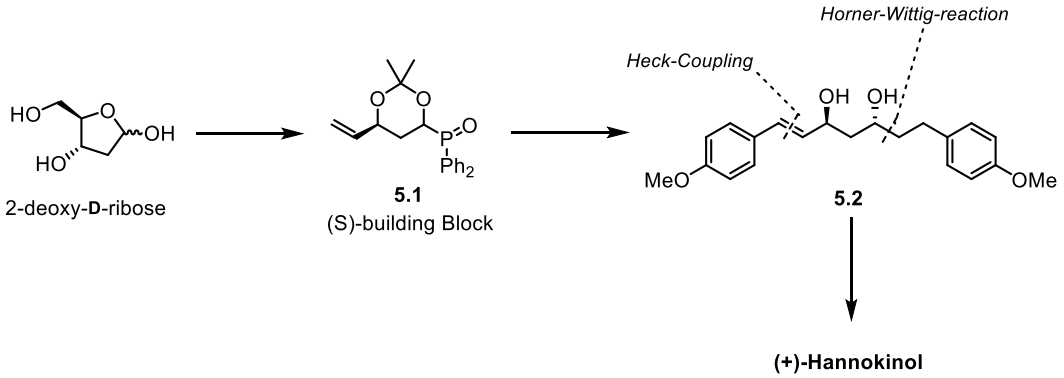

Scheme 5.4 Outline of the planned modular approach toward the formal synthesis of (+)-hannokinol.

5.6 Retrosynthesis

The retrosynthetic analysis of (+)-hannokinol was designed to enable a modular and stereocontrolled synthesis of the linear diarylheptanoid framework while minimizing non-strategic functional group manipulations (Scheme 5.5). (+)-Hannokinol could be accessed by aryl methyl ether demethylation of late-stage intermediate **5.3**.[244] This intermediate was envisioned to arise from catalytic hydrogenation of olefin **5.2**, thereby enabling installation of the fully saturated heptane backbone at a late stage of the synthesis. Olefin **5.2** was traced back to a palladium-catalyzed Heck cross-coupling between a *p*-methoxy-substituted aryl iodide fragment and olefin coupling partner **5.14**, providing a convergent entry to the diarylheptanoid framework. Olefin **5.14** was envisioned to arise from an Evans–Tishchenko anti-reduction of β-hydroxy ketone **5.4**, which in turn could be accessed via a Horner–Wittig olefination between aldehyde **5.5** and chiral phosphonate derivative **5.1**.

The chiral phosphonate building block **5.1** was selected due to its modularity and reliable stereochemical induction and was readily available from inexpensive and commercially accessible 2-deoxy-D-ribose. The aldehyde coupling partner **5.5** was envisioned to arise from reduction of the corresponding ester, itself prepared from commercially available aromatic carboxylic acid precursors. This retrosynthetic plan thus combines convergent fragment assembly with a robust stereochemical strategy, setting the stage for an efficient and flexible formal synthesis of (+)-hannokinol.

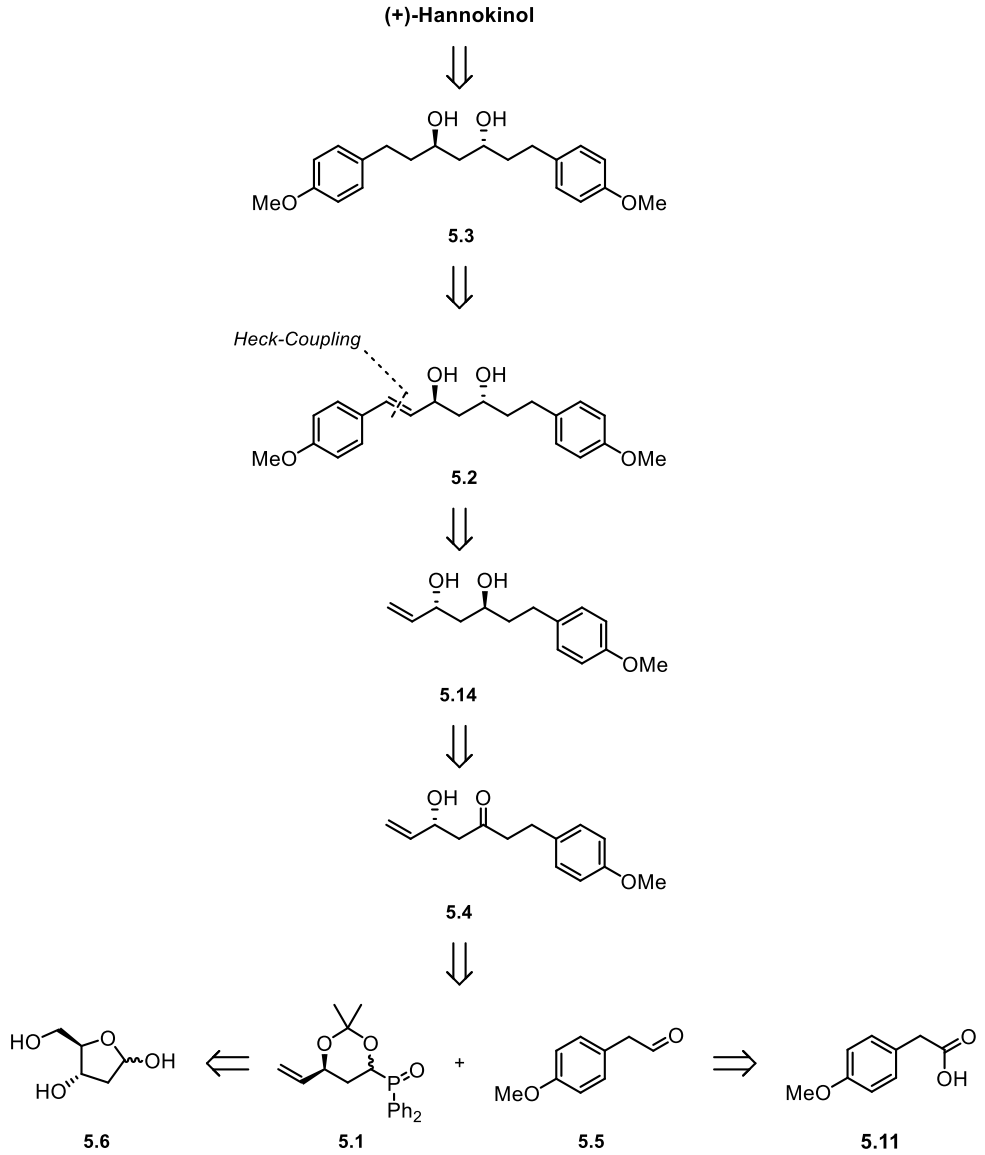

Scheme 5.5 Retrosynthetic analysis of (+)-hannokinol.

5.7 Results and Discussion

The forward synthesis toward (+)-hannokinol was initiated with the preparation of chiral phosphane oxide building block **5.1**, which serves as the cornerstone of the modular strategy for stereocontrolled construction of 1,3-polyol motifs developed by Kirsch and coworkers (Scheme 5.6).[251–253] This building block was selected due to its reliable induction of stereochemical information and its accessibility from inexpensive carbohydrate-derived starting materials. Accordingly, commercially available 2-deoxy-D-ribose **5.6** was used as the starting material and converted into acetal under standard protection conditions. Subsequent iodination furnished intermediate **5.7**, which upon *tert*-butyldimethylsilyl protection of the primary hydroxyl group afforded compound **5.8**. Vasella fragmentation of this iodinated intermediate, using zinc dust activated with 1 M

hydrochloric acid, efficiently generated aldehyde **5.9**. Treatment of the aldehyde with diphenylphosphane oxide **5.10** furnished phosphane oxide in 96% yield with a diastereomeric ratio of 60:40. Final TBS deprotection followed by acetal protection delivered the desired (*S*)-configured chiral building block **5.1** in 77% overall yield from 2-deoxy-D-ribose.

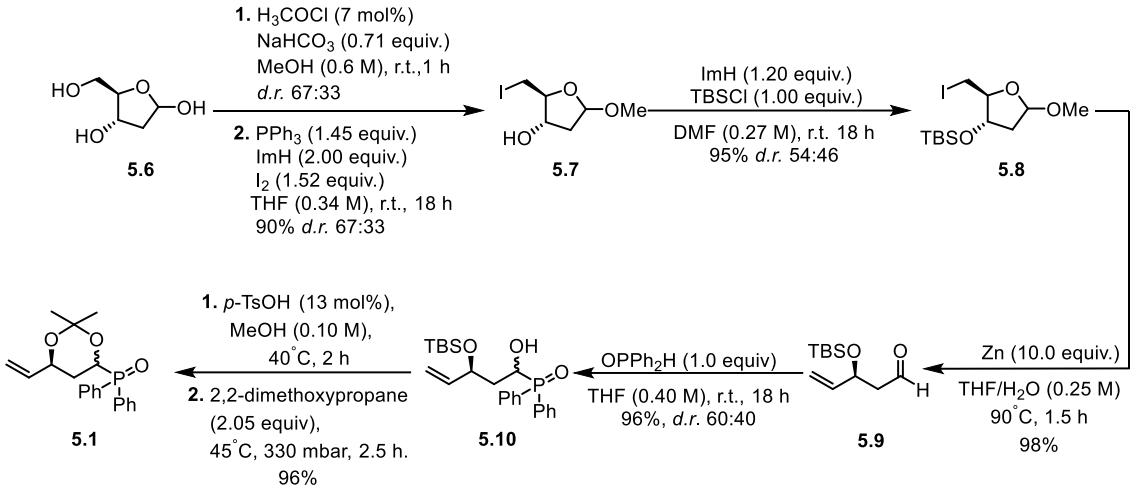

Scheme 5.6 Synthesis of the (*S*)-chiral phosphane oxide building block from 2-deoxy-D-ribose.

In parallel, the aromatic aldehyde coupling partner **5.5** was prepared from commercially available 4-methoxyphenylacetic acid (Scheme 5.7). Fischer esterification under acidic conditions afforded the corresponding methyl ester **5.11**, which was subsequently reduced under controlled conditions using diisobutylaluminum hydride (DIBAL-H) to furnish aldehyde **5.5** in good yield. This aldehyde served as the electrophilic partner for the key carbon–carbon bond-forming step.

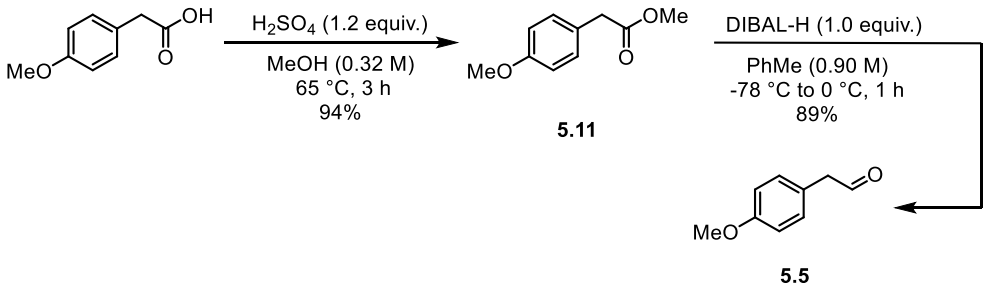

Scheme 5.7 Preparation of the aromatic aldehyde.

With both the chiral phosphane oxide building block **5.1** and aldehyde **5.5** in hand, attention was directed toward the pivotal Horner–Wittig olefination (Scheme 5.8). Reaction of aldehyde **5.5** with the phosphane oxide **5.1** proceeded smoothly to afford the corresponding β-hydroxy ketone **5.12** in 87% yield. Subsequent Evans–Tishchenko

anti-reduction of the β-hydroxy ketone, followed by deprotection, furnished the *anti*-1,3-diol **5.13** in 87% yield with excellent diastereoselectivity (*d.r.* > 20:1), thereby establishing the critical stereochemical motif of the target molecule. Protection of the 1,3-diol unit using *tert*-butyldimethylsilyl chloride (TBSCl) and imidazole afforded the corresponding *bis*-TBS-protected intermediate **5.14** in 95% yield.

Synthesis of the diarylheptanoid framework was accomplished through a palladium-catalyzed Heck cross-coupling between the *bis*-TBS-protected olefin **5.15** and 4 iodoanisole. Gratifyingly, the coupling proceeded efficiently, delivering the desired olefinic diarylheptanoid intermediate **5.17** in 84% yield. Subsequent catalytic hydrogenation of the alkene moiety using 10 mol% Pd/C under 1.0 bar of hydrogen smoothly afforded the fully saturated intermediate **5.18** in nearly quantitative yield 93%. Final global deprotection of the silyl ethers using an HF·pyridine complex furnished intermediate **5.3** in excellent yield (87%). This compound constitutes a late-stage precursor that can be converted into (+)-hannokinol via aryl methyl ether demethylation following the procedure reported by Yadav and co-workers,[244] thereby completing a formal total synthesis of (+)-hannokinol.

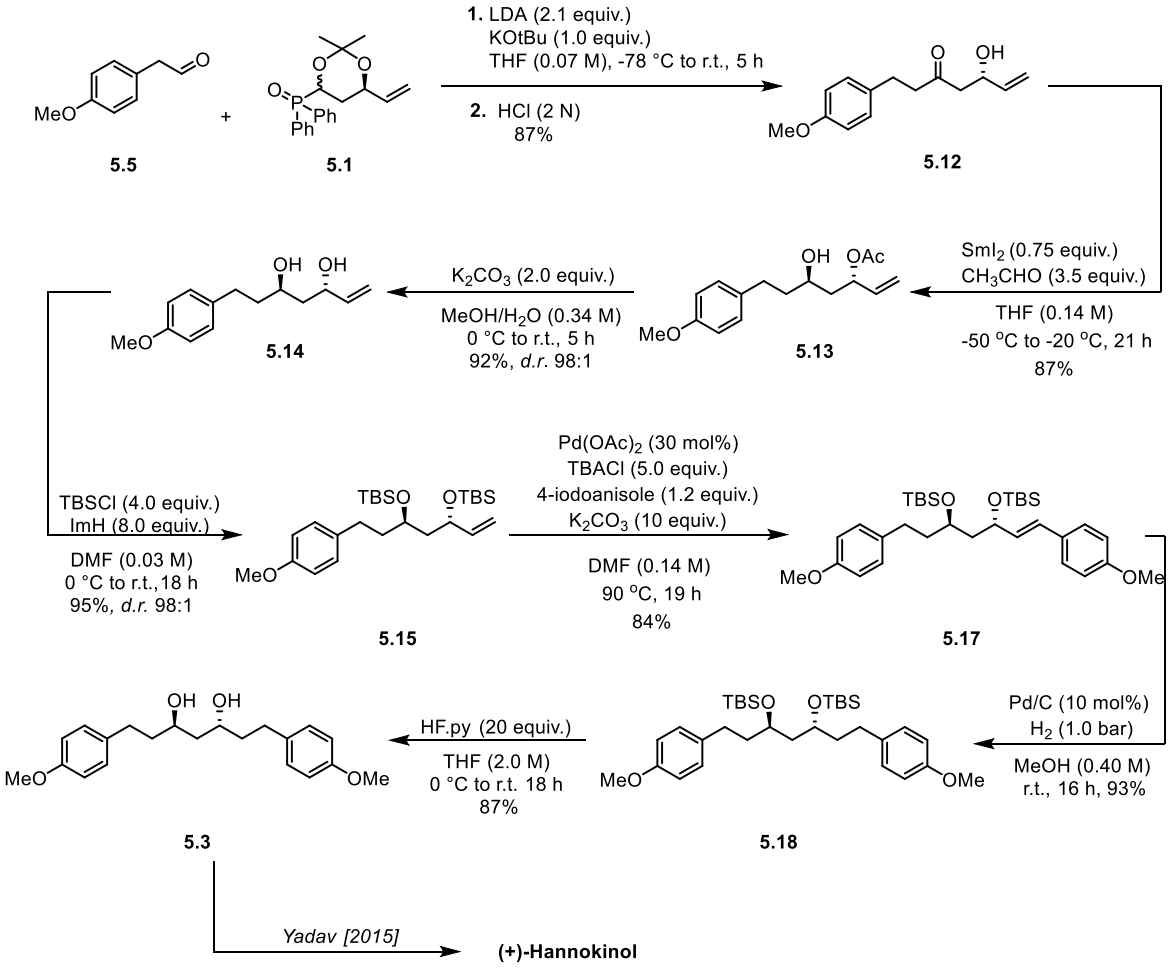

Scheme 5.8 Completion of the formal synthesis of (+)-hannokinol.

5.8 Summary and outlook

In conclusion, a modular and stereocontrolled synthetic strategy toward (+)-hannokinol has been developed, culminating in a formal total synthesis of this biologically significant linear diarylheptanoid. Key to this approach is the use of a chiral phosphane oxide-based building block derived from inexpensive and readily available 2-deoxy-D-ribose, enabling reliable installation of the synthetically challenging *anti*-1,3-diol motif with high diastereoselectivity. The convergent nature of the synthesis, featuring a key Horner-Wittig olefination followed by an Evans-Tishchenko *anti*-reduction, allowed efficient construction of the aliphatic backbone while maintaining strict stereochemical control. Assembly of the diarylheptanoid framework was achieved through a late-stage palladium-catalyzed Heck cross-coupling, providing a flexible and robust entry to the fully functionalized skeleton. The successful preparation of a late-stage intermediate convertible to (+)-hannokinol via known demethylation protocols achieved in an overall yield of 45% over seven linear steps, constitutes a formal total synthesis and validates the strategic design of the route.

Beyond the synthesis of (+)-hannokinol, the modularity of the present strategy offers significant potential for broader application. Variation of the aryl aldehyde **5.19** employed in the Horner-Wittig olefination and of the aryl halide **5.22** coupling partners enables this synthetic framework to be readily extended to linear diarylheptanoids bearing diverse substitution patterns on the aromatic rings, including hydroxyl, methoxy, and other functional groups, while preserving the core reaction sequence established in this work (Scheme 5.9). As such, this approach provides a general platform for the synthesis of both naturally occurring and non-natural diarylheptanoid analogues, facilitating systematic SAR studies and further biological evaluation. Moreover, the reliance on readily accessible starting materials, high stereochemical integrity, and efficient carbon-carbon bond-forming reactions underscores the potential of this strategy for adaptation to the synthesis of more complex diarylheptanoid derivatives and related polyol-containing natural products. Overall, this work contributes a versatile and scalable synthetic framework that expands access to an important class of bioactive natural products and sets the stage for future investigations in synthetic and medicinal chemistry.

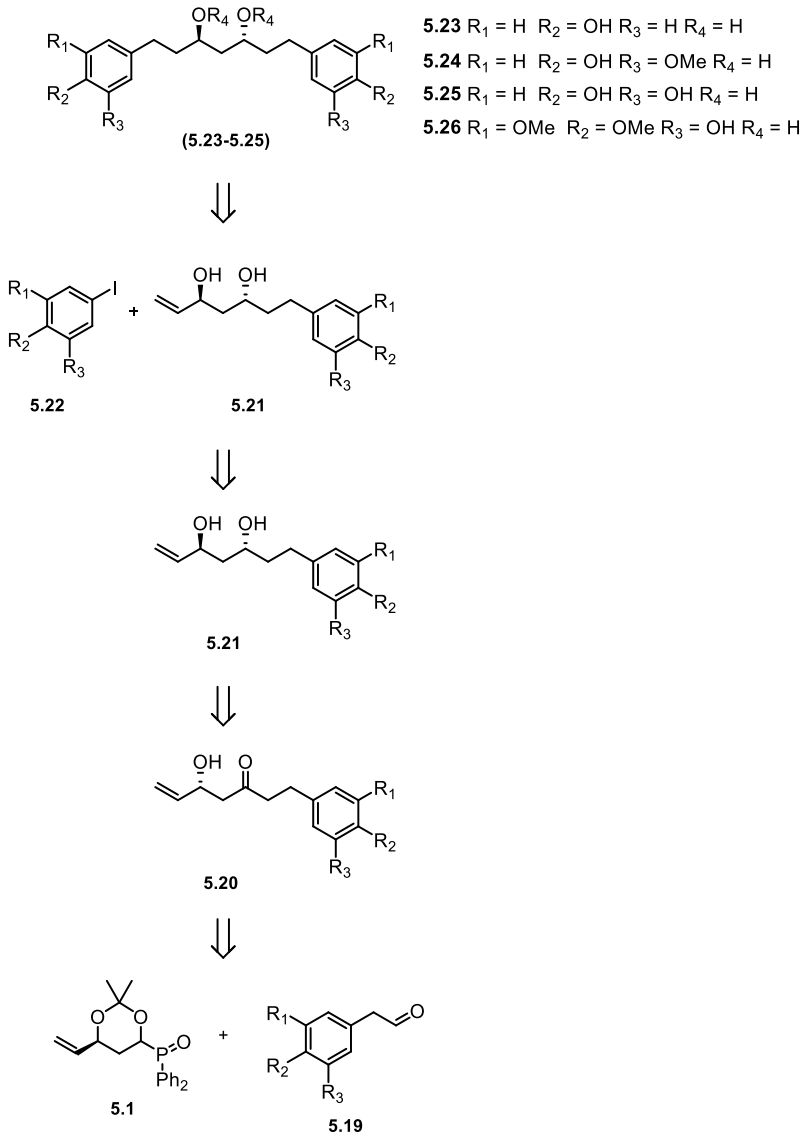

Scheme 5.9 Generalized synthetic strategy enabling access to linear diarylheptanoids with diverse aryl substitution patterns.

Chapter 6
Conclusion

The immobilization of organocatalytic systems represents an effective strategy for the development of sustainable oxidative transformations, enabling improved catalyst handling, enhanced operational stability, and efficient recyclability, while maintaining compatibility with mild reaction conditions and continuous-flow processing. Oxidation reactions remain indispensable in organic synthesis, yet their practical implementation is frequently limited by issues related to waste generation, catalyst recovery, safety, and long-term operational stability. By integrating organocatalysis with solid supports and flow chemistry, this dissertation addresses these challenges through the development of metal-free or low-waste oxidative methodologies that are operationally robust and amenable to scale-up. Collectively, the work establishes immobilization as a key design principle for advancing practical, sustainable oxidation processes.

Chapters 2 and 3 focus on the design and application of immobilized organocatalysts for oxidative transformations. In Chapter 2, a silica-supported hypervalent iodine(V) catalyst was developed, demonstrating significantly enhanced chemical and mechanical stability compared to polymer-supported analogues. This catalyst efficiently converted β-substituted alcohols into structurally diverse products, including γ-lactones, γ-lactams, and carbamates, in 33 examples with yields ranging from 26–92%, under mild, metal-free conditions with a short reaction time of 14.5 minutes. The system exhibited excellent recyclability over 15 consecutive cycles and performed robustly under continuous-flow conditions using green solvents, highlighting its potential for scalable and environmentally friendly oxidative processing (Scheme 6.1).

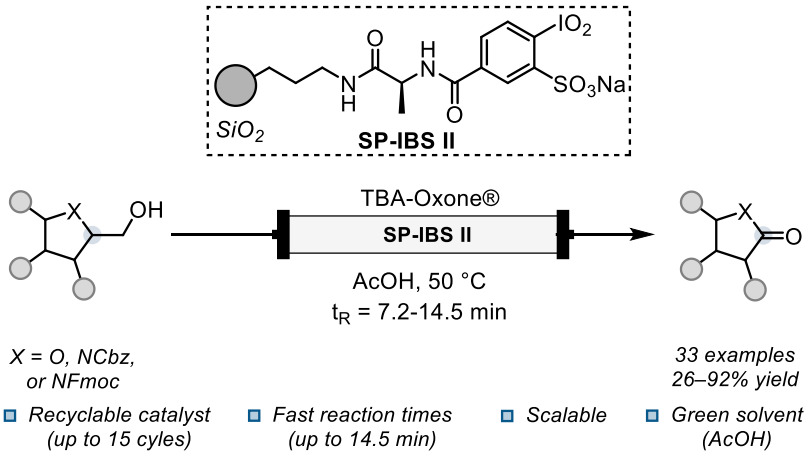

Scheme 6.1 Project summary for the immobilization of hypervalent iodine(V) catalysts and their application in flow.

Chapter 3 describes the design and preliminary evaluation of a benzoxathiazine-derived oxaziridine with a functional handle for future immobilization. While catalytic activity was

confirmed using oxone® as the terminal oxidant, reduced efficiency relative to homogeneous analogues was observed, delineating areas for future optimization with respect to oxidant compatibility and turnover (Scheme 6.2).

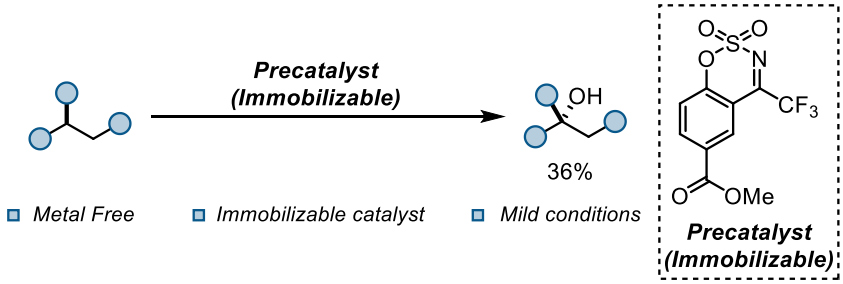

Scheme 6.2 Project summary for the synthesis of immobilizable oxaziridine-based organocatalyst and its investigation in batch.

Chapter 4 presents a metal- and catalyst-free approach for the *anti*-dihydroxylation of alkenes using in situ generated peracetic acid. This protocol efficiently converted 24 different alkenes into *anti*-1,2-diols with yields of up to 92% and demonstrated broad functional group tolerance. The method was successfully scaled up, providing multi-gram quantities of diols without loss of efficiency. Continuous-flow adaptation further confirmed the robustness and practical applicability of the approach, highlighting the importance of controlled reaction environments when handling reactive oxidants (Scheme 6.3).

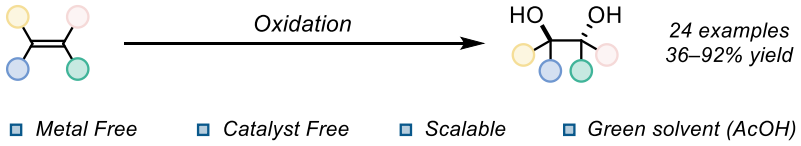

Scheme 6.3 Project summary for the metal- and catalyst-free *anti*-dihydroxylation of olefins in batch and flow.

Chapter 5 reports a side project on the modular, stereocontrolled synthesis of the diarylheptanoid (+)-hannokinol. The synthetic route comprised seven linear steps and delivered the target molecule in 18% overall yield. A chiral Horner–Wittig reagent derived from 2-deoxy-D-ribose enabled stereocontrolled installation of the 1,3-diol motif, while the modular design can permit variation of aromatic substitution patterns. Although independent of the oxidative methodology, this work illustrates broader applications of stereocontrolled synthesis in constructing linear diarylheptanoids.

Overall, this dissertation advances the development of sustainable oxidative methodologies by addressing critical challenges in oxidation chemistry, including catalyst recovery, operational safety, long-term stability, and scalability. The combined outcomes

provide a coherent framework for environmentally benign oxidation processes that integrate fundamental methodological innovation with practical synthetic utility. The strategies developed herein, combining immobilized organocatalysts with continuous-flow processing-offer a robust platform for future research in sustainable organocatalytic oxidation and broader applications in practical synthetic chemistry.

Chapter 7
Experimental Section

Used Materials and Equipment

7.1 Solvents & Reagents

Prior to use, anhydrous solvents including DCM, MeCN, THF, and Et_2O were purified using an MB-SPS 800 solvent purification system (MBraun GmbH). The purified solvents were subsequently stored over activated molecular sieves and transferred under an inert nitrogen atmosphere. Other anhydrous solvents were obtained from commercial suppliers and used as received without further purification. Cyclohexane and ethyl acetate employed for flash column chromatography were distilled prior to use. All commercially available reagents were used without additional purification. Compounds synthesized in-house were analyzed for purity prior to their use in subsequent reactions.

7.2 Reaction set up

Reactions sensitive to oxygen and/or moisture were conducted under an inert nitrogen atmosphere. Heating of reaction mixtures was achieved using an oil bath filled with paraffin oil, with temperature regulation ensured by a contact thermometer. Reactions requiring cooling were performed using appropriate cooling baths prepared in suitable plastic or Dewar vessels, or by employing a Julabo FT902 cryostat (Julabo GmbH). Ice–water and ice–sodium chloride baths were used to maintain temperatures in the range of 0 °C to −15 °C, whereas an acetone–dry ice bath was employed to achieve temperatures as low as −78 °C. Reaction temperatures were monitored and controlled using a calibrated cooling thermometer.

7.3 Analytics

Thin-layer chromatography (TLC) was carried out on precoated plates (silica gel 60, F_{254}, or ALUGRAM® ALOX N / UV_{254}). Visualization was achieved under ultraviolet light (254 nm) or by staining with basic potassium permanganate ($KMnO_4$), ninhydrin, cerium ammonium molybdate (CAM), or *p*-anisaldehyde solutions, followed by thermal development.

Flash column chromatography was performed using silica gel (40–60 µm) or neutral alumina (Brockmann Grade I, 58 Å) as the stationary phase. For selected transformations, the silica gel was deactivated prior to use by conditioning with a 1% (v/v) triethylamine solution in cyclohexane, followed by removal of excess triethylamine by washing with neat cyclohexane. Unless otherwise stated, cyclohexane and ethyl acetate were employed as the eluent system.

Nuclear magnetic resonance (NMR) spectra were recorded on Bruker Avance III 400 and 600 spectrometers. **^{1}H NMR** spectra were acquired at 400 or 600 MHz, **^{13}C NMR** spectra at 101 or 151 MHz, **^{19}F NMR** spectra at 376 MHz, and **^{11}B NMR** spectra at 128 MHz. Chemical shifts (δ) are reported in parts per million (ppm) relative to the residual solvent signal, and coupling constants (J) are given in hertz (Hz). Signal multiplicities are abbreviated according to standard notation. Unless otherwise specified, all NMR measurements were conducted at 300 K.

High-resolution mass spectrometry (HRMS) analyses were performed using a Bruker micrOTOF mass spectrometer equipped with an electrospray ionization (ESI) source operating in positive ion mode. Infrared (IR) spectra were recorded on a Bruker ALPHA spectrometer using attenuated total reflection (ATR). Spectral analysis was carried out using OPUS 7.5 software, and absorption bands were classified according to their relative intensities as weak (w), medium (m), or strong (s).

Optical rotations of chiral compounds were measured at 20 °C using a P8000-T polarimeter (A. Krüss Optronic GmbH). Samples were dissolved in the specified solvents at the stated concentrations (c = g/100 mL). Enantiomeric excesses were determined by high-performance liquid chromatography (HPLC) using an Agilent 1260 Infinity II system equipped with chiral stationary phases (CHIRALPAK IA and CHIRALCEL OJ-H, Daicel Chemical Industries Ltd.).

7.4 Chapter 2: Immobilization of Hypervalent Iodine(V) Catalysts and their application in Flow.

7.4.1 Synthesis & Characterization of Starting materials

General procedure for the synthesis (GP1):

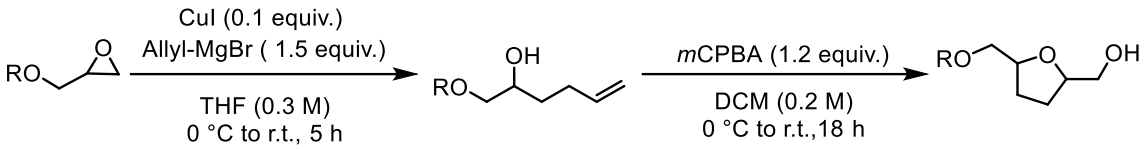

Following reported procedure,[254] to a solution of the oxirane derivative (1.0 equiv.) and copper(I) iodide (0.1 equiv.) in THF (0.3 M), cooled to 0 °C, allylmagnesium bromide (1.5 equiv.) was added dropwise. The reaction mixture was allowed to warm to room temperature and stirred for 5 hours. Upon completion, the reaction was quenched with saturated aqueous NH_4Cl. The mixture was extracted with EtOAc (3 times), and the combined organic layers were washed with brine, dried over anhydrous Na_2SO_4, filtered, and concentrated under reduced pressure. The resulting crude was used in the next step without further purification.

Following a reported procedure by Gravel and co-workers,[254] a solution of the corresponding alcohol in DCM (0.2 M) was cooled to 0 °C. To this solution, *m*CPBA (1.2 equiv.) was added in a single portion. The reaction mixture was subsequently allowed to warm to ambient temperature and stirred for 18 hours. Upon completion, the reaction was quenched by the addition of saturated aqueous $NaHCO_3$. The resulting mixture was extracted with DCM three times. The combined organic layers were dried over anhydrous Na_2SO_4, filtered, and concentrated under reduced pressure. The crude product was purified by flash column chromatography to afford substituted tetrahydrofuran-2-methanol derivatives.

General procedure for the synthesis (GP2):

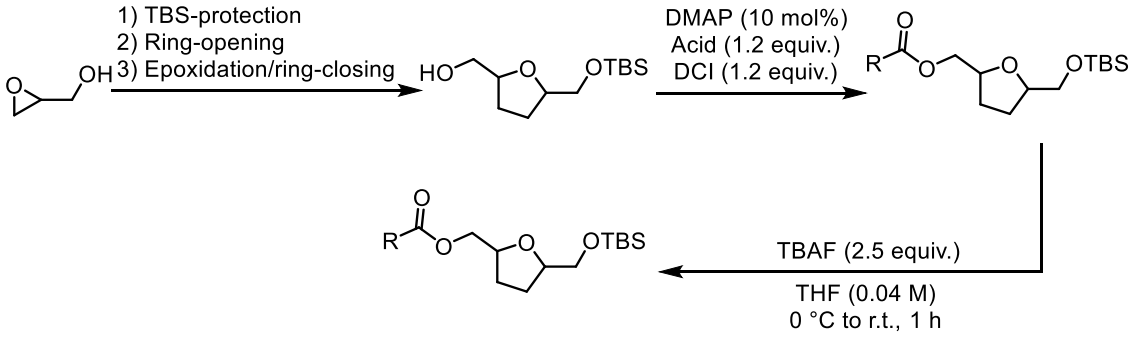

Following reported procedure,[255] to a solution of the oxirane derivative (1.0 equiv.) and copper(I) iodide (0.1 equiv.) in THF (0.3 M), cooled to 0 °C, allylmagnesium bromide (1.5 equiv.) was added dropwise. The reaction mixture was allowed to warm to room temperature and stirred for 5 hours. Upon completion, the reaction was quenched with saturated aqueous NH_4Cl. The mixture was extracted with EtOAc (3 times), and the combined organic layers were washed with brine, dried over anhydrous Na_2SO_4, filtered, and concentrated under reduced pressure. The resulting crude was used in the next step without further purification.

Following a reported procedure by Gravel and co-workers,[254] a solution of the corresponding alcohol in DCM (0.2 M) was cooled to 0 °C. To this solution, *m*CPBA (1.2 equiv.) was added in a single portion. The reaction mixture was subsequently allowed to warm to ambient temperature and stirred for 18 hours. Upon completion, the reaction was quenched by the addition of saturated aqueous $NaHCO_3$. The resulting mixture was extracted with DCM three times. The combined organic layers were dried over anhydrous Na_2SO_4, filtered, and concentrated under reduced pressure. The crude product was purified by flash column chromatography to afford substituted THF-M derivatives.

General procedure for the synthesis (GP3):

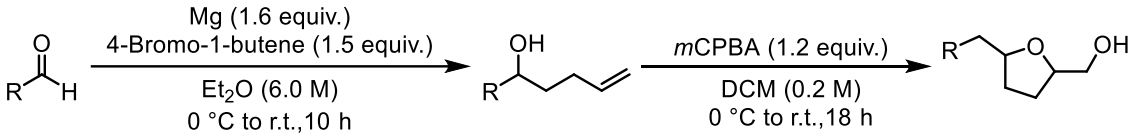

In an oven-dried round bottom flask equipped with a magnetic stirring bar was charged with Mg turnings (1.6 equiv.), and purged with argon. Anhydrous Et_2O (5 mL) was added, and the suspension was cooled to 0 °C. Neat 4-bromo-1-butene (1.5 equiv.) was added dropwise, and the resulting mixture was warmed to rt and stirred for 1 hour. A solution of the aldehyde (1.0 equiv) in Et_2O (10 M) was then added, and the reaction mixture was stirred at rt for 8 hours. The reaction was quenched by dropwise addition of saturated aqueous NH_4Cl. The layers were separated, and the aqueous phase was extracted with Et_2O (3 times). The combined organic extracts were dried over Na_2SO_4, filtered, and concentrated under reduced pressure. The crude product was used directly in the subsequent step without further purification.

Following a reported procedure by Gravel and co-workers,[254] a solution of the corresponding alcohol in DCM (0.2 M) was cooled to 0 °C. To this solution, *m*CPBA (1.2 equiv.) was added in a single portion. The reaction mixture was subsequently allowed to warm to ambient temperature and stirred for 18 hours. Upon completion, the reaction

was quenched by the addition of saturated aqueous $NaHCO_3$. The resulting mixture was extracted with DCM three times. The combined organic layers were dried over anhydrous Na_2SO_4, filtered, and concentrated under reduced pressure. The crude product was purified by flash column chromatography to afford substituted THF-M derivatives.

General procedure for the synthesis (GP4):

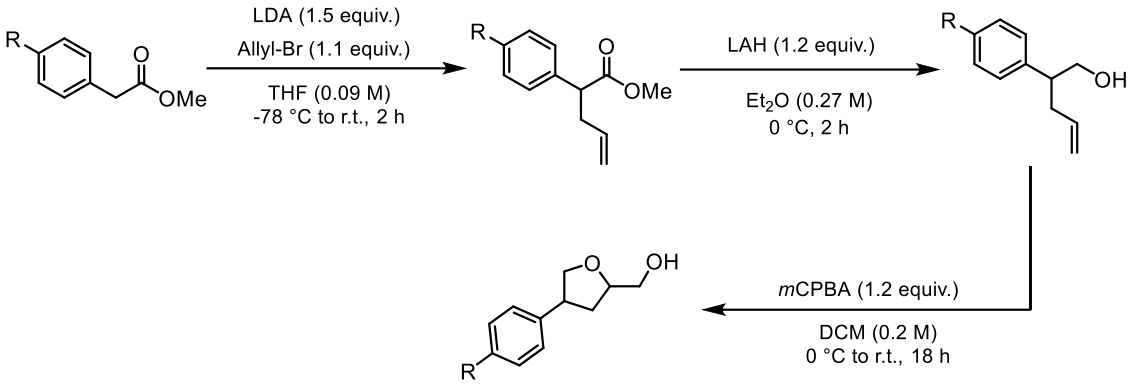

The reaction was carried out according to a modified literature procedure,[256] to a solution of diisopropylamine (1.3 equiv.) in dry THF (0.15 M) was added *n*-butyllithium (1.5 equiv.) dropwise at −78 °C. The resulting solution was stirred at 0 °C for 15 min and then cooled again to −78 °C. A solution of the ester (1.0 equiv.) in THF (0.5 M) was added dropwise, and the mixture was stirred for 40 min at −78 °C. Allyl bromide (1.1 equiv) was then added dropwise, and stirring was continued at −78 °C for 2 h. The reaction was quenched with saturated aqueous NH_4Cl (20 mL). The aqueous phase was extracted with Et_2O (3 times), and the combined organic layers were washed with 1 M HCl, then brine, dried over anhydrous Na_2SO_4, filtered, and concentrated under reduced pressure. The resulting crude was used in the next step without further purification.

Following a reported procedure by Szymoniak and co-workers,[256] a solution of the ester (1.0 equiv) in Et_2O (0.4 M) was added dropwise to a suspension of $LiAlH_4$ (1.2 equiv) in Et_2O (1.0 M) at 0 °C. The resulting mixture was stirred at room temperature for 2 hours. Cold distilled water (20 mL) was then added carefully to quench the reaction. The aqueous phase was extracted with Et_2O (3 times), and the combined organic layers were washed with brine, dried over anhydrous Na_2SO_4, filtered, and concentrated under reduced pressure. The crude mixture was purified by flash chromatography using silica gel to afford the corresponding reduced products.

Following a reported procedure by Gravel and co-workers,[254] a solution of the corresponding alcohol in DCM (0.2 M) was cooled to 0 °C. To this solution, *m*CPBA (1.2 equiv.) was added in a single portion. The reaction mixture was subsequently allowed to

warm to ambient temperature and stirred for 18 hours. Upon completion, the reaction was quenched by the addition of saturated aqueous $NaHCO_3$. The resulting mixture was extracted with DCM three times. The combined organic layers were dried over anhydrous Na_2SO_4, filtered, and concentrated under reduced pressure. The crude product was purified by flash column chromatography to afford substituted THF-M derivatives.

(5-(Phenoxymethyl)tetrahydrofuran-2-yl)methanol (7.1)

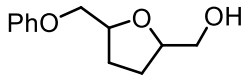

$C_{12}H_{16}O_3$
208.10 g/mol

Following **GP1**, starting from 1,2-epoxy-3-phenoxypropane (1.5 mL, 11.1 mmol, 1.0 equiv.). The crude mixture was purified by flash chromatography using silica gel (CyHex/EtOAc 8:2 → CyHex/EtOAc 6:4) affording (5-(phenoxymethyl)tetrahydrofuran-2-yl)methanol over 2 steps as a colorless liquid in 64% yield (1:1 mixture of diastereomers) (1.78 g, 8.53 mmol).

^{1}H NMR (400 MHz, $CDCl_3$) δ 7.32 – 7.23 (m, 2H), 7.02 – 6.85 (m, 3H), 4.45 – 4.35 (m, 0.49H), 4.39 – 4.30 (m, 0.46H), 4.24 – 4.15 (m, 0.49H), 4.18 – 4.08 (m, 0.48H), 4.08 – 3.89 (m, 2H), 3.82 – 3.62 (m, 1H), 3.59 – 3.50 (m, 1H), 2.87 (br, 1H), 2.19 – 1.70 (m, 4H).

^{13}C NMR (101 MHz, $CDCl_3$) δ 158.8, 158.7, 129.4, 129.4, 121.0, 120.9, 114.5, 114.5, 80.4, 80.1, 77.8, 77.4, 70.4, 70.0, 65.0, 64.7, 28.6, 28.1, 27.3, 27.1.

IR (ATR): $\tilde{\nu}$ [cm^{-1}] = 3419, 2924, 2872, 1598, 1587, 1454, 1292, 1243, 1172, 1076, 1041, 884, 807, 754, 691.

HRMS (ESI): [m/z] calculated for $C_{12}H_{16}NaO_3$ ($[M+Na]^+$): 231.0992; Found: 231.0994.

R_f (CyHex/EtOAc, 6:4) = 0.31 [$KMnO_4$]

2-((Benzyloxy)methyl)oxirane (7.2a)

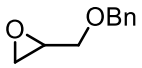

$C_{10}H_{12}O_2$
164.08 g/mol

Following reported procedure, [257] to a solution of (±)-glycidol (5.0 mL, 74.9 mmol. 1.0 equiv.) and benzyl bromide (11.6 mL, 97.4 mmol, 1.3 equiv) in DMF (150 mL, 0.5 M) at 0 °C was added NaH (3.30 g, 82.4 mmol, 1.1 equiv, 60 wt % dispersion in mineral oil). The cooling bath was removed, and the reaction mixture was stirred vigorously at rt for

20 h. The reaction mixture was diluted with DCM and quenched with water. The organic phase was separated, and the aqueous phase was extracted with DCM (5 times). The combined organic extracts were dried over anhydrous Na_2SO_4, filtered, and concentrated under reduced pressure. The crude mixture was purified by flash chromatography using silica gel (PE/EtOAc 20:1) affording product as a colorless oil in 82% yield (10.1 g, 61.4 mmol).

^{1}H NMR (600 MHz, $CDCl_3$) δ 7.35 (d, *J* = 4.5 Hz, 4H), 7.32 – 7.27 (m, 1H), 4.62 (d, *J* = 11.9 Hz, 1H), 4.57 (d, *J* = 11.9 Hz, 1H), 3.77 (dd, *J* = 11.4, 3.1 Hz, 1H), 3.45 (dd, *J* = 11.5, 5.8 Hz, 1H), 3.22 – 3.16 (m, 1H), 2.80 (dd, *J* = 5.1, 4.1 Hz, 1H), 2.62 (dd, *J* = 5.1, 2.7 Hz, 1H).
^{13}C NMR (151 MHz, $CDCl_3$) δ 138.0, 128.5, 127.9, 73.5, 70.9, 51.0, 44.4.
HRMS (ESI): [m/z] calculated for $C_{10}H_{12}NaO_2$ ($[M+Na]^+$): 187.0729; Found: 187.0730.
R_f (PE/EtOAc, 20:1) = 0.32 [$KMnO_4$].
The characterization data is consistent with the literature.[258]

(5-((Benzyloxy)methyl)tetrahydrofuran-2-yl)methanol (7.2)

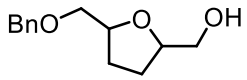

$C_{13}H_{18}O_3$
222.13 g/mol

Following reported procedure,[254] to a solution of the 2-((benzyloxy)methyl)oxirane (10.0 g. 60.9 mmol, 1.0 equiv.) and copper(I) iodide (1.16 g, 6.09 mmol, 0.1 equiv.) in THF (203 mL .0.3 M), cooled to 0 °C, allylmagnesium bromide (45.7 mL, 91.3 mmol, 1.5 equiv.) was added dropwise. The reaction mixture was allowed to warm to room temperature and stirred for 5 hours. Upon completion, the reaction was quenched with saturated aqueous NH_4Cl. The mixture was extracted with EtOAc (3 times), and the combined organic layers were washed with brine, dried over anhydrous Na_2SO_4, filtered, and concentrated under reduced pressure. The resulting crude was used in the next step without further purification.

Following reported procedure, [254] a solution of the corresponding alcohol (11.8 g, 57.2 mmol, 1.0 equiv.) in DCM (286 mL, 0.2 M) was cooled to 0 °C. To this solution, *m*CPBA (15.4 g, 68.6 mmol, 1.2 equiv.) was added in a single portion. The reaction mixture was subsequently allowed to warm to ambient temperature and stirred for 18 hours. Upon completion, the reaction was quenched by the addition of saturated aqueous $NaHCO_3$. The resulting mixture was extracted with DCM (3 times). The combined organic layers

were dried over anhydrous Na_2SO_4, filtered, and concentrated under reduced pressure. The crude mixture was purified by flash chromatography using silica gel (CyHex/EtOAc 3:2 → CyHex/EtOAc 1:1) affording product as a colorless oil in 94% yield (1:1 mixture of diastereomers) (11.9 g, 53.8 mmol).

^{1}H NMR (400 MHz, $CDCl_3$) δ 7.41 – 7.24 (m, 10H), 4.66 – 4.45 (m, 4H), 4.27 – 4.05 (m, 4H), 3.77 (dd, *J* = 11.7, 2.9 Hz, 1H), 3.68 (dd, *J* = 11.6, 3.3 Hz, 1H), 3.61 (dd, *J* = 10.1, 3.6 Hz, 1H), 3.54 – 3.43 (m, 5H), 2.24 (br, 2H), 2.10 – 1.80 (m, 6H), 1.80 – 1.59 (m, 2H).
^{13}C NMR (101 MHz, $CDCl_3$) δ 138.3, 138.0, 128.6, 128.5, 127.9, 127.9, 127.8, 80.3, 79.8, 78.8, 78.4, 73.5, 73.0, 72.5, 65.5, 64.8, 28.8, 28.3, 27.4, 27.3.
HRMS (ESI): [m/z] calculated for $C_{13}H_{18}NaO_3$ ($[M+Na]^+$): 245.1149; Found: 245.1148.
R_f (CyHex/EtOAc 3:2) = 0.24 [$KMnO_4$]
The characterization data is consistent with the literature.[254]

(5-(Hydroxymethyl)tetrahydrofuran-2-yl)methyl benzoate (7.3)

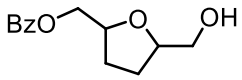

$C_{13}H_{16}O_4$
236.10 g/mol

Following a modified reported procedure,[106] to a solution of (5-((benzyloxy)methyl)-tetrahydrofuran-2-yl)methanol (1.50 g, 6.75 mmol, 1.0 equiv.) in anhydrous DCM (34 mL, 0.2 M) at 0 °C under N_2 were added benzoyl chloride (1.42 g, 10.1 mmol, 1.5 equiv.), pyridine (1.4 mL, 16.9 mmol, 2.5 equiv.), and DMAP (82.4 mg, 0.67 mmol, 0.1 equiv). The reaction mixture was warmed to rt and stirred for 18 h. The mixture was diluted with DCM and washed with brine. The combined organic layers were dried over anhydrous Na_2SO_4, filtered, and concentrated under reduced pressure to afford the crude product, which was used directly in the next step without further purification.

The crude product was dissolved in MeOH (31 mL, 0.2 M), and $Pd(OH)_2/C$ (43.0 mg, 61.3 µmol, 20 wt %) was added. The mixture was stirred under an atmosphere of H_2 for 5 h. Upon completion, the mixture was filtered through a pad of Celite and concentrated under reduced pressure. The crude mixture was purified by flash chromatography using silica gel (CyHex/EtOAc 3:2) affording product as a colorless oil in 86% yield over 2 steps (5:1 mixture of diastereomers) (1.25 g, 5.27 mmol).

^{1}H NMR (400 MHz, $CDCl_3$) δ 8.07 – 7.99 (m, 2H), 7.62 – 7.49 (m, 1H), 7.46 – 7.35 (m, 2H), 4.46 – 4.25 (m, 3H), 4.23 – 4.12 (m, 1H), 3.70 (ddd, *J* = 17.2, 11.7, 3.2 Hz, 1H), 3.51 (dd, *J* = 11.7, 5.8 Hz, 1H), 2.40 (br, 1H), 2.17 – 1.93 (m, 2H), 1.91 – 1.67 (m, 2H).

^{13}C NMR (101 MHz, $CDCl_3$) δ 166.8, 166.6, 133.2, 133.1, 130.1, 130.0, 129.8, 128.5, 128.4, 80.6, 80.1, 67.0, 66.9, 64.8, 64.6, 28.6, 28.1, 27.4, 26.8.
HRMS (ESI): [m/z] calculated for $C_{13}H_{16}NaO_4$ ($[M+Na]^+$): 259.0941; Found: 259.0941.
The characterization data is consistent with the literature.[259]

(5-((Benzyloxy)methyl)tetrahydrofuran-2-yl)methyl acetate (7.4a)

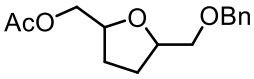

$C_{15}H_{20}O_4$
264.14 g/mol

Following a reported procedure,[106] to a solution of (5-((benzyloxy)-methyl)-tetrahydrofuran-2-yl)methanol (1.50 g, 6.75 mmol, 1.0 equiv.) in pyridine (34 mL, 0.2 M) at room temperature under nitrogen was added acetic anhydride (1.9 mL, 20.2 mmol, 3.0 equiv). The mixture was stirred for 18 h, then diluted with EtOAc and cold water. The organic phase was separated, and the aqueous phase was extracted with EtOAc (3 times). The combined organic layers were washed with brine, dried over anhydrous Na_2SO_4, filtered, and concentrated under reduced pressure. The crude mixture was purified by flash chromatography using silica gel (CyHex/EtOAc 8:2) affording (5-((benzyloxy)methyl)tetrahydrofuran-2-yl)methyl acetate as a colorless oil in 93% yield (2:1 mixture of diastereomers) (1.66 g, 6.28 mmol).

^{1}H NMR (600 MHz, $CDCl_3$) δ 7.34 – 7.33 (m, 5H,minor epimer), 7.33 – 7.32 (m, 5H, major epimer), 4.61 – 4.53 (m, 4H, both epimers), 4.36 – 4.08 (m, 6H, both epimers), 4.09 – 3.87 (m, 2H, both epimers), 3.55 – 3.39 (m, 4H, both epimers), 2.08 (s, 3H, minor epimer), 2.05 (s, 1H, major epimer), 2.00 – 1.93 (m, 2H, both epimers), 1.80 – 1.61 (m, 2H, both epimers).
^{13}C NMR (151 MHz, $CDCl_3$) δ 171.0, 171.0, 138.3, 133.0, 129.6, 128.3, 127.6, 127.5, 78.9, 78.4, 76.8, 73.4, 72.7, 72.6, 66.7, 66.6, 28.3, 28.2, 27.9, 27.8, 20.9, 20.9.
HRMS (ESI): [m/z] calculated for $C_{15}H_{20}NaO_4$ ($[M+Na]^+$): 287.1254; Found: 287.1254.

(5-(Hydroxymethyl)tetrahydrofuran-2-yl)methyl acetate (7.4)

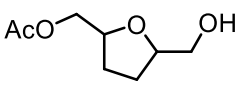

$C_8H_{14}O_4$
174.10 g/mol

Following a reported procedure,[106] to a solution of (5-((benzyloxy)-methyl)-tetrahydrofuran-2-yl)methyl acetate (1.61 g, 6.05 mmol, 1.0 equiv) in MeOH (30 mL, 0.2

M) was added $Pd(OH)_2/C$ (42.5 mg, 60.5 µmol, 20 wt %). The mixture was stirred under an atmosphere of H_2 for 5 h. Upon completion, the reaction mixture was filtered through a pad of Celite and concentrated under reduced pressure. The crude mixture was purified by flash chromatography using silica gel (CyHex/EtOAc 1:1) affording product as a colorless oil in 86% yield (2:1 mixture of diastereomers) (1.78 g, 8.53 mmol).

^{1}H NMR (600 MHz, $CDCl_3$) (both epimers) δ 4.27 – 3.87 (m, 8H), 3.67 (ddd, *J* = 2.5, 11.7, 3.3 Hz, 2H), 3.47 (ddd, *J* = 1.4, 11.7, 5.3 Hz, 2H), 2.38 (br, 2H), 2.06 (d, *J* = 1.5 Hz, 6H), 2.02 – 1.86 (m, 4H), 1.84 – 1.62 (m, 4H).
^{13}C NMR (151 MHz, $CDCl_3$) δ 171.2, 171.1, 80.6, 80.0, 77.4, 66.7, 66.6, 64.7, 64.6, 28.5, 28.1, 27.3, 26.8, 21.0.
HRMS (ESI): [m/z] calculated for $C_8H_{14}NaO_4$ ($[M+Na]^+$): 197.0784; Found: 197.0784.
The characterization data is consistent with the literature.[106]

(5-((Benzyloxy)methyl)tetrahydrofuran-2-yl)methyl-4-methylbenzenesulfonate (7.5a)

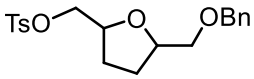

$C_{20}H_{24}O_5S$
376.13 g/mol

Following a reported procedure,[106] to a solution of (5-((benzyloxy)-methyl)-tetrahydrofuran-2-yl)methanol (3.5 g, 15.8 mmol, 1.0 equiv.) in anhydrous CH_2Cl_2 (121 mL, 0.13M) at 0 °C under N_2 were added *p*-toluenesulfonyl chloride (6.09 g, 31.9 mmol, 2.0 equiv), pyridine (31 mL, 0.5 M), and DMAP (196 mg, 1.60 mmol, 0.1 equiv). The mixture was stirred at room temperature for 7 h, then diluted with DCM and washed with water and brine. The combined organic layers was dried over anhydrous Na_2SO_4, filtered, and concentrated under reduced pressure. The crude mixture was purified by flash chromatography using silica gel (CyHex/EtOAc 3:2) affording (5-((benzyloxy)methyl)tetrahydrofuran-2-yl)methyl 4-methylbenzenesulfonate as a colorless oil in 88% yield (1:1 mixture of diastereomers) (5.32 g, 13.9 mmol).

^{1}H NMR (600 MHz, $CDCl_3$) δ 7.94 – 7.67 (m, 2H), 7.48 – 7.18 (m, 7H), 4.62 – 4.41 (m, 2H), 4.28 – 4.17 (m, 0.5H), 4.13 – 4.08 (m, 1.5H), 4.04 – 3.96 (m, 2H), 3.46 – 3.38 (m, 2H), 2.42 (d, *J* = 1.2 Hz, 3H), 2.19 – 1.87 (m, 2H), 1.79 – 1.63 (m, 2H).
^{13}C NMR (151 MHz, $CDCl_3$) δ 144.8, 144.8, 138.3, 133.1, 133.1, 129.9, 128.4, 128.0, 128.0, 127.7, 79.2, 78.7, 76.6, 76.4, 73.4, 73.4, 72.7, 72.6, 71.6, 71.6, 28.2, 28.1, 27.8, 27.8, 21.7.

HRMS (ESI): [m/z] calculated for $C_{20}H_{24}NaO_5S$ ([M+Na]$^+$): 399.1236; Found: 399.1236.

(5-(Hydroxymethyl)tetrahydrofuran-2-yl)methyl 4-methylbenzenesulfonate (7.5)

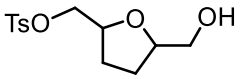

$C_{13}H_{18}O_5S$
286.09 g/mol

Following a reported procedure,[106] to solution of (5-((benzyloxy)-methyl)-tetrahydrofuran-2-yl)-methyl-4-methylbenzenesulfonate (5.2 g, 13.8 mmol, 1.0 equiv) in MeOH (69 mL, 0.2 M) was added $Pd(OH)_2/C$ (97 mg, 138 µmol, 20 wt %). The mixture was stirred under an atmosphere of H_2 for 5 h. Upon completion, the reaction mixture was filtered through a pad of Celite and concentrated under reduced pressure. The crude mixture was purified by flash chromatography using silica gel (CyHex/EtOAc 1:1) affording product as a colorless oil in 71% yield (1:1 mixture of diastereomers) (2.81 g, 9.81 mmol).

^{1}H NMR (600 MHz, $CDCl_3$) δ 7.77 (dd, *J* = 8.4, 2.1 Hz, 2H), 7.50 – 7.21 (m, 2H), 4.18 (tdd, *J* = 7.1, 5.6, 4.1 Hz, 0.5H), 4.15 – 4.10 (m, 0.5H), 4.06 (dd, *J* = 10.4, 3.9 Hz, 0.5H), 4.03 – 3.93 (m, 2.5H), 3.64 (dd, *J* = 11.8, 3.2 Hz, 0.5H), 3.58 (dd, *J* = 11.7, 3.3 Hz, 0.5H), 3.41 (ddd, *J* = 11.8, 8.5, 5.6 Hz, 1H), 2.42 (d, *J* = 1.3 Hz, 3H), 2.15 (br, 1H), 2.05 – 1.81 (m, 2H), 1.79 – 1.60 (m, 2H).
^{13}C NMR (151 MHz, $CDCl_3$) δ 145.0, 145.0, 133.1, 133.0, 129.9, 129.9, 128.0, 128.0, 80.7, 80.2, 76.6, 76.4, 71.7, 71.5, 64.7, 64.6, 28.3, 27.8, 27.2, 26.7, 21.7.
HRMS (ESI): [m/z] calculated for $C_{13}H_{18}NaO_5S$ ([M+Na]$^+$): 309.0768; Found: 309.0768.
The characterization data is consistent with the literature.[106]

((5-((Benzyloxy)methyl)tetrahydrofuran-2-yl)methoxy)(tert-butyl)diphenylsilane (7.6a)

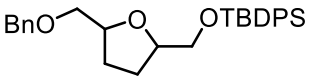

$C_{29}H_{36}O_3Si$
460.24 g/mol

Following a reported procedure,[106] to a solution of (5-((benzyloxy)-methyl)-tetrahydrofuran-2-yl)-methyl-4-methylbenzenesulfonate (1.10 g, 4.95 mmol, 1.0 equiv.) in DCM (71 mL, 0.07 M) at 0 °C under N_2 were added TBDPSCl (2.72 g, 9.89 mmol, 2.0 equiv) and imidazole (1.35 g, 19.8 mmol, 4.0 equiv). The mixture was stirred at rt for 4 h, then diluted with EtOAc and washed with water and brine. The combined organic layers were dried over anhydrous Na_2SO_4, filtered, and concentrated under reduced

pressure. The crude mixture was purified by flash chromatography using silica gel (CyHex/EtOAc 3:2) affording product as a colorless oil in 98% yield (1:2:1 mixture of diastereomers) (2.24 g, 4.87 mmol).

^{1}H NMR (400 MHz, $CDCl_3$) δ 7.78 – 7.65 (m, 8H), 7.47 – 7.26 (m, 17H), 4.70 – 4.40 (m, 2H), 4.31 – 3.94 (m, 2H), 3.88 – 3.60 (m, 2H), 3.60 – 3.38 (m, 2H), 2.13 – 1.80 (m, 5H), 1.79 – 1.57 (m, 1H), 1.13 – 1.01 (m, 18H).
^{13}C NMR (101 MHz, $CDCl_3$) δ 138.5, 135.8, 135.8, 135.3, 134.9, 133.8, 129.8, 129.7, 129.7, 128.4, 127.8, 127.8, 127.8, 127.6, 80.1, 78.8, 73.5, 73.4, 73.3, 73.0, 66.6, 66.4, 28.6, 28.3, 28.1, 27.7, 27.0, 26.7, 19.4, 19.1.
HRMS (ESI): [m/z] calculated for $C_{29}H_{36}NaO_3Si$ ($[M+Na]^+$): 483.2327; Found: 483.2327.

(5-(((*tert*-Butyldiphenylsilyl)oxy)methyl)tetrahydrofuran-2-yl)methanol (7.6)

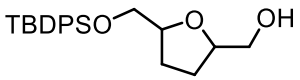

$C_{22}H_{30}O_3Si$
370.1964

Following a reported procedure,[106] to a solution of (5-((benzyloxy)-methyl)-tetrahydrofuran-2-yl)methyl-4-methylbenzenesulfonate (2.10 g, 4.56 mmol, 1.0 equiv) in MeOH (23 mL, 0.2 M) was added $Pd(OH)_2/C$ (32.0 mg, 45.6 µmol, 20 wt %). The mixture was stirred under an atmosphere of H_2 for 5 h. Upon completion, the reaction mixture was filtered through a pad of Celite and concentrated under reduced pressure. The crude mixture was purified by flash chromatography using silica gel (CyHex/EtOAc 9:1 → CyHex/EtOAc 9:1) affording product as a colorless oil in 64% yield (1:2:1 mixture of diastereomers) (1.08 g, 2.92 mmol).

^{1}H NMR (400 MHz, $CDCl_3$) δ 7.75 – 7.64 (m, 8H), 7.45 – 7.34 (m, 12H), 4.24 – 4.02 (m, 4H), 3.90 – 3.58 (m, 6H), 3.53 – 3.43 (m, 2H), 2.10 – 1.78 (m, 9zH), 1.75 – 1.62 (m, 1H), 1.07 (s, 9H), 1.06 (s, 9H).
^{13}C NMR (101 MHz, $CDCl_3$) δ 135.8, 135.8, 135.7, 133.8, 133.7, 133.5, 129.9, 129.8, 129.8, 127.9, 127.8, 127.8, 80.2, 80.0, 79.8, 66.6, 66.1, 65.6, 65.1, 28.3, 27.8, 27.5, 27.5, 27.0, 19.4, 19.4.
HRMS (ESI): [m/z] calculated for $C_{22}H_{30}NaO_3Si$ ($[M+Na]^+$): 393.1856; Found: 393.1856.
The characterization data is consistent with the literature.[106]

tert-Butyldimethyl(oxiran-2-ylmethoxy)silane (7.7a)

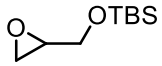

$C_9H_{20}O_2Si$
88.12 g/mol

Following a modified reported procedure,[254] to a solution of (±)-glycidol (7.2 mL, 108 mmol, 1 equiv.) in dry THF (360 mL, 0.3 M) at 0 °C under N_2 was added imidazole (9.56 g, 140 mmol, 1.3 equiv). TBSCl (21.6 g, 140 mmol, 1.3 equiv.) in THF (40 mL) was added dropwise, and the reaction mixture was warmed to rt and stirred for 18 h. Upon completion, the reaction mixture was diluted with EtOAc and washed sequentially with saturated aqueous $NaHCO_3$ and brine. The combined organic layers were dried over anhydrous Na_2SO_4, filtered, and concentrated under reduced pressure. The crude mixture was purified by flash chromatography using silica gel (PE/Et_2O 49:1) affording product as a colorless oil in 31% yield (1:1 mixture of diastereomers) (6.45 g, 34.3 mmol).

^{1}H NMR (600 MHz, $CDCl_3$) δ 3.84 (dd, *J* = 11.9, 3.2 Hz, 1H), 3.66 (dd, *J* = 11.9, 4.8 Hz, 1H), 3.13 – 3.03 (m, 1H), 2.76 (dd, *J* = 5.2, 4.0 Hz, 1H), 2.63 (dd, *J* = 5.2, 2.7 Hz, 1H), 0.90 (s, 9H), 0.08 (s, 3H), 0.07 (s, 3H).
^{13}C NMR (151 MHz, $CDCl_3$) δ 63.9, 52.6, 44.6, 26.0, 18.5, -5.2.
HRMS (ESI): [m/z] calculated for $C_9H_{20}NaO_2Si$ ([M+Na]$^+$): 211.1124; Found: 211.1125.
The characterization data is consistent with the literature. [254]

1-((_tert_-Butyldimethylsilyl)oxy)hex-5-en-2-ol (7.7b)

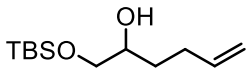

$C_{12}H_{26}O_2Si$
230.17 g/mol

Following reported procedure,[254] to a solution of the *tert*-butyldimethyl(oxiran-2-ylmethoxy)silane (6.40 g. 33.9 mmol, 1.0 equiv.) and copper(I) iodide (647 mg, 3.4 mmol, 0.1 equiv.) in THF (113 mL .0.3 M), cooled to 0 °C, allylmagnesium bromide (26 mL, 47.6 mmol, 1.5 equiv.) was added dropwise. The reaction mixture was allowed to warm to room temperature and stirred for 5 hours. Upon completion, the reaction was quenched with saturated aqueous NH_4Cl. The mixture was extracted with EtOAc (3 times), and the combined organic layers were washed with brine, dried over anhydrous Na_2SO_4, filtered, and concentrated under reduced pressure. . The crude mixture was purified by flash chromatography using silica gel (CyHex/EtOAc 3:2) affording product as a colorless oil in 73% yield (1:1 mixture of diastereomers) (5.78 g, 25.1 mmol).

^{1}H NMR (400 MHz, $CDCl_3$) δ 5.83 (ddt, *J* = 16.9, 10.2, 6.6 Hz, 1H), 5.09 – 4.92 (m, 2H), 3.69 – 3.60 (m, 2H), 3.45 – 3.36 (m, 1H), 2.30 – 2.06 (m, 3H), 1.61 – 1.41 (m, 2H), 0.90 (s, 9H), 0.07 (s, 6H).
^{13}C NMR (101 MHz, $CDCl_3$) δ 138.5, 114.9, 71.4, 67.3, 32.1, 30.0, 26.0, 18.4, -5.2, -5.3.
HRMS (ESI): [m/z] calculated for $C_{12}H_{26}NaO_2Si$ ($[M+Na]^+$): 253.1596; Found: 253.1596.
The characterization data is consistent with the literature.[254]

(5-(((*tert*-Butyldimethylsilyl)oxy)methyl)tetrahydrofuran-2-yl)methanol (7.7)

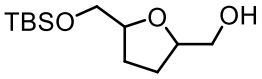

$C_{12}H_{26}O_3Si$
246.16 g/mol

Following reported procedure,[254] a solution of the corresponding alcohol 1-((*tert*-butyldimethylsilyl)oxy)hex-5-en-2-ol (5.80 g. 25.2 mmol, 1.0 equiv.) in DCM (125 mL, 0.2 M) was cooled to 0 °C. To this solution, *m*CPBA (6.76 g, 30.2 mmol, 1.2 equiv.) was added in a single portion. The reaction mixture was subsequently allowed to warm to ambient temperature and stirred for 18 hours. Upon completion, the reaction was quenched by the addition of saturated aqueous $NaHCO_3$. The resulting mixture was extracted with DCM (3 times). The combined organic layers were dried over anhydrous Na_2SO_4, filtered, and concentrated under reduced pressure. The crude mixture was purified by flash chromatography using silica gel (PE/Et_2O 3:2) affording product as a colorless oil in 86% yield (1:1 mixture of diastereomers) (5.33 g, 21.7 mmol).

^{1}H NMR (400 MHz, $CDCl_3$) δ 4.18 – 3.99 (m, 2H), 3.86 – 3.72 (m, 1H), 3.67 – 3.54 (m, 2H), 3.52 – 3.40 (m, 1H), 2.52 (br, 1H), 2.18 – 1.84 (m, 3H), 1.83 – 1.52 (m, 1H), 1.03 – 0.68 (m, 9H), 0.12 – -0.07 (m, 6H).
^{13}C NMR (101 MHz, $CDCl_3$) δ 80.2, 80.1, 80.0, 79.9, 66.0, 65.7, 65.5, 65.0, 28.3, 27.8, 27.7, 27.5, 26.1, -5.2, -5.3, -5.3.
HRMS (ESI): [m/z] calculated for $C_{12}H_{26}NaO_3Si$ ($[M+Na]^+$): 269.1544; Found: 269.1544.
The characterization data is consistent with the literature.[254]

(5-(Azidomethyl)tetrahydrofuran-2-yl)methanol (7.8)

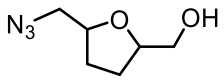

$C_6H_{11}N_3O_2$
157.08 g/mol

Following the reported procedure,[260] to a solution of (5-(hydroxymethyl)tetrahydrofuran-2-yl)methyl 4-methylbenzenesulfonate (950 mg, 3.32 mmol, 1.0 equiv.) in dry DMF (9 mL,0.36 M) was added NaN_3 (431 mg, 6.64 mmol, 2.0 equiv.). The reaction mixture was heated at 80 °C with stirring for 3 h. After cooling to rt, the mixture was diluted with EtOAc, washed with water and brine, dried over anhydrous Na_2SO_4, filtered, and concentrated under reduced pressure. The crude mixture was purified by flash chromatography using silica gel (CyHex/EtOAc 7:3) affording product as a colorless oil in 85% yield (1:1 mixture of diastereomers) (808 mg, 2.82 mmol).

^{1}H NMR (400 MHz, $CDCl_3$) δ 4.32 – 4.01 (m, 2H), 3.78 – 3.64 (m, 1H), 3.61 – 3.43 (m, 2H), 3.37 (dd, *J* = 12.8, 3.9 Hz, 0.5H), 3.30 – 3.20 (m, 0.5H), 2.22 (br, 1H), 2.09 – 1.90 (m, 2H), 1.84 – 1.57 (m, 2H).
^{13}C NMR (101 MHz, $CDCl_3$) δ 80.5, 80.0, 78.4, 78.2, 65.2, 64.8, 54.7, 54.7, 29.3, 28.7, 27.6, 27.1.
HRMS (ESI): [m/z] calculated for $C_6H_{11}N_3NaO_2$ ([M+Na]$^+$): 180.0748; Found: 180.0743.
The characterization data is consistent with the literature.[260]

2-((5-(((*tert*-Butyldimethylsilyl)oxy)methyl)tetrahydrofuran-2-yl)methyl)isoindoline-1,3-dione (7.9a)

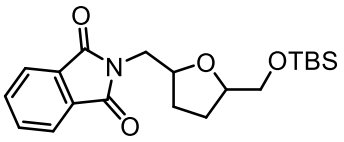

$C_{20}H_{29}NO_4Si$
375.18 g/mol

Following the reported procedure,[261] a stirred solution (5-(((*tert*-butyldimethylsilyl)-oxy)methyl)-tetrahydrofuran-2-yl)methanol (800 mg, 3.25mmol, 1.0 equiv.), PPh_3 (1.02 g, 3.90 mmol, 1.2 equiv.), and phthalimide (573 mg, 3.90 mmol, 1.2 equiv.) in THF (54 mL, 0.06M) was cooled to 0 °C under N_2. DEAD (1.8 mL, 3.90 mmol, 1.2 equiv) was added dropwise over 1 min, and the solution was warmed to rt and stirred for 18 h. The solvent was removed under reduced pressure, and the residue was taken up in EtOAc, washed sequentially with 0.1 N NaOH, 0.1 N HCl, and brine. The mixture was dried over anhydrous Na_2SO_4, filtered, and concentrated under reduced pressure. The crude mixture was purified by flash chromatography using silica gel (PE/Et_2O 8:2) affording product as a colorless oil in 78% yield (2:1 mixture of diastereomers) (952 mg, 2.53 mmol).

^{1}H NMR (600 MHz, $CDCl_3$) δ 7.87 – 7.80 (m, 2H), 7.76 – 7.65 (m, 2H), 4.36 (dq, *J* = 8.3, 6.0 Hz, 0.5H), 4.31 – 4.24 (m, 0.5H), 4.13 (tt, *J* = 6.4, 4.7 Hz, 0.5H), 4.00 – 3.93 (m, 0.5H), 3.87 – 3.77 (m, 1.5H), 3.70 (dd, *J* = 13.7, 5.8 Hz, 0.5H), 3.67 – 3.50 (m, 2H), 2.11 – 1.89 (m, 2H), 1.88 – 1.64 (m, 2H), 0.96 – 0.79 (m, 9H), 0.07 – -0.03 (m, 6H).
^{13}C NMR (151 MHz, $CDCl_3$) δ 168.9, 168.5, 168.4, 134.0, 134.0, 132.3, 132.3, 132.1, 132.0, 123.4, 123.2, 80.5, 79.4, 76.8, 76.5, 66.1, 65.8, 62.8, 53.6, 51.9, 47.3, 42.6, 42.0, 29.4, 29.2, 27.8, 27.5, 26.1, 26.0, 25.8, 18.5, -5.2, -5.2, -5.2, -5.4, -5.5.
HRMS (ESI): [m/z] calculated for $C_{20}H_{29}NNaO_4Si$ ([M+Na]$^+$): 398.1759; Found: 398.1759.

2-((5-(Hydroxymethyl)tetrahydrofuran-2-yl)methyl)isoindoline-1,3-dione (7.9)

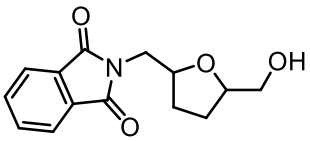

$C_{14}H_{15}NO_4$
261.10 g/mol

Following a modified literature procedure,[262] to a solution of 2-((5-(((*tert*-butyldimethylsilyl)oxy)methyl)tetrahydrofuran-2-yl)methyl)isoindoline-1,3-dione (930 mg, 2.48 mmol, 1.0 equiv.) in dry THF (0.04 M) at 0 °C was added TBAF 1.0 M in THF (6.2 mL, 6.19 mmol, 2.5 equiv.) dropwise, and the reaction mixture was stirred at room temperature for 1 h. The mixture was concentrated under reduced pressure, and the crude product was purified by was purified by flash chromatography using silica gel (CyHex/EtOAc 1:1) affording product as a colorless liquid in 42% yield (2:1 mixture of diastereomers) (271 mg, 1.04 mmol).

Major diastereomer
^{1}H NMR (600 MHz, $CDCl_3$) δ 7.87 – 7.79 (m, 2H), 7.72 – 7.68 (m, 2H), 4.43 – 4.34 (m, 1H), 4.22 – 4.16 (m, 1H), 3.81 (dd, J = 13.8, 8.0 Hz, 1H), 3.65 – 3.59 (m, 2H), 3.54 – 3.42 (m, 1H), 2.46 (br, 1H), 2.18 – 1.99 (m, 4H).
^{13}C NMR (151 MHz, $CDCl_3$) δ 168.5, 134.1, 132.2, 123.4, 79.2, 76.6, 64.8, 41.8, 29.7, 26.9.
Minor diastereomer
^{1}H NMR (600 MHz, $CDCl_3$) δ 7.88 – 7.80 (m, 2H), 7.73 – 7.68 (m, 2H), 4.34 – 4.27 (m, 1H), 4.07 – 3.98 (m, 1H), 3.77 (dd, J = 12.4, 2.7 Hz, 1H), 3.74 – 3.67 (m, 2H), 3.50 – 3.42 (m, 1H), 2.46 (br, 1H), 1.90 – 1.79 (m, 2H), 1.79 – 1.68 (m, 2H).
^{13}C NMR (151 MHz, $CDCl_3$) δ 169.0, 134.2, 132.1, 123.6, 81.4, 76.6, 63.1, 43.7, 29.6, 25.6.
HRMS (ESI): [m/z] calculated for $C_{14}H_{15}NNaO_4$ ([M+Na]$^+$): 284.0892; Found: 284.0892.

The characterization data is consistent with the literature.[106]

(5-(Chloromethyl)tetrahydrofuran-2-yl)methanol (7.10)

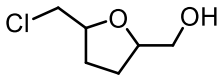

$C_6H_{11}ClO_2$
50.04 g/mol

Following **GP1**, starting from epichlorhydrin (1.0 mL, 12.8 mmol, 1.0 equiv.). The crude mixture was purified by flash chromatography using silica gel (PE: Et_2O 7:3) affording product over 2 steps as a colorless liquid in 82% yield (1:1 mixture of diastereomers) (1.58 g, 10.52 mmol).

^{1}H NMR (400 MHz, $CDCl_3$) δ 4.33 – 3.97 (m, 2H), 3.79 – 3.64 (m, 1H), 3.60 – 3.43 (m, 3H), 2.38 (br, 1H), 2.19 – 1.67 (m, 4H).
^{13}C NMR (101 MHz, $CDCl_3$) δ 80.6, 80.4, 78.9, 64.9, 64.8, 47.1, 29.9, 29.2, 27.4, 26.9.
HRMS (ESI): [m/z] calculated for $C_6H_{11}ClNaO_2$ ($[M+Na]^+$): 173.0338; Found: 173.0340.
R_f (PE: Et_2O 7:3) = 0.26 [$KMnO_4$]

(5-((Prop-2-yn-1-yloxy)methyl)tetrahydrofuran-2-yl)methanol (7.11)

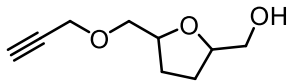

$C_9H_{14}O_3$
170.09 g/mol

Following **GP1**, starting from glycidylpropargylether (2.5 mL, 23.2 mmol, 1.0 equiv.). The crude mixture was purified by flash chromatography using silica gel (CyHex/EtOAc 1:1) affording product over 2 steps as a colorless liquid in 75% yield (1:1 mixture of diastereomers) (2.95 g, 17.3 mmol).

^{1}H NMR (400 MHz, $CDCl_3$) δ 4.27 – 4.15 (m, 3H), 4.17 – 4.07 (m, 1H), 3.70 – 3.60 (m, 1H), 3.56 (dd, *J* = 10.0, 3.7 Hz, 1H), 3.53 – 3.42 (m, 2H), 2.46 – 2.33 (m, 2H), 2.13 – 1.84 (m, 2H), 1.74 – 1.60 (m, 2H).
^{13}C NMR (151 MHz, $CDCl_3$) δ 80.3, 79.9, 79.7, 79.5, 78.4, 78.1, 74.8, 74.7, 72.5, 72.3, 58.6, 58.6, 28.6, 28.2, 27.3, 27.1.
IR (ATR): $\tilde{\nu}$ [cm^{-1}] = 3415, 3284, 2871, 1460, 1356, 1253, 1076, 1022, 939, 905, 811, 660.
HRMS (ESI): [m/z] calculated for $C_9H_{14}NaO_3$ ($[M+Na]^+$): 193.0835; Found: 193.0837.
R_f (CyHex/EtOAc, 3:2) = 0.29 [$KMnO_4$]

((5-((Allyloxy)methyl)tetrahydrofuran-2-yl)methoxy)(*tert*-butyl)dimethylsilane (7.12a)

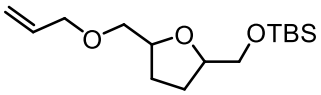

$C_{15}H_{30}O_3Si$
286.19 g/mol

Following a modified literature procedure,[263] to a solution of (5-(((*tert*-butyldimethylsilyl)-oxy)methyl)tetrahydrofuran-2-yl)methanol (1.0 g 4.06 mmol, 1.0 equiv.) in DMF (32 mL) cooled to 0 °C, NaH (0.2 g 4.87 mmol, 60% dispersion in mineral oil, 1.2 equiv.) was added carefully in portions. After gas evolution subsided, allyl bromide (0.5 mL, 5.78 mmol, 1.4 equiv.) was added dropwise over 30 min. The reaction mixture was stirred at room temperature fors 40 h and then quenched with water (15 mL). The mixture was diluted with additional water and extracted with CH_2Cl_2 (3 times). The combined organic layers were washed with brine, dried over Na_2SO_4, filtered, and concentrated under reduced pressure. The crude mixture was purified by flash chromatography using silica gel (CyHex/EtOAc 6:4) to afford product as a yellow oil in 78% yield (1:1 mixture of diastereomers) (910 mg, 3.18 mmol).

^{1}H NMR (600 MHz, $CDCl_3$) δ 5.97 – 5.86 (m, 1H), 5.32 – 5.22 (m, 1H), 5.21 – 5.13 (m, 1H), 4.17 (dtd, *J* = 7.4, 6.0, 4.7 Hz, 0.5H), 4.13 – 3.97 (m, 3.5H), 3.65 (ddd, *J* = 10.4, 4.4, 1.9 Hz, 1H), 3.55 (td, *J* = 10.5, 5.6 Hz, 1H), 3.48 – 3.39 (m, 2H), 2.05 – 1.96 (m, 1H), 1.96 – 1.88 (m, 1H), 1.82 – 1.74 (m, 1H), 1.71 – 1.63 (m, 1H), 0.89 (d, *J* = 1.6 Hz, 9H), 0.05 (s, 6H).
^{13}C NMR (151 MHz, $CDCl_3$) δ 135.1, 117.0, 80.3, 79.9, 78.7, 78.4, 73.3, 73.1, 72.5, 72.5, 66.0, 65.9, 28.6, 28.2, 28.2, 27.7, 26.1, 26.1, 18.5, -5.2.
HRMS (ESI): [m/z] calculated for $C_{15}H_{30}NaO_3Si$ ($[M+Na]^+$): 309.1856; Found: 309.1856.

(5-((Allyloxy)methyl)tetrahydrofuran-2-yl)methanol (7.12)

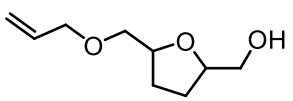

$C_9H_{16}O_3$
172.11 g/mol

Following a modified literature procedure,[262] to a solution of ((5-((allyloxy)-methyl)tetrahydrofuran-2-yl)methoxy)(*tert*-butyl)dimethylsilane (888 mg, 3.10 mmol, 1.0 equiv.) in dry THF (80 mL, 0.04 M) at 0 °C was added TBAF 1.0 M in THF (7.7 mL, 7.75 mmol, 2.5 equiv.) dropwise, and the reaction mixture was stirred at room temperature for

1 h. The mixture was concentrated under reduced pressure, and the crude product was purified by was purified by flash chromatography using silica gel (CyHex/EtOAc 1:1) affording product as a colorless liquid in 73% yield (1:1 mixture of diastereomers) (390 mg, 2.30 mmol).

^{1}H NMR (600 MHz, $CDCl_3$) δ 5.98 – 5.83 (m, 1H), 5.33 – 5.12 (m, 2H), 4.19 – 4.01 (m, 4H), 3.77 (dt, *J* = 11.6, 3.3 Hz, 0.53H), 3.67 (dt, *J* = 11.6, 3.3 Hz, 0.52H), 3.59 (dt, *J* = 10.0, 3.3 Hz, 0.55H), 3.51 – 3.43 (m, 2.64H), 2.22 (br, 1H), 2.03 – 1.86 (m, 3H), 1.76 – 1.67 (m, 1H).
^{13}C NMR (151 MHz, $CDCl_3$) δ 134.9, 134.6, 117.5, 117.3, 80.3, 79.8, 78.8, 78.4, 73.1, 72.7, 72.6, 72.5, 65.5, 64.9, 28.8, 28.3, 27.4, 27.4.
IR (ATR): $\tilde{\nu}$ [cm^{-1}] = 3393, 2921, 2871, 1725, 1456, 1421, 1349, 1257, 1048, 930, 882, 881.
HRMS (ESI): [m/z] calculated for $C_9H_{16}NaO_3$ ([M+Na]$^+$): 195.0985; Found: 195.0992.
R_f (CyHex/EtOAc 1:1) = 0.16 [$KMnO_4$].

(5-(((*tert*-Butyldimethylsilyl)oxy)methyl)tetrahydrofuran-2-yl)methyl 4-cyanobenzoate (7.13a)

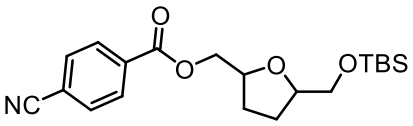

$C_{20}H_{29}NO_4Si$
375.19 g/mol

Following **GP4**, starting from 4-cyanobenzoic acid (502 mg, 3.41 mmol, 1.2 equiv) and (5-(((*tert*-butyldimethylsilyl)oxy)methyl)tetrahydrofuran-2-yl)methanol (700 mg, 2.84 mmol, 1.0 equiv). The crude mixture was purified by flash chromatography using silica gel (CyHex/EtOAc 8:2) to afford product as a colourless oil in 82% yield (1:1 mixture of diastereomers) (877 mg, 2.34 mmol).

^{1}H NMR (600 MHz, $CDCl_3$) δ 8.15 (dd, *J* = 7.8, 1.0 Hz, 2H), 7.74 (dd, *J* = 7.8, 1.1 Hz, 2H), 4.46 – 4.34 (m, 2H), 4.29 (dddd, *J* = 10.4, 7.3, 6.0, 2.6 Hz, 1.5H), 4.14 (tt, *J* = 6.7, 4.6 Hz, 0.5H), 4.07 (p, *J* = 5.6 Hz, 0.5H), 3.67 – 3.57 (m, 2H), 2.12 (td, *J* = 12.3, 5.3 Hz, 0.5H), 2.07 – 1.95 (m, 1.5H), 1.89 – 1.82 (m, 1H), 1.80 – 1.69 (m, 1H), 0.89 (dd, *J* = 4.0, 1.1 Hz, 9H), 0.10 – 0.01 (m, 6H).
^{13}C NMR (151 MHz, $CDCl_3$) δ 165.1, 165.0, 134.2, 132.3, 130.4, 118.1, 116.6, 80.7, 80.2, 68.1, 68.0, 65.8, 65.8, 28.5, 28.1, 27.9, 27.6, 26.1, 18.5, 18.5, -5.2, -5.2.
HRMS (ESI): [m/z] calculated for $C_{20}H_{29}NNaO_4Si$ ([M+Na]$^+$): 398.1758; Found: 398.1758.

R_f (CyHex/EtOAc, 8:2) = 0.23 [$KMnO_4$].

(5-(Hydroxymethyl)tetrahydrofuran-2-yl)methyl 4-cyanobenzoate (7.13)

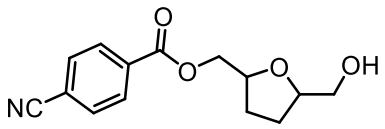

$C_{14}H_{15}NO_4$
261.10 g/mol

Following **GP4**, TBS-deprotection and flash chromatography using silica gel (CyHex/EtOAc 6:4) was isolated as a colorless liquid in 73% yield (1:1 mixture of diastereomers) (443 mg, 1.70 mmol).

^{1}H NMR (600 MHz, $CDCl_3$) δ 8.20 – 8.11 (m, 2H), 7.79 – 7.70 (m, 2H), 4.47 – 4.31 (m, 3H), 4.22 – 4.16 (m, 0.54H), 4.14 – 4.03 (m, 0.49H), 3.78 – 3.67 (m, 1H), 3.56 – 3.48 (m, 1H), 2.13 – 1.79 (m, 5H).
^{13}C NMR (151 MHz, $CDCl_3$) δ 165.2, 165.0, 134.0, 134.0, 132.4, 132.4, 130.4, 130.3, 118.1, 116.7, 116.7, 80.7, 80.1, 67.8, 67.7, 64.8, 64.6, 28.7, 28.2, 27.4, 26.8.
IR (ATR): $\tilde{\nu}$ [cm^{-1}] = 3428, 2946, 2876, 2231, 1719, 1450, 1405, 1358, 1310, 1268,1777, 1102, 1082, 1017, 978, 945, 914, 860, 765, 690.
HRMS (ESI): [m/z] calculated for $C_{14}H_{15}NNaO_4$ ($[M+Na]^+$): 284.0896; Found: 284.0893.
R_f (CyHex/EtOAc, 6:4) = 0.13 [$KMnO_4$].

(5-Hexyltetrahydrofuran-2-yl)methanol (7.14)

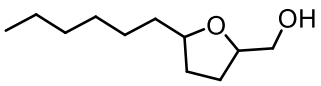

$C_{11}H_{22}O_2$
186.16 g/mol

Following **GP1**, starting from 1,2-epoxyoctane (1.5 mL, 9.77 mmol, 1.0 equiv.). The crude mixture was purified by flash chromatography using silica gel (CyHex/EtOAc 6:4 → CyHex/EtOAc 1:1) affording product over 2 steps as a colorless liquid in 76% yield (1:1 mixture of diastereomers) (1.57 g, 9.21 mmol).

^{1}H NMR (400 MHz, $CDCl_3$) δ 4.15 – 4.04 (m, 1H), 4.05 – 3.94 (m, 1H), 3.96 – 3.88 (m, 1H), 3.91 – 3.80 (m, 1H), 3.66 (ddd, *J* = 25.5, 11.5, 3.4 Hz, 2H), 3.47 (ddd, *J* = 11.5, 6.0, 3.9 Hz, 2H), 2.06 – 1.85 (m, 6H), 1.77 – 1.37 (m, 7H), 1.38 – 1.18 (m, 19H), 0.92 – 0.84 (m, 4H).

^{13}C NMR (101 MHz, $CDCl_3$) δ 80.2, 79.5, 79.1, 78.8, 65.3, 65.1, 35.9, 35.7, 32.0, 31.8 (d, *J* = 1.9 Hz), 31.4, 29.4, 27.5, 27.0, 26.2 (d, *J* = 3.9 Hz), 22.6, 14.1.

IR (ATR): $\tilde{\nu}$ [cm^{-1}] = 3412, 2954, 2926, 2857, 1721, 1460, 1431, 1378, 1286, 1242, 1132, 1098, 1039, 960, 899, 880, 813, 752, 724, 704, 674.

HRMS (ESI): [m/z] calculated for $C_{11}H_{22}NaO_2$ ($[M+Na]^+$): 209.1517; Found: 209.1517.

R_f (CyHex/EtOAc, 1:1) = 0.34 [$KMnO_4$]

The characterization data is consistent with the literature.[264]

(5-(4-Methoxyphenyl)tetrahydrofuran-2-yl)methanol (7.15)

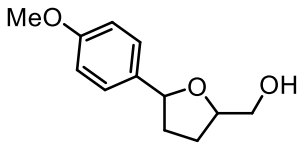

$C_{12}H_{16}O_3$
208.11 g/mol

Following **GP3**, starting from 4-methoxybenzaldehyde (1.0 mL, 8.23 mmol, 1.0 equiv.). The crude mixture was purified by flash chromatography using silica gel (CyHex/EtOAc 3:2) affording product over 2 steps as a colorless liquid in 84% yield (1:1 mixture of diastereomers) (1.44 g, 6.93 mmol).

^{1}H NMR (400 MHz, $CDCl_3$) δ 7.32 – 7.23 (m, 2H), 7.00 – 6.84 (m, 2H), 4.94 (dd, *J* = 8.4, 5.7 Hz, 0.5H), 4.86 (dd, *J* = 7.9, 6.3 Hz, 0.5H), 4.35 (dtd, *J* = 7.5, 6.5, 3.3 Hz, 0.5H), 4.18 (dtd, *J* = 7.8, 6.0, 3.4 Hz, 0.5H), 3.80 (s, 3H), 3.74 (dd, *J* = 26.7, 3.3 Hz, 1H), 3.61 (ddd, *J* = 18.0, 11.6, 6.1 Hz, 1H), 2.38 – 2.21 (m, 1H), 2.17 – 1.98 (m, 1H), 1.96 – 1.75 (m, 2H), 1.70 – 1.59 (m, 7H).

^{13}C NMR (101 MHz, $CDCl_3$) δ 162.6, 159.3, 127.5, 127.2, 114.0, 81.5, 80.8, 80.0, 79.8, 65.6, 65.4, 55.5, 35.5, 34.3, 28.1, 27.7.

HRMS (ESI): [m/z] calculated for $C_{12}H_{16}NaO_3$ ($[M+Na]^+$): 231.0993; Found: 231.0993.

The characterization data is consistent with the literature.[265]

(5-(4-Bromophenyl)tetrahydrofuran-2-yl)methanol (7.16)

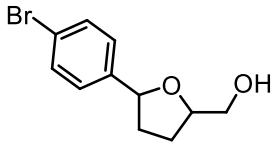

$C_{11}H_{13}BrO_2$
256.01 g/mol

Following **GP3**, starting from 4-bromobenzaldehyde (800 µL, 8.00 mmol, 1.0 equiv.). The crude mixture was purified by flash chromatography using silica gel (CyHex/EtOAc 1:1) affording product over 2 steps as a colorless liquid in 90% yield (1:1 mixture of diastereomers) (1.73 g, 6.972 mmol).

^{1}H NMR (400 MHz, $CDCl_3$) δ 7.48 – 7.43 (m, 2H), 7.25 – 7.18 (m, 2H), 4.95 (dd, *J* = 8.0, 6.2 Hz, 0.5H), 4.87 (dd, *J* = 8.0, 6.5 Hz, 0.5H), 4.40 – 4.30 (m, 0.5H), 4.19 (dtd, *J* = 7.6, 6.2, 3.4 Hz, 0.5H), 3.77 (ddd, *J* = 23.1, 11.6, 3.3 Hz, 1H), 3.61 (ddd, *J* = 22.0, 11.6, 6.1 Hz, 1H), 2.48 – 2.24 (m, 1H), 2.17 (br, 1H), 2.13 – 2.01 (m, 1H), 1.91 – 1.72 (m, 2H).
^{13}C NMR (101 MHz, $CDCl_3$) δ 142.2, 131.6, 131.6, 127.7, 127.4, 121.4, 121.2, 80.9, 80.4, 80.4, 80.2, 65.5, 65.3, 35.6, 34.4, 27.9, 27.6.
HRMS (ESI): [m/z] calculated for $C_{11}H_{13}BrNaO_2$ ($[M+Na]^+$): 278.9994; Found: 278.9991.
The characterization data is consistent with the literature.[265]

(5-(Thiophen-2-yl)tetrahydrofuran-2-yl)methanol (7.17)

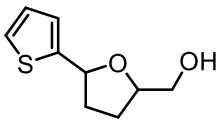

$C_9H_{12}O_2S$
184.06 g/mol

Following **GP3**, starting from thiophen-2-carbaldehyde (1.0 mL, 10.7 mmol, 1.0 equiv.). The crude mixture was purified by flash chromatography using silica gel (CyHex/EtOAc 4:1) affording product over 2 steps as a yellow oil in 83% yield (1:1 mixture of diastereomers) (1.63 g, 8.85 mmol).

^{1}H NMR (600 MHz, $CDCl_3$) δ 7.24 – 7.20 (m, 1H), 6.99 – 6.93 (m, 2H), 5.25 (t, *J* = 6.7 Hz, 1H), 5.19 (t, *J* = 6.7 Hz, 1H), 4.30 (tdd, *J* = 7.2, 5.9, 3.3 Hz, 1H), 4.16 (tdd, *J* = 7.0, 5.6, 3.3 Hz, 1H), 3.77 – 3.67 (m, 1H), 3.62 – 3.52 (m, 1H), 2.46 – 2.26 (m, 2H), 2.19 – 1.96 (m, 2H), 1.94 – 1.69 (m, 1H).
^{13}C NMR (151 MHz, $CDCl_3$) δ 146.8, 146.7, 126.9, 126.9, 124.8, 124.8, 124.3, 124.2, 80.5, 79.9, 77.5, 65.3, 65.1, 35.4, 34.9, 27.9, 27.7.

HRMS (ESI): [m/z] calculated for $C_9H_{12}NaO_2S$ ($[M+Na]^+$): 207.0450; Found: 207.0450. The characterization data is consistent with the literature.[266]

(5-(((1-(4-Bromophenyl)-1H-1,2,3-triazol-4-yl)methoxy)methyl)tetrahydrofuran-2-yl)methanol (7.18)

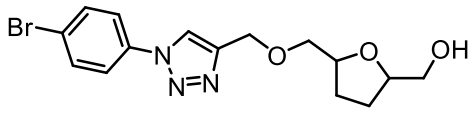

$C_{15}H_{18}BrN_3O_3$
367.05 g/mol

Following a modified literature procedure,[267] to a solution of (5-((prop-2-yn-1-yloxy)methyl)tetrahydrofuran-2-yl)methanol (100 mg, 0.59 mmol, 1.0 equiv) in *t*BuOH/H_2O (1:1, 15 mL) was added 1-azido-4-bromobenzene (1.41 mL, 0.71 mmol, 1.2 equiv), followed by sodium ascorbate (24 mg, 120 µmol, 0.2 equiv) and $CuSO_4 \cdot 5H_2O$ (15 mg, 60.0 µmol, 0.10 equiv.). The reaction mixture was stirred at rt for 21 h. The reaction was quenched with sat. aq. $NaHCO_3$ and extracted with EtOAc (3 times). The combined organic layers washed with brine, dried over anhydrous Na_2SO_4, filtered, and concentrated under reduced pressure. The crude mixture was purified by flash chromatography using silica gel (DCM/MeOH 9:1 → DCM/MeOH 7:3) to afford product as a colourless oil in 94% yield (1:1 mixture of diastereomers) (204 mg, 0.55 mmol).

^{1}H NMR (400 MHz, $CDCl_3$) δ 8.05 – 7.95 (m, 1H), 7.72 – 7.58 (m, 4H), 4.85 – 4.69 (m, 2H), 4.30 – 4.15 (m, 1H), 4.14 – 4.07 (m, 1H), 3.82 – 3.65 (m, 2H), 3.63 – 3.55 (m, 1H), 3.53 – 3.44 (m, 1H), 2.17 (br, 1H), 2.10 – 1.91 (m, 2H), 1.91 – 1.75 (m, 2H).
^{13}C NMR (101 MHz, $CDCl_3$) δ 146.0, 132.9, 122.4, 121.9, 120.6, 80.2, 78.6, 73.0, 65.2, 64.8, 28.1, 27.2.
IR (ATR): $\tilde{\nu}$ [cm^{-1}] = 3212, 2980, 2887, 1778, 1498, 1460, 1383, 1231, 1157, 1089, 1073, 988, 829.
HRMS (ESI): [m/z] calculated for $C_{15}H_{18}BrN_3NaO_3$ ($[M+Na]^+$): 390.0424; Found: 390.0424
R_f (DCM/MeOH, 4:1) = 0.24 [$KMnO_4$].

(5-(((*tert*-Butyldimethylsilyl)oxy)methyl)tetrahydrofuran-2-yl)methyl 3-(5-(2-fluorophenyl)-1,2,4-oxadiazol-3-yl)benzoate (7.19a)

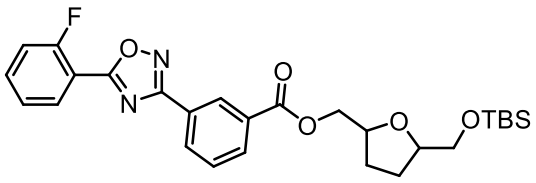

$C_{27}H_{33}FN_2O_5Si$
512.21 g/mol

Following **GP4**, using Ataluren (853 mg, 3.0 mmol, 1.2 equiv) and (5-(((*tert*-butyldimethylsilyl)oxy)methyl)tetrahydrofuran-2-yl)methanol (616 mg, 2.50 mmol, 1.0 equiv.). The crude mixture was purified by flash chromatography using silica gel (CyHex/EtOAc 17:3) to afford product as a colourless oil in 92% yield (1:1 mixture of diastereomers) (1.18 g, 2.30 mmol).

^{1}H NMR (600 MHz, $CDCl_3$) δ 8.91 – 8.81 (m, 1H), 8.37 (dt, *J* = 7.7, 1.5 Hz, 1H), 8.29 – 8.19 (m, 2H), 7.66 – 7.57 (m, 2H), 7.35 (tt, *J* = 7.7, 1.1 Hz, 1H), 7.32 – 7.27 (m, 1H), 4.48 – 4.30 (m, 3H), 4.22 – 4.05 (m, 2H), 3.72 – 3.58 (m, 2H), 2.19 – 2.05 (m, 1.5H), 2.02 – 1.97 (m, 0.5H), 1.90 – 1.77 (m, 1H), 0.89 (d, *J* = 6.2 Hz, 9H), 0.16 – -0.07 (m, 6H).
^{13}C NMR (151 MHz, $CDCl_3$) δ 168.2, 161.8, 160.1, 134.9, 132.5, 132.0, 131.2, 131.1, 129.2, 129.0, 129.0, 127.4, 124.9, 112.9, 80.7, 80.2, 67.7, 67.6, 65.9, 65.9, 60.5, 28.6, 28.2, 27.9, 27.8, 21.2, 18.5, 14.3, -5.1, -5.2, -5.2.
HRMS (ESI): [m/z] calculated for $C_{27}H_{33}FN_2NaO_5Si$ ($[M+Na]^+$): 535.2027; Found: 535.2035.
R_f (CyHex/EtOAc, 17:3) = 0.25 [$KMnO_4$].

(5-(Hydroxymethyl)tetrahydrofuran-2-yl)methyl 3-(5-(2-fluorophenyl)-1,2,4-oxadiazol-3-yl)benzoate (7.19)

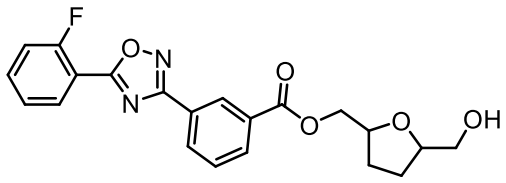

$C_{21}H_{19}FN_2O_5$
398.1278

Following **GP4** TBS-deprotection, the reaction mixture was purified by flash chromatography using silica gel (CyHex/EtOAc 4:6 → CyHex/EtOAc 1:1) to afford product as a white solid in 91% yield (1:1 mixture of diastereomers) (798 mg, 2.05 mmol).

^{1}H NMR (600 MHz, $CDCl_3$) δ 8.87 (d, *J* = 13.1 Hz, 1H), 8.38 (dd, 1H), 8.27 – 8.18 (m, 2H), 7.66 – 7.57 (m, 2H), 7.35 (t, *J* = 7.7 Hz, 1H), 7.33 – 7.26 (m, 1H), 4.54 – 4.48 (m, 0.55H), 4.46 – 4.34 (m, 2.55H), 4.27 – 4.20 (m, 0.54H), 4.16 – 4.12 (m, 0.55H), 3.75 (dd, *J* = 33.3, 11.8 Hz, 1H), 3.59 – 3.52 (m, 1H), 2.20 – 2.05 (m, 2H), 2.02 – 1.78 (m, 3H).
^{13}C NMR (151 MHz, $CDCl_3$) δ 173.2, 171.2, 168.2, 166.2, 165.9, 161.8, 160.1, 134.9, 134.8, 132.5, 132.5, 132.1, 132.0, 131.1, 131.1, 129.3, 129.2, 129.0, 129.0, 127.4, 127.4, 124.9, 117.4, 117.3, 112.9, 112.8, 80.7, 80.1, 67.4, 67.3, 64.9, 64.7, 60.5, 28.8, 28.3, 27.4, 26.9.
^{19}F NMR (376 MHz, $CDCl_3$) δ -108.2, -108.2.
IR (ATR): $\tilde{\nu}$ [cm^{-1}] =1719, 1619, 1552, 1461, 1351, 1264, 1225, 1150, 1055, 826, 744, 719.
HRMS (ESI): [m/z] calculated for $C_{21}H_{19}FN_2NaO_5$ ($[M+Na]^+$): 421.1170; Found: 421.1170.
R_f (CyHex/EtOAc, 6:4) = 0.09 [$KMnO_4$].

(4-Phenyltetrahydrofuran-2-yl)methanol (7.20)

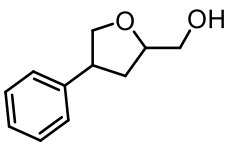

$C_{11}H_{14}O_2$
178.10 g/mol

Following **GP4**, starting from Methyl phenylacetate (1.5 g, 10.0 mmol, 1.0 equiv.). The crude mixture was purified by flash chromatography using silica gel (CyHex/EtOAc 3:2

→ CyHex/EtOAc 1:1) affording product over 3 steps as a colorless oil in 78% yield (2:1 mixture of diastereomers) (1.09 g, 6.13 mmol).

Major diastereomer

^{1}H NMR (400 MHz, $CDCl_3$) δ 7.32 – 7.23 (m, 5H), 4.32 – 4.23 (m, 2H), 3.91 – 3.75 (m, 2H), 3.67 (ddd, J = 24.8, 11.8, 5.9 Hz, 1H), 3.54 – 3.43 (m, 1H), 3.19 (br, J = 10.4 Hz, 1H), 2.32 – 2.20 (m, 1H), 2.18 – 2.06 (m, 1H).

^{13}C NMR (101 MHz, $CDCl_3$) δ 141.8, 128.6, 127.2, 126.6, 79.6, 74.7, 65.0, 44.8, 35.6.

Minor diastereomer

^{1}H NMR (400 MHz, $CDCl_3$) δ 7.40 – 7.33 (m, 5H), 4.42 – 4.33 (m, 2H), 3.85 – 3.73 (m, 2H), 3.74 – 3.60 (m, 1H), 3.54 (s, 1H), 3.19 (br, J = 10.4 Hz, 1H), 2.47 – 2.33 (m, 1H), 1.98 – 1.85 (m, 1H).

^{13}C NMR (101 MHz, $CDCl_3$) δ 141.0, 128.6, 127.2, 126.7, 80.6, 74.2, 64.6, 45.3, 35.7.

HRMS (ESI): [m/z] calculated for $C_{11}H_{14}NaO_2$ ($[M+Na]^+$): 201.0886; Found: 201.0886.

R_f (CyHex/EtOAc, 1:1) = 0.28 [$KMnO_4$].

The characterization data is consistent with the literature.[106]

Methyl 2-(4-methoxyphenyl)pent-4-enoate (7.21a)

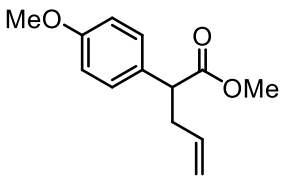

$C_{13}H_{16}O_3$
220.11 g/mol

Following the alkylation protocol of **GP4**, methyl 4-methoxyphenylacetate (1.2 mL, 6.66 mmol, 1.0 equiv.) was converted to methyl 2-(4-methoxyphenyl)pent-4-enoate. The crude mixture was purified by flash column chromatography on silica gel (PE/EtOAc 4:1) to afford product as a colorless oil in 96% yield (1.41 g, 6.39 mmol).

^{1}H NMR (400 MHz, $CDCl_3$) δ 7.23 (d, *J* = 8.7 Hz, 2H), 6.86 (d, *J* = 8.7 Hz, 2H), 5.71 (ddt, *J* = 17.1, 10.2, 6.8 Hz, 1H), 5.21 – 4.83 (m, 2H), 3.79 (s, 3H), 3.65 (s, 3H), 3.60 (t, 1H), 2.87 – 2.75 (m, 1H), 2.61 – 2.43 (m, 1H).

^{13}C NMR (101 MHz, $CDCl_3$) δ 174.3, 135.5, 130.7, 129.0, 117.0, 114.1, 55.4, 52.0, 50.6, 37.8.

HRMS (ESI): [m/z] calculated for $C_{13}H_{16}NaO_3$ ($[M+Na]^+$): 243.0992; Found: 243.0992.

The characterization data is consistent with the literature.[256]

2-(4-Methoxyphenyl)pent-4-en-1-ol (7.21b)

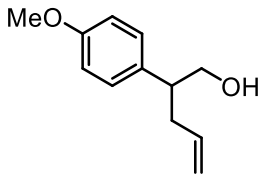

$C_{12}H_{16}O_2$
192.1150

Following the reduction protocol of **GP4**, methyl 2-(4-methoxyphenyl)pent-4-enoate (1.40 g, 6.36 mmol, 1.0 equiv) was converted to 2-(4-methoxyphenyl)pent-4-en-1-ol. The crude mixture was purified by flash column chromatography on silica gel (PE/EtOAc 3:2) to afford product as a colorless oil in 92% yield (1.12 g, 5.85 mmol).

^{1}H NMR (600 MHz, $CDCl_3$) δ 7.14 (d, *J* = 8.5 Hz, 2H), 6.88 (d, *J* = 8.7 Hz, 2H), 6.12 – 5.60 (m, 1H), 5.02 (dq, *J* = 17.1, 1.6 Hz, 1H), 4.96 (ddt, *J* = 10.2, 2.1, 1.1 Hz, 1H), 3.80 (s, 3H), 3.77 (dd, *J* = 10.8, 5.7 Hz, 1H), 3.70 (dd, *J* = 10.8, 7.5 Hz, 1H), 2.84 (tt, *J* = 7.7, 5.9 Hz, 1H), 2.55 – 2.41 (m, 1H), 2.39 – 2.32 (m, 1H), 1.41 (br, 1H).
^{13}C NMR (151 MHz, $CDCl_3$) δ 158.6, 136.6, 133.9, 129.1, 116.4, 114.2, 67.2, 55.4, 47.5, 36.9.
HRMS (ESI): [m/z] calculated for $C_{12}H_{16}NaO_2$ ($[M+Na]^+$): 215.1043; Found: 215.1043.

(4-(4-Methoxyphenyl)tetrahydrofuran-2-yl)methanol (7.21)

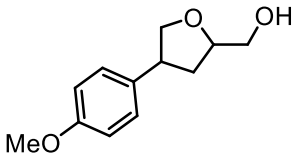

$C_{12}H_{16}O_3$
208.11 g/mol

Following the epoxide ring-closure protocol of **GP4**, 2-(4-methoxyphenyl)pent-4-en-1-ol (1.97 g, 10.3 mmol, 1.0 equiv) was converted to (4-(4-methoxyphenyl)tetrahydrofuran-2-yl)methanol. The crude mixture was purified by flash chromatography using silica gel (CyHex/EtOAc 7:3 → CyHex/EtOAc 1:1) affording product as a colorless oil in 89% yield (2:1 mixture of diastereomers) (1.15 g, 5.56 mmol).

Major diastereomer
^{1}H NMR (400 MHz, $CDCl_3$) δ 7.21 – 7.12 (m, 2H), 6.90 – 6.81 (m, 2H), 4.34 – 4.27 (m, 1H), 4.26 – 4.13 (m, 1H), 3.79 (s, 3H), 3.78 – 3.68 (m, 2H), 3.62 – 3.51 (m, 1H), 3.45 –

3.29 (m, 1H), 2.45 (br, 1H), 2.17 (ddd, J = 12.6, 8.6, 5.7 Hz, 1H), 2.04 (dt, J = 12.7, 7.9 Hz, 1H).

^{13}C NMR (101 MHz, $CDCl_3$) δ 158.4, 134.0, 128.3, 114.1, 79.7, 75.0, 65.3, 55.4, 44.3, 35.9.

Minor diastereomer

^{1}H NMR (400 MHz, $CDCl_3$) δ 7.22 – 7.10 (m, 2H), 6.90 – 6.81 (m, 2H), 4.35 – 4.25 (m, 1H), 4.22 – 4.10 (m, 1H), 3.79 (s, 3H), 3.78 – 3.68 (m, 2H), 3.68 – 3.60 (m, 1H), 3.52 – 3.42 (m, 1H), 2.45 (br, 1H), 2.37 – 2.27 (m, 1H), 1.92 – 1.78 (m, 1H).

^{13}C NMR (101 MHz, $CDCl_3$) δ 158.5, 133.2, 128.3, 114.1, 80.6, 74.6, 64.9, 55.4, 44.9, 36.0.

IR (ATR): $\tilde{\nu}$ [cm^{-1}] = 3407, 2933, 2870, 2836, 1611, 1512, 1455, 1302, 1243, 1178, 1113, 1030, 925, 826, 777, 752, 703, 673, 673, 638. **HRMS (ESI)**: [m/z] calculated for $C_{12}H_{16}NaO_3$ ([M+Na]$^+$): 231.0994; Found: 231.0992.

R_f (CyHex/EtOAc, 7:3) = 0.23 [$KMnO_4$].

Methyl 2-(4-bromophenyl)pent-4-enoate (7.22a)

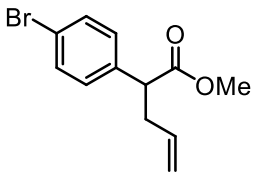

$C_{12}H_{13}BrO_2$
268.01 g/mol

Following the alkylation protocol of **GP4**, methyl 2-(4-bromophenyl)acetate (1.3 mL, 8.15 mmol, 1.0 equiv.) was converted to methyl 2-(4-bromophenyl)pent-4-enoate. The crude mixture was purified by flash column chromatography on silica gel (PE/EtOAc 5:1) to afford product as a yellow oil in 94% yield (2.06 g, 7.66 mmol).

^{1}H NMR (400 MHz, $CDCl_3$) δ 7.44 (d, *J* = 8.5 Hz, 2H), 7.18 (d, *J* = 8.3 Hz, 2H), 5.68 (ddt, *J* = 17.1, 10.2, 6.8 Hz, 1H), 5.13 – 4.93 (m, 2H), 3.65 (s, 3H), 3.61 (t, 1H), 2.80 (dddt, *J* = 14.3, 8.3, 7.0, 1.2 Hz, 1H), 2.63 – 2.38 (m, 1H).

^{13}C NMR (101 MHz, $CDCl_3$) δ 173.5, 137.6, 134.9, 131.8, 129.8, 121.4, 117.4, 52.2, 50.9, 37.5.

HRMS (ESI): [m/z] calculated for $C_{12}H_{13}BrNaO_2$ ([M+Na]$^+$): 290.9993; Found: 290.9991. The characterization data is consistent with the literature. [268]

2-(4-Bromophenyl)pent-4-en-1-ol (7.22b)

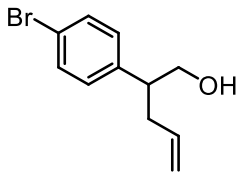

$C_{11}H_{13}BrO$
240.02 g/mol

Following the reduction protocol of **GP4**, 2-(4-bromophenyl)pent-4-enoate (2.00 g, 7.43 mmol, 1.0 equiv) was converted to 2-(4-bromophenyl)pent-4-en-1-ol. The crude mixture was purified by flash column chromatography on silica gel (PE/EtOAc = 4:1) to afford product as a yellow oil in 81% yield (1.45 g, 6.02 mmol).

^{1}H NMR (600 MHz, $CDCl_3$) δ 7.45 (d, *J* = 8.4 Hz, 2H), 7.10 (d, *J* = 8.4 Hz, 2H), 5.69 (ddt, *J* = 17.1, 10.2, 6.9 Hz, 1H), 5.16 – 4.89 (m, 2H), 3.79 (ddd, *J* = 10.9, 5.7, 1.3 Hz, 1H), 3.73 (ddd, *J* = 11.0, 7.3, 1.2 Hz, 1H), 2.92 – 2.75 (m, 1H), 2.64 – 2.44 (m, 1H), 2.41 – 2.23 (m, 1H), 1.40 (br, 1H).
^{13}C NMR (151 MHz, $CDCl_3$) δ 141.2, 136.0, 131.8, 129.9, 120.7, 116.9, 66.8, 47.8, 36.6.
HRMS (ESI): [m/z] calculated for $C_{11}H_{13}BrNaO$ ($[M+Na]^+$): 263.0041; Found: 263.0042.

(4-(4-Bromophenyl)tetrahydrofuran-2-yl)methanol (7.22)

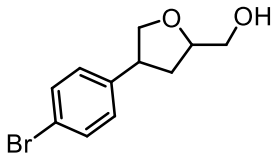

$C_{11}H_{13}BrO_2$
256.01 g/mol

Following the epoxide ring-closure protocol of **GP4**, 2-(4-bromophenyl)pent-4-en-1-ol (1.41 g, 5.85 mmol, 1.0 equiv) was converted to (4-(4-bromophenyl)tetrahydrofuran-2-yl)methanol. The crude mixture was purified by flash chromatography using silica gel (CyHex/EtOAc 8:2 → CyHex/EtOAc 6:4) affording product as a yellow oil in 78% yield (1:1 mixture of diastereomers) (1.17 g, 4.56 mmol).

^{1}H NMR (600 MHz, $CDCl_3$) δ 7.42 (dd, *J* = 8.4, 3.3 Hz, 2H), 7.12 (dd, *J* = 8.4, 1.7 Hz, 2H), 4.32 – 4.25 (m, 0.5H), 4.20 – 4.15 (m, 1.5H), 3.82 – 3.77 (m, 1H), 3.75 – 3.71 (m, 1H), 3.68 – 3.54 (m, 1H), 3.50 – 3.36 (m, 1H), 2.42 (br, 1H), 2.39 – 2.30 (m, 0.5H), 2.23 – 2.16 (m, 0.5H), 2.06 – 1.98 (m, 0.5H), 1.88 – 1.79 (m, 0.5H).

^{13}C NMR (151 MHz, $CDCl_3$) δ 141.2, 140.6, 131.8, 129.1, 120.6, 120.5, 80.7, 79.6, 74.6, 74.3, 65.2, 64.7, 45.1, 44.6, 35.9, 35.7.
IR (ATR): $\tilde{\nu}$ [cm^{-1}] = 3406, 2930, 2869, 1489, 1408, 1104, 1057, 1008, 972, 816.759, 630.
HRMS (ESI): [m/z] calculated for $C_{11}H_{13}BrNaO_2$ ([M+Na]$^+$): 278.9991; Found: 278.9991.
R_f (CyHex/EtOAc, 7:3) = 0.20 [$KMnO_4$].

Methyl 2-(4-chlorophenyl)pent-4-enoate (7.23a)

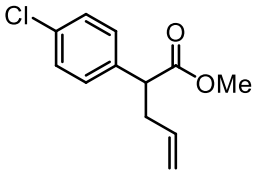

$C_{12}H_{13}ClO_2$
224.06 g/mol

Following the alkylation protocol of **GP4**, methyl 4-chlorophenylacetate (1.2 mL, 8.15 mmol, 1.0 equiv.) was converted to methyl 2-(4-chlorophenyl)pent-4-enoate. The crude mixture was purified by flash column chromatography on silica gel (PE/EtOAc = 5:1) to afford product as a colorless oil in 90% yield (1.56 g, 6.95 mmol).

^{1}H NMR (400 MHz, $CDCl_3$) δ 7.29 (d, *J* = 8.6 Hz, 2H), 7.24 (d, *J* = 8.6 Hz, 2H), 5.69 (ddt, *J* = 17.0, 10.2, 6.8 Hz, 1H), 5.30 – 4.84 (m, 2H), 3.66 (s, 3H), 3.62 (t, 1H), 2.91 – 2.72 (m, 1H), 2.66 – 2.36 (m, 1H).
^{13}C NMR (101 MHz, $CDCl_3$) δ 173.6, 137.1, 134.9, 133.4, 129.5, 128.9, 117.5, 52.2, 50.9, 37.6.
HRMS (ESI): [m/z] calculated for $C_{12}H_{13}ClNaO_2$ ([M+Na]$^+$): 247.0496; Found: 247.0496.
The characterization data is consistent with the literature.[269]

2-(4-Chlorophenyl)pent-4-en-1-ol (7.23b)

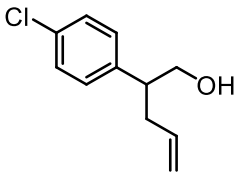

$C_{11}H_{13}ClO$
196.07 g/mol

Following the reduction protocol of **GP4**, methyl 2-(4-chlorophenyl)pent-4-enoate (1.52 g, 6.77 mmol, 1.0 equiv) was converted to 2-(4-chlorophenyl)pent-4-en-1-ol. The crude mixture was purified by flash column chromatography on silica gel (PE/EtOAc = 3:2) to afford product as a colorless oil in 95% yield (1.26 g, 6.43 mmol).

^{1}H NMR (600 MHz, $CDCl_3$) δ 7.30 (d, *J* = 8.5 Hz, 2H), 7.15 (d, *J* = 8.4 Hz, 2H), 6.05 – 5.41 (m, 1H), 5.16 – 4.78 (m, 2H), 3.78 (dd, *J* = 10.9, 5.7 Hz, 1H), 3.72 (dd, *J* = 10.9, 7.4 Hz, 1H), 2.91 – 2.81 (m, 1H), 2.55 – 2.43 (m, 1H), 2.42 – 2.29 (m, 1H), 1.44 (br, 1H).
^{13}C NMR (151 MHz, $CDCl_3$) δ 140.6, 136.0, 132.6, 129.5, 128.9, 116.9, 66.9, 47.7, 36.7.
The characterization data is consistent with the literature.[255]

(4-(4-Chlorophenyl)tetrahydrofuran-2-yl)methanol (7.23)

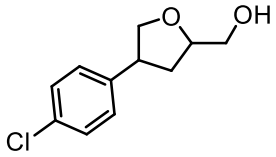

$C_{11}H_{13}ClO_2$
212.06 g/mol

Following the epoxide ring-closure protocol of **GP4**, 2-(4-chlorophenyl)pent-4-en-1-ol (1.23 g, 6.25 mmol, 1.0 equiv) was converted to (4-(4-chlorophenyl)tetrahydrofuran-2-yl)methanol. The crude mixture was purified by flash chromatography using silica gel (CyHex/EtOAc 8:2 → CyHex/EtOAc 6:4) affording product as a colorless oil in 85% yield (1:1 mixture of diastereomers) (1.13 g, 5.32 mmol).

^{1}H NMR (600 MHz, $CDCl_3$) δ 7.37 – 7.29 (m, 2H), 7.28 – 7.19 (m, 2H), 4.39 – 4.30 (m, 0.5H), 4.30 – 4.19 (m, 1.5H), 3.89 – 3.82 (m, 0.5H), 3.82 – 3.75 (m, 1.5H), 3.73 – 3.61 (m, 1H), 3.57 – 3.43 (m, 1H), 2.67 (br, 1H), 2.44 – 2.36 (m, 0.5H), 2.28 – 2.21 (m, 0.5H), 2.08 (ddd, *J* = 12.7, 8.1, 7.2 Hz, 0.5H), 1.93 – 1.86 (m, 0.5H).
^{13}C NMR (151 MHz, $CDCl_3$) δ 140.7, 140.1, 132.5, 132.4, 129.4, 128.9, 128.8, 128.8, 128.7, 128.6, 80.7, 79.7, 74.6, 74.3, 65.1, 64.7, 44.9, 44.5, 35.9, 35.7.
IR (ATR): $\tilde{\nu}$ [cm^{-1}] = 3405, 2929, 2869, 1492, 1412, 1090, 1047, 1012, 924, 818, 756, 718, 702, 658, 607.
HRMS (ESI): [m/z] calculated for $C_{11}H_{13}ClNaO_2$ ($[M+Na]^+$): 235.0496; Found: 235.0496.
R_f (CyHex/EtOAc, 7:3) = 0.25 [$KMnO_4$].

2-(4-(Trifluoromethyl)phenyl)pent-4-enoate (7.24a)

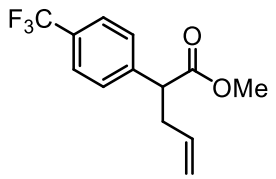

$C_{13}H_{13}F_3O_2$
258.09 g/mol

Following the alkylation protocol of **GP4**, [4-(trifluoromethyl)phenyl]acetic acid methyl ester (950 µL, 5.12 mmol, 1.0 equiv.) was converted to methyl-2-(4-(trifluoromethyl)phenyl)pent-4-enoate. The crude mixture was purified by flash column chromatography on silica gel (PE/EtOAc 3:2) to afford product as a colorless oil in 91% yield (1.20 g, 4.66 mmol).

^{1}H NMR (400 MHz, $CDCl_3$) δ 7.58 (d, *J* = 8.1 Hz, 2H), 7.43 (d, *J* = 8.4 Hz, 2H), 5.69 (ddt, *J* = 17.1, 10.2, 6.8 Hz, 1H), 5.19 – 4.99 (m, 2H), 3.71 (t, 1H), 3.67 (s, 3H), 2.98 – 2.76 (m, 1H), 2.62 – 2.45 (m, 1H).
^{13}C NMR (101 MHz, $CDCl_3$) δ 173.3, 142.5, 134.7, 128.5, 125.8, 125.7, 117.7, 52.4, 51.4, 37.6.
^{19}F NMR (376 MHz, $CDCl_3$) δ -62.54.
The characterization data is consistent with the literature. [270]

(4-(4-(Trifluoromethyl)phenyl)tetrahydrofuran-2-yl)methanol (7.24b)

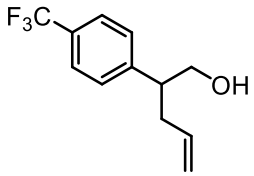

$C_{12}H_{13}F_3O$
230.09
g/mol

Following the reduction protocol of **GP4**, methyl 2-(4-(trifluoromethyl)phenyl)pent-4-enoate (1.19 g, 4.61 mmol, 1.0 equiv) was converted to 2-(4-(trifluoromethyl)phenyl)pent-4-en-1-ol. The crude mixture was purified by flash column chromatography on silica gel (PE/EtOAc 3:2) to afford product as a colorless oil in 86% yield (912 mg, 3.96 mmol).

^{1}H NMR (400 MHz, $CDCl_3$) δ 7.59 (d, *J* = 7.9 Hz, 2H), 7.34 (d, *J* = 8.1 Hz, 2H), 5.78 – 5.62 (m, 1H), 5.11 – 4.90 (m, 2H), 3.89 – 3.74 (m, 2H), 3.05 – 2.89 (m, 1H), 2.52 (dddt, *J* = 14.1, 7.7, 6.7, 1.2 Hz, 1H), 2.40 (dddt, *J* = 14.4, 8.1, 6.6, 1.4 Hz, 1H), 1.44 (br, 1H).
^{13}C NMR (101 MHz, $CDCl_3$) δ 146.4, 135.8, 128.5, 125.7, 117.1, 66.7, 48.1, 36.5.
^{19}F NMR (376 MHz, $CDCl_3$) δ -62.41.

(4-(4-(Trifluoromethyl)phenyl)tetrahydrofuran-2-yl)methanol (7.24)

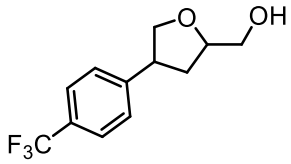

$C_{12}H_{13}F_3O_2$
246.09 g/mol

Following the epoxide ring-closure protocol of **GP4**, 2-(4-(trifluoromethyl)phenyl)pent-4-en-1-ol (1.23 g, 6.25 mmol, 1.0 equiv) was converted to (4-(4-(Trifluoromethyl)phenyl)tetrahydrofuran-2-yl)methanol. The crude mixture was purified by flash chromatography using silica gel (CyHex/EtOAc 8:2 → CyHex/EtOAc 6:4) affording product as a colorless oil in 85% yield (1:1 mixture of diastereomers) (1.13 g, 5.32 mmol).

^{1}H NMR (400 MHz, $CDCl_3$) δ 7.56 (dd, *J* = 8.3, 2.7 Hz, 2H), 7.44 – 7.32 (m, 2H), 4.38 – 4.27 (m, 0.5H), 4.30 – 4.14 (m, 1.5H), 3.88 – 3.71 (m, 2H), 3.70 – 3.43 (m, 2H), 2.85 – 2.47 (br, 1H), 2.45 – 2.34 (m, 0.5H), 2.30 – 2.19 (m, 0.5H), 2.12 – 2.01 (m, 0.5H), 1.95 – 1.83 (m, 0.5H).

^{13}C NMR (101 MHz, $CDCl_3$) δ 146.4, 145.9, 129.3, 129.3, 129.0, 128.9, 128.3, 127.7, 127.7, 125.7, 125.7, 125.7, 125.6, 122.9, 80.8, 79.7, 74.5, 74.3, 65.1, 64.6, 45.4, 45.0, 35.8, 35.7.

^{19}F NMR (376 MHz, $CDCl_3$) δ -62.43, -62.44.

IR (ATR): $\tilde{\nu}$ [cm^{-1}] = 3407, 2938, 2873, 1619, 1421, 1322, 1253, 1161, 1111, 1066, 1015, 954, 926, 891, 834, 723, 667.

HRMS (APCI): [m/z] calculated for $C_{12}H_{14}F_3O_2$ ($[M+H]^+$): 247.0941; Found: 247.0940.

R_f (CyHex/EtOAc, 6:4) = 0.19 [$KMnO_4$].

(2,8-Dioxaspiro[4.5]decan-3-yl)methanol (7.25)

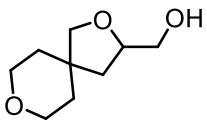

$C_9H_{16}O_3$
172.11 g/mol

Following modified literature procedure,[271] to a solution of diisopropylamine (2.2 mL,15.7 mmol, 1.5 equiv.) in dry THF (69 mL. 0.15 M) was added *n*-butyllithium (8.1 mL, 15.6 mmol, 1.5 equiv.) dropwise at −78 °C. The resulting solution was stirred at 0 °C for 15 min and then cooled again to −78 °C. A solution of the methyl tetrahydro-2*H*-pyran-4-

carboxylater (1.5 g, 10.4 mmol,1.0 equiv.) in THF (20 mL, 0.5 M) was added dropwise, and the mixture was stirred for 40 min at −78 °C. Allyl bromide (1 mL, 11.4 mmol, 1.1 equiv) was then added dropwise, and stirring was continued at −78 °C for 2 h. The reaction was quenched with saturated aqueous NH_4Cl (20 mL). The aqueous phase was extracted with Et_2O (3 times), and the combined organic layers were washed with 1 M HCl, then brine, dried over anhydrous Na_2SO_4, filtered, and concentrated under reduced pressure. The resulting crude was used in the next step without further purification.

Following a reported procedure by Szymoniak and co-workers,[256] a solution of the ester (1.8 g, 9.77 mmol, 1.0 equiv) in Et_2O (24 mL, 0.4 M) was added dropwise to a suspension of $LiAlH_4$ (445 mg, 11.72 mmol, 1.2 equiv.) in Et_2O (1.0 M) at 0 °C. The resulting mixture was stirred at room temperature for 2 hours. Cold distilled water (20 mL) was then added carefully to quench the reaction. The aqueous phase was extracted with Et_2O (3 times), and the combined organic layers were washed with brine, dried over anhydrous Na_2SO_4, filtered, and concentrated under reduced pressure. The crude mixture was purified by flash chromatography using silica gel to afford the corresponding reduced products.

Following a reported procedure by Gravel and co-workers,[254] a solution of the corresponding alcohol (1.3 g, 8.32 mmol, 1.0 equiv.) in DCM (42 mL, 0.2 M) was cooled to 0 °C. To this solution, *m*CPBA (2.24 g, 9.99 mmol,1.2 equiv.) was added in a single portion. The reaction mixture was subsequently allowed to warm to ambient temperature and stirred for 18 hours. Upon completion, the reaction was quenched by the addition of saturated aqueous $NaHCO_3$. The resulting mixture was extracted with DCM three times. The combined organic layers were dried over anhydrous Na_2SO_4, filtered, and concentrated under reduced pressure. The crude mixture was purified by flash chromatography using silica gel (CyHex/EtOAc 4:1) affording product over 3 steps as a colorless oil in 70% yield (1.23 g, 7.16 mmol).

^{1}H NMR (400 MHz, $CDCl_3$) δ 4.17 – 4.06 (m, 1H), 3.75 – 3.59 (m, 7H), 3.52 (dd, *J* = 11.7, 5.9 Hz, 1H), 2.03 (br, 1H), 1.89 (dd, *J* = 12.5, 7.0 Hz, 1H), 1.72 – 1.49 (m, 5H).
^{13}C NMR (101 MHz, $CDCl_3$) δ 79.1, 78.1, 65.9, 65.5, 64.9, 41.8, 39.0, 36.2, 35.6.
HRMS (ESI): [m/z] calculated for $C_9H_{16}NaO_3$ ($[M+Na]^+$): 195.0989; Found: 195.0992.
The characterization data is consistent with the literature. [272]

(3-Phenyltetrahydrofuran-2-yl)methanol (7.27)

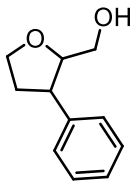

$C_{11}H_{14}O_2$
178.10 g/mol

To a solution of cinnamyl alcohol (1.00 g, 7.50 mmol, 1.0 equiv) and triethyl orthoacetate (6.00 g, 37.4 mmol, 5.0 equiv) in toluene (30 mL) was added propionic acid (28.5 µL, 0.38 mmol, 0.05 equiv.). The reaction mixture was heated at 150 °C and stirred for 15 h. After cooling to room temperature, the mixture was concentrated under reduced pressure, diluted with hexanes, and filtered through a short plug of silica. The filtrate was concentrated under reduced pressure and the residue of ester was directly used for the next step without further purification.

Following a modified literature procedure,[256] a solution of the ester (1.42 g, 6.95 mmol, 1.0 equiv.) in THF (0.6 M) was added dropwise to a suspension of $LiAlH_4$ (317 mg, 8.34 mmol, 1.2 equiv.) in THF (0.3 M) at 0 °C. The resulting mixture was stirred at room temperature for 2 hours. Cold distilled water was then added carefully to quench the reaction. The aqueous phase was extracted with Et_2O (3 times), and the combined organic layers were washed with brine, dried over anhydrous Na_2SO_4, filtered, and concentrated under reduced pressure. The residue of the alcohol was directly used for the next step without further purification.

Following a reported procedure by Gravel and co-workers,[254] a solution of alcohol (940 mg, 5.79 mmol, 1.0 equiv.) in DCM (29 mL, 0.2 M) was cooled to 0 °C. To this solution, *m*CPBA (1.70 g, 6.95 mmol, 1.2 equiv.) was added in a single portion. The reaction mixture was subsequently allowed to warm to ambient temperature and stirred for 18 hours. Upon completion, the reaction was quenched by the addition of saturated aqueous $NaHCO_3$. The resulting mixture was extracted with DCM three times. The combined organic layers were dried over anhydrous Na_2SO_4, filtered, and concentrated under reduced pressure. The crude product was purified by was purified by flash chromatography using silica gel (CyHex/EtOAc 1:1) affording product as a colorless liquid in 79% yield (1:1 mixture of diastereomers) (816 mg, 4.58 mmol).

^{1}H NMR (400 MHz, $CDCl_3$) δ 7.44 – 7.36 (m, 1H), 7.35 – 7.23 (m, 4H), 4.31 – 4.12 (m, 0.5H), 4.07 (td, *J* = 8.3, 6.8 Hz, 0.5H), 4.00 (ddd, *J* = 8.2, 5.1, 2.8 Hz, 0.5H), 3.86 – 3.76 (m, 1.5H), 3.68 (ddd, *J* = 11.0, 7.0, 5.9 Hz, 1H), 3.62 – 3.55 (m, 0.5H), 3.32 – 3.22 (m,

1H), 3.20 – 3.12 (m, 1H), 2.86 – 2.77 (m, 1H), 2.68 – 2.61 (m, 1H), 2.60 – 2.52 (m, 1H), 2.51 – 2.18 (m, 4H), 2.15 – 2.04 (m, 1H).

^{13}C NMR (101 MHz, $CDCl_3$) δ 141.3, 141.0, 128.8, 128.8, 127.8, 127.7, 127.1, 126.9, 86.4, 68.4, 62.9, 60.6, 56.4, 47.1, 46.2, 46.0, 36.6, 35.5.
HRMS (ESI): [m/z] calculated for $C_{11}H_{14}NaO_2$ ($[M+Na]^+$): 201.0889; Found: 201.0889.
R_f (CyHex/EtOAc, 1:1) = 0.19 [$KMnO_4$].
The characterization data is consistent with the literature.[273]

((3a*S*,7a*R*)-Octahydrobenzofuran-2-yl)methanol (7.28)

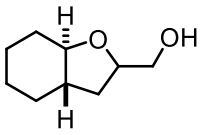

$C_9H_{16}O_2$
156.12 g/mol

Following reported procedure,[254] to a solution of cyclohexene oxide (1.0 mL, 9.88 mmol, 1.0 equiv.) and copper(I) iodide (188 mg, 0.99 mmol, 0.1 equiv.) in THF (33 mL, 0.3 M), cooled to 0 °C, allylmagnesium bromide (7.4 mL, 14.8 mmol, 1.5 equiv. 2.0 M) was added dropwise. The reaction mixture was allowed to warm to room temperature and stirred for 5 hours. Upon completion, the reaction was quenched with saturated aqueous NH_4Cl. The mixture was extracted with EtOAc (3 times), and the combined organic layers were washed with brine, dried over anhydrous Na_2SO_4, filtered, and concentrated under reduced pressure. The resulting crude was used in the next step without further purification.

Following a reported procedure by Gravel and co-workers, a solution of the crude mixture of the alcohol prepared above (1.28 g, 9.13 mmol, 1.0 equiv.) in DCM (45 mL, 0.2 M) was cooled to 0 °C. To this solution, *m*CPBA (1.89 g, 10.95 mmol, 1.2 equiv.) was added in a single portion. The reaction mixture was subsequently allowed to warm to ambient temperature and stirred for 18 hours. Upon completion, the reaction was quenched by the addition of saturated aqueous $NaHCO_3$. The resulting mixture was extracted with DCM three times. The combined organic layers were dried over anhydrous Na_2SO_4, filtered, and concentrated under reduced pressure. The crude mixture was purified by flash chromatography using silica gel (CyHex/EtOAc 8:2) affording (Octahydrobenzofuran-2-yl)methanol **7.28** over 2 steps as a colorless liquid in 79% yield (2:1 mixture of diastereomers) (1.23 g, 7.85 mmol).

^{1}H NMR (400 MHz, $CDCl_3$) δ 4.18 – 4.05 (m, 1H), 3.73 – 3.57 (m, 1H), 3.53 – 3.41 (m, 1H), 3.18 – 2.97 (m, 1H), 2.26 (br, 1H), 2.15 – 2.05 (m, 1H), 1.96 – 1.87 (m, 1H), 1.87 – 1.74 (m, 2H), 1.74 – 1.54 (m, 2H), 1.42 – 0.96 (m, 5H).
^{13}C NMR (101 MHz, $CDCl_3$) δ 84.2, 82.6, 79.0, 77.9, 66.0, 65.7, 46.0, 45.2, 33.3, 33.2, 31.4, 31.4, 29.3, 29.1, 25.9, 25.8, 24.4, 24.4.
HRMS (ESI): [m/z] calculated for $C_9H_{16}NaO_2$ ([M+Na]$^+$): 179.1042; Found: 179.1043.
The characterization data is consistent with the literature.[254]

(2,3-Dihydrobenzofuran-2-yl)methanol (7.29)

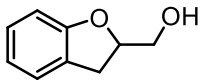

$C_9H_{10}O_2$
150.07 g/mol

Following a reported procedure by Gravel and co-workers,[254] a solution of 2-allylphenol (1.0 mL, 7.66 mmol, 1.0 equiv.) in DCM (38 mL, 0.2 M) was cooled to 0 °C. To this solution, *m*CPBA (2.06 g, 9.19 mmol, 1.2 equiv.) was added in a single portion. The reaction mixture was subsequently allowed to warm to ambient temperature and stirred for 18 hours. Upon completion, the reaction was quenched by the addition of saturated aqueous $NaHCO_3$. The resulting mixture was extracted with DCM three times. The combined organic layers were dried over anhydrous Na_2SO_4, filtered, and concentrated under reduced pressure. The crude product was purified by was purified by flash chromatography using silica gel (PE/Et_2O 4:1) affording product as a colorless liquid in 79% yield (816 mg, 4.58 mmol).

^{1}H NMR (400 MHz, $CDCl_3$) δ 7.20 – 7.15 (m, 1H), 7.15 – 7.07 (m, 1H), 6.86 (td, *J* = 7.4, 1.0 Hz, 1H), 6.82 – 6.76 (m, 1H), 4.95 – 4.84 (m, 1H), 3.83 (dd, *J* = 12.0, 3.3 Hz, 1H), 3.73 (dd, *J* = 12.1, 6.3 Hz, 1H), 3.36 – 3.18 (m, 1H), 3.11 – 2.92 (m, 1H), 2.63 (s, 1H).
^{13}C NMR (101 MHz, $CDCl_3$) δ 159.2, 128.1, 126.6, 125.1, 120.7, 109.5, 83.1, 64.9, 31.3.
HRMS (ESI): [m/z] calculated for $C_9H_{10}NaO_2$ ([M+Na]$^+$): 173.0572; Found: 173.0573.
R_f (CyHex/EtOAc, 1:1) = 0.19 [$KMnO_4$].
The characterization data is consistent with the literature.[274]

2-(Benzyloxy)-3-hydroxypropyl 4-methylbenzenesulfonate (7.30)

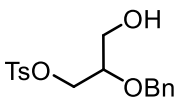

$C_{17}H_{20}O_5S$
336.10 g/mol

To a solution of 2-benzyloxy-1,3-propanediol (1.00 g, 5.49 mmol, 1.0 equiv.) in anhydrous DCM (43 mL, 0.13 M) were added pyridine (4.4 mL, 54.9 mmol, 10 equiv) and 4-(dimethylamino)pyridine (DMAP, 31 mg, 0.25 mmol, 0.05 equiv.). The reaction mixture was cooled to 0 °C under a nitrogen atmosphere, and a solution of *p*-toluenesulfonyl chloride (TsCl, 523 mg, 2.74 mmol, 0.5 equiv.) in DCM (10 mL, 0.27M) was added dropwise over 30 min. The reaction was allowed to warm to room temperature and stirred for 7 h. The mixture was diluted with DCM, washed with water and brine, and the organic layer was dried over anhydrous Na_2SO_4, filtered, and concentrated under reduced pressure. The crude mixture was purified by flash chromatography using silica gel (PE/ EtOAc 7:3 →PE/ EtOAc 1:1) to afford product as a colorless oil in 43% yield (794 mg, 2.36 mmol).

^{1}H NMR (400 MHz, $CDCl_3$) δ 7.82 – 7.75 (m, 2H), 7.41 – 7.23 (m, 7H), 4.58 (dd, 2H), 4.13 (dd, *J* = 5.2, 1.1 Hz, 2H), 3.76 – 3.66 (m, 2H), 3.63 – 3.53 (m, 1H), 2.44 (s, 3H), 1.83 (br, 1H).

^{13}C NMR (101 MHz, $CDCl_3$) δ 145.1, 137.6, 132.8, 130.1, 128.7, 128.2, 128.1, 128.0, 72.6, 68.8, 61.6, 21.8.

HRMS (ESI): [m/z] calculated for $C_{17}H_{20}NaO_5$ ($[M+Na]^+$): 359.0925; Found: 359.0924.

R_f (PE/EtOAc, 1:1) = 0.19 [CAM].

The characterization data is consistent with the literature.[275]

(9*H*-fluoren-9-yl)methyl 2-(hydroxymethyl)pyrrolidine-1-carboxylate (7.31)

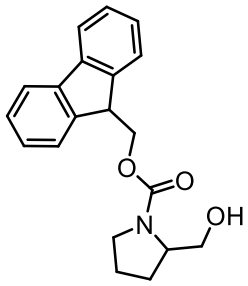

$C_{20}H_{21}NO_3$
323.15 g/mol

Following a reported procedure, [276] to a solution of pyrrolidin-2-ylmethanol (500 mg, 4.93 mmol, 1.0 equiv.) in THF/H_2O (2:3, 33 mL/49 mL) at 0 °C was added $NaHCO_3$ (5.00 g, 59.3 mmol, 12 equiv.) and N-(9-fluorenylmethoxycarbonyloxy)succinimide (2.17 g, 6.43 mmol, 1.3 equiv.). The mixture was stirred at room temperature for 17 h, THF was removed under reduced pressure, and the resulting aqueous layer was extracted with EtOAc 3 times. The combined organic extracts were washed with water and brine, dried over Na_2SO_4, filtered, and concentrated under reduced pressure. The crude mixture was

purified by flash chromatography using silica gel (CyHex/EtOAc 6:4) affording product as a yellowish oil in 92% yield (1.47 g, 4.55 mmol).

^{1}H NMR (400 MHz, $CDCl_3$) δ 7.84 – 7.71 (m, 2H), 7.64 – 7.54 (m, 2H), 7.45 – 7.36 (m, 2H), 7.32 (td, *J* = 7.5, 1.2 Hz, 2H), 4.49 – 4.38 (m, 2H), 4.24 (t, *J* = 6.7 Hz, 1H), 4.05 – 3.14 (m, 6H), 2.10 – 1.53 (m, 4H).
^{13}C NMR (101 MHz, $CDCl_3$) δ 157.1, 144.0, 141.4, 127.8, 127.1, 125.0, 120.0, 67.5, 66.7, 60.7, 47.4, 31.0, 28.6, 24.1.
HRMS (ESI): [m/z] calculated for $C_{20}H_{21}NNaO_3$ ($[M+Na]^+$): 346.1414; Found: 346.1414.
The characterization data are consistent with the literature.[276]

Benzyl 3-(hydroxymethyl)-2-oxa-8-azaspiro[4.5]decane-8-carboxylate (7.26)

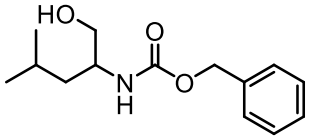

$C_{14}H_{21}NO_3$
251.15 g/mol

Following a reported procedure, [276] Leucinol (800 mg, 8.53 mmol, 1.0 equiv.) and Na_2CO_3 (1.44 g, 13.6 mmol, 2.0 equiv) were dissolved in a mixture of H_2O (6.4 mL) and dioxane (6.4 mL). The resulting suspension was cooled to 0 °C, and benzyl chloroformate (1.5 mL, 10.24 mmol, 1.5 equiv) was added dropwise. The reaction mixture was stirred at room temperature for 19 h. After concentration under reduced pressure, the mixture was extracted with DCM (3 times). The combined organic layers were washed sequentially with 5% aqueous citric acid (10 mL), saturated aqueous $NaHCO_3$, and brine, dried over Na_2SO_4, filtered, and concentrated. The crude mixture was purified by flash chromatography using silica gel (PE/EtOAc 7:3) to afford *N*-Cbz-protected leucinol as a viscous oil in 92% yield (1.58 g, 6.28 mmol).

^{1}H NMR (600 MHz, $CDCl_3$) δ 7.30 – 7.20 (m, 5H), 5.01 (s, 2H), 4.86 (s, 1H), 3.72 – 3.68 (m, 1H), 3.60 – 3.55 (m, 1H), 3.46 – 3.37 (m, 1H), 2.44 (br, 1H), 1.66 – 1.51 (m, 1H), 1.41 – 1.17 (m, 2H), 0.84 (d, *J* = 6.1 Hz, 6H).
^{13}C NMR (151 MHz, $CDCl_3$) δ 156.9, 136.6, 128.6, 128.2, 128.2, 67.0, 66.0, 51.6, 40.6, 24.9, 23.1, 22.3.
The characterization data are consistent with the literature.[276]

(5-(Pyridin-2-yl)tetrahydrofuran-2-yl)methanol (7.34)

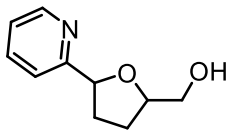

$C_{10}H_{13}NO_2$
179.09 g/mol

Following **GP3**, starting from 2-Pyridincarbaldehyde (0.9 mL, 10.0 mmol, 1.0 equiv.). The crude mixture was purified by flash chromatography using silica gel (CyHex/EtOAc 4:2) affording product over 2 steps as a yellow oil in 49% yield (1:1 mixture of diastereomers) (700 mg, 3.91 mmol).

^{1}H NMR (600 MHz, $CDCl_3$) δ 8.21 (d, *J* = 6.6 Hz, 1H), 7.40 – 7.27 (m, 2H), 7.26 – 7.13 (m, 1H), 5.90 – 5.77 (m, 1H), 5.73 (d, *J* = 6.9 Hz, 1H), 5.23 – 4.74 (m, 3H), 2.38 – 2.16 (m, 2H), 2.13 – 1.92 (m, 2H).
^{13}C NMR (151 MHz, $CDCl_3$) δ 152.2, 140.2, 140.1, 137.8, 127.3, 127.2, 124.6, 124.6, 124.3, 124.2, 124.1, 115.5, 70.4, 70.4, 60.5, 51.9, 47.2, 32.7, 30.0, 29.9, 29.7, 29.0, 28.6.
HRMS (ESI): [m/z] calculated for $C_{10}H_{13}NaO_2$ ($[M+Na]^+$): 202.0838; Found: 202.0837.

Synthesis of 5-(phenoxymethyl)tetrahydrofuran-2-carbaldehyde (2.44)

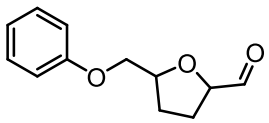

$C_{12}H_{14}O_3$
206.09 g/mol

A suspension of alcohol **6.1** (850 mg, 4.08 mmol, 1.0 equiv) and IBX (1.60 g, 5.71 mmol, 1.4 equiv.) in MeCN (20 mL) was heated at 80 °C for approximately 2 h. Upon completion (as monitored by TLC), the reaction mixture was cooled to room temperature and filtered through a pad of basic alumina or Celite, eluting with EtOAc. The combined filtrates were concentrated under reduced pressure. The crude mixture was purified by flash chromatography using silica gel (PE/DE 9:1) to afford the corresponding product as a colourless oil in 91% yield (1:1 mixture of diastereomers) (766 mg, 3.71 mmol).

^{1}H NMR (400 MHz, $CDCl_3$) δ 9.72 (t, *J* = 1.8 Hz, 1H), 7.32 – 7.26 (m, 2H), 7.01 – 6.86 (m, 3H), 4.58 – 4.42 (m, 1.5H), 4.38 – 4.32 (m, 0.5H), 2.33 – 1.83 (m, 4H).
^{13}C NMR (101 MHz, $CDCl_3$) δ 203.4, 202.6, 158.8, 158.7, 129.6, 129.6, 121.2, 114.7, 114.6, 83.9, 83.5, 79.3, 79.0, 70.2, 70.0, 27.9, 27.9, 27.3.

IR (ATR): $\tilde{\nu}$ [cm^{-1}] = 2924, 2874, 1731, 1598, 1587, 1495, 1455, 1292, 1244, 1173, 1154, 1078, 1043, 948, 886, 847, 808, 755, 692.

HRMS (ESI): [m/z] calculated for $C_{12}H_{14}NaO_3$ ($[M+Na]^+$): 229.0836; Found: 229.0835.

Synthesis of precatalyst.

Sodium 2-iodobenzenesulfonate (pre-IBS)

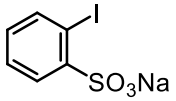

$C_6H_4INaO_3S$
305.88 g/mol

Following a reported procedure,[79] in an oven-dried round-bottom flask equipped with a magnetic stir bar, aniline-2-sulfonic acid (7.0 g, 40.4 mmol, 1.0 equiv.) was suspended in concentrated hydrochloric acid (15 mL, 37%, 185 mmol, 4.6 equiv.) containing crushed ice (28 g). A solution of sodium nitrite (3.07 g, 44.5 mmol, 1.1 equiv.) in water (12 mL) was added very slowly at 0 °C over 40 min, while maintaining the internal temperature below 5 °C to avoid the formation of nitrous gases. The resulting diazonium suspension was stirred at this temperature for an additional 40 min. Subsequently, a solution of sodium iodide (7.3 g, 48.5 mmol, 1.2 equiv.) in water (12 mL) was added dropwise at 0 °C, keeping the temperature below 5 °C. After completion of the addition, the reaction mixture was stirred at 0 °C for 1 h, then allowed to warm to room temperature and stirred for a further 1 h. The mixture was then heated at 50 °C for 12 h. Upon cooling in a refrigerator for approximately 8 h, a yellow solid precipitated, which was collected by filtration and washed sequentially with cold ethanol and a cold 1:1 mixture of methanol and diethyl ether (10 mL). The filtrate was concentrated and cooled again, affording a second crop of solid, which was isolated by filtration and washed using the same cold solvent system. The combined solids afforded sodium 2-iodobenzenesulfonate as a yellow solid in 59% yield (7.3 g, 23.9 mmol).

^{1}H NMR (600 MHz, D_2O) δ 8.19 – 8.14 (m, 3H), 8.06 (d, *J* = 7.8 Hz, 2H), 7.57 (t, *J* = 7.5 Hz, 2H), 7.27 (t, *J* = 7.3 Hz, 2H).

^{13}C NMR (151 MHz, D_2O) δ 146.1, 143.4, 133.7, 129.7, 129.6, 92.2.

The characterization data is consistent with the literature.[70]

Sodium 2-iodo-5-methylbenzenesulfonate (2.1)

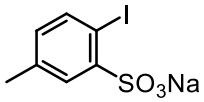

$C_7H_6INaO_3S$
319.89 g/mol

Following a reported procedure,[79] in an oven-dried round-bottom flask equipped with a magnetic stir bar, 2-amino-5-methylbenzenesulfonic acid (10.0 g, 53.4 mmol, 1.0 equiv.) was suspended in concentrated hydrochloric acid (20 mL, 37%, 245 mmol, 4.6 equiv.) containing crushed ice (40 g). A solution of sodium nitrite (4.05 g, 58.8 mmol, 1.1 equiv.) in water (20 mL) was added very slowly at 0 °C over 40 min, while maintaining the internal temperature below 5 °C to suppress the formation of nitrous gases. The resulting diazonium suspension was stirred at this temperature for an additional 40 min. Subsequently, a solution of sodium iodide (9.61 g, 64.1 mmol, 1.2 equiv.) in water (20 mL) was added dropwise at 0 °C, keeping the temperature below 5 °C. Upon completion of the addition, the reaction mixture was stirred at 0 °C for 1 h, then allowed to warm to room temperature and stirred for an additional 1 h. The mixture was then heated at 50 °C for 12 h. After cooling in a refrigerator for approximately 3 h, a yellowish solid precipitated, which was collected by filtration and washed sequentially with cold ethanol and a cold 1:1 mixture of methanol and diethyl ether (20 mL). The filtrate was concentrated and cooled again, affording a second crop of solid, which was isolated by filtration and washed using the same cold solvent system. The combined solids afforded sodium 2-iodo-4-methylbenzenesulfonate as a yellowish solid in 62% yield (10.7 g, 33.3 mmol).

^{1}H NMR (400 MHz, D_2O) δ 7.95 (d, *J* = 8.0 Hz, 1H), 7.84 (dd, *J* = 2.2, 0.8 Hz, 1H), 7.08 – 7.01 (m, 1H), 2.32 (d, *J* = 0.8 Hz, 3H).
^{13}C NMR (101 MHz, D_2O) δ 146.3, 143.6, 141.0, 135.0, 130.8, 88.4, 21.8.
HRMS (ESI): [m/z] calculated for $C_7H_6IO_3S$ ($[M-Na]^-$): 296.9109; Found: 296.9188.
The characterization data is consistent with the literature.[70]

Sodium 5-carboxy-2-iodobenzenesulfonate (2.2)

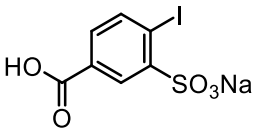

$C_7H_4INaO_5S$
349.87 g/mol

Following a reported procedure,[79] in an oven-dried round-bottom flask equipped with a magnetic stir bar, sodium hydroxide (3.15 g, 78.7 mmol, 2.4 equiv.) was dissolved in water (256 mL, 0.13 M). Sodium 2-iodo-5-methylbenzenesulfonate 2.1 (10.5 g, 32.8 mmol, 1.0 equiv.) was added, and the resulting solution was heated to 40 °C. Potassium permanganate (15.6 g, 98.4 mmol, 3.0 equiv.) was then added portionwise over 10 min intervals. The reaction mixture was heated to 75–80 °C and stirred at this temperature for 16 h. Upon completion, a 1:1 methanol/water mixture (1.1 mL) was added at 60 °C to quench excess oxidant. The mixture was cooled to 35–40 °C and filtered to remove manganese dioxide. The filtrate was acidified to approximately pH 1 by the slow addition of concentrated HCl, resulting in the formation of a precipitate, which was collected by suction filtration and washed with minimal amounts of cold acetonitrile and diethyl ether. Approximately one-third of the filtrate volume was removed under reduced pressure, and the remaining solution was cooled to 0 °C and stirred for 3–4 h. The resulting suspension was filtered, washed with small amounts of cold acetonitrile and diethyl ether, and dried under high vacuum to afford sodium 4-carboxy-2-iodobenzenesulfonate as a fluffy white solid in 94% yield (10.8 g, 30.84 mmol).

^{1}H NMR (400 MHz, DMSO) δ 13.11 (s, 1H), 8.45 (d, *J* = 2.2 Hz, 1H), 8.02 (d, *J* = 8.1 Hz, 1H), 7.51 (dd, *J* = 8.0, 2.2 Hz, 1H).
^{13}C NMR (101 MHz, DMSO) δ 166.9, 150.5, 141.4, 130.2, 130.0, 128.5, 99.7.
HRMS (ESI): [m/z] calculated for $C_7H_4IO_5S([M-H]^-)$: 326.8829; Found: 326.8630.
The characterization data is consistent with the literature.[79]

Tetrabutylammonium peroxomonosulfate

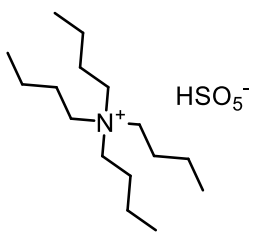

$C_{16}H_{37}NO_5S$
355.23 g/mol

Following a modified literature procedure,[277] Oxone® (51.8 g, 169 mmol, 1.1 equiv.) was dissolved in water (519 mL, 0.3 M). Tetrabutylammonium hydrogen sulfate (52.0 g, 153 mmol, 1.0 equiv.) was added, and the mixture was stirred at room temperature for 30 min. DCM was then added, and the phases were separated. The aqueous phase was extracted with DCM 2 times. The combined organic layers were dried over sodium sulfate and concentrated under reduced pressure. The resulting residue was washed with hexane and dried under reduced pressure to afford tetrabutylammonium peroxomonosulfate (51.8 g, 146 mmol, 95% yield, 91% purity).

The peroxo content was determined by iodometric titration. For this purpose, an aqueous iodide solution (10 wt% sodium iodide in water) and an aqueous sodium thiosulfate solution (1.27 g) dissolved in 50 mL of water was prepared. A sample of the synthesized tetrabutylammonium peroxomonosulfate (150 mg) was dissolved in anhydrous acetic acid (1 mL), followed by the addition of the iodide solution (2 mL). The mixture was diluted to a total volume of 10 mL with THF and titrated with the sodium thiosulfate solution until the color changed from yellow to colorless. The amount of peroxo species was calculated from the volume of sodium thiosulfate solution consumed.

7.4.2 Synthesis of SP-IBS I and II by solid-phase peptide synthesis

SP-IBS I was prepared according to our previously reported procedure.[80] **SP-IBS II** was synthesized using a modified protocol with silica gel as the solid support.

Stock solutions

Fmoc-Ala-OH (A, 0.51 M in DMF)

HBTU (B, 0.49 M in DMF)

DIPEA (C, 2.04 M in NMP)

Piperidine (D, 40% v/v in DMF)

Preparation of silica gel

3-Aminopropyl-functionalized silica gel (200 mg, 200 µmol, 1.0 equiv) was suspended in anhydrous DCM (2.0 mL) in a 10 mL PP reactor. The suspension was vortexed intermittently (15 s vortex, 2 min break) for 2 h, after which the solvent was removed by suction. The procedure was performed in five parallel reactions to afford 1000 µmol of functionalized silica gel.

Peptide coupling

To each PP reactor with silica gel (200 mg, 200 µmol, 1.0 equiv.) were added Fmoc-Ala-OH (1.6 mL, 800 µmol, 4 equiv.), HBTU (1.7 mL, 800 µmol, 4 equiv.), and DIPEA (1.2 mL, 800 µmol, 4 equiv.). The mixture was vortexed for 24 h(15 s vortex, 2 min break). Solvent was removed by suction, and the silica gel was washed with DMF (3 × 2 mL).

End-capping of silica gel

Silica gel was suspended in DCM (1 mL) with acetic anhydride (1.89 mL, 20 mmol, 100 equiv.) and vortexed for 3 h(15 s vortex, 2 min break), then filtered by suction. The solid was washed sequentially with DMF (3 × 2 mL) and DCM (6 × 2 mL).

Fmoc deprotection

Piperidine solution D (2.4 mL, 9.2 mmol, 48 equiv.) was added and vortexed for 20 min. After suction removal of solvent, a second deprotection was performed with piperidine (1.2 mL, 4.6 mmol, 24 equiv.) and DMF (1.2 mL) for 40 min. The resin was washed with DMF (6 × 2 mL), and theoretical loading was determined according to a previously reported procedure.[80]

Theoretical loading is determined using the following equation 1

$$\boldsymbol{theo.Loading}\left(\frac{mmol}{g}\right) = \boldsymbol{B}\left(\frac{mmol}{g}\right).\frac{1000}{\left(1000 + \left(\boldsymbol{B}\left(\frac{mmol}{g}\right).(\boldsymbol{M} - 18)\right)\right)}$$

where *B* equals the loading of starting resin and M equals the molecular weight of the amino acid chain with protective groups.[79]

Coupling of IBS catalyst to solid support

IBS catalyst (210 mg, 600 µmol, 3 equiv.), HATU (228 mg, 600 µmol, 3 equiv.), and DMSO (2 mL) were added to the PP reactor, followed by DIPEA (1.2 mL, 800 µmol, 4 equiv.). The mixture was vortexed for 48 h, then solvent was removed by suction. Silica gel was washed with DMSO (4 × 2 mL) and DCM (6 × 2 mL).

Final end-capping

DCM (2 mL) and acetic anhydride (1.89 mL, 20 mmol, 100 equiv.) were added, vortexed for 4 h, and filtered by suction. The resin was washed with DMF (3 × 2 mL) and DCM (6 × 2 mL).

Determination of catalyst loading

Solid-supported catalysts **I** and **II** were oxidized as previously reported.[75] Preoxidized solid-supported IBS (30 mol%) was added to L-(−)-borneol (4.56 mg, 29.0 µmol, 1.0 equiv.) in acetonitrile (0.2 mL, 0.15 M) and stirred at 70 °C for 18 h. The mixture was filtered, and the filtrate analyzed by GC-FID. The observed conversion was divided by the theoretically possible conversion (30%). Multiplying this factor with the theoretical loading gave the real loading in mmol/g.

Information about the catalyst cartridge

The catalyst cartridge was prepared according to our previously reported procedure.[80] The reactor volume was determined by weighing the cartridge before and after flushing it with the corresponding solvent. The mass difference was then divided by the solvent's density to calculate the volume. For clarity, the average packed-bed volumes of polystyrene-supported IBS (3.6 mL) and silica-supported IBS (1.2 mL) are used throughout.

7.4.3 Protocol for optimization studies

Batch reaction

In a 4 mL screw-cap vial equipped with a magnetic stir bar, tetrahydrofurfuryl alcohol (29.5 µL, 0.3 mmol, 1.0 equiv.), IBS (27.5 mg, 0.3 mmol, 0.3 equiv.) and TBA-Oxone® (5 equiv., unless otherwise noted) were dissolved in the appropriate solvent (0.3 M, unless otherwise noted). The mixture was stirred at various temperatures for 2–24 h. Upon completion, methyl laurate (76.2 µL, 0.3 mmol, 1.0 equiv.) was then added as an internal standard, and the mixture was diluted with EtOAc (ca. 2 mL). An aliquot (60 µL) was withdrawn; where necessary, the crude mixture was passed through a short pad of Na_2SO_4 in a glass pipette, eluting with EtOAc. The eluent was collected in a 1.5 mL glass vial and analyzed by GC-FID to determine the conversion based on the relative amounts of product and remaining starting material.

Continuous flow reactions

A flow reactor packed with **SP-IBS I/II** or the corresponding solid support without catalyst was placed in a water bath preheated to 50 °C. Tetrahydrofurfuryl alcohol (98.3 µL, 1.0 mmol, 1.0 equiv) was dissolved in AcOH (6 mL), and TBA-Oxone® (nBu$_4$NHSO$_5$, 5.0 equiv) was dissolved separately in AcOH (4 mL), affording a total solution volume of 10 mL. The two solutions were delivered using a dual syringe pump at various combined flow rates and residence times. Prior to entering the reactor, the streams were merged

via a three-way valve (T-mixer), and the resulting mixture was passed through the packed bed and collected in a receiving flask. After complete passage of the reaction mixture, the reactor was flushed with AcOH (10 mL) under identical flow conditions, yielding a total of 20 mL of product solution. Methyl laurate (254 µL, 1.0 mmol, 1.0 equiv) was then added as an internal standard. An aliquot (2 mL) of the product solution was taken and diluted with EtOAc (2 mL) in a 4 mL vial; 1 mL of this mixture was transferred to a 1.5 mL glass vial and analyzed by GC-FID to determine the conversion based on the amounts of product and remaining starting material.

Recycling experiments

A flow reactor packed with **SP-IBS I or SP-IBS II** was placed in a water bath preheated to 50 °C. Tetrahydrofurfuryl alcohol (98.3 µL, 1.0 mmol, 1.0 equiv) was dissolved in AcOH (6 mL), and TBA-Oxone® (nBu$_4$NHSO$_5$, 1.95 g, 5 mmol, 5 equiv, 91%) was dissolved separately in AcOH (4 mL), affording a total solution volume of 10 mL. Using a dual syringe pump, the two solutions were then conducted with a preadjusted flow-rate of 5 mL/h through the reactor, first passing a three-way valve where they were mixed together, next passing through the catalyst cartridge and at last being collected into a flask. After complete passage of the reaction mixture, the reactor was flushed with AcOH (10 mL) with the same flow rate, yielding a total of 20 mL of product solution. Methyl laurate (254 µL, 1.0 mmol, 1.0 equiv) was then added as an internal standard. An aliquot (2 mL) of the product solution was taken and diluted with EtOAc (2 mL) in a 4 mL vial; 1 mL of this mixture was transferred to a 1.5 mL glass vial and analyzed by GC-FID to determine the conversion based on the amounts of product and remaining starting material. This procedure was repeated for 20 consecutive cycles to assess catalyst recyclability.

Control experiments

Protocol for the reaction without catalyst:

A flow reactor packed with SiO_2 - without catalyst was placed in a water bath preheated to 50 °C. The substrate (5-(Phenoxymethyl)tetrahydrofuran-2-yl)methanol, **6.1** (104 mg, 0.5 mmol, 1.0 equiv.) was dissolved in AcOH (3 mL), and TBA-Oxone® (nBu$_4$NHSO$_5$, 977 mg, 2.5 mmol, 5 equiv., 91%) was dissolved separately in AcOH (2 mL), affording a total solution volume of 5 mL. The two solutions were delivered using a dual syringe pump at a preset flow rate of 5 mL/h, combined at a three-way valve, passed through the catalyst cartridge, and collected in a round-bottom flask. After the solutions had completely passed through the reactor, the system was flushed with AcOH (10 mL),

resulting in a total product volume of 15 mL. Methyl laurate (127 µL, 0.5 mmol, 1.0 equiv) was then added as an internal standard. An aliquot (1.5 mL) of the product solution and internal standard was taken and diluted with EtOAc (1.5 mL) in a 4 mL vial; 1 mL of this mixture was transferred to a 1.5 mL glass vial and analyzed by GC-FID to determine the conversion based on the amounts of product and remaining starting material.

Protocol for the reaction without TBA-Oxone®:

A flow reactor packed with preoxidized **SP-IBS II** (1.10 g, 0.38 mmol/g) was placed in a water bath preheated to 50 °C. The substrate (5-(Phenoxymethyl)tetrahydrofuran-2-yl)methanol, **6.1** (104 mg, 0.42 mmol, 1.0 equiv) was dissolved in AcOH (4.2 mL), The solution was delivered using a syringe pump at a preset flow rate of 5 mL/h, passed through the catalyst cartridge, and collected in a round-bottom flask. After the solution had completely passed through the reactor, the system was flushed with AcOH (5 mL), resulting in a total product volume of 9.2 mL. Methyl laurate (107 µL, 0.42 mmol, 1.0 equiv) was then added as an internal standard. An aliquot (1.5 mL) of the product solution and internal standard was taken and diluted with EtOAc (1.5 mL) in a 4 mL vial; 1 mL of this mixture was transferred to a 1.5 mL glass vial and analyzed by GC-FID to determine the product yield.

7.4.4 Synthesis & Characterization of products

General procedure for flow reactions in 0.5 or 1.0 mmol scale (GP5):

A flow reactor packed with **SP-IBS II** (1.10 g, 0.38 mmol/g) was placed in a water bath preheated to 50 °C. The substrate (0.5 or 1.0 mmol, 1.0 equiv) was dissolved in AcOH (3.0 or 6.0 mL), and TBA-Oxone® (nBu$_4$NHSO$_5$, 0. 98–1.95 g, 5.0–10.0 mmol, 5 equiv, 91%) was dissolved separately in AcOH (2.0–4.0 mL), affording a total solution volume of 5.0-10.0 mL. Using a dual syringe pump, the two solutions were then conducted with a preadjusted flow-rate 5 mL/h through the reactor, first passing a three-way valve where they were mixed together, next passing through the catalyst cartridge and at last being collected into a flask. After the two solutions were passed through the reactor completely, it was additionally washed with AcOH (10 mL) using the syringe pump, which led to a total volume of 15.0-20.0 mL product solution. The reaction mixture was concentrated under reduced pressure and purified by flash chromatography using silica gel to yield the desired product.

5-(Phenoxymethyl)dihydrofuran-2(3H)-one (2.5)

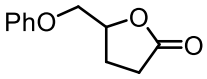

$C_{11}H_{12}O_3$
192.08 g/mol

Synthesized following **GP5** using (5-(phenoxymethyl)tetrahydrofuran-2-yl)methanol (208 mg, 1.0 mmol, 1.0 equiv.). Purification via flash chromatography using silica gel (CyHex/EtOAc, 8:2 → CyHex/EtOAc, 7:3) afforded product as a colourless oil in 85% yield (163 mg, 0.83 mmol).

^{1}H NMR (400 MHz, $CDCl_3$) δ 7.36 – 7.24 (m, 2H), 6.98 (t, *J* = 7.4 Hz, 1H), 6.90 (dd, *J* = 8.8, 0.9 Hz, 2H), 4.91 – 4.81 (m, 1H), 4.17 (dd, *J* = 10.4, 3.6 Hz, 1H), 4.08 (dd, *J* = 10.4, 4.1 Hz, 1H), 2.80 – 2.66 (m, 1H), 2.63 – 2.50 (m, 1H), 2.48 – 2.35 (m, 1H), 2.33 – 2.20 (m, 1H).
^{13}C NMR (101 MHz, $CDCl_3$) δ 177.1, 158.3, 129.7, 121.6, 114.7, 78.0, 69.3, 28.4, 24.2.
IR (ATR): $\tilde{\nu}$ [cm^{-1}] = 2923, 2854, 1769, 1598, 1587, 1493, 1456, 1418, 1346, 1292, 1241, 1154, 1110, 1080, 1038, 982, 945, 919, 887, 856,809, 754, 691, 650.
HRMS (ESI): [m/z] calculated for $C_{11}H_{12}NaO_3$ ($[M+Na]^+$): 215.0678; Found: 215.0679.
R_f (CyHex/EtOAc, 7:3) = 0.36 [$KMnO_4$].
All the characterization data are consistent with the literature.[278]

5-((Benzyloxy)methyl)dihydrofuran-2(3*H*)-one (2.6)

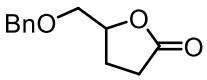

$C_{12}H_{14}O_3$
206.09 g/mol

Synthesized following **GP5** using (5-((benzyloxy)methyl)tetrahydrofuran-2-yl)methanol (222 mg, 1.0 mmol, 1.0 equiv.). Purification via flash chromatography using silica gel (PE/EtOAc, 4:1) afforded product as a colourless oil in 52% yield (107 mg, 0.52 mmol).

^{1}H NMR (600 MHz, $CDCl_3$) δ 7.41 – 7.36 (m, 2H), 7.36 – 7.31 (m, 3H), 4.70 (dddd, J = 7.7, 5.8, 4.2, 3.4 Hz, 1H), 4.64 – 4.55 (m, 2H), 3.71 (dd, J = 10.7, 3.4 Hz, 1H), 3.62 (dd, J = 10.7, 4.2 Hz, 1H), 2.71 – 2.58 (m, 1H), 2.58 – 2.43 (m, 1H), 2.41 – 2.25 (m, 1H), 2.23 – 2.10 (m, 1H).
^{13}C NMR (151 MHz, $CDCl_3$) δ 177.4, 137.8, 128.6, 128.0, 127.8, 79.1, 73.8, 71.7, 28.5, 24.3.
IR (ATR): $\tilde{\nu}$ [cm^{-1}] = 3369, 3242, 1671, 1615, 1382, 1108, 831, 749, 648, 617.

HRMS (ESI): [m/z] calculated for C12H14NaO3 ([M+Na]+): 229.0835; Found: 229.0835.
R_f (PE/EtOAc, 4:1) = 0.25 [$KMnO_4$].
All the characterization data are consistent with the literature.[259]

(5-Oxotetrahydrofuran-2-yl)methyl benzoate (2.7)

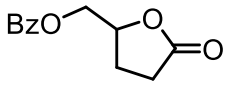

$C_{12}H_{12}O_4$
220.07 g/mol

Synthesized following **GP5** using (5-(hydroxymethyl)tetrahydrofuran-2-yl)methyl benzoate (236 mg, 1.0 mmol, 1.0 equiv.). Purification via flash chromatography using silica gel (CyHex/EtOAc, 7:3) afforded product as a colourless oil in 90% yield (198 mg, 0.90 mmol).

^{1}H NMR (400 MHz, $CDCl_3$) δ 8.07 – 7.98 (m, 2H), 7.62 – 7.53 (m, 1H), 7.52 – 7.37 (m, 2H), 4.92 – 4.82 (m, 1H), 4.54 (dd, *J* = 12.2, 3.2 Hz, 1H), 4.44 (dd, *J* = 12.2, 5.3 Hz, 1H), 2.71 – 2.52 (m, 2H), 2.49 – 2.34 (m, 1H), 2.21 – 2.05 (m, 1H).
^{13}C NMR (101 MHz, $CDCl_3$) δ 176.6, 166.3, 133.6, 129.8, 129.4, 128.7, 77.5, 65.8, 28.3, 24.1.
IR (ATR): $\tilde{\nu}$ [cm^{-1}] = 2954, 1777, 1718, 1601, 1584, 1451, 1381, 1360, 1315, 1270, 1176, 1116, 1068, 1026, 945, 920, 805, 711, 687, 649.
HRMS (ESI): [m/z] calculated for $C_{12}H_{12}NaO_4$ ([M+Na]$^+$): 243.0625; Found: 243.0628.
R_f (CyHex/EtOAc, 7:3) = 0.19 [$KMnO_4$].
All the characterization data are consistent with the literature.[259]

(5-Oxotetrahydrofuran-2-yl)methyl acetate (2.8)

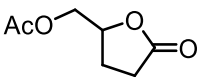

$C_7H_{10}O_4$
158.06 g/mol

Synthesized following **GP5** using (5-(hydroxymethyl)tetrahydrofuran-2-yl)methyl acetate (174 mg, 1.0 mmol, 1.0 equiv.). Purification via flash chromatography using silica gel (CyHex/EtOAc, 8:2) afforded product as a colourless oil in 87% yield (138 mg, 0.87 mmol).

^{1}H NMR (400 MHz, $CDCl_3$) δ 4.73 (dddd, *J* = 7.5, 6.8, 5.5, 3.1 Hz, 1H), 4.31 (dd, *J* = 12.2, 3.2 Hz, 1H), 4.14 (dd, *J* = 12.2, 5.5 Hz, 1H), 2.67 – 2.48 (m, 2H), 2.35 (dddd, *J* = 13.0, 9.2, 7.6, 6.4 Hz, 1H), 2.09 (s, 3H), 2.09 – 1.98 (m, 1H).

^{13}C NMR (101 MHz, $CDCl_3$) δ 176.6, 170.7, 65.4, 28.3, 24.1, 20.9.

IR (ATR): $\tilde{\nu}$ [cm^{-1}] = 3980, 1772, 1735, 1371, 1230, 1160, 1073, 1038969, 943, 893, 848, 804, 651, 603.

HRMS (ESI): [m/z] calculated for $C_7H_{10}NaO_4$ ($[M+Na]^+$): 181.0469; Found: 181.0471.

R_f (CyHex/EtOAc, 8:2) = 0.19 [$KMnO_4$].

All the characterization data are consistent with the literature.[106]

(5-Oxotetrahydrofuran-2-yl)methyl 4-methylbenzenesulfonate (2.9)

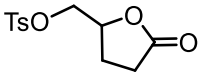

$C_{12}H_{14}O_5S$
270.07 g/mol

Synthesized following **GP5** using (5-(hydroxymethyl)tetrahydrofuran-2-yl)methyl 4-methylbenzenesulfonate (286 mg, 1.0 mmol, 1.0 equiv.). Purification via flash chromatography using silica gel (CyHex/EtOAc, 7:3) afforded product as a white solid in 89% yield (241 mg, 0.89 mmol).

^{1}H NMR (600 MHz, $CDCl_3$) δ 7.83 – 7.69 (m, 2H), 7.35 (d, *J* = 7.8 Hz, 2H), 4.71 – 4.62 (m, 1H), 4.18 (dd, *J* = 11.1, 3.4 Hz, 1H), 4.12 (dd, *J* = 11.0, 4.3 Hz, 1H), 2.73 – 2.49 (m, 2H), 2.44 (s, 3H), 2.40 – 2.27 (m, 1H), 2.16 – 2.08 (m, 1H).

^{13}C NMR (151 MHz, $CDCl_3$) δ 176.1, 145.5, 132.4, 130.2, 128.1, 76.5, 70.1, 28.0, 23.6, 21.8.

IR (ATR): $\tilde{\nu}$ [cm^{-1}] = 2954, 1781, 1732, 1598, 1452, 1357, 1357, 1307, 1292, 1189, 1175, 1096, 1019, 958, 815, 790, 665, 554.

HRMS (ESI): [m/z] calculated for $C_{12}H_{14}NaO_5S$ ($[M+Na]^+$): 293.0453; Found: 293.0454.

R_f (CyHex/EtOAc, 7:3) = 0.11 [$KMnO_4$].

All the characterization data are consistent with the literature.[259]

5-(((*tert*-Butyldiphenylsilyl)oxy)methyl)dihydrofuran-2(3*H*)-one (2.10)

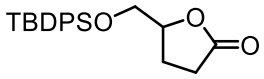

$C_{21}H_{26}O_3Si$
354.16 g/mol

Synthesized following **GP5** using (5-(((tert-butyldiphenylsilyl)oxy)methyl)tetrahydrofuran-2-yl)methanol (371 mg, 1.0 mmol, 1.0 equiv.). Purification via flash chromatography using silica gel (CyHex/EtOAc, 7:3) afforded product as a colourless oil in 71% yield (252 mg, 0.71 mmol).

^{1}H NMR (400 MHz, $CDCl_3$) δ 7.72 – 7.60 (m, 4H), 7.52 – 7.35 (m, 6H), 4.80 – 4.53 (m, 1H), 3.88 (dd, *J* = 11.3, 3.3 Hz, 1H), 3.69 (dd, *J* = 11.4, 3.4 Hz, 1H), 2.68 (ddd, *J* = 17.4, 10.1, 7.2 Hz, 1H), 2.51 (ddd, *J* = 17.7, 9.9, 6.6 Hz, 1H), 2.37 – 2.15 (m, 2H), 1.06 (s, 9H).
^{13}C NMR (101 MHz, $CDCl_3$) δ 177.6, 135.8, 135.7, 133.1, 132.7, 130.1, 128.0, 80.1, 65.6, 28.7, 26.9, 23.8, 19.3.
IR (ATR): $\tilde{\nu}$ [cm^{-1}] = 3071, 2956, 2931, 2892, 2857, 1776, 1471, 1461, 1427, 1390, 1346, 1262, 1174, 1112, 1083, 1031, 995, 941, 914, 886, 858, 822, 799, 742, 702, 504, 489.
HRMS (ESI): [m/z] calculated for $C_{21}H_{26}NaO_3Si$ ($[M+Na]^+$): 377.1546; Found: 377.1543.
R_f (CyHex/EtOAc, 7:3) = 0.26 [$KMnO_4$].
All the characterization data are consistent with the literature.[106]

5-(Azidomethyl)dihydrofuran-2(3*H*)-one (2.11)

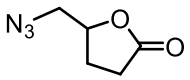

$C_5H_7N_3O_2$
141.05 g/mol

Synthesized following **GP5** using (5-(azidomethyl)tetrahydrofuran-2-yl)methanol (79 mg, 0.5 mmol, 1.0 equiv.). Purification via flash chromatography using silica gel (CyHex/EtOAc, 4:1) afforded product as a colourless oil in 56% yield (40 mg, 0.28 mmol).

^{1}H NMR (400 MHz, $CDCl_3$) δ 4.68 – 4.56 (m, 1H), 3.58 (dd, *J* = 13.3, 3.7 Hz, 1H), 3.43 (dd, *J* = 13.3, 5.0 Hz, 1H), 2.69 – 2.42 (m, 2H), 2.37 – 2.23 (m, 1H), 2.11 – 1.92 (m, 1H).
^{13}C NMR (101 MHz, $CDCl_3$) δ 176.4, 78.1, 54.1, 28.2, 24.5.
IR (ATR): $\tilde{\nu}$ [cm^{-1}] = 2938, 2094, 1768, 1672, 1449, 1439, 1350, 1217, 1097, 941, 913, 803, 730, 650.
HRMS (ESI): [m/z] calculated for $C_5H_7N_3NaO_2$ ($[M+Na]^+$): 164.0431; Found: 164.0430.
R_f (CyHex/EtOAc, 7:3) = 0.26 [$KMnO_4$].

5-(Chloromethyl)dihydrofuran-2(3*H*)-one (2.12)

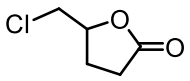

$C_5H_7ClO_2$
134.01 g/mol

Synthesized following **GP5** using (5-(chloromethyl)tetrahydrofuran-2-yl)methanol (151 mg, 1.0 mmol, 1.0 equiv.). Purification via flash chromatography using silica gel (CyHex/EtOAc, CyHex/EtOAc, 8:1 → 7:3) afforded product as a yellow oil in 77% yield (104 mg, 0.77 mmol).

^{1}H NMR (400 MHz, $CDCl_3$) δ 4.90 – 4.71 (m, 1H), 3.76 – 3.71 (m, 1H), 3.70 – 3.66 (m, 1H), 2.72 – 2.51 (m, 2H), 2.47 – 2.36 (m, 1H), 2.23 – 2.11 (m, 1H).
^{13}C NMR (101 MHz, $CDCl_3$) δ 176.4, 78.2, 46.1, 28.3, 25.1.
IR (ATR): $\tilde{\nu}$ [cm^{-1}] = 2960, 1767, 1660, 1420, 1342, 1283, 1283, 1259, 1169, 1142, 1043, 993, 919, 832, 740, 653.
HRMS (ESI): [m/z] calculated for $C_5H_7ClNaO_2$ ($[M+Na]^+$): 157.0026; Found: 157.0027.
R_f (CyHex/EtOAc, 8:2) = 0.15 [$KMnO_4$].
All the characterization data are consistent with the literature.[279]

2-((5-Oxotetrahydrofuran-2-yl)methyl)isoindoline-1,3-dione (2.13)

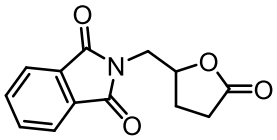

$C_{13}H_{11}NO_4$
245.07 g/mol

Synthesized following **GP5** using 2-((5-(hydroxymethyl)tetrahydrofuran-2-yl)methyl)isoindoline-1,3-dione (261 mg, 1.0 mmol, 1.0 equiv.). Purification via flash chromatography using silica gel (CyHex/EtOAc, 7:3) afforded product as a white solid in 66% yield (162 mg, 0.66 mmol).

^{1}H NMR (600 MHz, $CDCl_3$) δ 7.90 – 7.83 (m, 2H), 7.76 – 7.72 (m, 2H), 4.90 – 4.81 (m, 1H), 4.00 (dd, *J* = 14.2, 7.7 Hz, 1H), 3.83 (dd, *J* = 14.2, 5.3 Hz, 1H), 2.67 – 2.58 (m, 1H), 2.58 – 2.49 (m, 1H), 2.45 – 2.29 (m, 1H), 2.13 – 1.98 (m, 1H).
^{13}C NMR (151 MHz, $CDCl_3$) δ 176.1, 168.1, 134.4, 131.9, 123.7, 76.8, 41.5, 28.1, 25.6.
IR (ATR): $\tilde{\nu}$ [cm^{-1}] = 2928, 1773, 1713, 1613, 1467, 1467, 1423, 1394, 1314, 1291, 1172, 1118, 1069, 1032, 917, 799, 721, 615, 530.

HRMS (ESI): [m/z] calculated for $C_{13}H_{11}NNaO_4$ ([M+Na]$^+$): 268.0581; Found: 268.0580.
R_f (CyHex/EtOAc, 7:3) = 0.29 [$KMnO_4$].
All the characterization data are consistent with the literature.[280]

5-((Prop-2-yn-1-yloxy)methyl)dihydrofuran-2(3*H*)-one (2.14)

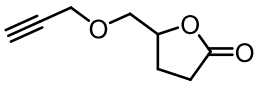

$C_8H_{10}O_3$
154.06 g/mol

Synthesized following **GP5** using (5-((prop-2-yn-1-yloxy)methyl)tetrahydrofuran-2-yl)methanol (170 mg, 1.0 mmol, 1.0 equiv.). Purification via flash chromatography using silica gel (CyHex/EtOAc, 9:1 → CyHex/EtOAc, 8:2) afforded product as a colourless liquid in 79% yield (122 mg, 0.79 mmol).

^{1}H NMR (400 MHz, $CDCl_3$) δ 4.74 – 4.57 (m, 1H), 4.18 (qd, 2H), 3.71 (dd, *J* = 10.7, 3.4 Hz, 1H), 3.65 (dd, *J* = 10.7, 4.4 Hz, 1H), 2.65 – 2.54 (m, 1H), 2.52 – 2.40 (m, 2H), 2.35 – 2.22 (m, 1H), 2.17 – 2.05 (m, 1H).
^{13}C NMR (101 MHz, $CDCl_3$) δ 177.3, 79.1, 78.7, 75.2, 71.2, 58.8, 28.4, 24.1.
IR (ATR): $\tilde{\nu}$ [cm^{-1}] = 3272, 2980, 1764,1460, 1418, 1355, 1264, 1219, 1180, 1111, 1053, 1008, 941, 914, 804, 649.
HRMS (ESI): [m/z] calculated for $C_8H_{10}NaO_3$ ([M+Na]$^+$): 177.0523; Found: 177.0522.
R_f (CyHex/EtOAc, 8:2) = 0.31 [$KMnO_4$].

5-((Allyloxy)methyl)dihydrofuran-2(3*H*)-one (2.15)

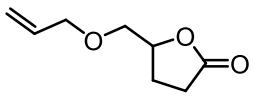

$C_8H_{12}O_3$
156.08 g/mol

Synthesized following **GP5** using (5-((allyloxy)methyl)tetrahydrofuran-2-yl)methanol (86.1 mg, 0.5 mmol, 1.0 equiv.). Purification via flash chromatography using silica gel (CyHex/EtOAc, 7:3) afforded product as a colourless liquid in 33% yield (26.0 mg, 0.17 mmol).

^{1}H NMR (400 MHz, $CDCl_3$) δ 6.05 – 5.72 (m, 1H), 5.29 – 5.21 (m, 1H), 5.21 – 5.15 (m, 1H), 4.69 – 4.59 (m, 1H), 4.04 – 3.99 (m, 2H), 3.63 (dd, *J* = 10.8, 3.4 Hz, 1H), 3.55 (dd, *J* = 10.8, 4.3 Hz, 1H), 2.72 – 2.55 (m, 1H), 2.53 – 2.42 (m, 1H), 2.35 – 2.22 (m, 1H), 2.17 – 2.05 (m, 1H).

^{13}C NMR (101 MHz, $CDCl_3$) δ 177.4, 134.3, 117.5, 79.1, 72.6, 71.6, 28.5, 24.2.
IR (ATR): $\tilde{\nu}$ [cm^{-1}] = 2862, 1767, 1645, 1460, 1421, 1348, 1269, 1167, 1118, 1115, 1084, 1055, 998, 940, 886, 804, 651.
HRMS (ESI): [m/z] calculated for $C_8H_{12}NaO_3$ ([M+Na]$^+$): 179.0679; Found: 179.0679.
R_f (CyHex/EtOAc, 7:3) = 0.24 [$KMnO_4$].

(5-Oxotetrahydrofuran-2-yl)methyl 4-cyanobenzoate (2.16)

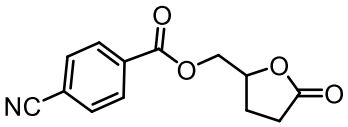

$C_{13}H_{11}NO_4$
245.07 g/mol

Synthesized following **GP5** using (5-(hydroxymethyl)tetrahydrofuran-2-yl)methyl 4-cyanobenzoate (131 mg, 0.5 mmol, 1.0 equiv.). Purification via flash chromatography using silica gel (CyHex/EtOAc, 7:3) afforded product as a colourless liquid in 38% yield (46.8 mg, 0.19 mmol).

^{1}H NMR (400 MHz, $CDCl_3$) δ 8.11 (d, *J* = 8.7 Hz, 2H), 7.74 (d, *J* = 8.8 Hz, 2H), 4.87 (tdd, *J* = 7.3, 6.0, 3.0 Hz, 1H), 4.57 (dd, *J* = 12.3, 3.0 Hz, 1H), 4.43 (dd, *J* = 12.3, 6.0 Hz, 1H), 2.69 – 2.56 (m, 2H), 2.43 (dq, *J* = 13.0, 7.6 Hz, 1H), 2.19 – 2.02 (m, 1H).
^{13}C NMR (101 MHz, $CDCl_3$) δ 176.4, 164.6, 133.2, 132.4, 130.3, 117.9, 116.9, 77.2, 66.5, 28.2, 24.0.
IR (ATR): $\tilde{\nu}$ [cm^{-1}] = 2955, 2231, 1774, 1723, 1610, 1459, 1406, 1361, 1310, 1268, 1220, 1163, 1119, 1108, 1067, 1018, 944, 911, 860, 765, 726, 690, 646.
HRMS (ESI): [m/z] calculated for $C_{13}H_{11}NNaO_4$ ([M+Na]$^+$): 268.0579; Found: 268.0580.
R_f (CyHex/EtOAc, 4:6) = 0.16 [$KMnO_4$].

5-Hexyldihydrofuran-2(3*H*)-one (2.17)

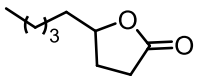

$C_{10}H_{18}O_2$
170.13 g/mol

Synthesized following GP5 using (5-hexyltetrahydrofuran-2-yl)methanol (186 mg, 1.0 mmol, 1.0 equiv.). Purification via flash chromatography using silica gel (CyHex/EtOAc, 7:3) afforded product as a white solid in 86% yield (146 mg, 0.86 mmol).

^{1}H NMR (400 MHz, $CDCl_3$) δ 4.56 – 4.43 (m, 1H), 2.60 – 2.48 (m, 2H), 2.40 – 2.27 (m, 1H), 1.87 (dtd, *J* = 12.7, 9.5, 8.0 Hz, 1H), 1.81 – 1.69 (m, 1H), 1.67 – 1.54 (m, 1H), 1.51 – 1.24 (m, 8H), 0.94 – 0.86 (m, 3H).
^{13}C NMR (101 MHz, $CDCl_3$) δ 177.4, 81.1, 35.7, 31.7, 29.1, 28.9, 28.1, 25.3, 22.6, 14.1.
IR (ATR): $\tilde{\nu}$ [cm^{-1}] = 29802924, 1767, 1598, 5186, 1493, 1456, 1363, 1347, 1292, 1240, 1155, 1113, 990, 753.
HRMS (ESI): [m/z] calculated for $C_{10}H_{18}NaO_2$ ($[M+Na]^+$): 193.1199; Found: 193.1199.
R_f (CyHex/EtOAc, 7:3) = 0.22 [$KMnO_4$].
The characterization data is consistent with the literature.[281]

5-(4-Methoxyphenyl)dihydrofuran-2(3*H*)-one (2.18)

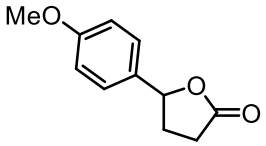

$C_{11}H_{12}O_3$
192.08 g/mol

Synthesized following **GP5** using (5-(4-methoxyphenyl)tetrahydrofuran-2-yl)methanol (208 mg, 1.0 mmol, 1.0 equiv.). Purification via flash chromatography using silica gel (CyHex/EtOAc, 7:3) afforded product as a white solid in 70% yield (135 mg, 0.70 mmol).

^{1}H NMR (600 MHz, $CDCl_3$) δ 7.26 (d, *J* = 8.3 Hz, 2H), 6.91 (d, *J* = 8.9 Hz, 2H), 5.60 – 5.37 (m, 1H), 3.81 (s, 3H), 2.70 – 2.53 (m, 3H), 2.30 – 2.08 (m, 1H).
^{13}C NMR (151 MHz, $CDCl_3$) δ 177.0, 160.0, 131.4, 127.1, 114.3, 81.5, 55.5, 31.0, 29.3.
IR (ATR): $\tilde{\nu}$ [cm^{-1}] = 2937, 2838, 1767, 1612, 1587, 1515, 1459, 1420, 1373, 1328, 1292, 1247, 1216, 1172, 1141, 1111, 1029, 981, 936, 892, 834, 807, 772, 698, 673.
HRMS (ESI): [m/z] calculated for $C_{11}H_{12}NaO_3$ ($[M+Na]^+$): 215.0679; Found: 215.0679.
R_f (CyHex/EtOAc, 9:1) = 0.15 [$KMnO_4$].
The characterization data is consistent with the literature.[280]

5-(4-Bromophenyl)dihydrofuran-2(3*H*)-one (2.19)

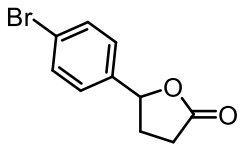

$C_{10}H_9BrO_2$
239.99 g/mol

Synthesized following **GP5** using (5-(4-bromophenyl)tetrahydrofuran-2-yl)methanol (129 mg, 0.5 mmol, 1.0 equiv.). Purification via flash chromatography using silica gel (CyHex/EtOAc, 7:3) afforded product as a brown solid in 73% yield (87.9 mg, 0.36 mmol).

^{1}H NMR (400 MHz, $CDCl_3$) δ 7.52 (d, *J* = 8.5 Hz, 2H), 7.21 (d, *J* = 8.1 Hz, 2H), 5.53 – 5.42 (m, 1H), 2.73 – 2.60 (m, 3H), 2.20 – 2.09 (m, 1H).
^{13}C NMR (101 MHz, $CDCl_3$) δ 176.7, 138.6, 132.1, 127.1, 122.6, 80.6, 31.1, 29.0.
IR (ATR): $\tilde{\nu}$ [cm^{-1}] = 2950, 1780, 1686, 1586, 1490, 1456, 1399, 1359, 1326, 1296, 1214, 1173, 1141, 1104, 1070, 1028, 1010, 988, 938, 889, 834, 806, 758, 715, 671.
HRMS (ESI): [m/z] calculated for $C_{10}H_9BrNaO_2$ ($[M+Na]^+$): 262.9674; Found: 262.9678.
R_f (CyHex/EtOAc, 7:3) = 0.39 [$KMnO_4$].
The characterization data is consistent with the literature.[282]

5-(Thiophen-2-yl)dihydrofuran-2(3*H*)-one (2.20)

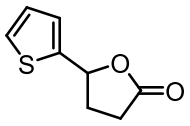

$C_8H_8O_2S$
168.02 g/mol

Synthesized following **GP5** using (5-(thiophen-2-yl)tetrahydrofuran-2-yl)methanol (92.1 mg, 0.5 mmol, 1.0 equiv.). Purification via flash chromatography using silica gel (CyHex/EtOAc, 7:3) afforded product as a brown solid in 22% yield (18.5 mg, 0.11 mmol).

^{1}H NMR (600 MHz, $CDCl_3$) δ 7.34 (dd, *J* = 5.1, 1.2 Hz, 1H), 7.09 (d, *J* = 3.5 Hz, 1H), 7.01 (dd, *J* = 5.1, 3.5 Hz, 1H), 5.75 – 5.70 (m, 1H), 2.71 – 2.64 (m, 3H), 2.45 – 2.32 (m, 1H).
^{13}C NMR (151 MHz, $CDCl_3$) δ 176.2, 141.9, 127.1, 126.3, 126.0, 77.4, 30.9, 29.1.
IR (ATR): $\tilde{\nu}$ [cm^{-1}] = 3107, 2931, 1770, 1538, 1457, 1438, 1419, 1381, 1327, 1297, 1275, 1205, 1171, 1135, 1080, 1012, 978, 920, 879, 852, 807, 759, 708, 671, 629.
HRMS (ESI): [m/z] calculated for $C_8H_8NaO_2S$ ($[M+Na]^+$): 191.0138; Found: 191.0137.
R_f (CyHex/EtOAc, 7:3) = 0.32 [$KMnO_4$].

The characterization data is consistent with the literature.[283]

(5-Oxotetrahydrofuran-2-yl)methyl-3-(5-(2-fluorophenyl)-1,2,4-oxadiazol-3-yl)benzoate (2.21)

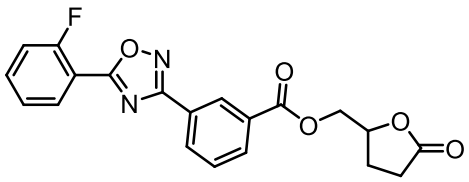

$C_{20}H_{15}FN_2O_5$
382.10 g/mol

Synthesized following **GP5** using (5-(hydroxymethyl)tetrahydrofuran-2-yl)methyl 3-(5-(2-fluorophenyl)-1,2,4-oxadiazol-3-yl)benzoate (199 mg, 0.5 mmol, 1.0 equiv.). Purification via flash chromatography using silica gel (CyHex/EtOAc, 7:3) afforded product as a white solid in 62% yield (118 mg, 0.31 mmol).

^{1}H NMR (400 MHz, CD_2Cl_2) δ 8.84 – 8.74 (m, 1H), 8.39 (d, *J* = 8.0 Hz, 1H), 8.23 (d, *J* = 21.2 Hz, 2H), 7.71 – 7.57 (m, 2H), 7.44 – 7.27 (m, 2H), 4.96 – 4.84 (m, 1H), 4.65 – 4.52 (m, 1H), 4.52 – 4.41 (m, 1H), 2.71 – 2.53 (m, 2H), 2.52 – 2.37 (m, 1H), 2.22 – 2.07 (m, 1H).

^{13}C NMR (101 MHz, CD_2Cl_2) δ 176.6, 168.2, 165.6, 162.4, 135.2 (d, *J* = 9.0 Hz), 132.5, 132.3, 131.3, 130.8, 129.6, 128.9, 127.8, 117.4 (d, *J* = 21.1 Hz), 112.9 (d, *J* = 11.1 Hz), 77.7, 66.5, 28.4, 24.3.

^{19}F NMR (376 MHz, CD_2Cl_2) δ -109.24.

IR (ATR): $\tilde{\nu}$ [cm^{-1}] = 2958, 1775, 1721, 1620, 1595, 1595, 1555, 1523, 1494, 1462, 1413, 1367, 1349, 1287, 1253, 1226, 1166, 1143, 1110, 1067, 1030, 987, 973, 944, 923, 824, 803, 782, 767, 747, 721, 693, 669, 653.

HRMS (ESI): [m/z] calculated for $C_{20}H_{15}FN_2NaO_5$ ($[M+Na]^+$): 405.0858; Found: 405.0858.

R_f (CyHex/EtOAc, 7:3) = 0.17 [$KMnO_4$].

5-(((1-(4-Bromophenyl)-1*H*-1,2,3-triazol-4-yl)methoxy)methyl)dihydrofuran-2(3*H*)-one (2.22)

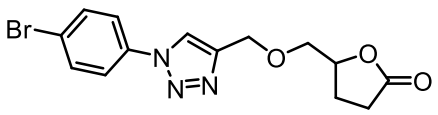

$C_{14}H_{14}BrN_3O_3$
351.02 g/mol

Synthesized following **GP5** using (5-(((1-(4-bromophenyl)-1*H*-1,2,3-triazol-4-yl)methoxy)methyl)tetrahydrofuran-2-yl)methanol (184 mg, 0.5 mmol, 1.0 equiv.). Purification via flash chromatography using silica gel (CyHex/EtOAc, 7:3) afforded product as a colorless oil in 72% yield (128 mg, 0.36 mmol).

^{1}H NMR (400 MHz, $CDCl_3$) δ 7.99 (s, 1H), 7.73 – 7.59 (m, 4H), 4.80 (dd, *J* = 12.7, 0.6 Hz, 1H), 4.75 (dd, *J* = 12.6, 0.6 Hz, 1H), 4.74 – 4.64 (m, 1H), 3.81 (dd, *J* = 10.8, 3.0 Hz, 1H), 3.69 (dd, *J* = 10.8, 4.3 Hz, 1H), 2.67 – 2.54 (m, 1H), 2.56 – 2.43 (m, 1H), 2.37 – 2.24 (m, 1H), 2.20 – 2.06 (m, 1H).
^{13}C NMR (101 MHz, $CDCl_3$) δ 177.4, 136.1, 133.1, 122.7, 122.1, 120.9, 78.9, 72.2, 65.0, 28.6, 24.1.
IR (ATR): $\tilde{\nu}$ [cm^{-1}] = 3140, 3099, 2925, 2867, 1768, 1497, 1459, 1418, 1402, 1346, 1229, 1185, 1115, 1072, 1042, 1013, 988, 941, 916, 886, 827, 770, 725, 689, 651.
HRMS (ESI): [m/z] calculated for $C_{14}H_{14}BrN_3NaO_3$ ($[M+Na]^+$): 374.0111; Found: 374.0111.
R_f (CyHex/EtOAc, 4:6) = 0.15 [$KMnO_4$].

4-Phenyldihydrofuran-2(3*H*)-one (2.23)

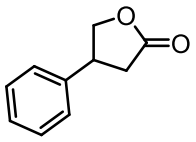

$C_{10}H_{10}O_2$
162.07 g/mol

Synthesized following **GP5** using (4-phenyltetrahydrofuran-2-yl)methanol (178 mg, 1.0 mmol, 1.0 equiv.). Purification via flash chromatography using silica gel (CyHex/EtOAc, 9:1 → CyHex/EtOAc, 7:3) afforded product as a colorless oil in 88% yield (143 mg, 0.88 mmol).

^{1}H NMR (400 MHz, $CDCl_3$) δ 7.41 – 7.34 (m, 2H), 7.33 – 7.27 (m, 1H), 7.26 – 7.20 (m, 2H), 4.67 (dd, *J* = 9.0, 7.9 Hz, 1H), 4.27 (dd, *J* = 9.1, 7.9 Hz, 1H), 3.91 – 3.70 (m, 1H), 2.93 (dd, *J* = 17.5, 8.7 Hz, 1H), 2.68 (dd, *J* = 17.5, 9.1 Hz, 1H).
^{13}C NMR (101 MHz, $CDCl_3$) δ 176.5, 139.5, 129.2, 127.8, 126.8, 74.1, 41.2, 35.8.
IR (ATR): $\tilde{\nu}$ [cm^{-1}] = 3062, 3031, 2908, 1770, 1603, 1496, 1479, 1454, 1421, 1374, 1352, 1307, 1285, 1225, 1165, 1072, 1016, 947, 900, 851, 817, 758, 699, 641.
HRMS (ESI): [m/z] calculated for $C_{10}H_{10}NaO_2$ ($[M+Na]^+$): 185.0573; Found: 185.0573.
R_f (CyHex/EtOAc, 7:3) = 0.47 [$KMnO_4$].
The characterization data is consistent with the literature.[284]

4-(4-Methoxyphenyl)dihydrofuran-2(3*H*)-one (2.24)

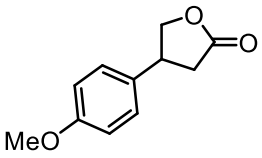

$C_{11}H_{12}O_3$
192.08 g/mol

Synthesized following **GP5** using (4-(4-methoxyphenyl)tetrahydrofuran-2-yl)methanol (208 mg, 1.0 mmol, 1.0 equiv.). Purification via flash chromatography using silica gel (CyHex/EtOAc, 7:3) afforded product as a colorless oil in 61% yield (117 mg, 0.61 mmol).

^{1}H NMR (400 MHz, $CDCl_3$) δ 7.15 (d, *J* = 8.4 Hz, 2H), 6.89 (d, *J* = 8.7 Hz, 2H), 4.63 (dd, *J* = 9.0, 7.8 Hz, 1H), 4.22 (dd, *J* = 9.0, 8.1 Hz, 1H), 3.80 (s, 3H), 3.77 – 3.66 (m, 1H), 2.89 (dd, *J* = 17.5, 8.6 Hz, 1H), 2.63 (dd, *J* = 17.5, 9.3 Hz, 1H).
^{13}C NMR (101 MHz, $CDCl_3$) δ 176.7, 159.2, 131.4, 127.9, 114.6, 74.4, 55.5, 40.6, 36.0.
IR (ATR): $\tilde{\nu}$ [cm^{-1}] = 2980, 2906, 1768, 1612, 1514, 1463, 1443, 1429, 1377, 1294, 1247, 1207, 1165, 1116, 1017, 830.
HRMS (ESI): [m/z] calculated for $C_{11}H_{12}NaO_3$ ($[M+Na]^+$): 215.0679; Found: 215.0679.
R_f (CyHex/EtOAc, 7:3) = 0.49 [$KMnO_4$].
The characterization data is consistent with the literature.[284]

4-(4-Bromophenyl)dihydrofuran-2(3*H*)-one (2.25)

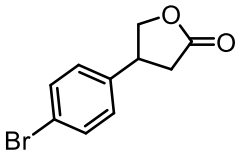

$C_{10}H_9BrO_2$
239.99 g/mol

Synthesized following **GP5** using (5-(4-bromophenyl)tetrahydrofuran-2-yl)methanol (257 mg, 1.0 mmol, 1.0 equiv.). Purification via flash chromatography using silica gel (CyHex/EtOAc, 7:3) afforded product as a colorless oil in 83% yield (201 mg, 0.83 mmol).

^{1}H NMR (400 MHz, $CDCl_3$) δ 7.49 (d, *J* = 8.4 Hz, 2H), 7.11 (d, *J* = 8.3 Hz, 2H), 4.65 (dd, *J* = 9.1, 7.8 Hz, 1H), 4.22 (dd, *J* = 9.1, 7.7 Hz, 1H), 3.75 (p, *J* = 8.2 Hz, 1H), 2.92 (dd, *J* = 17.5, 8.7 Hz, 1H), 2.62 (dd, *J* = 17.5, 8.9 Hz, 1H).
^{13}C NMR (101 MHz, $CDCl_3$) δ 176.1, 138.6, 132.4, 128.5, 121.7, 73.8, 40.7, 35.7.
IR (ATR): $\tilde{\nu}$ [cm^{-1}] = 2979, 2908, 1772, 1491, 1408, 1372, 1342, 1301, 1276, 1224, 1204, 1164, 1109, 1073, 1044, 1020, 1009, 947, 901, 853, 754, 714, 691, 672.

HRMS (ESI): [m/z] calculated for $C_{10}H_9BrNaO_2$ ([M+Na]$^+$): 262.9675; Found: 262.9678.
R_f (CyHex/EtOAc, 8:2) = 0.17 [$KMnO_4$].
The characterization data is consistent with the literature.[284]

4-(4-Chlorophenyl)dihydrofuran-2(3*H*)-one (2.26)

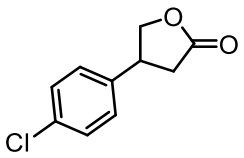

$C_{10}H_9ClO_2$
196.03 g/mol

Synthesized following **GP5** using (4-(4-chlorophenyl)tetrahydrofuran-2-yl)methanol (213 mg, 1.0 mmol, 1.0 equiv.). Purification via flash chromatography using silica gel (CyHex/EtOAc, 7:3) afforded product as a colorless oil in 84% yield (166 mg, 0.84 mmol).

^{1}H NMR (400 MHz, $CDCl_3$) δ 7.34 (d, *J* = 8.5 Hz, 2H), 7.17 (d, *J* = 8.3 Hz, 2H), 4.65 (dd, *J* = 9.1, 7.8 Hz, 1H), 4.23 (dd, *J* = 9.1, 7.7 Hz, 1H), 3.83 – 3.70 (m, 1H), 2.93 (dd, *J* = 17.5, 8.7 Hz, 1H), 2.63 (dd, *J* = 17.5, 8.8 Hz, 1H).
^{13}C NMR (101 MHz, $CDCl_3$) δ 176.1, 138.1, 133.7, 129.4, 128.2, 73.9, 40.6, 35.8.
IR (ATR): $\tilde{\nu}$ [cm^{-1}] = 2970, 2909, 1772, 1596, 1493, 1424, 1372, 1342, 1301, 1277, 1224, 1205, 1161, 1091, 1044, 1012, 945, 901, 852, 824, 759, 718, 704, 675, 632, 622.
HRMS (ESI): [m/z] calculated for $C_{10}H_9ClNaO_2$ ([M+Na]$^+$): 219.0185; Found: 219.0185.
R_f (CyHex/EtOAc, 7:3) = 0.21 [$KMnO_4$].
The characterization data is consistent with the literature.[284]

4-(4-(Trifluoromethyl)phenyl)dihydrofuran-2(3*H*)-one (2.27)

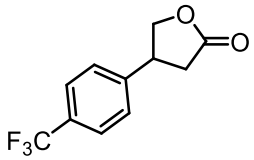

$C_{11}H_9F_3O_2$
230.06 g/mol

Synthesized following **GP5** using (4-(4-(trifluoromethyl)phenyl)tetrahydrofuran-2-yl)methanol (246 mg, 1.0 mmol, 1.0 equiv.). Purification via flash chromatography using silica gel (CyHex/EtOAc, 7:3) afforded product as a colorless oil in 76% yield (176 mg, 0.76 mmol).

^{1}H NMR (400 MHz, $CDCl_3$) δ 7.63 (d, *J* = 7.9 Hz, 2H), 7.37 (d, *J* = 8.1 Hz, 2H), 4.70 (dd, *J* = 9.2, 7.8 Hz, 1H), 4.28 (dd, *J* = 9.2, 7.5 Hz, 1H), 3.86 (p, *J* = 8.1 Hz, 1H), 2.97 (dd, *J* = 17.5, 8.8 Hz, 1H), 2.67 (dd, *J* = 17.5, 8.6 Hz, 1H).

^{13}C NMR (101 MHz, $CDCl_3$) δ 175.9, 143.7, 130.4, 130.1, 126.3 (q, *J* = 3.8 Hz), 73.6, 41.0, 35.6.

^{19}F NMR (376 MHz, $CDCl_3$) δ -62.64.

IR (ATR): $\tilde{\nu}$ [cm^{-1}] = 2979, 2915, 1776, 1620, 1481, 1427, 1375, 1323, 1227, 1160, 1111, 1067, 1045, 1016, 948, 903, 836, 765, 726, 687, 665, 606.

HRMS (ESI): [m/z] calculated for $C_{11}H_9F_3NaO_2$ ([M+Na]$^+$): 253.0446; Found: 253.0447.

R_f (CyHex/EtOAc, 7:3) = 0.18 [$KMnO_4$].

The characterization data is consistent with the literature.[284]

2,8-Dioxaspiro[4.5]decan-3-one (2.28)

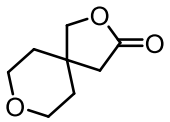

$C_8H_{12}O_3$
156.08 g/mol

Synthesized following **GP5** using (2,8-dioxaspiro[4.5]decan-3-yl)methanol (86 mg, 0.5 mmol, 1.0 equiv.). Purification via flash chromatography using silica gel (CyHex/EtOAc, 7:3) afforded product as a colorless oil in 64% yield (50 mg, 0.32 mmol).

^{1}H NMR (400 MHz, $CDCl_3$) δ 4.10 (s, 2H), 3.72 (ddd, *J* = 12.1, 6.0, 4.1 Hz, 2H), 3.61 (ddd, *J* = 11.7, 7.7, 3.7 Hz, 2H), 2.46 (s, 2H), 1.75 – 1.59 (m, 4H).

^{13}C NMR (101 MHz, $CDCl_3$) δ 176.1, 77.6, 64.7, 40.0, 38.3, 35.1.

IR (ATR): $\tilde{\nu}$ [cm^{-1}] = 2922, 2848, 1769, 1417, 1391, 1377, 1285, 1232, 1210, 1165, 1138, 1104, 1088, 1036, 1012, 980, 949, 890, 842.

HRMS (ESI): [m/z] calculated for $C_8H_{12}NaO_3$ ([M+Na]$^+$): 179.0679; Found: 179.0679.

R_f (CyHex/EtOAc, 7:3) = 0.18 [$KMnO_4$].

The characterization data is consistent with the literature.[285]

Benzyl 3-oxo-2-oxa-8-azaspiro[4.5]decane-8-carboxylate (2.29)

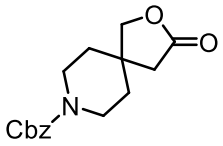

$C_{16}H_{19}NO_4$
289.13 g/mol

Synthesized following **GP5** using benzyl 3-(hydroxymethyl)-2-oxa-8-azaspiro[4.5]decane-8-carboxylate (153 mg, 0.5 mmol, 1.0 equiv.). Purification via flash chromatography using silica gel (CyHex/EtOAc, 7:3) afforded product as a colorless oil in 51% yield (74 mg, 0.26 mmol).

^{1}H NMR (600 MHz, $CDCl_3$) δ 7.39 – 7.32 (m, 5H), 5.13 (s, 2H), 4.08 (s, 2H), 3.73 – 3.62 (m, 2H), 3.38 – 3.30 (m, 2H), 2.43 (s, 2H), 1.64 (s, 4H).
^{13}C NMR (151 MHz, $CDCl_3$) δ 175.8, 155.2, 136.7, 128.7, 128.3, 128.1, 67.5, 41.0, 39.5, 39.1, 34.3.
IR (ATR): $\tilde{\nu}$ [cm^{-1}] = 2989, 1771, 1688, 1472, 1429, 1383, 1359,1272, 1241, 1209, 1161, 1085, 1012, 964, 763, 737,698.
HRMS (ESI): [m/z] calculated for $C_{16}H_{19}NNaO_4$ ($[M+Na]^+$): 312.1207; Found: 312.1207.
R_f (CyHex/EtOAc, 7:3) = 0.11 [$KMnO_4$].
The characterization data is consistent with the literature.[285]

3-Phenyldihydrofuran-2(3*H*)-one (2.30)

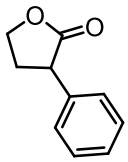

$C_{10}H_{10}O_2$
162.07 g/mol

Synthesized following **GP5** using (3-phenyltetrahydrofuran-2-yl)methanol (178 mg, 1.0 mmol, 1.0 equiv.). Purification via flash chromatography using silica gel (CyHex/EtOAc, 7:3) afforded product as a colorless oil in 70% yield (114 mg, 0.70 mmol).

^{1}H NMR (400 MHz, $CDCl_3$) δ 7.42 – 7.33 (m, 2H), 7.35 – 7.26 (m, 3H), 4.49 (ddd, *J* = 9.1, 8.2, 3.3 Hz, 1H), 4.36 (td, *J* = 9.2, 6.7 Hz, 1H), 3.82 (dd, *J* = 10.2, 8.9 Hz, 1H), 2.79 – 2.66 (m, 1H), 2.53 – 2.37 (m, 1H).
^{13}C NMR (101 MHz, $CDCl_3$) δ 177.5, 136.8, 129.1, 128.0, 127.8, 66.6, 45.6, 31.7.
IR (ATR): $\tilde{\nu}$ [cm^{-1}] = 2980, 2914, 1768, 1686, 1497, 1453, 1373, 1265, 1216, 1151, 1096, 1071, 1024, 953, 919, 753, 699.
HRMS (ESI): [m/z] calculated for $C_{10}H_{10}NaO_2$ ($[M+Na]^+$): 185.0576; Found: 185.0573.
R_f (CyHex/EtOAc, 7:3) = 0.27 [$KMnO_4$].
The characterization data is consistent with the literature.[286]

(3a*S*,7a*R*)-Hexahydrobenzofuran-2(3*H*)-one (2.31)

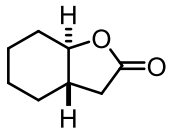

$C_8H_{12}O_2$
140.08 g/mol

Synthesized following **GP5** using ((3a*S*,7a*R*)-octahydrobenzofuran-2-yl)methanol (156 mg, 1.0 mmol, 1.0 equiv.). Purification via flash chromatography using silica gel (CyHex/EtOAc, 7:3) afforded product as a colorless oil in 59% yield (83 mg, 0.59 mmol).

^{1}H NMR (600 MHz, $CDCl_3$) δ 3.76 (dt, *J* = 10.4, 3.8 Hz, 1H), 2.47 (dd, *J* = 16.2, 6.4 Hz, 1H), 2.25 – 2.16 (m, 2H), 1.98 – 1.83 (m, 3H), 1.80 – 1.73 (m, 1H), 1.51 (qd, *J* = 11.8, 3.8 Hz, 1H), 1.43 – 1.23 (m, 3H).
^{13}C NMR (151 MHz, $CDCl_3$) δ 176.6, 85.2, 44.9, 35.9, 28.4, 25.4, 24.1.
IR (ATR): $\tilde{\nu}$ [cm^{-1}] = 2936, 2863, 1775, 1447, 1211, 1187, 1170, 1130, 1113, 1074, 1026, 929, 875, 835, 696.
HRMS (ESI): [m/z] calculated for $C_8H_{12}NaO_2$ ($[M+Na]^+$): 163.0727; Found: 163.0730.
R_f (CyHex/EtOAc, 8:2) = 0.24 [$KMnO_4$].
The characterization data is consistent with the literature.[287]

Tetrahydro-2*H*-pyran-2-one (2.32)

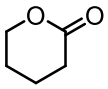

$C_5H_8O_2$
100.05 g/mol

Synthesized following **GP5** using (tetrahydro-2*H*-pyran-2-yl)methanol (119 mg, 1.0 mmol, 1.0 equiv.). Purification via flash chromatography using silica gel (CyHex/EtOAc, 7:3) afforded product as a colorless oil in 45% yield (45 mg, 0.45 mmol).

^{1}H NMR (600 MHz, $CDCl_3$) δ 4.34 (t, *J* = 5.7 Hz, 2H), 2.55 (t, *J* = 7.1 Hz, 2H), 1.95 – 1.88 (m, 2H), 1.88 – 1.82 (m, 2H).
^{13}C NMR (151 MHz, $CDCl_3$) δ 171.4, 69.5, 30.0, 22.5, 19.3.
IR (ATR): $\tilde{\nu}$ [cm^{-1}] = 2957, 2922, 1729, 1400, 1342, 1238, 1158, 1078, 1054, 930.
HRMS (ESI): [m/z] calculated for $C_5H_8NaO_2$ ($[M+Na]^+$): 123.0415; Found: 123.0417.
R_f (CyHex/EtOAc, 7:3) = 0.19 [$KMnO_4$].
The characterization data is consistent with the literature.[283]

Benzyl 2-(tosyloxy)acetate (2.33)

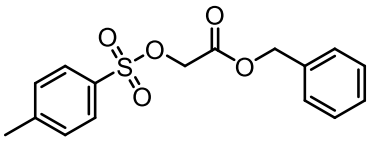

$C_{16}H_{16}O_5S$
320.07 g/mol

Synthesized following **GP5** using 2-(benzyloxy)-3-hydroxypropyl 4-methylbenzenesulfonate (168 mg, 0.5 mmol, 1.0 equiv.). Purification via flash chromatography using silica gel (CyHex/EtOAc, 7:3) afforded product as a colorless oil in 28% yield (45 mg, 0.14 mmol).

^{1}H NMR (400 MHz, $CDCl_3$) δ 7.81 (d, *J* = 8.4 Hz, 2H), 7.38 – 7.34 (m, 3H), 7.34 – 7.29 (m, 4H), 5.15 (s, 2H), 4.63 (s, 2H), 2.44 (s, 3H).
^{13}C NMR (101 MHz, $CDCl_3$) δ 165.9, 145.3, 134.6, 132.6, 129.9, 128.7, 128.6, 128.5, 67.5, 64.6, 21.7.
IR (ATR): $\tilde{\nu}$ [cm^{-1}] = 3034, 2926, 1764, 1597, 1497, 1455, 1365, 1289, 1189, 1175, 1120, 1096, 1044, 815, 771, 751, 698, 663.
HRMS (ESI): [m/z] calculated for $C_{16}H_{16}NaO_5S$ ($[M+Na]^+$): 343.0611; Found: 343.0611.
R_f (CyHex/EtOAc, 9:1) = 0.29 [$KMnO_4$].

Benzyl 2-oxopyrrolidine-1-carboxylate (2.34)

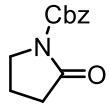

$C_{12}H_{13}NO_3$
219.09 g/mol

Synthesized following **GP5** using benzyl 2-(hydroxymethyl)pyrrolidine-1-carboxylate (235 mg, 1.0 mmol, 1.0 equiv.). Purification via flash chromatography using silica gel (CyHex/EtOAc, 7:3) afforded product as a colorless oil in 43% yield (94 mg, 0.43 mmol).

^{1}H NMR (400 MHz, $CDCl_3$) δ 7.46 – 7.38 (m, 2H), 7.40 – 7.29 (m, 3H), 5.29 – 5.25 (m, 2H), 3.84 – 3.76 (m, 2H), 2.52 (t, *J* = 8.1 Hz, 2H), 2.08 – 1.96 (m, 2H).
^{13}C NMR (101 MHz, $CDCl_3$) δ 174.1, 151.6, 135.4, 128.7, 128.5, 128.3, 68.0, 46.5, 32.8, 17.6.
IR (ATR): $\tilde{\nu}$ [cm^{-1}] = 2924, 2853, 1787, 1749, 1713, 1478, 1450, 1419, 1383, 1368, 1295, 1248, 1174, 1153, 1104, 1077, 1034, 970, 843, 759, 740, 621.
HRMS (ESI): [m/z] calculated for $C_{12}H_{13}NNaO_3$ ($[M+Na]^+$): 242.0787; Found: 242.0788.

R_f (CyHex/EtOAc, 7:3) = 0.25 [$KMnO_4$].
The characterization data is consistent with the literature.[259]

(9*H*-Fluoren-9-yl)methyl 2-oxopyrrolidine-1-carboxylate (2.35)

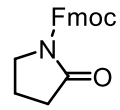

$C_{19}H_{17}NO_3$
307.12 g/mol

Synthesized following **GP5** using (9H-fluoren-9-yl)methyl 2-(hydroxymethyl)pyrrolidine-1-carboxylate (232 mg, 1.0 mmol, 1.0 equiv.). Purification via flash chromatography using silica gel (CyHex/EtOAc, 7:3) afforded product as a colorless oil in 80% yield (246 mg, 0.80 mmol).

^{1}H NMR (400 MHz, $CDCl_3$) δ 7.77 (d, *J* = 7.5 Hz, 2H), 7.73 (d, *J* = 7.5 Hz, 2H), 7.41 (t, *J* = 7.3 Hz, 2H), 7.33 (td, *J* = 7.5, 1.2 Hz, 2H), 4.50 (d, *J* = 7.3 Hz, 2H), 4.31 (t, *J* = 7.3 Hz, 1H), 3.80 (dd, *J* = 7.5, 6.8 Hz, 2H), 2.59 (dd, *J* = 8.4, 7.8 Hz, 2H), 2.22 – 1.86 (m, 2H).
^{13}C NMR (101 MHz, $CDCl_3$) δ 174.0, 151.9, 143.6, 141.4, 128.0, 127.4, 125.5, 120.1, 68.7, 46.8, 46.6, 33.0, 17.7.
IR (ATR): $\tilde{\nu}$ [cm^{-1}] = 2924, 2853, 1787, 1749, 1713, 1478, 1450, 1419, 1383, 1368, 1295, 1248, 1174, 1153, 1104, 1077, 1034, 970, 843, 759, 740, 621.
HRMS (ESI): [m/z] calculated for $C_{19}H_{17}NNaO_3$ ($[M+Na]^+$): 330.1101; Found: 330.1101.
R_f (CyHex/EtOAc, 7:3) = 0.29 [$KMnO_4$].
The characterization data is consistent with the literature.[259]

Benzyl (3-methylbutanoyl)carbamate (2.36)

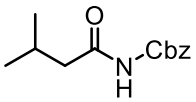

$C_{13}H_{17}NO_3$
235.12 g/mol

Synthesized following **GP5** using benzyl (1-hydroxy-4-methylpentan-2-yl)carbamate (126 mg, 0.5 mmol, 1.0 equiv.). Purification via flash chromatography using silica gel (CyHex/EtOAc, 7:3) afforded product as a colorless oil in 39% yield (46 mg, 0.2 mmol).

^{1}H NMR (400 MHz, $CDCl_3$) δ 7.54 – 7.34 (m, 5H), 5.17 (s, 2H), 2.29 (d, *J* = 7.3 Hz, 2H), 2.25 – 2.07 (m, 1H), 1.02 (s, 3H), 1.00 (s, 3H).

^{13}C NMR (101 MHz, $CDCl_3$) δ 173.1, 136.3, 128.8, 128.6, 128.3, 128.3, 66.1, 43.5, 25.9, 22.5.

IR (ATR): $\tilde{\nu}$ [cm^{-1}] = 2959, 2872, 1733, 1455, 1377, 1356, 1292, 1255, 1183, 1165, 1118, 1095, 1000, 748, 696.

HRMS (ESI): [m/z] calculated for $C_{13}H_{17}NNaO_3$ ($[M+Na]^+$): 258.1103; Found: 258.1103.

R_f (CyHex/EtOAc, 9:1) = 0.31 [$KMnO_4$].

7.5 Chapter 3: Development of an Immobilized Oxaziridine-Based Organocatalyst

7.5.1 Synthesis & Characterization of Starting materials

3,7-Dimethyloctanoic acid (3.17)

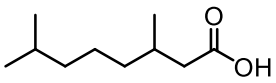

$C_{10}H_{20}O_2$
172.15 g/mol

Following the reported procedure,[288] in an oven-dried round-bottom flask equipped with a magnetic stir bar, geranic acid (1.0 mL, 5.77 mmol, 1.0 equiv.) was dissolved in methanol (58 mL, 0.10 M), and Pd/C (10% on activated charcoal, 607 mg, 0.57 mmol, 0.10 equiv.) was added. The reaction mixture was stirred at room temperature under a hydrogen atmosphere (1 atm) for 8 h. The suspension was filtered through a pad of Celite and washed with ethyl acetate (3 × 10 mL). The combined filtrates were concentrated under reduced pressure, and the crude residue was purified by flash column chromatography on silica gel (CyHex/ EtOAc, 1:9) to afford the product as a colorless oil in 94% yield (933 mg, 5.42 mmol).

^{1}H NMR (400 MHz, $CDCl_3$) δ 11.19 (s, 1H), 2.35 (dd, *J* = 14.9, 5.9 Hz, 1H), 2.13 (dd, *J* = 14.9, 8.2 Hz, 1H), 2.00 – 1.91 (m, 1H), 1.52 (dp, *J* = 13.3, 6.7 Hz, 1H), 1.39 – 1.08 (m, 6H), 0.96 (d, *J* = 6.7 Hz, 3H), 0.86 (d, *J* = 6.7 Hz, 6H).

^{13}C NMR (101 MHz, $CDCl_3$) δ 180.2, 41.7, 39.0, 36.9, 30.1, 27.9, 24.6, 22.6, 22.5, 19.7.

The characterization data is consistent with the literature. [288]

Methyl 3,7-dimethyloctanoate

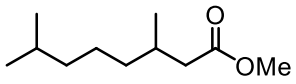

$C_{11}H_{22}O_2$
186.16 g/mol

In an oven-dried round-bottom flask equipped with a magnetic stir bar, 3,7-dimethyloctanoic acid (500 mg, 3.16 mmol, 1.0 equiv.) was dissolved in MeOH (8.0 mL, 0.40 M), and concentrated H_2SO_4 (1.2 equiv.) was added. The reaction mixture was heated to reflux (65 °C) for 3 h. After cooling to room temperature, the mixture was concentrated under reduced pressure, and the residue was dissolved in EtOAc. The solution was dried over anhydrous Na_2SO_4, filtered, and concentrated under reduced pressure to afford the corresponding methyl ester as a colorless oil in 97% yield (521 mg, 2.80 mmol).

^{1}H NMR (400 MHz, $CDCl_3$) δ 3.66 (s, 3H), 2.30 (dd, *J* = 14.7, 6.0 Hz, 1H), 2.11 (dd, *J* = 14.7, 8.2 Hz, 1H), 2.00 – 1.86 (m, 1H), 1.51 (dq, *J* = 13.2, 6.7 Hz, 1H), 1.37 – 1.07 (m, 6H), 0.92 (d, *J* = 6.7 Hz, 3H), 0.86 (dd, *J* = 6.6, 0.8 Hz,6H).
^{13}C NMR (101 MHz, $CDCl_3$) δ 173.8, 51.3, 41.7, 39.0, 36.9, 30.4, 27.9, 24.6, 22.6, 22.5, 19.7.
The characterization data is consistent with the literature.[288]

Benzyl 3,7-dimethyloctanoate

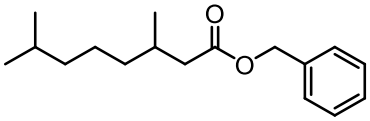

$C_{17}H_{26}O_2$
262.19 g/mol

In an oven-dried round-bottom flask equipped with a magnetic stir bar, 3,7-dimethyloctanoic acid (500 mg, 2.97 mmol, 1.0 equiv.) was dissolved in acetone (6 mL, 0.50 M), and benzyl bromide (1.01 g, 5.94 mmol, 2.0 equiv.) and K_2CO_3 (1.23 g, 8.92 mmol, 3.0 equiv.) were added at room temperature. The reaction mixture was heated at 50 °C for 12 h. After completion, the solvent was removed under reduced pressure, and the crude residue was purified by flash column chromatography on silica gel (hexanes/EtOAc 100:1, v/v) to afford benzyl 3,7-dimethyloctanoate as a colorless liquid in 72% yield (561 mg, 2.14 mmol).

^{1}H NMR (600 MHz, $CDCl_3$) δ 7.39 (s, 5H), 5.15 (s, 2H), 2.38 (dd, *J* = 14.7, 6.1 Hz, 1H), 2.20 (dd, *J* = 14.7, 8.1 Hz, 1H), 2.05 – 1.96 (m, *J* = 6.8 Hz, 1H), 1.59 – 1.49 (m, 1H), 1.37 – 1.24 (m, 3H), 1.16 (ddd, *J* = 8.7, 7.0, 4.9 Hz, 3H), 0.96 (d, *J* = 6.7 Hz, 3H), 0.89 (d, *J* = 6.6 Hz, 6H).

^{13}C NMR (151 MHz, $CDCl_3$) δ 173.1, 136.2, 128.5, 128.2, 128.1, 66.0, 41.9, 39.0, 36.9, 30.4, 27.9, 24.6, 22.6, 22.5, 19.7.

The characterization data is consistent with the literature.[289]

3-Methylbut-2-en-1-yl benzoate (3.15)

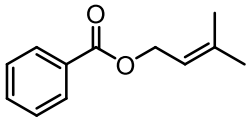

$C_{12}H_{14}O_2$
190.09 g/mol

Following the reported procedure,[290] in an oven-dried round-bottom flask equipped with a magnetic stir bar, 3-methylbut-2-en-1-ol (1.02 mL, 10.0 mmol, 1.0 equiv.) and Et_3N (2.77 mL, 20.0 mmol, 2.0 equiv.) were dissolved in dry DCM (20 mL, 0.50 M). DMAP (12.3 mg, 0.10 mmol, 0.01 equiv.) was added at room temperature. The reaction mixture was cooled to 0 °C, and benzyl chloride (1.39 mL, 12.1 mmol, 1.2 equiv.) was added dropwise. The mixture was allowed to warm to room temperature and stirred overnight. The reaction mixture was diluted with DCM (50 mL) and washed sequentially with 1 M aqueous HCl (2 × 20 mL), saturated aqueous $NaHCO_3$ (20 mL), and brine (20 mL). The organic layer was dried over anhydrous Na_2SO_4, filtered, and concentrated under reduced pressure. The crude residue was purified by flash column chromatography on silica gel (CyHex/EtOAc, 7:3) to afford the desired ester as a colorless liquid in 95% yield (1.8 g).

^{1}H NMR (400 MHz, $CDCl_3$) δ 8.08 – 8.00 (m, 2H), 7.58 – 7.50 (m, 2H), 7.47 – 7.38 (m, 1H), 5.64 – 5.31 (m, 1H), 4.82 (dt, *J* = 7.2, 0.9 Hz, 2H), 1.93 – 1.68 (m, 6H).

^{13}C NMR (101 MHz, $CDCl_3$) δ 166.7, 139.1, 132.8, 130.5, 129.6, 128.3, 118.7, 61.9, 25.8, 18.1.

HRMS (ESI) m/z: $[M+Na]^+$ calcd for $C_{12}H_{14}NaO_2$: 213.0994; Found: 213.0461.

R_f (CyHex/EtOAc, 7:3) = 0.31 [$KMnO_4$].

The characterization data is consistent with the literature. [290]

7.5.2 Synthesis & Characterization of the catalyst

Methyl 3-formyl-4-methoxybenzoate (3.5)

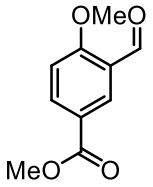

$C_{10}H_{10}O_4$
194.06 g/mol

In an oven-dried round-bottom flask equipped with a magnetic stir bar, methyl 3-formyl-4-hydroxybenzoic acid (5.00 g, 27.0 mmol, 1.0 equiv.) and potassium carbonate (5.80 g, 41.6 mmol, 1.5 equiv.) were dissolved in dry DMF (8 mL, 3.4 M). Methyl iodide (7.4 mL, 41.6 mmol, 1.5 equiv.) was added dropwise, and the reaction mixture was stirred at room temperature overnight. Upon completion, the reaction mixture was concentrated under reduced pressure, and the residue was partitioned between ethyl acetate and saturated aqueous Na_2CO_3. The aqueous layer was extracted with ethyl acetate (3 × 20 mL), and the combined organic layers were dried over anhydrous $MgSO_4$, filtered, and concentrated under reduced pressure. The crude product was purified by flash column chromatography on silica gel (CyHex/EtOAc, 10:1) to afford the desired methyl ether as a colorless solid in 95% yield (5.12 g, 26.4 mmol).

^{1}H NMR (600 MHz, $CDCl_3$) δ 10.39 (s, 1H), 8.43 (d, *J* = 2.3 Hz, 1H), 8.18 (dd, *J* = 8.8, 2.4 Hz, 1H), 7.00 (d, *J* = 8.8 Hz, 1H), 3.96 (s, 3H), 3.86 (s, 3H).
^{13}C NMR (151 MHz, $CDCl_3$) δ 188.6, 165.8, 164.6, 136.9, 130.4, 124.36, 122.8, 111.5, 55.9, 51.9.
IR (ATR): $\tilde{\nu}$ [cm^{-1}] = 1720, 1685, 1650, 1589, 1436, 1387, 1366, 1296, 1205, 1168, 1123, 1003, 930, 815, 772.
HRMS (ESI) m/z: $[M+Na]^+$ calcd for $C_{10}H_{10}NaO_4$:217.0321; Found: 217.0322.
R_f (CyHex/EtOAc, 10:1) = 0.25 [$KMnO_4$].
The characterization data is consistent with the literature.[291]

Methyl 4-methoxybenzoate (3.7)

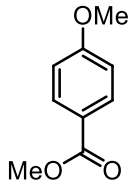

$C_9H_{10}O_3$
166.06 g/mol

Following the reported procedure, [292] in an oven-dried round-bottom flask equipped with a magnetic stir bar, 4-methoxybenzoic acid (2.00 g, 13.1 mmol, 1.0 equiv.) was dissolved in methanol (65 mL, 0.20 M), and concentrated sulfuric acid (98%, 7.1 µL, 0.13 mmol, 1 mol%) was added. The reaction mixture was heated to reflux for 3 h. After cooling to room temperature, the reaction solution was concentrated under reduced pressure. The resulting crude residue was dissolved in saturated aqueous $NaHCO_3$ and extracted with DCM. The combined organic layers were washed with brine, dried over anhydrous Na_2SO_4, filtered, and concentrated under reduced pressure. The crude product was purified by flash column chromatography on silica gel (CyHex/EtOAc, 5:2) to afford the desired ester as a white solid in 98% yield (2.14 g, 12.9 mmol).

^{1}H NMR (400 MHz, $CDCl_3$) δ 8.03 – 7.94 (m, 2H), 6.96 – 6.86 (m, 2H), 3.87 (s, 3H), 3.84 (s, 3H).
^{13}C NMR (101 MHz, $CDCl_3$) δ 166.7, 163.2, 131.5, 122.5, 113.5, 55.3, 51.7.
IR (ATR): $\tilde{\nu}$ [cm^{-1}] = 1705, 1604, 1508, 1466, 1453, 1427, 1317, 1280, 1251, 1191, 1166, 1104, 1020, 959, 847, 828.
HRMS (ESI) m/z: $[M+Na]^+$ calcd for $C_9H_{10}NaO_3$: 189.0630; Found: 189.0631.
R_f (CyHex/EtOAc, 5:2) = 0.23 [$KMnO_4$].
The characterization data is consistent with the literature. [292]

3-Formyl-4-hydroxybenzoic acid (3.8)

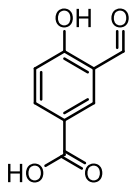

$C_8H_6O_4$
166.02 g/mol

Following a reported procedure,[162] in an oven-dried round-bottom flask equipped with a magnetic stir bar, 4-hydroxybenzoic acid (15.0 g, 108 mmol, 1.0 equiv.) was suspended

in trifluoroacetic acid (40 mL) under a nitrogen atmosphere. A solution of hexamethylenetetramine (15.3 g, 109 mmol, 1.0 equiv.) in trifluoroacetic acid (45 mL) was added dropwise, and the resulting mixture was heated to reflux under nitrogen. Reaction progress was monitored by TLC ($CHCl_3$/MeOH = 10:1.5), and reflux was maintained until complete consumption of 4-hydroxybenzoic acid (ca. 2 h). After cooling to room temperature, the reaction mixture was poured into 4 M aqueous HCl (300 mL) and stirred for an additional 3 h. The resulting yellow precipitate was collected by filtration and washed thoroughly with water. The solid was dried under reduced pressure to afford the corresponding product as a yellow solid in 43% yield (7.76 g, 46.7 mmol).

^{1}H NMR (400 MHz, DMSO) δ 13.11 (br, 1H), 11.45 (br, 1H), 10.28 (s, 1H), 8.26 – 8.20 (m, 1H), 8.03 (dd, *J* = 8.7, 1.1 Hz, 1H), 7.07 (d, *J* = 8.7 Hz, 1H).
^{13}C NMR (101 MHz, DMSO) δ 191.9, 165.5, 164.9, 137.6, 130.7, 123.6, 122.6, 117.5.
The characterization data is consistent with the literature. [162]

Methyl 4-methoxy-3-(2,2,2-trifluoro-1-hydroxyethyl)benzoate (3.9)

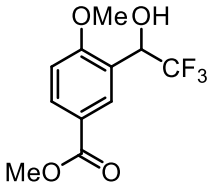

$C_{11}H_{11}F_3O_4$
264.06 g/mol

Following a similar reported procedure,[293] in an oven-dried round-bottom flask equipped with a magnetic stir bar, aldehyde (2.72 g, 14.0 mmol, 1.0 equiv.) was dissolved in THF (16 mL, 0.83 M). (Trifluoromethyl)trimethylsilane (2.69 mL, 18.2 mmol, 1.3 equiv.) was added, and the reaction mixture was cooled to −78 °C and stirred for 10 min. TBAF (1 M in THF, 0.14 mL, 0.20 mmol, 1 mol%) was added dropwise, and the reaction mixture was allowed to warm to room temperature and stirred for 6 h. To cleave the silyl ether intermediate, the reaction mixture was cooled to 0 °C, water (3.6 mL) was added, followed by TBAF (1 M in THF, 1.4 mL, 1.40 mmol, 0.10 equiv.). After stirring for 1 h, the ice bath was removed, and the mixture was stirred at room temperature. Brine (50 mL) and Et_2O (60 mL) were added, and the layers were separated. The aqueous layer was back-extracted with Et_2O (3 × 40 mL). The combined organic layers were dried over anhydrous Na_2SO_4, filtered, and concentrated under reduced pressure. The crude product was purified by flash column chromatography on silica gel (EtOAc/CyHex 1:4) to afford methyl 4-methoxy-3-(2,2,2-trifluoro-1-hydroxyethyl)benzoate as a yellow oil in 84% yield (3.11 g, 11.8 mmol).

^{1}H NMR (600 MHz, $CDCl_3$) δ 8.15 (d, *J* = 2.2 Hz, 1H), 8.08 (dd, *J* = 8.7, 2.2 Hz, 1H), 6.97 (d, *J* = 8.7 Hz, 1H), 5.39 (q, *J* = 6.9 Hz, 1H), 3.94 (s, 3H), 3.90 (s, 3H), 3.74 (br, 1H).

^{13}C NMR (151 MHz, $CDCl_3$) δ 166.3, 160.9, 132.6, 130.8, 110.7, 68.4, 68.0, 56.1, 52.1, 25.6.

^{19}F NMR (376 MHz, $CDCl_3$): δ -78.6.

IR (ATR): $\tilde{\nu}$ [cm^{-1}] = 1623, 1558, 1474, 1396, 1153, 983, 868, 831, 803, 761, 643.

HRMS (ESI) m/z: $[M-H]^-$ calcd for $C_{11}H_{11}F_3O_4$:263.0526; Found: 263.0530.

Methyl 4-methoxy-3-(2,2,2-trifluoroacetyl)benzoate (3.10)

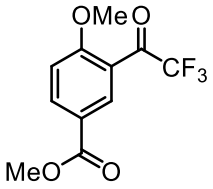

$C_{11}H_9F_3O_4$
262.04 g/mol

Following a similar reported procedure,[152] in an oven-dried round-bottom flask equipped with a magnetic stir bar, methyl 4-methoxy-3-(2,2,2-trifluoroacetyl)benzoate (2.00 g, 7.57 mmol, 1.0 equiv.) was dissolved in CH_2Cl_2 (108 mL, 0.07 M). TEMPO (115 mg, 0.76 mmol, 0.10 equiv.) was added, followed by PIDA (5.60 g, 17.41 mmol, 2.3 equiv.) at room temperature. The reaction mixture was stirred for 13 h, then quenched with 1.0 M aqueous $Na_2S_2O_3$ (250 mL). The mixture was transferred to a separatory funnel, and the organic layer was collected. The aqueous phase was extracted with CH_2Cl_2 (3 × 200 mL). The combined organic layers were dried over anhydrous Na_2SO_4, filtered, and concentrated under reduced pressure. The crude product was purified by flash column chromatography on silica gel (EtOAc/CyHex 1:4) to afford the desired product as an oily, peach-colored residue that solidified upon standing in 89% yield (1.77 g, 6.76 mmol).

^{1}H NMR (600 MHz, $CDCl_3$) δ 8.33 (d, *J* = 2.2 Hz, 1H), 8.25 (dd, *J* = 8.8, 2.2 Hz, 1H), 7.06 (d, *J* = 8.8 Hz, 1H), 3.97 (s, 3H), 3.91 (s, 3H).

^{13}C NMR (151 MHz, $CDCl_3$) δ 182.6, 182.3, 165.4, 162.7, 136.9, 133.0, 123.1, 121.8, 116.9, 114.9, 111.8, 56.3, 52.3.

^{19}F NMR (376 MHz, $CDCl_3$) δ -72.8.

IR (ATR): $\tilde{\nu}$ [cm^{-1}] = 3414, 2957, 2848, 1713, 1601, 1503, 1461, 1438, 14414, 1272, 1193, 1167, 1139, 1119, 1059, 1004, 948, 935.

HRMS (ESI) m/z: $[M+Na]^+$ calcd for $C_{11}H_9F_3NaO_4$: 285.0453; Found: 285.0455.

TLC: R_f= 0.34 (EtOAc/CyHex = 1:4) [$KMnO_4$]

4-Hydroxy-3-(2,2,2-trifluoroacetyl)benzoic acid (3.11)

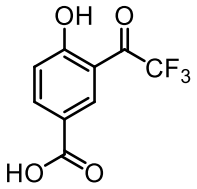

$C_9H_5F_3O_4$
234.01 g/mol

Following a similar reported procedure,[152] in an oven-dried round-bottom flask equipped with a magnetic stir bar, methyl 4-methoxy-3-(2,2,2-trifluoroacetyl)benzoate (2.10 g, 8.01 mmol, 1.0 equiv.) was dissolved in CH_2Cl_2 (80 mL, 0.10 M) and cooled to −78 °C. A 1.0 M solution of BBr_3 in CH_2Cl_2 (20.0 mL, 20.0 mmol, 2.5 equiv.) was added dropwise. The reaction mixture was allowed to warm slowly to room temperature and stirred for 10 h. The mixture was then cooled to 0 °C and carefully quenched with H_2O (30 mL). The resulting biphasic mixture was transferred to a separatory funnel and extracted with CH_2Cl_2 (3 × 20 mL). The combined organic layers were dried over anhydrous Na_2SO_4, filtered, and concentrated under reduced pressure. The crude product was obtained as a brown oil in 54% yield (1.01 g, 4.33 mmol) and was used without further purification.

^{1}H NMR (400 MHz, DMSO) δ 12.97 (br, 1H), 11.75 (br, 1H), 8.21 (dd, *J* = 2.1, 1.0 Hz, 1H), 8.10 (dd, *J* = 8.7, 2.2 Hz, 1H), 7.12 (d, *J* = 8.7 Hz, 1H).
^{13}C NMR (101 MHz, DMSO) δ 181.5, 181.2, 166.0, 162.6, 137.2, 132.8, 121.9, 118.1, 117.8.
^{19}F NMR (376 MHz, DMSO) δ -72.8.
IR (ATR): $\tilde{\nu}$ [cm^{-1}] = 1666, 1616, 1296, 1198, 1172, 1152, 1119, 969, 936, 922, 852, 790.
HRMS (ESI) m/z: $[M+Na]^+$ calcd for $C_9H_5F_3NaO_4$: 257.1423; Found: 257.1426.

Methyl 4-hydroxy-3-(2,2,2-trifluoroacetyl)benzoate (3.12)

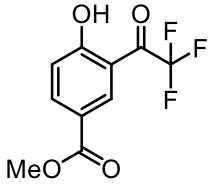

$C_{10}H_7F_3O_4$
248.03 g/mol

Following a similar reported procedure,[152] in an oven-dried round-bottom flask, 4-hydroxy-3-(2,2,2-trifluoroacetyl)benzoic acid (970 mg, 4.14 mmol, 1.0 equiv.) was dissolved in methanol (9.7 mL, 0.20 M). Concentrated sulfuric acid (98%, 2.2 µL, 41.4

µmol, 1 mol%) was added, and the reaction mixture was heated to reflux for 6 h. After cooling to room temperature, the solution was concentrated under reduced pressure. The crude residue was dissolved in saturated aqueous $NaHCO_3$ and extracted with CH_2Cl_2. The combined organic layers were washed with brine, dried over anhydrous Na_2SO_4, filtered, and concentrated under reduced pressure. The crude product was purified by flash column chromatography on silica gel (EtOAc/CyHex 1:6) to afford the methyl ester as a white solid in 92% yield (946 mg, 3.81 mmol).

^{1}H NMR (400 MHz, $CDCl_3$) δ 11.36 (br, 1H), 8.57 (d, *J* = 2.0 Hz, 1H), 8.28 (ddd, *J* = 8.9, 2.1, 0.5 Hz, 1H), 7.14 (d, *J* = 8.9 Hz, 1H), 3.94 (s, 3H).
^{13}C NMR (101 MHz, $CDCl_3$) δ 185.1, 184.8, 184.4, 184.1, 167.5, 165.13, 139.4, 133.2, 133.2, 122.4, 119.3, 113.3, 52.5.
IR (ATR): $\tilde{\nu}$ [cm^{-1}] = 3217, 1726, 1671, 1621, 1437, 1313, 1283, 1269, 1169, 1196, 1141, 1115, 980, 952, 860.
^{19}F NMR (376 MHz, $CDCl_3$) δ -70.4.
HRMS (ESI) m/z: $[M+Na]^+$ calcd for $C_{10}H_7F_3NaO_4$: 271.0741; Found: 271.0743.
R_f (CyHex/EtOAc, 6:1) = 0.29 [$KMnO_4$].

Methyl-4-(trifluoromethyl)benzo[e][1,2,3]oxathiazine-6-carboxylate-2,2-dioxide (3.13)

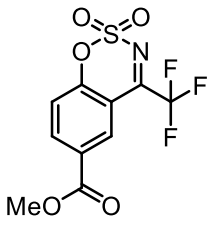

$C_{10}H_6F_3NO_5S$
308.99 g/mol

Following a similar reported procedure,[152] in an oven-dried round-bottom flask equipped with a magnetic stir bar, methyl 4-hydroxy-3-(2,2,2-trifluoroacetyl)benzoate (0.11 g, 0.44 mmol, 1.0 equiv.) was dissolved in DMA (0.8 mL, 0.5 M) and cooled to 0 °C. Solid H_2NSO_2Cl (0.15 g, 1.33 mmol, 3.0 equiv.) was added in one portion. The reaction mixture was allowed to warm to room temperature and stirred for 21 h until completion, as monitored by TLC. The reaction was quenched with pH 7 NaH_2PO_4/NaOH buffer (5 mL) and transferred to a separatory funnel containing Et_2O (10 mL). The organic layer was collected, and the aqueous layer was extracted with Et_2O (2 × 5 mL). The combined organic layers were washed with water (2 × 3 mL) and brine (5 mL), dried over anhydrous $MgSO_4$, filtered, and concentrated under reduced pressure. The crude residue was

purified by flash column chromatography on silica gel (EtOAc/CyHex 3:7) to afford the desired product as a pale solid in 32% yield (43.9 mg, 0.14 mmol).

^{1}H NMR (400 MHz, $CDCl_3$) δ 8.61 (s, 1H), 8.50 (d, *J* = 2.0 Hz, 1H), 7.49 (d, *J* = 8.7 Hz, 1H), 4.00 (s, 3H).
^{13}C NMR (101 MHz, $CDCl_3$) δ 163.9, 157.6, 139.4, 130.2, 130.1, 128.9, 119.9, 111.2, 53.2.
^{19}F NMR (376 MHz, $CDCl_3$) δ -66.9.
IR (ATR): $\tilde{\nu}$ [cm^{-1}] = 1729, 1615, 1412, 1295, 1179, 1113, 995, 963, 850, 819.
HRMS (ESI) m/z: $[M+Na]^+$ calcd for $C_{10}H_6F_3NaNO_5S$: 331.9819; Found: 331. 9824.
R_f (CyHex/EtOAc, 7:3) = 0.31 [$KMnO_4$].

Methyl 8b-(trifluoromethyl)-8bH-benzo[*e*][1,2]oxazireno[2,3-c][1,2,3]oxathiazine-7-carboxylate 3,3-dioxide (3.13a)

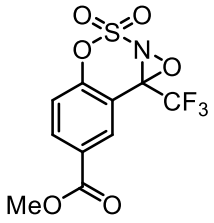

$C_{10}H_6F_3NO_6S$
324.98 g/mol

Following a similar reported procedure,[151] in an oven-dried round-bottom flask equipped with a magnetic stir bar, methyl 4-(trifluoromethyl)benzo[e][1,2,3]oxathiazine-6-carboxylate 2,2-dioxide (50 mg, 0.16 mmol, 1.0 equiv.) was dissolved in 1,2-dichloroethane (DCE, 1.1 mL, 0.15 M). *m*CPBA (31.2 mg, 0.18 mmol, 1.1 equiv.) was added at room temperature, and the reaction mixture was stirred for 75 min. Upon completion, the solvent was partially removed under reduced pressure to a volume of approximately 2 mL. The resulting white suspension was applied directly to a silica gel column and eluted with (EtOAc/hexanes 1:9) to afford the desired oxaziridine as a white solid in 77% yield (33.7 mg, 0.12 mmol).

^{1}H NMR (400 MHz, $CDCl_3$) δ 8.65 – 8.59 (m, 1H), 8.38 (dd, *J* = 8.6, 1.9 Hz, 1H), 7.40 (d, *J* = 8.6 Hz, 1H), 4.00 (s, 3H).
^{13}C NMR (101 MHz, $CDCl_3$) δ 167.4, 150.3, 136.1, 133.6, 126.1, 124.8, 120.7, 94.9, 53.2.
^{19}F NMR (376 MHz, $CDCl_3$) δ -73.3.
IR (ATR): $\tilde{\nu}$ [cm^{-1}] = 1727, 1615, 1411, 1295, 1178, 1155, 1110, 994, 962, 846, 817, 759.

Methyl 3-formyl-4-hydroxybenzoate (3.14)

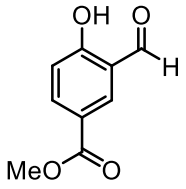

$C_9H_8O_4$
180.04 g/mol

In an oven-dried round-bottom flask equipped with a magnetic stir bar, 3-formyl-4-hydroxybenzoic acid (2.00 g, 12.04 mmol, 1.0 equiv.) was dissolved in methanol (60 mL, 0.20 M), and concentrated sulfuric acid (98%, 6.5 µL, 0.12 mmol, 1 mol%) was added. The reaction mixture was heated to reflux for 6 h. After cooling to room temperature, the solvent was removed under reduced pressure. The crude residue was dissolved in saturated aqueous $NaHCO_3$ and extracted with dichloromethane. The combined organic layers were washed with brine, dried over anhydrous Na_2SO_4, filtered, and concentrated under reduced pressure. The resulting crude product was purified by flash column chromatography on silica gel (CyHex/EtOAc, 8:2) to afford the desired methyl ester as a white solid in 92% yield (1.99 g, 11.1 mmol).

^{1}H NMR (600 MHz, $CDCl_3$) δ 11.39 (s, 1H), 9.96 (br, 1H), 8.32 (d, *J* = 2.2 Hz, 1H), 8.19 (dd, *J* = 8.8, 2.1 Hz, 1H), 7.04 (d, *J* = 8.8 Hz, 1H), 3.93 (s, 3H).
^{13}C NMR (151 MHz, $CDCl_3$) δ 196.3, 165.6, 165.1, 137.8, 136.1, 120.1, 118.0, 52.2.
IR (ATR): $\tilde{\nu}$ [cm^{-1}] = 3156, 1740, 1695, 1670, 1597, 1448, 1383, 1366, 1310, 1220, 1183, 1122, 930, 815.
R_f (CyHex/EtOAc, 7:3) = 0.37 [$KMnO_4$].
The characterization data is consistent with the literature.[294]

Methyl benzo[*e*][1,2,3]oxathiazine-6-carboxylate 2,2-dioxide (3.16)

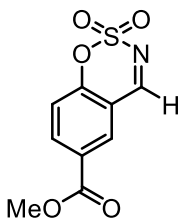

$C_9H_7NO_5S$
241.01 g/mol

Following a similar reported procedure, in an oven-dried round-bottom flask equipped with a magnetic stir bar, a vigorously stirring ice-cold solution of $ClSO_2NCO$ (2.51 mL,

28.8 mmol, 4.0 equiv.) was treated dropwise with formic acid (HCO_2H, 1.09 mL, 28.6 mmol, 4.0 equiv.) over 5-10 min. The flask was vented carefully during the addition due to gas evolution, and a white solid formed. After completion, CH_3CN (6.4 mL, 1.3 M) was added, resulting in a clear solution that was stirred at room temperature for 6 h. The reaction mixture was then cooled to 0 °C, and a solution of methyl 3-formyl-4-hydroxybenzoate (1.30 g, 7.22 mmol, 1.0 equiv.) in DMA (22 mL) was added dropwise. The mixture was allowed to warm to room temperature and stirred for 13 h, after which it was quenched with H_2O (20 mL). The mixture was transferred to a separatory funnel containing EtOAc (20 mL), and the organic layer was collected. The aqueous phase was extracted with EtOAc (2 × 25 mL), and the combined organic layers were washed with water (2 × 20 mL) and saturated aqueous NaCl (40 mL). The organic layer was dried over anhydrous Na_2SO_4, filtered, and concentrated under reduced pressure. The crude product was purified by flash column chromatography on silica gel (EtOAc/CyHex 3:7) to afford the desired product as an off-white solid in 55% yield (964 mg, 4.00 mmol).

^{1}H NMR (600 MHz, $CDCl_3$) δ 8.63 (s, 1H), 7.70 (dd, *J* = 8.8, 2.5 Hz, 1H), 7.67 (s, 1H), 7.27 (d, *J* = 8.9 Hz, 1H), 3.93 (s, 3H).
^{13}C NMR (151 MHz, $CDCl_3$) δ 166.3, 152.7, 137.3, 131.7, 129.9, 120.2, 116.1.
IR (ATR): $\tilde{\nu}$ [cm^{-1}] = 1705, 1598, 1494, 1431, 1396, 1262, 1232, 1195, 1171, 1135, 1015, 835.
All the characterization data are consistent with the literature.[295]

6-Chlorobenzo[*e*][1,2,3]oxathiazine 2,2-dioxide (3.17)

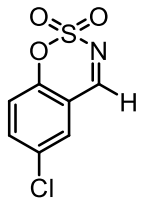

$C_7H_4ClNO_3S$
216.96 g/mol

To a vigorously stirring ice-cold solution of $ClSO_2NCO$ (1.11 mL, 12.7 mmol, 4.0 equiv.) was added formic acid (HCO_2H, 0.48 mL, 12.7 mmol, 4.0 equiv.) dropwise over 5–10 min. The flask was well vented during the addition, as gas evolution occurred and a white solid formed. After completion of the addition, CH_3CN (2.83 mL, 1.3 M) was added, resulting in a clear solution that was stirred at rt for 6 h. The solution was then cooled to 0 °C, and a solution of 5-chloro-2-hydroxybenzaldehyde (0.50 g, 3.19 mmol, 1.0 equiv.) in DMA (10 mL) was added dropwise. The reaction mixture was allowed to warm to rt

and stirred for 13 h, after which it was quenched with H_2O (5 mL). The mixture was transferred to a separatory funnel containing EtOAc (20 mL), and the organic layer was collected. The aqueous phase was extracted with EtOAc (2 × 25 mL). The combined organic layers were washed with water (2 × 20 mL) and saturated aqueous NaCl (40 mL), dried over anhydrous Na_2SO_4, filtered, and concentrated under reduced pressure. The crude product was purified by flash column chromatography on silica gel (EtOAc/CyHex 3:7) to afford the desired product as an off-white solid in 70% yield.

^{1}H NMR (600 MHz, $CDCl_3$) δ 8.63 (s, 1H), 7.70 (dd, *J* = 8.8, 2.5 Hz, 1H), 7.67 (s, 1H), 7.27 (d, *J* = 8.9 Hz, 1H).
^{13}C NMR (151 MHz, $CDCl_3$) δ 166.3, 152.7, 137.3, 131.7, 129.9, 120.2, 116.1.
The characterization data is consistent with the literature.[152]

Methyl-4-(trifluoromethyl)-3,4-dihydrobenzo[*e*][1,2,3]oxathiazine-6-carboxylate 2,2-dioxide (3.14)

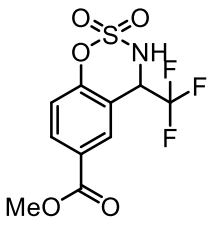

$C_{10}H_8F_3NO_5S$
311.01 g/mol

To a flask containing CsF (744 mg, 4.90 mmol, 1.25 equiv.) was added benzoxathiazine (945 mg, 3.92 mmol, 1.0 equiv.) and DMF (38 mL, 0.10 M). The flask was sealed with a rubber septum and heated in an oil bath at 40 °C. Neat Me_3SiCF_3 (0.725 mL, 4.90 mmol, 1.25 equiv.) was added dropwise, and the resulting dark amber/red mixture was stirred for 13 h. The reaction mixture was cooled to rt and slowly quenched with saturated aqueous NH_4Cl (20 mL, pH ~5.0). The mixture was transferred to a separatory funnel containing Et_2O, and the organic layer was collected. The aqueous phase was extracted with Et_2O (100 mL), and the combined organic layers were washed with saturated aqueous NaCl (2 × 100 mL), dried over anhydrous Na_2SO_4, filtered, and concentrated under reduced pressure to afford a dark orange oily residue. The crude product was purified by flash column chromatography on silica gel (EtOAc/CyHex 1:9) to afford the desired compound in 54% yield.

^{1}H NMR (600 MHz, $CDCl_3$) δ 7.48 (s, 1H), 7.45 (dd, *J* = 8.8, 2.5 Hz, 1H), 5.40 (d, *J* = 7.9 Hz, 1H), 5.27 – 5.16 (m, 1H), 3.93 (s, 3H).

^{13}C NMR (151 MHz, $CDCl_3$) δ 150.0, 131.6, 127.2 (d, *J* = 3.2 Hz), 121.1, 115.1, 58.0, 26.9.

IR (ATR): $\tilde{\nu}$ [cm^{-1}] = 1729, 1615, 1412, 1295, 1179, 1113, 995, 963, 850, 819, 762, 720, 634.

^{19}F NMR (376 MHz, $CDCl_3$) δ -68.2.

HRMS (ESI): [m/z] calculated for $C_{10}H_7F_3NO_5S$ ($[M-H]^-$): 310.0003; Found: 309.9994.

X-Ray Crystallography Data

Compound code	3.18
Identification code	OCMTA1118
Empirical formula	$C_{10}H_8F_3NO_5S$
Formula weight	311.23
Temperature/K	150
Crystal system	monoclinic
Space group	$P2_1/n$
a/Å	6.3107(3)
b/Å	15.4091(8)
c/Å	11.7684(6)
α/°	90
β/°	90.950(5)
γ/°	90
Volume/Å^3	1144.23(10)
Z	4
ρ_{calc}g/cm^3	1.807
μ/mm^{-1}	0.346
F(000)	632.0
Crystal size/mm^3	0.09 × 0.08 × 0.03
Radiation	Mo Kα (λ = 0.71073)
2Θ range for data collection/°	5.288 to 58.622
Index ranges	-8 ≤ h ≤ 7, -21 ≤ k ≤ 17, -13 ≤ l ≤ 14
Reflections collected	6055
Independent reflections	2651 [R_{int} = 0.0278, R_{sigma} = 0.0470]
Data/restraints/parameters	2651/0/182
Goodness-of-fit on F^2	1.045
Final R indexes [I>=2σ (I)]	R_1 = 0.0452, wR_2 = 0.1007
Final R indexes [all data]	R_1 = 0.0652, wR_2 = 0.1118
Largest diff. peak/hole / e Å^{-3}	0.42/-0.49

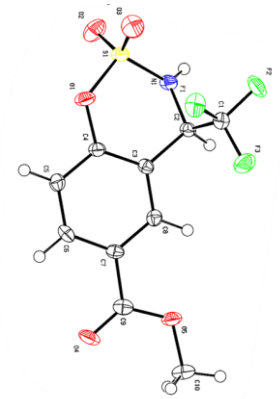

Figure 7.1 Molecular structure of **2.18**.

6-Chloro-4-(trifluoromethyl)-3,4-dihydrobenzo[e][1,2,3]oxathiazine 2,2-dioxide (3.19)

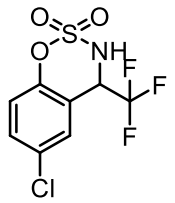

$C_8H_5ClF_3NO_3S$
286.96 g/mol

To a flask containing CsF (393 mg, 2.58 mmol, 1.25 equiv.) was added benzoxathiazine (450 mg, 2.07 mmol, 1.0 equiv.) and DMF (20 mL, 0.10 M). The flask was sealed with a rubber septum and heated in an oil bath at 40 °C. Neat Me_3SiCF_3 (0.383 mL, 2.58 mmol, 1.25 equiv.) was added dropwise, and the resulting dark amber/red mixture was stirred for 13 h. The reaction mixture was cooled to rt and slowly quenched with saturated aqueous NH_4Cl (20 mL, pH ~5.0). The mixture was transferred to a separatory funnel containing Et_2O, and the organic layer was collected. The aqueous phase was extracted with Et_2O (100 mL), and the combined organic layers were washed with saturated aqueous NaCl (2 × 100 mL), dried over anhydrous Na_2SO_4, filtered, and concentrated under reduced pressure to give a dark orange oily residue. The crude product was purified by flash column chromatography on silica gel (EtOAc/CyHex 1:9) to afford the desired compound in 51% yield.

^{1}H NMR (600 MHz, $CDCl_3$) δ 7.48 (s, 1H), 7.45 (dd, *J* = 8.8, 2.5 Hz, 1H), 5.40 (d, *J* = 7.9 Hz, 1H), 5.27 – 5.16 (m, 1H).
^{13}C NMR (151 MHz, $CDCl_3$) δ 150.0, 131.6, 127.2 (d, *J* = 3.2 Hz), 121.1, 115.1, 58.0, 26.9.
The characterization data is consistent with the literature.[152]

6-Chloro-4-(trifluoromethyl)benzo[*e*][1,2,3]oxathiazine 2,2-dioxide (3.20)

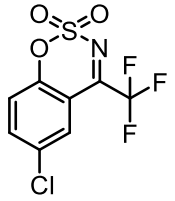

$C_8H_3ClF_3NO_3S$
284.94 g/mol

To a solution of benzoxathiazine **3.17** (250 mg, 0.87 mmol, 1.0 equiv.) in EtOAc (29 mL, 0.03 M) was added I_2 (221 mg, 1.87 mmol, 1.0 equiv.) followed by $PhI(OAc)_2$ (840 mg, 2.61 mmol, 3.0 equiv.) sequentially. The resulting dark brown mixture was stirred at rt for 14 h. The reaction was quenched with saturated aqueous $Na_2S_2O_3$ (50 mL), and the mixture was transferred to a separatory funnel containing EtOAc (100 mL). The organic layer was collected, and the aqueous phase was extracted with EtOAc (2 × 100 mL). The combined organic layers were washed with saturated aqueous NaCl (70 mL), dried over anhydrous Na_2SO_4, filtered, and concentrated under reduced pressure to give a yellow solid residue. The crude product was purified by flash column chromatography on silica gel (EtOAc/CyHex 7:3) to afford the desired product in 29% yield.

^{1}H NMR (400 MHz, $CDCl_3$) δ 7.90 (dq, *J* = 3.2, 1.7 Hz, 1H), 7.81 (dd, *J* = 8.9, 2.4 Hz, 1H), 7.40 (d, *J* = 8.9 Hz, 1H).
^{13}C NMR (101 MHz, $CDCl_3$) δ 161.3, 153.5, 138.8, 132.7, 128.1, 121.2, 112.5.
^{19}F NMR (376 MHz, $CDCl_3$) δ -67.1.
The characterization data is consistent with the literature.[152]

7.6 Chapter 4: Metal- and Catalyst-Free *anti*-Dihydroxylation of Olefins in Batch and Flow

7.6.1 Synthesis & Characterization of Starting materials

(*N*-(2-Cyclohex-1-enyl-ethyl)-4-methyl-benzenesulfonamide)

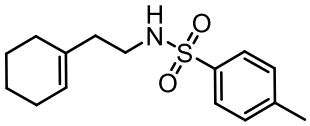

$C_{15}H_{21}NO_2S$
279.12 g/mol

Synthesized according to literature procedure [296] : To a solution of 2-cyclohex-1-enyl-ethylamine (1.00 g, 7.80 mmol, 1.0 equiv.) and Et_3N (1.19 mL, 8.60 mmol, 1.1 equiv.) in dry DCM (16 mL, 0.49 M) under a nitrogen atmosphere was added 4-methylbenzenesulfonyl chloride (1.66 g, 8.60 mmol, 1.1 equiv.) dropwise at 0 °C. The reaction mixture was allowed to warm to rt and stirred for 16 h. Upon completion, H_2O (25 mL) was added, and the mixture was extracted with DCM (3 × 25 mL). The combined organic layers were washed with brine (10 mL), dried over anhydrous Na_2SO_4, filtered, and concentrated under reduced pressure. The crude residue was purified by flash column chromatography on silica gel (petroleum ether/EtOAc, 100:1 → 2:1) to afford the desired product as a white solid in 88% yield (1.93 g, 6.91 mmol).

^{1}H NMR (400 MHz, $CDCl_3$) 7.73 (d, *J* = 8.3 Hz, 2H), 7.28 (d, *J* = 7.8 Hz, 2H), 5.38 – 5.30 (m, 1H), 4.70 (s, 1H), 2.96 (t, *J* = 6.8 Hz, 2H), 2.40 (s, 3H), 2.03 (t, 2H), 1.91 (s, 2H), 1.68 (s, 2H), 1.56 – 1.41 (m, 4H).

^{13}C NMR (101 MHz, $CDCl_3$) 143.3, 136.9, 133.5, 129.7, 127.1, 124.6, 40.7, 37.4, 27.6, 25.2, 22.7, 22.2, 21.5.

The characterization data is consistent with the literature. [296]

7.6.1 Synthesis & Characterization of products

(±)-*trans*-Cyclohexane-1,2-diol (4.4)

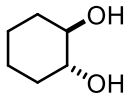

$C_6H_{12}O_2$
116.08 g/mol

In an oven-dried round bottom flask equipped with a magnetic stirring bar, cyclohexene (50.6 µL, 0.50 mmol, 1.0 equiv.) was dissolved in acetic acid (1.0 mL, 0.5 M) as the solvent and reagent. To this mixture, 35% aqueous H_2O_2 (85.6 µL, 1.0 mmol, 2.0 equiv.) was added as the oxidant, and the reaction was stirred in an oil bath preheated at 50 °C until complete conversion of the starting material was achieved. For the saponification step, the excess H_2O_2 was quenched by adding 1 M aqueous $Na_2S_2O_3$ solution (1.0 mL) to the same flask. The potassium-iodine starch paper was used to monitor the absence of H_2O_2. Following this, 5 M aqueous NaOH (5.0 mL) was added to the solution and stirred until the complete conversion of side products to furnish diol (reaction monitored by TLC). After completion of the reaction, the solution was neutralized with the addition of sat. aqueous NH_4Cl and extracted with ethyl acetate six times. The organic layer was washed with brine, dried over Na_2SO_4, filtered. The filtrate was concentrated in a vacuum and flash chromatography (CyHex/EtOAc 3:7) on silica gel afforded (±)-*trans*-cyclohexane-1,2-diol in 90% yield (52.3 mg, 0.45 mmol) as a white solid.

^{1}H NMR (600 MHz, $CDCl_3$) 3.71 (br s, 2H), 3.38 – 3.27 (m, 2H), 1.94 (d, *J* = 5.9 Hz, 2H), 1.74 – 1.60 (m, 2H), 1.23 (d, *J* = 5.5 Hz, 4H).

^{13}C NMR (151 MHz, $CDCl_3$) 75.8, 33.0, 24.5.

HRMS (ESI): [m/z] calculated for $C_6H_{12}NaO_2$ ($[M+Na]^+$): 139.0733; Found: 139.0730.

R_f (CyHex/EtOAc, 2:3) = 0.21 [UV Inactive] [$KMnO_4$].

The characterization data is consistent with the literature. [297]

(±)-*trans*-Cycloheptane-1,2-diol (4.5)

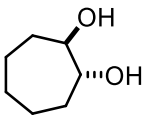

$C_7H_{14}O_2$
130.09 g/mol

In an oven-dried round bottom flask equipped with a magnetic stirring bar, cycloheptene (50.6 µL, 0.50 mmol, 1.0 equiv.) was dissolved in acetic acid (1.0 mL, 0.5 M) as the solvent and reagent. To this mixture, 35% aqueous H_2O_2 (85.6 µL, 1.0 mmol, 2.0 equiv.) was added as the oxidant, and the reaction was stirred in an oil bath preheated at 50 °C until complete conversion of the starting material was achieved. For the saponification step, the excess H_2O_2 was quenched by adding 1 M aqueous $Na_2S_2O_3$ solution (1.0 mL) to the same flask. The potassium-iodine starch paper was used to monitor the absence of H_2O_2. Following this, 5 M aqueous NaOH (5.0 mL) was added to the solution and stirred until the complete conversion of side products to furnish diol (reaction monitored by TLC). After completion of the reaction, the solution was neutralized with the addition of sat. aqueous NH_4Cl and extracted with ethyl acetate six times. The organic layer was washed with brine, dried over Na_2SO_4, filtered. The filtrate was concentrated in a vacuum and flash chromatography (CyHex/EtOAc 3:7) on silica gel afforded (±)-*trans*-cycloheptane-1,2-diolin 77% yield (50.0 mg, 0.38 mmol) as a white solid.

^{1}H NMR (600 MHz, $CDCl_3$) 3.49 – 3.36 (m, 2H), 3.16 (br s, 2H), 1.92 – 1.80 (m, 2H), 1.65 (dq, *J* = 13.7, 6.2 Hz, 2H), 1.55 – 1.38 (m, 6H).
^{13}C NMR (151 MHz, $CDCl_3$) 78.0, 32.6, 26.6, 22.3.
HRMS (ESI): [m/z] calculated for $C_7H_{14}NaO_2$ ($[M+Na]^+$): 153.0886; Found: 153.0887.
R_f (CyHex/EtOAc, 3:2) = 0.91 [UV Inactive] [$KMnO_4$].
The characterization data is consistent with the literature. [298]

(±)-*trans*-*N*-(2-(1,2-Dihydroxycyclohexyl)ethyl)-4-methylbenzenesulfonamide (4.8)

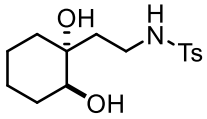

$C_{15}H_{23}NO_4S$
313.13 g/mol

In an oven-dried round bottom flask equipped with a magnetic stirring bar, (N-(2-cyclohex-1-enyl-ethyl)-4-methyl-benzenesulfonamide) (140 mg, 0.50 mmol, 1.0 equiv.) was dissolved in acetic acid (1.0 mL, 0.5 M) as the solvent and reagent. To this mixture, 35% aqueous H_2O_2 (85.6 µL, 1.0 mmol, 2.0 equiv.) was added as the oxidant, and the reaction was stirred in an oil bath preheated at 50 °C until complete conversion of the

starting material was achieved. For the saponification step, the excess H_2O_2 was quenched by adding 1 M aqueous $Na_2S_2O_3$ solution (1.0 mL) to the same flask. The potassium-iodine starch paper was used to monitor the absence of H_2O_2. Following this, 5 M aqueous NaOH (5.0 mL) was added to the solution and stirred until the complete conversion of side products to furnish diol (reaction monitored by TLC). After completion of the reaction, the solution was neutralized with the addition of sat. aqueous NH_4Cl and extracted with ethyl acetate six times. The organic layer was washed with brine, dried over Na_2SO_4, filtered. The filtrate was concentrated in a vacuum and flash chromatography (EA/MeOH 3:7) on silica gel afforded (±)-*trans*-*N*-(2-(1,2-dihydroxycyclohexyl)ethyl)-4-methylbenzenesulfonamide in 36% yield (56.1 mg, 0.18 mmol) as a white solid.

^{1}H NMR (600 MHz, $CDCl_3$) 7.75 (d, *J* = 8.2 Hz, 2H), 7.30 (d, *J* = 8.0 Hz, 2H), 3.49 (dd, *J* = 9.3, 4.1 Hz, 1H), 3.24 (br s, 2H), 3.16 – 3.04 (m, 2H), 2.42 (s, 3H), 1.95 – 1.85 (m, 1H), 1.85 – 1.78 (m, 1H), 1.74 – 1.59 (m, 3H), 1.55 – 1.45 (m, 1H), 1.39 – 1.12 (m, 5H).
^{13}C NMR (151 MHz, $CDCl_3$) 143.5, 136.9, 129.8, 127.3, 76.6, 75.4, 38.8, 34.9, 30.6, 23.2, 22.4, 21.6.
HRMS (ESI): [m/z] calculated for $C_{15}H_{23}NNaO_4S$ ($[M+Na]^+$): 336.1240; Found: 336.1240.
R_f (CyHex/EtOAc, 4:1) = 0.23 [UV Inactive] [$KMnO_4$].

(±)-Hexane-1,3,4-triol (4.10)

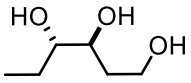

$C_6H_{14}O_3$
134.09 g/mol

In an oven-dried round bottom flask equipped with a magnetic stirring bar, *cis*-hex-3-en-1-ol (61.0 µL, 0.50 mmol, 1.0 equiv.) was dissolved in acetic acid (1.0 mL, 0.5 M) as the solvent and reagent. To this mixture, 35% aqueous H_2O_2 (85.6 µL, 1.0 mmol, 2.0 equiv.) was added as the oxidant, and the reaction was stirred in an oil bath preheated at 50 °C until complete conversion of the starting material was achieved. For the saponification step, the excess H_2O_2 was quenched by adding 1 M aqueous $Na_2S_2O_3$ solution (1.0 mL) to the same flask. The potassium-iodine starch paper was used to monitor the absence of H_2O_2. Following this, 5 M aqueous NaOH (5.0 mL) was added to the solution and stirred until the complete conversion of side products to furnish diol (reaction monitored by TLC). After completion of the reaction, the solution was neutralized with the addition of sat. aqueous NH_4Cl and extracted with ethyl acetate six times. The organic layer was washed with brine, dried over Na_2SO_4, filtered. The filtrate was concentrated in a vacuum

and flash chromatography (CyHex/EtOAc 3:7) on silica gel afforded (±)-*trans*-hexane-1,3,4-triol in 58% yield (39.1 mg, 0.29 mmol) as a white solid.

^{1}H NMR (400 MHz, $CDCl_3$) 3.92 – 3.82 (m, 2H), 3.74 – 3.68 (m, 1H), 3.39 (dt, *J* = 8.9, 4.6 Hz, 1H), 2.78 (br s, 3H), 1.76 (dq, *J* = 12.3, 4.7 Hz, 2H), 1.58 (ddd, *J* = 14.0, 7.4, 4.3 Hz, 1H), 1.47 (dt, *J* = 13.5, 7.5 Hz, 1H), 0.99 (t, *J* = 7.4 Hz, 3H).
^{13}C NMR (101 MHz, $CDCl_3$) 75.9, 73.6, 60.9, 35.1, 26.3, 9.9.
HRMS (ESI): [m/z] calculated for $C_6H_{14}NaO_3$ ($[M+Na]^+$): 157.0869; Found: 157.0870.
R_f (EtOAc/MeOH, 4:1) = 0.39 [UV Inactive] [$KMnO_4$].
The characterization data is consistent with the literature. [184]

(±)-Octane-1,2,3-triol (4.11)

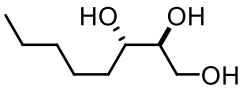

$C_8H_{18}O_3$
162.13 g/mol

In an oven-dried round bottom flask equipped with a magnetic stirring bar, (*E*)-oct-2-en-1-ol (76.1 µL, 0.50 mmol, 1.0 equiv.) was dissolved in acetic acid (1.0 mL, 0.5 M) as the solvent and reagent. To this mixture, 35% aqueous H_2O_2 (85.6 µL, 1.0 mmol, 2.0 equiv.) was added as the oxidant, and the reaction was stirred in an oil bath preheated at 50 °C until complete conversion of the starting material was achieved. For the saponification step, the excess H_2O_2 was quenched by adding 1 M aqueous $Na_2S_2O_3$ solution (1.0 mL) to the same flask. The potassium-iodine starch paper was used to monitor the absence of H_2O_2. Following this, 5 M aqueous NaOH (5.0 mL) was added to the solution and stirred until the complete conversion of side products to furnish diol (reaction monitored by TLC). After completion of the reaction, the solution was neutralized with the addition of sat. aqueous NH_4Cl and extracted with ethyl acetate six times. The organic layer was washed with brine, dried over Na_2SO_4, filtered. The filtrate was concentrated in a vacuum and flash chromatography (CyHex/EtOAc 3:7) on silica gel afforded (±)-octane-1,2,3-triol in 86% yield (69.7 mg, 0.43 mmol) as a white solid.

^{1}H NMR (600 MHz, DMSO-d_6): δ 4.34 (d, *J* = 5.3 Hz, 1H), 4.28 (d, *J* = 5.5 Hz, 1H), 4.27 (br s, 1H), 3.51 (ddd, *J* = 10.5, 5.9, 4.0 Hz, 1H), 3.37 – 3.30 (m, 1H), 3.29 – 3.25 (m, 1H), 3.21 (p, *J* = 6.0 Hz, 1H), 1.54 (tt, *J* = 12.1, 3.4 Hz, 1H), 1.49 – 1.39 (m, 1H), 1.33 – 1.16 (m, 6H), 0.86 (t, *J* = 7.0 Hz, 3H).
^{13}C NMR (151 MHz, DMSO-d_6): δ 74.8, 71.4, 63.5, 32.7, 31.5, 24.9, 22.2, 13.9.
HRMS (ESI): [m/z] calculated for $C_8H_{18}NaO_3$ ($[M+Na]^+$): 185.1148; Found: 185.1150.
R_f (CyHex/EtOAc 3:7**)** = 0.2 [UV Inactive] [$KMnO_4$]

The characterization data is consistent with the literature. [299]

(±)-*trans*-9,10-Dihydroxyoctadecanoic acid (4.12)

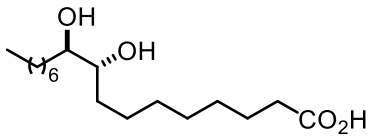

$C_{18}H_{36}O_4$
316.26 g/mol

In an oven-dried round bottom flask equipped with a magnetic stirring bar, oleic acid oleic acid (151 µL, 0.50 mmol, 1.0 equiv.) was dissolved in acetic acid (1.0 mL, 0.5 M) as the solvent and reagent. To this mixture, 35% aqueous H_2O_2 (0.343 mL, 4.0 mmol, 8.0 equiv.) was added as the oxidant, and the reaction was stirred in an oil bath preheated at 50 °C until complete conversion of the starting material was achieved. For the saponification step, the excess H_2O_2 was quenched by adding 1 M aqueous $Na_2S_2O_3$ solution (1.0 mL) to the same flask. The potassium-iodine starch paper was used to monitor the absence of H_2O_2. Following this, 5 M aqueous NaOH (5.0 mL) was added to the solution and stirred until the complete conversion of side products to furnish diol (reaction monitored by TLC). After completion of the reaction, the solution was neutralized with the addition of sat. aqueous NH_4Cl and extracted with warm ethyl acetate six times. The organic layer was washed with brine, dried over Na_2SO_4, filtered. The filtrate was concentrated in a vacuum and the residure was isolated by recrystallization to afforded (±)-9,10-dihydroxyoctadecanoic acid in 78% yield (0.117 g, 0.39 mmol) yield as a white solid.

^{1}H NMR (600 MHz, DMSO) δ 11.93 (s, 1H), 4.13 – 4.09 (m, 2H), 3.19 (d, *J* = 6.0 Hz, 2H), 2.18 (t, *J* = 7.4 Hz, 2H), 1.48 (br s, 2H), 1.41 – 1.34 (m, 4H), 1.24 (h, *J* = 7.5 Hz, 20H), 0.86 (t, *J* = 6.8 Hz, 3H).
^{13}C NMR (151 MHz, DMSO) 174.4, 73.1, 33.6, 32.2, 31.3, 29.2, 29.1, 29.0, 28.8, 28.7, 28.5, 25.6 (d, J = 3.6 Hz), 24.5, 22.0, 13.9.
HRMS (ESI): [m/z] calculated for $C_{18}H_{36}NaO_4$ ($[M+Na]^+$): 339.2495; Found: 339.2506.
R_f (DCM/MeOH, 4:1) = 0.81 [UV Inactive] [$KMnO_4$].
The characterization data is consistent with the literature. [300]

(±)-1-Cyclohexylethane-1,2-diol (4.13)

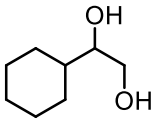

$C_8H_{16}O_2$
144.11 g/mol

In an oven-dried round bottom flask equipped with a magnetic stirring bar, vinylcyclohexane (68.5 µL, 0.50 mmol, 1.0 equiv.) was dissolved in acetic acid (1.0 mL, 0.5 M) as the solvent and reagent. To this mixture, 35% aqueous H_2O_2 (85.6 µL, 1.0 mmol, 2.0 equiv.) was added as the oxidant, and the reaction was stirred in an oil bath preheated at 50 °C until complete conversion of the starting material was achieved. For the saponification step, the excess H_2O_2 was quenched by adding 1 M aqueous $Na_2S_2O_3$ solution (1.0 mL) to the same flask. The potassium-iodine starch paper was used to monitor the absence of H_2O_2. Following this, 5 M aqueous NaOH (5.0 mL) was added to the solution and stirred until the complete conversion of side products to furnish diol (reaction monitored by TLC). After completion of the reaction, the solution was neutralized with the addition of sat. aqueous NH_4Cl and extracted with ethyl acetate six times. The organic layer was washed with brine, dried over Na_2SO_4, filtered. The filtrate was concentrated in a vacuum and flash chromatography (CyHex/EtOAc 3:7) on silica gel afforded (±)-1-cyclohexylethane-1,2-diol in 67% yield (48.0 mg, 0.33 mmol) yield as a white solid.

^{1}H NMR (600 MHz, $CDCl_3$) 3.71 (s, 1H), 3.55 – 3.49 (m, 1H), 3.44 (td, *J* = 7.4, 2.9 Hz, 1H), 2.41 (br s, 2H), 1.86 (d, *J* = 12.7 Hz, 1H), 1.80 – 1.70 (m, 2H), 1.69 – 1.61 (m, 2H), 1.40 (dtd, *J* = 11.6, 7.5, 3.3 Hz, 1H), 1.29 – 1.09 (m, 3H), 1.04 (t, *J* = 12.1 Hz, 2H).
^{13}C NMR (151 MHz, $CDCl_3$) 76.7, 65.0, 29.1, 28.8, 26.5, 26.2, 26.1.
HRMS (ESI): [m/z] calculated for $C_8H_{16}NaO_2$ ($[M+Na]^+$): 167.1052; Found: 167.1043.
R_f (CyHex/EtOAc, 3:2) = 0.26 [UV Inactive] [$KMnO_4$].
The characterization data is consistent with the literature. [301]

(±)-1,2-Hexadecanediol (4.15)

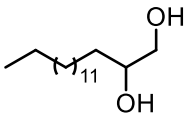

$C_{16}H_{34}O_2$
258.26 g/mol

In an oven-dried round bottom flask equipped with a magnetic stirring bar, hexadec-1-ene (143.7 µL, 0.50 mmol, 1.0 equiv.) was dissolved in acetic acid (1.0 mL, 0.5 M) as

the solvent and reagent. To this mixture, 35% aqueous H_2O_2 (0.343 mL, 4.0 mmol, 8.0 equiv.) was added as the oxidant, and the reaction was stirred in an oil bath preheated at 50 °C until complete conversion of the starting material was achieved. For the saponification step, the excess H_2O_2 was quenched by adding 1 M aqueous $Na_2S_2O_3$ solution (1.0 mL) to the same flask. The potassium-iodine starch paper was used to monitor the absence of H_2O_2. Following this, 5 M aqueous NaOH (5.0 mL) was added to the solution and stirred until the complete conversion of side products to furnish diol (reaction monitored by TLC). After completion of the reaction, the solution was neutralized with the addition of sat. aqueous NH_4Cl and extracted with ethyl acetate six times. The organic layer was washed with brine, dried over Na_2SO_4, filtered. The filtrate was concentrated in a vacuum and flash chromatography (CyHex/EtOAc 3:7) on silica gel afforded (±)-trans-1,2-Hexadecanediolin 81% yield (105 mg, 0.41 mmol) yield as a yellowish oil.

^{1}H NMR (600 MHz, $CDCl_3$) 3.77 – 3.69 (m, 1H), 3.66 (dd, *J* = 11.0, 3.0 Hz, 1H), 3.44 (dd, *J* = 11.0, 7.6 Hz, 1H), 1.76 (s, 3H), 1.44 (s, 2H), 1.37 – 1.21 (m, 23H), 0.88 (t, *J* = 6.9 Hz, 3H).
^{13}C NMR (151 MHz, $CDCl_3$) 72.3, 66.8, 33.2, 31.9, 29.6 (d, J = 5.5 Hz), 29.5, 29.5, 29.3, 25.5, 22.6, 14.0.
HRMS (ESI): [m/z] calculated for $C_{16}H_{34}NaO_2$ ($[M+Na]^+$): 281.2451; Found: 281.2452.
R_f (CyHex/EtOAc, 3:2) = 0.14 [UV Inactive] [$KMnO_4$].
The characterization data is consistent with the literature. [302]

(±)-3-Phenoxypropane-1,2-diol (4.16)

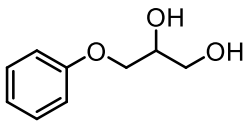

$C_9H_{12}O_3$
168.08 g/mol

In an oven-dried round bottom flask equipped with a magnetic stirring bar, allyl phenyl ether (68.6 µL, 0.50 mmol, 1.0 equiv.) was dissolved in acetic acid (1.0 mL, 0.5 M) as the solvent and reagent. To this mixture, 35% aqueous H_2O_2 (342.5 µL, 4.0 mmol, 8.0 equiv.) was added as the oxidant, and the reaction was stirred in an oil bath preheated at 50 °C until complete conversion of the starting material was achieved. For the saponification step, the excess H_2O_2 was quenched by adding 1 M aqueous $Na_2S_2O_3$ solution (1.0 mL) to the same flask. The potassium-iodine starch paper was used to monitor the absence of H_2O_2. Following this, 5 M aqueous NaOH (5.0 mL) was added to

the solution and stirred until the complete conversion of side products to furnish diol (reaction monitored by TLC). After completion of the reaction, the solution was neutralized with the addition of sat. aqueous NH_4Cl and extracted with ethyl acetate six times. The organic layer was washed with brine, dried over Na_2SO_4, filtered. The filtrate was concentrated in a vacuum and flash chromatography (CyHex/EtOAc 3:7) on silica gel afforded (±)-3-phenoxypropane-1,2-diol in 74% yield (62.2 mg, 0.37 mmol) yield as a yellowish oil.

^{1}H NMR (600 MHz, $CDCl_3$): δ [ppm] = 7.32 – 7.24 (m, 2H), 6.98 (t, *J* = 7.3 Hz, 1H), 6.92 (d, *J* = 8.1 Hz, 2H), 4.15 – 4.06 (m, 1H), 4.05 (t, *J* = 4.6 Hz, 2H), 3.85 (dd, *J* = 11.4, 3.9 Hz, 1H), 3.76 (dd, *J* = 11.4, 5.5 Hz, 1H), 2.26 (br s, 2H).
^{13}C NMR (151 MHz, $CDCl_3$): δ [ppm] = 158.6, 129.7, 121.5, 114.7, 70.5, 69.3, 63.8.
HRMS (ESI): [m/z] calculated for $C_9H_{12}NaO_3$ ($[M+Na]^+$): 191.0705; Found: 191.0706.
R_f (CyHex/EtOAc, 4:1) = 0.19 [UV Inactive] [$KMnO_4$].
The characterization data is consistent with the literature. [303]

(±)-4-Phenylbutane-1,2-diol (4.17)

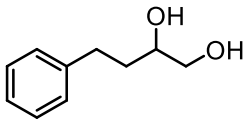

$C_{10}H_{14}O_2$
166.10 g/mol

In an oven-dried round bottom flask equipped with a magnetic stirring bar, 4-phenyl-1-butene (76.7 µL, 0.50 mmol, 1.0 equiv.) was dissolved in acetic acid (1.0 mL, 0.5 M) as the solvent and reagent. To this mixture, 35% aqueous H_2O_2 (85.6 µL, 1.0 mmol, 2.0 equiv.) was added as the oxidant, and the reaction was stirred in an oil bath preheated at 50 °C until complete conversion of the starting material was achieved. For the saponification step, the excess H_2O_2 was quenched by adding 1 M aqueous $Na_2S_2O_3$ solution (1.0 mL) to the same flask. The potassium-iodine starch paper was used to monitor the absence of H_2O_2. Following this, 5 M aqueous NaOH (5.0 mL) was added to the solution and stirred until the complete conversion of side products to furnish diol (reaction monitored by TLC). After completion of the reaction, the solution was neutralized with the addition of sat. aqueous NH_4Cl and extracted with ethyl acetate six times. The organic layer was washed with brine, dried over Na_2SO_4, filtered. The filtrate was concentrated in a vacuum and flash chromatography (CyHex/EtOAc 3:7) on silica gel afforded (±)-4-Phenylbutane-1,2-diol in 57% yield (47.4 mg, 0.28 mmol) as a white solid.

^{1}H NMR (400 MHz, $CDCl_3$) δ 7.38 – 7.28 (m, 2H), 7.27 – 7.23 (m, 3H), 3.76 (tdd, *J* = 7.8, 5.0, 2.9 Hz, 1H), 3.67 (dd, *J* = 11.3, 2.9 Hz, 1H), 3.62 (br s, 1H), 3.50 (dd, *J* = 11.3, 7.8 Hz, 1H), 2.79 (dd, *J* = 2.1, 13.8, 9.0, 6.7 Hz, 2H), 1.88 – 1.70 (m, 2H).
^{13}C NMR (101 MHz, $CDCl_3$) δ 141.8, 128.5, 126.0, 71.7, 66.8, 34.7, 31.9.
HRMS (ESI): [m/z] calculated for $C_{10}H_{14}NaO_2$ ($[M+Na]^+$): 189.0886; Found: 189.0886.
R_f (CyHex/EtOAc, 5:1) = 0.23 [UV Inactive] [$KMnO_4$].
The characterization data is consistent with the literature. [302]

(±)-1-(4-(Trifluoromethyl)phenyl)ethane-1,2-diol (4.19)

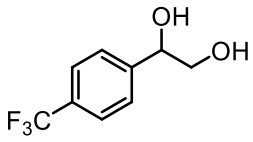

$C_9H_9F_3O_2$
206.06 g/mol

In an oven-dried round bottom flask equipped with a magnetic stirring bar, 4-(trifluormethyl)styrol (73.9 µL, 0.50 mmol, 1.0 equiv.) was dissolved in acetic acid (1.0 mL, 0.5 M) as the solvent and reagent. To this mixture, 35% aqueous H_2O_2 (0.343 mL, 4.0 mmol, 8.0 equiv.) was added as the oxidant, and the reaction was stirred in an oil bath preheated at 50 °C until complete conversion of the starting material was achieved. For the saponification step, the excess H_2O_2 was quenched by adding 1 M aqueous $Na_2S_2O_3$ solution (1.0 mL) to the same flask. The potassium-iodine starch paper was used to monitor the absence of H_2O_2. Following this, 5 M aqueous NaOH (5.0 mL) was added to the solution and stirred until the complete conversion of side products to furnish diol (reaction monitored by TLC). After completion of the reaction, the solution was neutralized with the addition of sat. aqueous NH_4Cl and extracted with ethyl acetate six times. The organic layer was washed with brine, dried over Na_2SO_4, filtered. The filtrate was concentrated in a vacuum and flash chromatography (CyHex/EtOAc 3:7) on silica gel afforded (±)-1-(4-(trifluoromethyl)phenyl)ethane-1,2-diol in 40% yield (41.3 mg, 0.20 mmol) as a colourless liquid.

^{1}H NMR (400 MHz, DMSO-d_6) 7.67 (d, *J* = 8.1 Hz, 2H), 7.57 (d, *J* = 8.1 Hz, 2H), 5.47 (br s, 1H), 4.80 (br s, 1H), 4.63 (t, *J* = 6.0 Hz, 1H), 3.46 (dd, *J* = 7.4, 5.9 Hz, 2H).
^{13}C NMR (101 MHz, DMSO-d_6) 148.6, 127.8, 127.5, 124.9, 124.9, 124.8, 124.8, 73.4, 67.3.
^{19}F NMR (376 MHz, DMSO-d_6): δ [ppm] = -60.7.
HRMS (ESI): [m/z] calculated for $C_9H_9F_3NaO_2$ ($[M+Na]^+$): 229.0452; Found 229.0453.
R_f (CyHex/EtOAc, 3:2) = 0.24 [UV Inactive] [$KMnO_4$].

The characterization data is consistent with the literature. [304]

(±)-1-(4-(*tert*-Butyl)phenyl)ethane-1,2-diol (4.20)

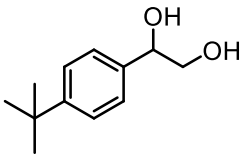

$C_{12}H_{18}O_2$
194.13 g/mol

In an oven-dried round bottom flask equipped with a magnetic stirring bar, 4-*tert*-butylstyrene (90.6 µL, 0.50 mmol, 1.0 equiv.) was dissolved in acetic acid (1.0 mL, 0.5 M) as the solvent and reagent. To this mixture, 35% aqueous H_2O_2 (85.6 µL, 1.0 mmol, 2.0 equiv.) was added as the oxidant, and the reaction was stirred in an oil bath preheated at 50 °C until complete conversion of the starting material was achieved. For the saponification step, the excess H_2O_2 was quenched by adding 1 M aqueous $Na_2S_2O_3$ solution (1.0 mL) to the same flask. The potassium-iodine starch paper was used to monitor the absence of H_2O_2. Following this, 5 M aqueous NaOH (5.0 mL) was added to the solution and stirred until the complete conversion of side products to furnish diol (reaction monitored by TLC). After completion of the reaction, the solution was neutralized with the addition of sat. aqueous NH_4Cl and extracted with ethyl acetate six times. The organic layer was washed with brine, dried over Na_2SO_4, filtered. The filtrate was concentrated in a vacuum and flash chromatography (CyHex/EtOAc 3:7) on silica gel afforded (±)-1-(4-(*tert*-butyl)phenyl)ethane-1,2-diol in 72% yield (70.0 mg, 0.36 mmol) as a white solid.

^{1}H NMR (600 MHz, $CDCl_3$) 7.39 (d, *J* = 8.0 Hz, 2H), 7.30 (d, *J* = 8.0 Hz, 2H), 4.80 (dd, *J* = 8.3, 3.5 Hz, 1H), 3.87 – 3.52 (m, 2H), 2.40 (br s, 2H), 1.32 (s, 9H).
^{13}C NMR (151 MHz, $CDCl_3$) 151.0, 137.5, 125.8, 125.4, 74.5, 67.9, 34.5, 31.3.
HRMS (ESI): [m/z] calculated for $C_{12}H_{18}NaO_2$ ($[M+Na]^+$): 217.1200; Found: 217.1199.
R_f (CyHex/EtOAc, 1:1) = 0.35 [UV Inactive] [$KMnO_4$].
The characterization data is consistent with the literature. [305]

(±)-1-(2-Bromophenyl)ethane-1,2-diol (4.22)

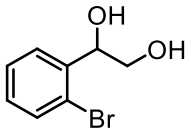

$C_8H_9BrO_2$
215.98 g/mol

In an oven-dried round bottom flask equipped with a magnetic stirring bar, 2-bromostyrene (62.7 µL, 0.50 mmol, 1.0 equiv.) was dissolved in acetic acid (1.0 mL, 0.5 M) as the solvent and reagent. To this mixture, 35% aqueous H_2O_2 (85.6 µL, 1.0 mmol, 2.0 equiv.) was added as the oxidant, and the reaction was stirred in an oil bath preheated at 50 °C until complete conversion of the starting material was achieved. For the saponification step, the excess H_2O_2 was quenched by adding 1 M aqueous $Na_2S_2O_3$ solution (1.0 mL) to the same flask. The potassium-iodine starch paper was used to monitor the absence of H_2O_2. Following this, 5 M aqueous NaOH (5.0 mL) was added to the solution and stirred until the complete conversion of side products to furnish diol (reaction monitored by TLC). After completion of the reaction, the solution was neutralized with the addition of sat. aqueous NH_4Cl and extracted with ethyl acetate six times. The organic layer was washed with brine, dried over Na_2SO_4, filtered. The filtrate was concentrated in a vacuum and flash chromatography (CyHex/EtOAc 3:7) on silica gel afforded (±)-1-(2-bromophenyl)ethane-1,2-diol in 42% yield (46.0 mg, 0.21 mmol) as a colourless liquid.

^{1}H NMR (600 MHz, DMSO-d_6): δ [ppm] = 7.59 – 7.51 (m, 2H), 7.38 (t, *J* = 7.5 Hz, 1H), 7.22 – 7.15 (m, 1H), 5.45 (br s, 1H), 4.86 (dd, *J* = 7.6, 3.4 Hz, 1H), 3.51 (dd, *J* = 11.2, 3.4 Hz, 1H), 3.38 – 3.26 (m, 2H).
^{13}C NMR (151 MHz, DMSO-d_6): δ [ppm] = 141.9, 132.0, 128.9, 128.6, 127.5, 121.6, 72.9, 65.8.
HRMS (ESI): [m/z] calculated for $C_8H_9BrNaO_2$ ($[M+Na]^+$): 238.9678; Found: 238.9678.
R_f (CyHex/EtOAc, 1:1) = 0.35 [UV Inactive] [$KMnO_4$].
The characterization data is consistent with the literature. [306]

(±)-1,1-Diphenylethane-1,2-diol (4.25)

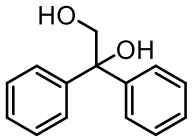

$C_{14}H_{14}O_2$
214.10 g/mol

In an oven-dried round bottom flask equipped with a magnetic stirring bar, 1,1-diphenylethylene (90.1 µL, 0.50 mmol, 1.0 equiv.) was dissolved in acetic acid (1.0 mL, 0.5 M) as the solvent and reagent. To this mixture, 35% aqueous H_2O_2 (0.34 mL, 4.0 mmol, 8.0 equiv.) was added as the oxidant, and the reaction was stirred in an oil bath preheated at 50 °C until complete conversion of the starting material was achieved. For the saponification step, the excess H_2O_2 was quenched by adding 1 M aqueous $Na_2S_2O_3$ solution (1.0 mL) to the same flask. The potassium-iodine starch paper was used to monitor the absence of H_2O_2. Following this, 5 M aqueous NaOH (5.0 mL) was added to the solution and stirred until the complete conversion of side products to furnish diol (reaction monitored by TLC). After completion of the reaction, the solution was neutralized with the addition of sat. aqueous NH_4Cl and extracted with ethyl acetate six times. The organic layer was washed with brine, dried over Na_2SO_4, filtered. The filtrate was concentrated in a vacuum and flash chromatography (CyHex/EtOAc 3:7) on silica gel afforded (±)-1,1-diphenylethane-1,2-diol in 65% yield (69.4 mg, 0.32 mmol) as a white solid.

^{1}H NMR (400 MHz, $CDCl_3$) 7.48 – 7.37 (m, 4H), 7.37 – 7.31 (m, 4H), 7.29 – 7.25 (m, 2H), 4.15 (s, 2H), 2.30 (br, 2H).
^{13}C NMR (101 MHz, $CDCl_3$) 143.6, 129.0, 128.8, 128.3, 127.3, 126.2, 78.4, 69.2.
HRMS (ESI): [m/z] calculated for $C_{14}H_{14}NaO_2$ ($[M+Na]^+$): 237.0889; Found: 237.0889.
R_f (CyHex/EtOAc, 4:1) = 0.25 [UV Inactive] [$KMnO_4$].
The characterization data is consistent with the literature. [307]

(±)-2-Phenylpropane-1,2-diol (4.26)

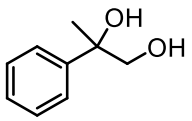

$C_9H_{12}O_2$
152.08 g/mol

In an oven-dried round bottom flask equipped with a magnetic stirring bar, prop-1-en-2-ylbenzene (76.2 mg, 0.50 mmol, 1.0 equiv.) was dissolved in acetic acid (1.0 mL, 0.5 M)

as the solvent and reagent. To this mixture, 35% aqueous H_2O_2 (85.6 µL, 1.0 mmol, 2.0 equiv.) was added as the oxidant, and the reaction was stirred in an oil bath preheated at 50 °C until complete conversion of the starting material was achieved. For the saponification step, the excess H_2O_2 was quenched by adding 1 M aqueous $Na_2S_2O_3$ solution (1.0 mL) to the same flask. The potassium-iodine starch paper was used to monitor the absence of H_2O_2. Following this, 5 M aqueous NaOH (5.0 mL) was added to the solution and stirred until the complete conversion of side products to furnish diol (reaction monitored by TLC). After completion of the reaction, the solution was neutralized with the addition of sat. aqueous NH_4Cl and extracted with ethyl acetate six times. The organic layer was washed with brine, dried over Na_2SO_4, filtered. The filtrate was concentrated in a vacuum and flash chromatography (CyHex/EtOAc 3:7) on silica gel afforded (±)-trans-cyclohexane-1,2-diol in 90% yield as a white solid.

^{1}H NMR (600 MHz, $CDCl_3$) δ 7.46 – 7.42 (m, 2H), 7.36 (t, *J* = 7.8 Hz, 2H), 7.27 (td, *J* = 7.2, 1.4 Hz, 1H), 3.75 (d, *J* = 11.2 Hz, 1H), 3.60 (d, *J* = 11.2 Hz, 2H), 2.66 (s, 1H), 1.51 (s, 3H).
^{13}C NMR (151 MHz, $CDCl_3$) δ 144.97, 128.35, 127.10, 125.05, 74.83, 70.95, 25.95.
HRMS (ESI) m/z: $[M+Na]^+$ calcd for $C_{16}H_{34}NaO$: 175.2559; Found: 175.2552.
R_f (CyHex/EtOAc, 3:2) = 0.26 [UV Inactive] [$KMnO_4$].
The characterization data is consistent with the literature. [308]

(±)-1-Phenylcyclohexane-1,2-diol (4.27)

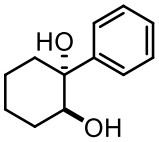

$C_{12}H_{16}O_2$
192.12 g/mol

In an oven-dried round bottom flask equipped with a magnetic stirring bar, 1-Phenyl-1-cyclohexene (79.6 µL, 0.50 mmol, 1.0 equiv.) was dissolved in acetic acid (1.0 mL, 0.5 M) as the solvent and reagent. To this mixture, 35% aqueous H_2O_2 (85.6 µL, 1.0 mmol, 2.0 equiv.) was added as the oxidant, and the reaction was stirred in an oil bath preheated at 50 °C until complete conversion of the starting material was achieved. For the saponification step, the excess H_2O_2 was quenched by adding 1 M aqueous $Na_2S_2O_3$ solution (1.0 mL) to the same flask. The potassium-iodine starch paper was used to monitor the absence of H_2O_2. Following this, 5 M aqueous NaOH (5.0 mL) was added to the solution and stirred until the complete conversion of side products to furnish diol (reaction monitored by TLC). After completion of the reaction, the solution was

neutralized with the addition of sat. aqueous NH_4Cl and extracted with ethyl acetate six times. The organic layer was washed with brine, dried over Na_2SO_4, filtered. The filtrate was concentrated in a vacuum and flash chromatography (CyHex/EtOAc 3:7) on silica gel afforded (±)-1-phenylcyclohexane-1,2-diol in 83% yield (79.6 mg, 0.41 mmol) as a yellowish solid.

^{1}H NMR (600 MHz, $CDCl_3$) δ 7.51 (dd, *J* = 8.2, 1.5 Hz, 2H), 7.38 (t, *J* = 7.8 Hz, 2H), 7.30 – 7.24 (m, 1H), 3.99 (dd, *J* = 11.1, 4.6 Hz, 1H), 2.20 – 1.93 (m, 2H), 1.92 – 1.81 (m, 3H), 1.81 – 1.62 (m, 3H), 1.59 – 1.51 (m, 1H), 1.42 (dt, *J* = 13.2, 3.7 Hz, 1H).
^{13}C NMR (151 MHz, $CDCl_3$) δ 146.34, 128.44, 126.98, 125.10, 75.75, 74.50, 38.50, 29.22, 24.34, 21.06.
HRMS (ESI) m/z: $[M+Na]^+$ calcd for $C_{12}H_{16}NaO_2$: 215.1150; Found: 215.1039.
R_f (CyHex/EtOAc, 3:2) = 0.26 [UV Inactive] [$KMnO_4$].
The characterization data is consistent with the literature. [309]

7.7 Chapter 5: A Modular Approach to the Formal Total Synthesis of (+)-Hannokinol

7.7.1 Synthesis & Characterization of Starting materials

(2*S*,3*S*)-2-(Iodomethyl)-5-methoxytetrahydrofuran-3-ol (5.7)

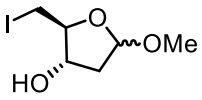

$C_6H_{11}IO_3$
257.98 g/mol

Following reported procedure,[251] in an oven-dried round bottom flask equipped with a magnetic stirring bar, 0.07 equiv.) was added to a solution of 2-deoxy-D-ribose (10.0 g, 74.6 mmol, 1.0 equiv.) in methanol (125 mL). The reaction mixture was stirred at rt for 1 h, after which sodium bicarbonate (4.38 g, 52.2 mmol, 0.70 equiv.) was added portionwise and the resulting suspension was stirred for an additional 5 min. The mixture was filtered through a pad of Celite, and the residue was washed with methanol (3 × 10 mL). The combined filtrates were concentrated in vacuo at a bath temperature of 40 °C to afford the crude acetal (11.0 g, 75.3 mmol), which was used directly in the next step. The crude acetal was dissolved in THF (220 mL), and triphenylphosphine (29.2 g, 111 mmol, 1.5 equiv.), imidazole (10.1 g, 148 mmol, 2.0 equiv.), and iodine (28.3 g, 111 mmol, 1.5 equiv.) were added sequentially. The resulting suspension was stirred at rt for 18 h, then filtered through a pad of Celite and washed with ethyl acetate (3 × 50 mL). The filtrate was concentrated under reduced pressure, and the crude residue was purified by flash column chromatography on silica gel (CyH/EtOAc = 7:3) to afford the desired product as a colorless oil in 90% yield (17.4 g, 67.4 mmol, *d.r* = 67:33).

^{1}H NMR (600 MHz, $CDCl_3$) δ 5.13 (d, J = 4.7 Hz, 1H), 5.10 (dd, J = 5.4, 1.8 Hz, 1H), 4.46 (ddd, J= 10.7, 6.7, 4.1 Hz, 1H), 4.14−4.06 (m, 3H), 3.38 (s, 3H), 3.35 (s,3H), 3.30 (dd, J = 9.8, 5.7 Hz, 1H), 3.25 (dd, J = 10.5, 4.9 Hz, 1H),3.21−3.16 (m, 2H), 2.31 (ddd, J = 13.6, 6.9, 1.7 Hz, 1H), 2.23 (ddd, J= 14.0, 6.6, 4.7 Hz, 1H), 2.12 (ddd, J = 13.6, 6.2, 5.4 Hz, 1H), 2.00(dd, J = 14.0, 1.3 Hz, 1H).

^{13}C NMR (151 MHz, $CDCl_3$) δ 105.9, 105.5, 86.2, 86.1, 75.8, 75.6, 55.4, 55.1, 42.0, 41.0, 7.9, 6.7.

R_f (CyHex/EtOAc, 7:3) = 0.19 [$KMnO_4$].

The characterization data is consistent with the literature.[251]

tert-Butyl(((2S,3S)-2-(iodomethyl)-5-methoxytetrahydrofuran-3-yl)oxy)dimethylsilane (5.8)

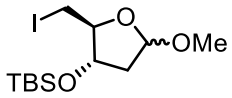

$C_{12}H_{25}IO_3Si$
372.06 g/mol

Following reported procedure,[251] in an oven-dried round bottom flask equipped with a magnetic stirring bar, (2*S*,3*S*)-2-(iodomethyl)-5-methoxytetrahydrofuran-3-ol (16.7 g, 64.8 mmol, 1.0 equiv.) was dissolved in DMF (236 mL), and the solution was cooled to 0 °C. Imidazole (5.29 g, 77.7 mmol, 1.2 equiv.) was added, followed by *tert*-butyldimethylsilyl chloride (11.7 g, 77.7 mmol, 1.2 equiv.) dissolved in dichloromethane (78 mL). The reaction mixture was allowed to warm to rt and stirred for 18 h. The mixture was then diluted with heptane (100 mL), and the organic phase was washed with H_2O (3 × 50 mL) and brine (50 mL), dried over anhydrous Na_2SO_4, and filtered. The filtrate was concentrated in vacuo, and the crude residue was purified by flash column chromatography on silica gel (CyH/EtOAc = 9:1) to afford the desired product as a colorless oil in 95% yield (22.9 g, 61.4 mmol, *d.r.*= 54:46).

^{1}H NMR (600 MHz,$CDCl_3$) δ 5.10 (dd, J = 5.4, 1.9 Hz, 0.5H), 5.00 (dd, J = 5.9, 3.0 Hz,0.5H), 4.43−4.29 (m, 0.5H), 4.00−3.87 (m, 1H), 3.60−3.54 (m,0.5H), 3.47 (dd, J = 10.8, 3.6 Hz, 0.5H), 3.39 (s, 1.5H), 3.37 (s,1.5H), 3.33−3.18 (m, 1.5H), 2.48 (ddd, J = 13.6, 8.6, 5.9 Hz, 0.5H),2.21 (ddd, J = 13.2, 6.6, 1.9 Hz, 0.5H), 2.06 (ddd, J = 13.2, 6.2, 5.4Hz, 0.5H), 1.84 (ddd, J = 13.6, 6.0, 3.0 Hz, 0.5H), 0.88 (s, 9H), 0.11(s, 1.5H), 0.08 (d, J = 0.9 Hz, 3H), 0.07 (s, 1.5H).

^{13}C NMR (151 MHz, CDCl3) δ 105.4, 104.2, 86.0, 80.8, 75.7, 75.4, 55.42,55.40, 42.6, 42.1, 25.90, 25.86, 18.1, 18.0, 8.0, 7.9, −4.35, −4.36, −4.46, −4.51.

R_f (CyHex/EtOAc, 9:1) = 0.19 [$KMnO_4$].

The characterization data is consistent with the literature. [310]

(*S*)-3-((*tert*-Butyldimethylsilyl)oxy)pent-4-enal (5.9)

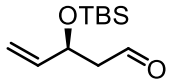

$C_{11}H_{22}O_2Si$
214.14 g/mol

Following reported procedure,[251] in an oven-dried round bottom flask equipped with a magnetic stirring bar, activated zinc powder (24.6 g, 376 mmol, 10 equiv.; activated by stirring in 1 M HCl for 15 min) was added to a solution of the silyl ether (14.0 g, 37.6 mmol, 1.0 equiv.) in THF/H_2O (150 mL, 4:1). The reaction mixture was heated to 90 °C and stirred for 1.5 h, then allowed to cool to room temperature and filtered through a pad of Celite. The residue was washed with diethyl ether (3 × 50 mL), and the combined filtrates were diluted with H_2O (100 mL). The layers were separated, and the aqueous phase was extracted with diethyl ether (3 × 50 mL). The combined organic layers were washed with brine (50 mL), dried over anhydrous Na_2SO_4, filtered, and concentrated in vacuo. Purification by flash column chromatography on silica gel (CyH/EtOAc = 9:1) afforded the desired product as a colorless oil in 98% yield (7.90 g, 37.0 mmol).

^{1}H NMR (400 MHz, $CDCl_3$) δ 9.77 (dd, J = 2.7, 2.2 Hz, 1H), 5.87 (ddd, J = 17.1, 10.4, 5.8 Hz,1H), 5.26 (dt, J = 17.2, 1.5 Hz, 1H), 5.12 (dt, J = 10.4, 1.4 Hz, 1H),4.70−4.60 (m, 1H), 2.60 (ddd, J = 15.7, 6.8, 2.7 Hz, 1H), 2.52 (ddd, J= 15.7, 5.0, 2.2 Hz, 1H), 0.88 (s, 9H), 0.07 (s, 6H), 0.05 (s, 3H).
^{13}C NMR (101 MHz, $CDCl_3$) δ 201.7, 140.1, 115.0, 69.6, 51.4,25.9, 18.2, −4.2, −4.9.
R_f (CyHex/EtOAc, 9:1) = 0.58 [$KMnO_4$].
The characterization data is consistent with the literature. [311]

(*S*)-3-((*tert*-Butyldimethylsilyl)oxy)-1-(diphenylphosphoryl)-pent-4-en-1-one (5.10)

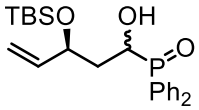

$C_{23}H_{31}O_3PSi$
414.18 g/mol

Following reported procedure,[251] in an oven-dried round bottom flask equipped with a magnetic stirring bar, a solution of (*S*)-3-((*tert*-butyldimethylsilyl)oxy)-1-(diphenylphosphoryl)pent-4-en-1-one (10.0 g, 24.0 mmol, 1.0 equiv.) in methanol (240 mL) was treated with *p*-toluenesulfonic acid monohydrate (594 mg, 3.12 mmol, 0.13 equiv.). The reaction mixture was stirred at 40 °C for 2.5 h, after which the solvent was

removed under reduced pressure. The resulting residue was dissolved in 2,2-dimethoxypropane (63.8 g, 600 mmol, 25 equiv.), and the mixture was rotated at 45 °C for 2.5 h at 330 mbar using a rotary evaporator. The reaction mixture was then diluted with dichloromethane (100 mL) and washed with saturated aqueous $NaHCO_3$ solution (50 mL). The organic layer was dried over Na_2SO_4, filtered, and concentrated in vacuo. Purification by flash column chromatography on silica gel (DCM/EtOAc = 4:6) afforded the desired product as a colorless solid in 96% yield (7.88 g, 23.0 mmol, *d.r.* = 70:30).

^{1}H NMR (600 MHz, $CDCl_3$) δ 8.01−7.65 (m, 4H), 7.60−7.38 (m,6H), 5.84 (ddd, J = 17.1, 10.5, 4.9 Hz, 0.6H), 5.75 (ddd, J = 17.2,10.3, 6.9 Hz, 0.4H), 5.27 (dt, J = 17.2, 1.6 Hz, 0.6H), 5.22−5.12 (m,1H), 5.06 (dt, J = 10.4, 1.2 Hz, 0.4H), 4.82 (dt, J = 11.7, 2.1 Hz,0.6H), 4.68 (ddd, J = 11.0, 3.8, 1.5 Hz, 0.4H), 4.63−4.55 (m, 0.6H),4.52−4.43 (m, 0.4H), 2.18−2.10 (m, 0.4H), 2.03−1.96 (m, 0.6H),1.92−1.83 (m, 0.6H), 1.79−1.68 (m, 0.4H), 0.87 (s, 3H), 0.86 (s,6H), 0.08 (s, 1H), 0.04 (s, 1H), 0.02 (s, 2H), 0.02 (s, 2H).
^{13}CNMR (151 MHz, $CDCl_3$) δ 140.7, 139.0, 132.5, 132.4, 132.4,132.4, 132.1, 132.0, 131.8, 131.7, 131.7, 131.7, 128.7, 128.7,128.6, 128.6, 128.5, 128.4, 115.5, 115.4, 75.7, 75.7, 72.6, 72.5,70.5, 69.9, 68.5, 67.9, 37.8, 36.3, 26.0, 25.9, 18.21, 18.16, −3.9, −4.5,−4.6, −5.3.
R_f (DCM/EtOAc, 3:2) = 0.31 [$KMnO_4$].
The characterization data is consistent with the literature.[312]

((6S)-2,2-Dimethyl-6-vinyl-1,3-dioxan-4-yl)diphenylphosphine oxide (5.1)

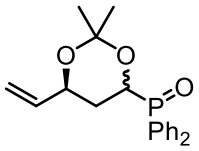

$C_{20}H_{23}O_3P$
342.14 g/mol

To a solution of alcohol (10 g, 24.0 mmol, 1.0 equiv.) in methanol (240 mL) was added *p*-toluenesulfonic acid monohydrate (594 mg, 3.12 mmol, 0.13 equiv.). The solution was stirred at 40 °C for 2.5 h. The solvent was removed in vacuo, and the residue was dissolved in 2,2-dimethoxypropane (75.3 mL, 63.8 g, 600 mmol, 25 equiv.). The reaction mixture was rotated at 45 °C for 2.5 h at 330 mbar in a rotavap and then diluted with dichloromethane (100 mL). The mixture was washed with saturated aqueous sodium bicarbonate solution (50 mL), dried with sodium sulfate, and filtered. The filtrate was concentrated in vacuo, and flash chromatography (DCM/EtOAc 4:6) on silica gel afforded product in 96% yield as a colorless solid (7.88 g, 23.0 mmol, *dr* 70:30).

^{1}H NMR (600 MHz, C_6D_6) δ 8.25−7.93 (m, 4H), 7.15−7.06 (m, 6H), 5.67 (ddd, J = 17.3, 10.6, 5.3Hz, 0.3H), 5.58 (ddd, J = 17.3, 10.6, 5.1 Hz, 0.7H), 5.13−4.99 (m,1H), 4.93−4.81 (m, 1H), 4.78−4.65 (m, 1H), 4.26−4.15 (m, 0.3H),4.15−4.01 (m, 0.7H), 2.42−2.30 (m, 0.3H), 2.12−2.04 (m, 0.7H),2.03−1.93 (m, 0.3H), 1.76−1.62 (m, 0.7H), 1.37 (s, 2H), 1.24 (s,1H), 1.22 (s, 1H), 1.14 (s, 2H).

^{13}C NMR (151 MHz, C_6D_6) δ 138.6, 138.4, 132.92, 132.87, 132.8, 132.7, 131.89, 131.87, 131.82,131.80, 131.75, 131.72, 128.7, 128.65, 128.61, 128.5, 128.44, 128.40,128.37, 128.32, 114.8, 114.5, 101.5, 101.4, 99.53, 99.46, 70.2, 70.1,69.7, 69.1, 67.35, 67.75, 66.4, 65.7, 31.1, 30.2, 30.0, 25.1, 25.0, 19.1.

R_f (DCM/EtOAc, 6:4) = 0.64 [$KMnO_4$].

The characterization data is consistent with the literature. [251]

Methyl 2-(4-methoxyphenyl)acetate (5.11)

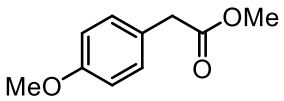

$C_{10}H_{12}O_3$
180.08 g/mol

Following reported procedure,[251] in an oven-dried round bottom flask equipped with a magnetic stirring bar, a solution of 4-methoxyphenylacetic acid (6.00 g, 36.0 mmol, 1.0 equiv.) in methanol (112 mL) was treated with concentrated H_2SO_4 (2.32 mL, 43.3 mmol, 1.2 equiv.). The reaction mixture was heated under reflux for 3 h, then allowed to cool to room temperature. The solvent was removed under reduced pressure, and the crude residue was redissolved in ethyl acetate. The organic phase was dried over anhydrous Na_2SO_4, filtered, and concentrated in vacuo. Purification by flash column chromatography on silica gel (CyHex/EtOAc = 1:1) afforded the corresponding methyl ester as a colourless oil in 94% yield (6.12 g, 33.9 mmol).

^{1}H NMR (600 MHz, $CDCl_3$) δ 7.20 (d, *J* = 8.6 Hz, 2H), 6.86 (d, *J* = 8.6 Hz, 2H), 3.79 (s, 3H), 3.69 (s, 3H), 3.57 (s, 2H).

^{13}C NMR (151 MHz, $CDCl_3$) δ 172.4, 158.9, 130.4, 126.2, 114.1, 55.4, 52.1, 40.4.

IR (ATR): $\tilde{\nu}$ [cm^{-1}] = 2952, 1732, 1612, 1511, 1299, 1242, 1151, 1012, 788.

HRMS (ESI) m/z: [M+Na^+] calcd for $C_{10}H_{12}NaO_3$:203.0678; Found: 203.0679.

R_f (CyHex/EtOAc, 1:1) = 0.82 [$KMnO_4$].

The characterization data is consistent with the literature. [313]

2-(4-Methoxyphenyl)acetaldehyde (5.5)

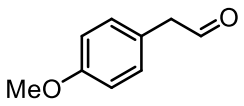

$C_9H_{10}O_2$
150.07 g/mol

In an oven-dried round bottom flask equipped with a magnetic stirring bar, a solution of methyl 2-(4-methoxyphenyl)acetate (5.00 g, 27.8 mmol, 1.0 equiv.) in anhydrous toluene (72 mL) was cooled to −78 °C. Diisobutylaluminium hydride (1.0 M solution in toluene, 25.4 mL, 1.1 equiv.) was added dropwise, and the reaction mixture was stirred at −78 °C for 1 h. The reaction was quenched by careful addition of methanol (10 mL) and then poured into dichloromethane (100 mL). The resulting mixture was washed sequentially with 1 M aqueous HCl (50 mL) and brine (50 mL). The organic phase was dried over anhydrous Na_2SO_4, filtered, and concentrated under reduced pressure. Purification of the crude residue by flash column chromatography on silica gel (PE/Et_2O = 10:1) afforded the corresponding aldehyde as a colourless oil in 83% yield (3.71 g, 24.5 mmol).

^{1}H NMR (400 MHz, $CDCl_3$) δ 9.72 (s, 1H), 7.18 – 7.09 (m, 2H), 6.91 (d, *J* = 8.7 Hz, 2H), 3.81 (s, 3H), 3.63 (d, *J* = 2.4 Hz, 2H).
^{13}C NMR (101 MHz, $CDCl_3$) δ 199.6, 158.94, 130.6, 123.6, 114.4, 55.2, 49.6.
IR (ATR): $\tilde{\nu}$ [cm^{-1}] = 1721, 1611, 1511, 1245, 1177, 1032, 906, 825, 726, 648, 524.
HRMS (ESI) m/z: $[M+Na]^+$ calcd for $C_9H_{10}NaO_2$: 173.0681; Found: 173.0568.
R_f (PE/DE, 10:1) = 0.81 [$KMnO_4$].
The characterization data is consistent with the literature.[314]

5-Hydroxy-1-(4-methoxyphenyl)hept-6-en-3-one (5.12)

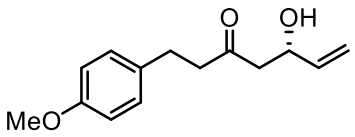

$C_{14}H_{18}O_3$
234.13 g/mol

To a solution of diisopropylamine (1.72 mL, 12.27 mmol, 2.1 equiv.) in anhydrous THF (58 mL) was added *n*-butyllithium (2.5 M in hexanes, 6.39 mL, 12.27 mmol, 2.1 equiv.) at −78 °C to generate LDA. After stirring for 15 min at this temperature, a solution of the (*S*)-building block (2.00 g, 5.84 mmol, 1.0 equiv.) in anhydrous THF (19 mL) was added dropwise at −78 °C. The reaction mixture was stirred at −78 °C for 1 h, after which a

solution of the aldehyde (2.63 g, 17.52 mmol, 3.0 equiv.) in anhydrous THF (9 mL) was added. The reaction mixture was allowed to warm to room temperature over 1 h, then potassium *tert*-butoxide (0.69 g, 5.84 mmol, 1.0 equiv.) was added, and stirring was continued at room temperature for an additional 1 h. The reaction was quenched with saturated aqueous NH_4Cl (30 mL), and the aqueous phase was extracted with CH_2Cl_2 (3 × 50 mL). The combined organic layers were washed with 2 M HCl (2 × 50 mL), and the aqueous phases were re-extracted with CH_2Cl_2 (3 × 50 mL). The combined organic extracts were washed with brine (100 mL), dried over anhydrous Na_2SO_4, filtered, and concentrated under reduced pressure. Purification of the crude residue by flash column chromatography on silica gel (PE/EtOAc = 4:1) afforded the β-hydroxy ketone as a light yellow oil in 87% yield (1.19 g, 5.08 mmol).

^{1}H NMR (600 MHz, $CDCl_3$) δ 7.08 (d, *J* = 8.6 Hz, 2H), 6.82 (d, *J* = 8.6 Hz, 2H), 5.83 (ddd, *J* = 16.6, 10.6, 5.6 Hz, 1H), 5.27 (d, *J* = 17.1 Hz, 1H), 5.14 – 5.08 (m, 1H), 4.61 – 4.52 (m, 1H), 3.77 (s, 3H), 2.88 (s, 1H), 2.84 (t, *J* = 7.6 Hz, 2H), 2.73 (t, *J* = 7.6 Hz, 2H), 2.60 (d, *J* = 6.4 Hz, 2H).
^{13}C NMR (151 MHz, $CDCl_3$) δ 210.1, 157.9, 139.1, 132.7, 129.1, 114.9, 113.9, 68.5, 55.2, 48.9, 45.3, 28.5.
IR (ATR): $\tilde{\nu}$ [cm^{-1}] = 2932, 1707, 1611, 1583, 1510, 1463, 1441, 1404, 1365, 1299, 1242, 1177, 1108, 1084, 1032, 976, 927, 823.
HRMS (ESI) m/z: [M+Na]+ calcd for $C_{14}H_{18}NaO_3$: 257.1256; Found: 257.1148.
$[\alpha]^{20}_D$ = +11.3 (c = 1.21, DCM).
R_f (PE/EtOAc, 4:1) = 0.26 [$KMnO_4$].

(3*S*,5*R*)-5-Hydroxy-7-(4-methoxyphenyl)hept-1-en-3-yl acetate (5.13)

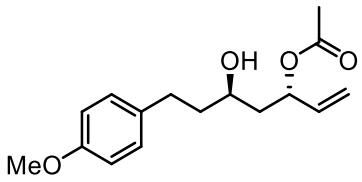

$C_{16}H_{22}O_4$
278.15 g/mol

In an oven-dried round bottom flask equipped with a magnetic stirring bar, β-hydroxy ketone (350 mg, 1.40 mmol, 1.0 equiv.) was dissolved in THF (3 mL) and cooled to −50 °C. Acetaldehyde (0.29 mL, 5.23 mmol, 3.5 equiv.) was added, and samarium(II) iodide (0.1 M in THF, 11.2 mL, 1.12 mmol, 0.75 equiv.) was added dropwise under exclusion of light. The reaction mixture was allowed to warm to −20 °C and stirred for 18 h. The reaction was quenched with saturated aqueous $NaHCO_3$ (15 mL), and the layers were

separated. The aqueous phase was extracted with ethyl acetate (3 × 10 mL), and the combined organic layers were washed with brine (20 mL), dried over anhydrous Na_2SO_4, filtered, and concentrated under reduced pressure. Purification by flash column chromatography on silica gel (CyHex/EtOAc = 4:1) afforded the ester as a colourless oil in 87% yield (362 mg, 1.30 mmol).

^{1}H NMR (600 MHz, $CDCl_3$) δ 7.16 – 7.07 (m, 2H), 6.88 – 6.78 (m, 2H), 5.84 (ddd, *J* = 16.9, 10.5, 6.0 Hz, 1H), 5.52 (ddt, *J* = 9.5, 5.6, 3.6 Hz, 1H), 5.27 (dt, *J* = 17.3, 1.3 Hz, 1H), 5.16 (dt, *J* = 10.5, 1.3 Hz, 1H), 3.56 (tt, *J* = 7.8, 3.5 Hz, 3H), 2.75 (ddd, *J* = 14.8, 9.8, 5.5 Hz, 1H), 2.62 (ddd, *J* = 13.8, 9.7, 6.6 Hz, 1H), 2.08 (s, 3H), 1.84 – 1.63 (m, 4H).
^{13}C NMR (151 MHz, $CDCl_3$) δ 171.3, 157.8, 136.4, 134.1, 129.3, 116.3, 113.8, 72.1, 66.6, 55.23, 42.6, 39.1, 31.1, 21.1.
IR (ATR): $\tilde{\nu}$ [cm^{-1}] = 2928, 1608, 1510, 1463, 1247, 1174, 1037, 834, 774.
HRMS (ESI) m/z: $[M+Na]^+$ calcd for $C_{16}H_{22}NaO_4$: 301.1518; Found: 301.1154.
$[\alpha]^{20}_D$ = -3.1 (c = 1.0, DCM).
R_f (CyHex/EtOAc, 4:1) = 0.17 [$KMnO_4$].

(3*S*,5*R*)-7-(4-Methoxyphenyl)hept-1-ene-3,5-diol (5.14)

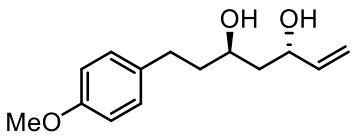

$C_{14}H_{20}O_3$
236.14 g/mol

In an oven-dried round bottom flask equipped with a magnetic stirring bar, a solution of (3*S*,5*R*)-5-hydroxy-7-(4-methoxyphenyl)hept-1-en-3-yl acetate (300 mg, 1.08 mmol, 1.0 equiv.) in MeOH/H_2O (4 mL, 3:1) was cooled to 0 °C, and potassium carbonate (297 mg, 2.15 mmol, 2.0 equiv.) was added. The reaction mixture was stirred at 0 °C for 1 h and then allowed to warm to room temperature. Upon completion as indicated by TLC, water (10 mL) and ethyl acetate (10 mL) were added, and the layers were separated. The aqueous phase was extracted with ethyl acetate (3 × 10 mL), and the combined organic layers were washed with brine (15 mL), dried over anhydrous Na_2SO_4, filtered, and concentrated under reduced pressure. Purification by flash column chromatography on silica gel (CyHex/EtOAc = 7:3) afforded the corresponding diol as a colourless oil in 92% yield (234 mg, 0.99 mmol).

^{1}H NMR (600 MHz, $CDCl_3$) δ 7.11 (d, *J* = 8.6 Hz, 2H), 6.83 (d, *J* = 8.6 Hz, 2H), 5.92 (ddd, *J* = 17.1, 10.5, 5.5 Hz, 1H), 5.28 (dt, *J* = 17.3, 1.5 Hz, 1H), 5.14 (dd, *J* = 10.5, 1.4 Hz,

1H), 4.51 – 4.44 (m, 1H), 4.00 – 3.93 (m, 1H), 3.78 (s, 3H), 2.73 (ddd, *J* = 13.8, 9.9, 5.7 Hz, 1H), 2.62 (ddd, *J* = 13.9, 9.7, 6.4 Hz, 2H), 2.25 (s, 2H), 1.87 – 1.61 (m, 4H).

^{13}C NMR (151 MHz, $CDCl_3$) δ 157.8, 140.7, 133.9, 129.3, 114.5, 113.9, 70.7, 68.7, 55.3, 42.3, 39.4, 31.1.

IR (ATR): $\tilde{\nu}$ [cm^{-1}] = 3354, 2935, 1611, 1510, 1242, 1177, 1034, 922, 822, 526.

HRMS (ESI) m/z: $[M+Na]^+$ calcd for $C_{14}H_{20}NaO_3$: 259.1412; Found: 259.1305.

$[\alpha]^{20}_D$ = +15.4 (c = 1.0, DCM).

R_f (CyHex/EtOAc, 7:3) = 0.24 [$KMnO_4$].

(5*R*,7*S*)-5-(4-Methoxyphenethyl)-2,2,3,3,9,9,10,10-octamethyl-7-vinyl-4,8-dioxa-3,9-disilaundecane (5.15)

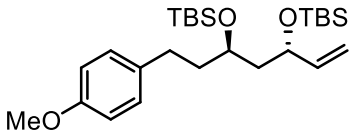

$C_{26}H_{48}O_3Si_2$
464.31 g/mol

In an oven-dried round bottom flask equipped with a magnetic stirring bar, a solution of (3*S*,5*R*)-7-(4-methoxyphenyl)hept-1-ene-3,5-diol (200 mg, 0.85 mmol, 1.0 equiv.) in DMF (5 mL) was cooled to 0 °C for 20 min. Imidazole (461 mg, 6.77 mmol, 8.0 equiv.) and *tert*-butyldimethylsilyl chloride (0.51 g, 3.39 mmol, 4.0 equiv.) were added, and the reaction mixture was stirred at room temperature for 18 h. Upon completion, water (15 mL) and diethyl ether (15 mL) were added, and the layers were separated. The aqueous phase was extracted with diethyl ether (3 × 15 mL), and the combined organic layers were washed with brine (15 mL), dried over anhydrous Na_2SO_4, filtered, and concentrated under reduced pressure. Purification by flash column chromatography on silica gel (CyHex/EtOAc = 7:3) afforded the silylated product as a colorless oil in 95% yield (373 mg, 0.80 mmol, *d.r.* > 99:1).

^{1}H NMR (600 MHz, $CDCl_3$) δ 7.10 (d, *J* = 8.4 Hz, 2H), 6.83 (d, *J* = 8.4 Hz, 2H), 5.81 (ddd, *J* = 17.2, 10.3, 7.0 Hz, 1H), 5.12 (d, *J* = 17.2 Hz, 1H), 5.03 (d, *J* = 10.3 Hz, 1H), 4.19 (d, *J* = 6.7 Hz, 1H), 3.87 – 3.80 (m, 1H), 3.79 (s, 3H), 2.60 (dddd, *J* = 38.9, 13.7, 10.6, 5.7 Hz, 1H), 1.82 – 1.69 (m, 3H), 1.65 (dt, *J* = 13.5, 6.0 Hz, 1H), 0.92 (s, 9H), 0.89 (s, 9H), 0.19 – -0.17 (m, 12H).

^{13}C NMR (151 MHz, $CDCl_3$) δ 157.7, 134.7, 129.2, 114.2, 113.8, 71.9, 69.2, 55.3, 46.2, 39.9, 30.5, 25.9, 18.2, -3.8, -3.9, -4.1, -4.5.

IR (ATR): $\tilde{\nu}$ [cm^{-1}] = 2928, 1511, 1463, 1246, 1073, 833, 773.

HRMS (ESI) m/z: $[M+Na]^+$ calcd for $C_{26}H_{48}O_3NaSi_2$: 487.3142; Found: 487.3034.
$[\alpha]^{20}_D$ = +1.0 (c = 1.0, DCM).
R_f (CyHex/EtOAc, 7:3) = 0.23 [$KMnO_4$].

(5*R*,7*S*)-5-(4-Methoxyphenethyl)-7-((E)-4-methoxystyryl)-2,2,3,3,9,9,10,10-octamethyl-4,8-dioxa-3,9-disilaundecane (5.17)

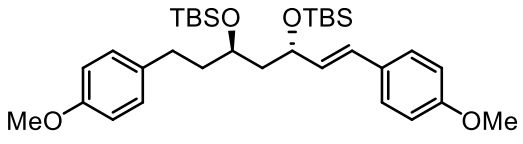

$C_{33}H_{54}O_4Si_2$
570.36 g/mol

In an oven-dried round bottom flask equipped with a magnetic stirring bar, (5*R*,7*S*)-5-(4-methoxyphenethyl)-2,2,3,3,9,9,10,10-octamethyl-7-vinyl-4,8-dioxa-3,9-disilaundecane (320 mg, 0.69 mmol, 1.0 equiv.) was combined with palladium(II) acetate (46.4 mg, 0.21 mmol, 0.30 equiv.), potassium carbonate (951 mg, 6.88 mmol, 10 equiv.), and tetrabutylammonium chloride (957 mg, 3.44 mmol, 5.0 equiv.). The flask was evacuated and backfilled with argon three times. A solution of 4-iodoanisole (242 mg, 1.03 mmol, 1.5 equiv.) in degassed DMF (32 mL) was added, and the mixture was stirred at 90 °C for 19 h. Upon completion, the reaction was cooled to room temperature and diluted with ethyl acetate (10 mL) and water (10 mL). The aqueous phase was extracted with ethyl acetate (3 × 10 mL), and the combined organic layers were washed with brine (8 mL), dried over anhydrous Na_2SO_4, filtered, and concentrated under reduced pressure. Purification by flash column chromatography on silica gel (PE/DE = 50:1) afforded the desired olefin as a colorless oil in 84% yield (330 mg, 0.58 mmol, *d.r.* > 99:1).

^{1}H NMR (600 MHz, $CDCl_3$) δ 7.29 (d, *J* = 8.6 Hz, 2H), 7.12 – 7.05 (m, 2H), 6.89 – 6.83 (m, 2H), 6.83 – 6.78 (m, 2H), 6.37 (d, *J* = 15.9 Hz, 1H), 6.00 (dd, *J* = 15.8, 7.5 Hz, 1H), 4.34 (q, *J* = 6.9 Hz, 1H), 3.87 (p, *J* = 5.8 Hz, 1H), 3.82 (s, 3H), 3.78 (s, 3H), 2.60 (tq, *J* = 19.6, 6.8 Hz, 2H), 1.89 – 1.68 (m, 4H), 0.92 (s, 9H), 0.90 (s, 9H), 0.09 – 0.03 (m, 12H).
^{13}C NMR (151 MHz, $CDCl_3$) δ 159.2, 157.7, 134.7, 131.4, 129.8, 129.2, 127.5, 114.1, 113.8, 71.7, 69.1, 55.3, 55.3, 46.6, 30.4, 25.9, 18.2, 18.2, -4.2, -4.1, -4.5.
IR (ATR): $\tilde{\nu}$ [cm^{-1}] = 2929, 1607, 1502, 1275, 1250, 1182, 1040, 906, 823, 809, 731.
HRMS (ESI) m/z: $[M+Na]^+$ calcd for $C_{33}H_{54}O_4NaSi_2$: 593.3561; Found: 593.3452.
$[\alpha]^{20}_D$ -23.0 (c = 1.0, DCM).
R_f (PE/DE, 50:1) = 0.21 [$KMnO_4$].

(5*R*,7*R*)-5,7-*bis*(4-Methoxyphenethyl)-2,2,3,3,9,9,10,10-octamethyl-4,8-dioxa-3,9-disilaundecane (5.18)

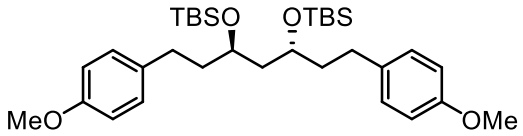

$C_{33}H_{56}O_4Si_2$
572.37 g/mol

In an oven-dried round bottom flask equipped with a magnetic stirring bar, (5*R*,7*S*)-5-(4-methoxyphenethyl)-7-((E)-4-methoxystyryl)-2,2,3,3,9,9,10,10-octamethyl-4,8-dioxa-3,9-disilaundecane (200 mg, 0.35 mmol, 1.0 equiv.) was dissolved in methanol (8.0 mL), and Pd/C (10% on activated charcoal, 0.10 g, 0.10 mmol, 0.3 equiv.) was added. The reaction mixture was stirred at room temperature under a hydrogen atmosphere (1 atm) for 8 h. The suspension was filtered through a pad of celite and washed with ethyl acetate (3 × 10 mL). The combined filtrate was concentrated under reduced pressure, and the crude residue was purified by flash column chromatography on silica gel (CyHex/EtOAc = 17:1) to afford the reduced product as a colorless oil in 93% yield (193 mg, 0.33 mmol).

^{1}H NMR (600 MHz, $CDCl_3$) δ 7.09 (d, *J* = 8.1 Hz, 4H), 6.87 – 6.80 (m, 4H), 3.80 (d, *J* = 6.2 Hz, 8H), 2.67 – 2.53 (m, 4H), 1.72 (dt, *J* = 12.1, 5.8 Hz, 6H), 0.91 (s, 18H), 0.07 (d, *J* = 6.8 Hz, 12H).
^{13}C NMR (151 MHz, $CDCl_3$) δ 157.7, 134.6, 113.8, 69.8, 55.3, 45.2, 39.9, 30.4, 25.9, 18.1, -3.9, -4.07.
IR (ATR): $\tilde{\nu}$ [cm^{-1}] = 2928, 1511, 1462, 1244, 1176, 1037, 832, 771.
HRMS (ESI) m/z: $[M+Na]^+$ calcd for $C_{33}H_{56}O_4NaSi_2$: 595.3717; Found: 595.3608.
$[\alpha]^{20}_D$ = +2.1 (c = 1.0, DCM).
R_f (CyHex/EtOAc, 17:1) = 0.21 [$KMnO_4$].

(3*R*,5*R*)-1,7-*bis*(4-Methoxyphenyl)heptane-3,5-diol (5.3)

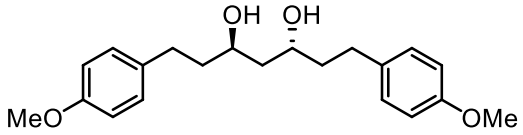

$C_{21}H_{28}O_4$
344.19 g/mol

In a Teflon vial, HF-pyridine (70% HF, 0.50 mL, 3.49 mmol, 20 equiv.) was dissolved in pyridine/MeOH (1.76 mL, 6:1) at 0 °C. In a separate Teflon vial, the silyl ether (100 mg, 175 µmol, 1.0 equiv.) was dissolved in THF (1.52 mL) and cooled to 0 °C. The HF-

pyridine solution was added to the THF solution, and the reaction mixture was stirred at room temperature for 18 h. Upon completion, excess methoxytrimethylsilane (10 mL) was added at 0 °C, followed by dilution with toluene (10 mL), and volatiles were removed under reduced pressure. This toluene addition and evaporation cycle was repeated three times to ensure complete removal of pyridine. The crude product was purified by flash column chromatography on silica gel (CyHex/EtOAc = 5:2) to afford the corresponding 1,3-diol as a white solid in 87% yield (48.1 mg, 151 µmol).

^{1}H NMR (600 MHz, $CDCl_3$) δ 7.11 (d, *J* = 8.4 Hz, 4H), 6.83 (d, *J* = 8.6 Hz, 4H), 3.97 (dd, *J* = 8.4, 5.1 Hz, 2H), 3.78 (s, 6H), 2.71 (ddd, *J* = 15.0, 9.7, 5.7 Hz, 2H), 2.61 (ddd, *J* = 13.8, 9.5, 6.5 Hz, 2H), 2.12 (s, 2H), 1.83 (ddd, *J* = 14.3, 8.7, 5.6 Hz, 2H), 1.80 (d, *J* = 5.7 Hz, 2H), 1.73 (dddd, *J* = 13.9, 10.4, 6.5, 4.6 Hz, 2H), 1.66 (t, *J* = 5.6 Hz, 2H).
^{13}C NMR (151 MHz, $CDCl_3$) δ 157.9, 133.9, 129.3, 113.9, 68.9, 55.3, 42.6, 39.3, 31.2.
IR (ATR): $\tilde{\nu}$ [cm^{-1}] = 3374, 2939, 1612, 1511, 1300, 1244, 1176, 1033, 814, 514.
HRMS (ESI) m/z: $[M+Na]^+$ calcd for $C_{21}H_{28}NaO_4$: 367.1988; Found: 367.1879.
$[\alpha]^{20}_D$ = +6.5 (c = 1.0, DCM).
R_f (CyHex/EtOAc, 5:2) = 0.24 [$KMnO_4$].

Abbreviation

2,2-DMP	2,2-Dimethoxypropane
Ac	Acetyl
AcOH	Acetic acid
Ala	Alanine
Ar	Aryl
Aq.	Aqueous
ATR	Attenuated total reflection
Bn	Benzyl
Boc	*tert*-Butyloxycarbonyl
Bu	Butyl
Bz	Benzoyl
CAM	Ceric ammonium molybdate
Cat.	Catalyst
Cbz	Benzyloxycarbonyl
CSA	Camphorsulfonic acid
CuAAC	Copper(I)-catalyzed azide–alkyne cycloaddition
CyHex	Cyclohexane
DCM	Dichloromethane
DCE	1,2-Dichloroethane
DDQ	2,3-Dichloro-5,6-dicyano-p-benzoquinone
DEAD	Diethyl azodicarboxylate
DIBAL	Diisobutylaluminium hydride
DIC	*N*,*N'*-Diisopropylcarbodiimide
DIPA	Diisopropylamine

DIPEA	*N,N*-Diisopropylethylamine
DMA	Dimethylacetamide
DMAP	4-Dimethylaminopyridine
DME	1,2-Dimethoxyethane
DMF	*N,N*-Dimethylformamide
DMP	Dess–Martin periodinane
DMSO	Dimethyl sulfoxide
d.r.	Diastereomeric ratio
e.e.	Enantiomeric excess
e.r.	Enantiomeric ratio
EDG	Electron-donating group
EDTA	Ethylenediaminetetraacetic acid
ESI	Electrospray ionization
Et	Ethyl
EtOAc	Ethyl acetate
EtOH	Ethanol
Equiv.	Molar equivalents
EWG	Electron-withdrawing group
FDA	United States Food and Drug Administration
FG	Functional group
Fmoc	Fluorenylmethoxycarbonyl
Gln	Glutamine
HAT	Hydrogen-atom transfer
HATU	Hexafluorophosphate azabenzotriazole tetramethyl uronium
HBTU	Hexafluorophosphate benzotriazole tetramethyl uronium
HCl	Hydrochloric acid

HMTA	Hexamethylenetetramine
HOBt	1-Hydroxybenzotriazole
IBS	2-Iodoxybenzenesulfonic acid
IBX	2-Iodoxybenzoic acid
ImH	Imidazole
iPr	Isopropyl
IR	Infrared spectroscopy
LA	Lewis acid
LDA	Lithium diisopropylamide
M	Molarity
m	Meta (substituent orientation in phenyl ring)
***m*CPBA**	*meta*-Chloroperbenzoic acid
Me	Methyl
MeOH	Methanol
MHz	Megahertz
MSA	Methanesulfonic acid
Ms	Mesyl (methanesulfonyl)
MTBE	Methyl tert-butyl ether
NMP	N-Methyl-2-pyrrolidone
NMR	Nuclear magnetic resonance spectroscopy
o	Ortho (substituent orientation in phenyl ring)
p	Para (substituent orientation in phenyl ring)
Pd/C	Palladium on carbon
PE	Petroleum ether
PG	Protecting group
Ph	Phenyl

Phth	Phthaloyl
PhthN	Phthalimide
PIDA	Phenyliodine diacetate
PIFA	*Bis*(trifluoroacetoxy)iodobenzene
PMB	4-Methoxybenzyl
PPA	Propionic acid
PPTS	Pyridinium p-toluenesulfonate
PP-reactor	Polypropylene reactor
PTFE	Poly(tetrafluoroethylene)
***p*TsOH**	*p*-Toluenesulfonic acid
Rf	Retention factor
RSM	Recovered starting material
r.t.	Room temperature
SET	Single-electron transfer
SPPS	Solid-phase peptide synthesis
TBA	Tetrabutylammonium
TBAF	Tetrabutylammonium fluoride
TBDPSCl	*tert*-Butyldiphenylsilyl chloride
TBS	*tert*-Butyldimethylsilyl
TEA	Triethylamine
TEMPO	2,2,6,6-Tetramethylpiperidin-1-oxyl
Tf	Triflyl
TFA	Trifluoroacetic acid
TFE	2,2,2-Trifluoroethanol
THF	Tetrahydrofuran
THF-M	Tetrahydrofuran-2-methanol

TLC Thin-layer chromatography

TMS Tetramethylsilane

References

[1] J.-E. Bäckvall, *Modern Oxidation Methods*, Wiley-VCH, **2011**.

[2] S. Caron, R. W. Dugger, S. G. Ruggeri, J. A. Ragan, D. H. B. Ripin, *Chem. Rev.* **2006**, 106, 2943–2989.

[3] V. H. Masand, M. K. Patil, S. A. Al-Hussain, A. Samad, V. Rastija, R. D. Jawarkar, G. S. Masand, R. G. Gawali, M. E. A. Zaki, *Chem. Biol. Drug Des.* **2025**, 105, e70060.

[4] M. S. Chen, M. C. White, *Science* **2007**, 318, 783–787.

[5] F. P. Guengerich, F. K. Yoshimoto, *Chem. Rev.* **2018**, 118, 6573–6655.

[6] W. J. Mijs, C. de Jonge, *Organic Syntheses by Oxidation with Metal Compounds*, Springer Science & Business Media, **2013**.

[7] N. Jiao and S. S. Stahl, ed., *Green oxidation in organic synthesis*, Wiley-VCH **2019**.

[8] P. Anastas, N. Eghbali, *Chem. Soc. Rev.* **2010**, 39, 301–312.

[9] M. E. Ali, M. M. Rahman, S. M. Sarkar, S. B. A. Hamid, *J. Nanomater.* **2014**, 1920, 1–23.

[10] G. D. Yadav, R. K. Mewada, D. P. Wagh, H. G. Manyar, *Catal. Sci. Technol.* **2022**, 12, 7245–7269.

[11] R. Saha, R. Nandi, B. Saha, *J. Coord. Chem.* **2011**, 64, 1782–1806.

[12] J. C. Védrine, *ChemSusChem* **2019**, 12, 577–588.

[13] Z. Guo, B. Liu, Q. Zhang, W. Deng, Y. Wang, Y. Yang, *Chem. Soc. Rev.* **2014**, 43, 3480–3524.

[14] T. A. Gazis, J. Wuyts, A. Moutsiou, G. Volpin, M. J. Ford, R. I. Teixeira, K. M. P. Wheelhouse, P. Natho, P. Žnidaršič-Plazl, S. Jost, R. Luisi, B. Benyahia, B. U. W. Maes, G. Vilé, *Chem. Soc. Rev.* **2026**, 55, 619–674.

[15] M. Waris, M. A. Salam, A. Akram, F. Shafeeq, M. Malik, A. u. Rehman, F. Bashir, M. A. Khan, T. Hasan, *Physical Education, Health and Social Sciences* **2025**, 3, 73–86.

[16] B. List, *Chem. Rev.* **2007**, 107, 5413–5415.

[17] M. H. Aukland, B. List, *Pure Appl. Chem.* **2021**, 93, 1371–1381.

[18] Q.-L. Zhou, *Angew. Chem. Int. Ed.* **2016**, 55, 5352–5353.

[19] A. Antenucci, S. Dughera, P. Renzi, *ChemSusChem* **2021**, 14, 2785–2853.

[20] J. Veselý, M. Kamlar, *Catal. Today* **2026**, 461, 115518.

[21] Z. Fehér, D. Richter, G. Dargó, J. Kupai, *Beilstein J. Org. Chem.* **2024**, 20, 2129–2142.

[22] J. Lu, P. H. Toy, *Chem. Rev.* **2009**, 109, 815–838.

[23] F. Cozzi, *Adv. Synth. Catal.* **2006**, 348, 1367–1390.

[24] S. Kobayashi, *Chem. Asian J.* **2016**, 11, 425–436.

[25] H. Pennemann, G. Kolb, *Catal. Today* **2016**, 278, 3–21.

[26] M. B. Plutschack, B. Pieber, K. Gilmore, P. H. Seeberger, *Chem. Rev.* **2017**, 117, 11796–11893.

[27] M. Movsisyan, E. I. P. Delbeke, J. K. E. T. Berton, C. Battilocchio, S. V. Ley, C. V. Stevens, *Chem. Soc. Rev.* **2016**, 45, 4892–4928.

[28] H. Westphal, R. Warias, H. Becker, M. Spanka, D. Ragno, R. Gläser, C. Schneider, A. Massi, D. Belder, *ChemCatChem* **2021**, 13, 5089–5096.

[29] P. H. R. de Oliveira, B. M. Da S. Santos, R. A. C. Leão, L. S. M. Miranda, R. A. S. San Gil, R. O. M. A. de Souza, F. G. Finelli, *ChemCatChem* **2019**, 11, 5553–5561.

[30] A. Duschek, S. F. Kirsch, *Angew. Chem. Int. Ed.* **2011**, 50, 1524–1552.

[31] T. Kitamura, Y. Fujiwara, *Org. Prep. Proc. Int.* **1997**, 29, 409–458.

[32] A. Yoshimura, V. V. Zhdankin, *Chem. Rev.* **2016**, 116, 3328–3435.

[33] V. V. Zhdankin, *Hypervalent Iodine Chemistry*, Wiley-VCH, **2013**.

[34] M. S. Yusubov, V. V. Zhdankin, *Resource-Efficient Technologies* **2015**, 1, 49–67.

[35] A. Varvoglis, *Tetrahedron* **1997**, 53, 1179–1255.

[36] R. Varala, V. Seema, M. Amanullah, S. Ramanaiah, M. M. Alam, *Curr. Org. Chem.* **2024**, 28, 489–509.

[37] C. Hartmann, V. Meyer, *Ber. Dtsch. Chem. Ges.* **1893**, 26, 1727–1732.

[38] A. R. Katritzky, B. L. Duell, J. K. Gallos, H. D. Durst, *Magn. Reson. Chem.* **1989**, 27, 1007–1011.

[39] P. Kazmierczak, L. Skulski, L. Kraszkiewicz, *Molecules* **2001**, 6, 881–891.

[40] F. R. Greenbaum, *Am. J. Pharm.* **1936**, 108, 17–22.

[41] D. B. Dess, J. C. Martin, *J. Org. Chem.* **1983**, 48, 4155–4156.

[42] D. B. Dess, J. C. Martin, *J. Am. Chem. Soc.* **1991**, 113, 7277–7287.

[43] J. B. Plumb, D. J. Harper, *ChemInform* **1990**, 21.

[44] M. Frigerio, M. Santagostino, S. Sputore, *J. Org. Chem.* **1999**, 64, 4537–4538.

[45] U. Ladziata, V. V. Zhdankin, *Arkivoc.* **2007**, 9, 26–58.

[46] V. V. Zhdankin, *J. Org. Chem.* **2011**, 76, 1185–1197.

[47] S. E. Shetgaonkar, S. Jothish, T. Dohi, F. V. Singh, *Molecules* **2023**, 28, 5250.

[48] F. V. Singh, T. Wirth, *Chem. Asian J.* **2014**, 9, 950–971.

[49] T. Dohi, Y. Kita, *Chem. Commun.* **2009**, 2073–2085.

[50] A. P. Thottumkara, T. K. Vinod, *Tetrahedron Lett.* **2002**, 43, 569–572.

[51] A. Kommreddy, M. S. Bowsher, M. R. Gunna, K. Botha, T. K. Vinod, *Tetrahedron Lett.* **2008**, 49, 4378–4382.

[52] J. N. Moorthy, N. Singhal, K. Senapati, *Tetrahedron Lett.* **2008**, 49, 80–84.

[53] R. D. Richardson, J. M. Zayed, S. Altermann, D. Smith, T. Wirth, *Angew. Chem. Int. Ed.* **2007**, 46, 6529–6532.

[54] A. Y. Koposov, D. N. Litvinov, V. V. Zhdankin, M. J. Ferguson, R. McDonald, R. R. Tykwinski, *Eur. J. Org. Chem.* **2006**, 2006, 4791–4795.

[55] I. M. Kumanyaev, M. A. Lapitskaya, L. L. Vasiljeva, K. K. Pivnitsky, *Mendeleev Commun.* **2012**, 22, 129–131.

[56] S. de Munari, M. Frigerio, M. Santagostino, *J. Org. Chem.* **1996**, 61, 9272–9279.

[57] L. McDermott, D. Aljovic, Z. G. Walters, F. Peng, R. Zhao, K. R. Campos, N. K. Garg, *Org. Lett.* **2025**, 27, 13165–13169.

[58] R. Rimi, S. Soni, B. Uttam, H. China, T. Dohi, V. V. Zhdankin, R. Kumar, *Synthesis* **2022**, 54, 2731–2748.

[59] B. Frey, A. Maity, H. Tan, P. Roychowdhury, D. C. Powers, *Sustainable Methods in Hypervalent Iodine Chemistry*, Wiley-VCH, **2022**.

[60] B. H. Lipshutz, S. Handa, *Green Chem.* **2026** *Advance Article*. DOI: 10.1039/D5GC05289K.

[61] F. Kurul, B. Doruk, S. N. Topkaya, *Discov. Chem.* **2025**, 2, 68.

[62] J. H. Clark, *Green Chem.* **1999**, 1, 1–8.

[63] A. P. Thottumkara, M. S. Bowsher, T. K. Vinod, *Org. Lett.* **2005**, 7, 2933–2936.

[64] S. Seth, S. Jhulki, J. N. Moorthy, *Eur. J. Org. Chem.* **2013**, 2013, 2445–2452.

[65] S. Jhulki, S. Seth, M. Mondal, J. N. Moorthy, *Tetrahedron* **2014**, 70, 2286–2293.

[66] A. K. Mishra, J. N. Moorthy, *Org. Chem. Front.* **2017**, 4, 343–349.

[67] A. Schulze, A. Giannis, *Synthesis* **2006**, 257–260.

[68] P. Page, L. Appleby, B. Buckley, S. Allin, M. McKenzie, *Synlett* **2007**, 2007, 1565–1568.

[69] J. N. Moorthy, K. Senapati, K. N. Parida, S. Jhulki, K. Sooraj, N. N. Nair, *J. Org. Chem.* **2011**, 76, 9593–9601.

[70] M. Uyanik, M. Akakura, K. Ishihara, *J. Am. Chem. Soc.* **2009**, 131, 251–262.

[71] J. Zong, J. Yue, *Ind. Eng. Chem. Res.* **2022**, 61, 6269–6291.

[72] D. D. Eley, W. O. Haag, B. Gates, ed., *Advances in Catalysis*, Academic Press **1998**.

[73] O. Piermatti, R. Abu-Reziq, L. Vaccaro, in *Catalyst Immobilization*, ed. M. Benaglia and A. Puglisi, Wiley **2020**, pp. 1–22.

[74] M. Mülbaier, A. Giannis, *Angew. Chem. Int. Ed.* **2001**, 40, 4393.

[75] G. Sorg, A. Mengel, G. Jung, J. Rademann, *Angew. Chem. Int. Ed.* **2001**, 40, 4395.

[76] N. N. Reed, M. Delgado, K. Hereford, B. Clapham, K. D. Janda, *Bioorg. Med. Chem. Lett.* **2002**, 12, 2047–2049.

[77] B. M. Bizzarri, I. Abdalghani, L. Botta, A. R. Taddei, S. Nisi, M. Ferrante, M. Passacantando, M. Crucianelli, R. Saladino, *J. Nanomater.* **2018**, 8, 516–529.

[78] Y.-H. Kim, H.-S. Jang, Y.-O. Kim, S.-D. Ahn, S. Yeo, S.-M. Lee, Y.-S. Lee, *Synlett* **2013**, 24, 2282–2286.

[79] F. Ballaschk, S. F. Kirsch, *Green Chem.* **2019**, 21, 5896–5903.

[80] K. Bensberg, A. Savvidis, F. Ballaschk, A. Gómez-Suárez, S. F. Kirsch, *Chem. Eur. J.* **2024**, 30, e202304011.

[81] Z. Zhou, M. Liu, L. Lv, C.-J. Li, *Angew. Chem. Int. Ed.* **2018**, 57, 2646–2650.

[82] C.-H. Jun, *Chem. Soc. Rev.* **2004**, 33, 610–618.

[83] F. Song, B. Wang, Z.-J. Shi, *Acc. Chem. Res.* **2023**, 56, 2867–2886.

[84] M. Murakami, N. Ishida, *J. Am. Chem. Soc.* **2016**, 138, 13759–13769.

[85] S. P. Morcillo, *Angew. Chem. Int. Ed.* **2019**, 58, 14044–14054.

[86] P. Sivaguru, Z. Wang, G. Zanoni, X. Bi, *Chem. Soc. Rev.* **2019**, 48, 2615–2656.

[87] M. Maitre, J.-P. Humbert, V. Kemmel, D. Aunis, C. Andriamampandry, *médecine/sciences* **2005**, 21, 284–289.

[88] A. G. Malykh, M. R. Sadaie, *Drugs* **2010**, 70, 287–312.

[89] S. Liu, Y. Jin, S. Huang, Q. Zhu, S. Shao, J. C.-H. Lam, *Nat. Commun.* **2024**, 15, 1141.

[90] D. W. Hwang, P. Kashinathan, J. M. Lee, J. H. Lee, U. Lee, J.-S. Hwang, Y. K. Hwang, J.-S. Chang, *Green Chem.* **2011**, 13, 1672–1675.

[91] M. Hong, E. Y.-X. Chen, *Nat. Chem.* **2016**, 8, 42–49.

[92] W. Schwarz, J. Schossig, R. Rossbacher, R. Pinkos, H. Höke, in *Ullmann's Encyclopedia of Industrial Chemistry*, Wiley **2000**, pp. 1–7.

[93] D. Cavuoto, A. Gervasini, F. Zaccheria, N. Scotti, M. Marelli, C. Bisio, F. Begni, N. Ravasio, *Catal. Today* **2023**, 418, 114104.

[94] N. Ichikawa, S. Sato, R. Takahashi, T. Sodesawa, K. Inui, *J. Mol. Catal. A Chem.* **2004**, 212, 197–203.

[95] K. H. Kang, U. G. Hong, J. O. Jun, J. H. Song, Y. Bang, J. H. Choi, S. J. Han, I. K. Song, *J. Mol. Catal. A Chem.* **2014**, 395, 234–242.

[96] X. Li, X. Lan, T. Wang, *Green Chem.* **2016**, 18, 638–642.

[97] B. Chen, F. Li, G. Yuan, *RSC Adv.* **2017**, 7, 21145–21152.

[98] R. Zhu, G. Zhou, J. Teng, W. Liang, X. Li, Y. Fu, *Green Chem.* **2021**, 23, 1758–1765.

[99] R. Ghalta, R. Srivastava, *Sustain. Energy Fuels* **2023**, 7, 1707–1723.

[100] S. Baskaran, S. Chandrasekaran, *Tetrahedron Lett.* **1990**, 31, 2775–2778.

[101] S. H. Mahadevegowda, F. A. Khan, *Tetrahedron Lett.* **2014**, 55, 2266–2269.

[102] F. Urabe, S. Nagashima, K. Takahashi, J. Ishihara, S. Hatakeyama, *J. Org. Chem.* **2013**, 78, 3847–3857.

[103] K. Tomooka, M. Kikuchi, K. Igawa, M. Suzuki, P.-H. Keong, T. Nakai, *Angew. Chem. Int. Ed.* **2000**, 39, 4502–4505.

[104] R. P. Robinson, V. Mascitti, C. M. Boustany-Kari, C. L. Carr, P. M. Foley, E. Kimoto, M. T. Leininger, A. Lowe, M. K. Klenotic, J. I. Macdonald, R. J. Maguire, V. M.

Masterson, T. S. Maurer, Z. Miao, J. D. Patel, C. Préville, M. R. Reese, L. She, C. M. Steppan, B. A. Thuma, T. Zhu, *Bioorg. Med. Chem. Lett.* **2010**, 20, 1569–1572.

[105] T. Yakura, T. Fujiwara, H. Nishi, Y. Nishimura, H. Nambu, *Synlett* **2018**, 29, 2316–2320.

[106] T. Yakura, Y. Horiuchi, Y. Nishimura, A. Yamada, H. Nambu, T. Fujiwara, *Adv. Synth. Catal.* **2016**, 358, 869–873.

[107] A. Trommer, J. Hessling, P. R. Schreiner, M. Schönhoff, B. M. Smarsly, *ACS Appl. Mater. Interfaces* **2025**, 17, 24283–24299.

[108] P. S. Shinde, P. S. Suryawanshi, K. K. Patil, V. M. Belekar, S. A. Sankpal, S. D. Delekar, S. A. Jadhav, *J. Compos. Sci.* **2021**, 5, 75.

[109] D. Tran, C. Zhang, K. Y. Choi, *Macromol. React. Eng.* **2022**, 16, 2200020.

[110] R. W. Murray, *Chem. Rev.* **1989**, 89, 1187–1201.

[111] D. K. Naritoku, J. A. Levine, D. F. Covey, J. A. Ferrendelli, *Biochem. Pharmacol.* **1987**, 36, 797–800.

[112] J. A. Levine, J. A. Ferrendelli, D. F. Covey, *Biochem. Pharmacol.* **1985**, 34, 4187–4190.

[113] S. S. Thorat, R. Kontham, *Org. Biomol. Chem.* **2019**, 17, 7270–7292.

[114] K. Hiesinger, D. Dar'in, E. Proschak, M. Krasavin, *J. Med. Chem.* **2021**, 64, 150–183.

[115] S. Youssif, *ChemInform* **2003**, 34, 242–268.

[116] F. A. Davis, A. C. Sheppard, *Tetrahedron* **1989**, 45, 5703–5742.

[117] F. A. Davis, A. C. Sheppard, *J. Org. Chem.* **1987**, 52, 954–955.

[118] F. A. Davis, U. K. Nadir, E. W. Kluger, *J. Chem. Soc., Chem. Commun.* **1977**, 25–26.

[119] H. W. Heine, in *Chemistry of Heterocyclic Compounds*, ed. A. Hassner, Wiley **1983**, pp. 547–628.

[120] K. S. Williamson, D. J. Michaelis, T. P. Yoon, *Chem. Rev.* **2014**, 114, 8016–8036.

[121] W. D. Emmons, *J. Am. Chem. Soc.* **1957**, 79, 5739–5754.

[122] B.-C. Chen, F. A. Davis, *in Encyclopedia of Reagents for Organic Synthesis, John Wiley & Sons, Ltd.,* **2001**.

[123] F. A. Davis, J. Lamendola, U. Nadir, E. W. Kluger, T. C. Sedergran, T. W. Panunto, R. Billmers, R. Jenkins, I. J. Turchi, *J. Am. Chem. Soc.* **1980**, 102, 2000–2005.

[124] W. B. Jennings, S. P. Watson, M. S. Tolley, *J. Am. Chem. Soc.* **1987**, 109, 8099–8100.

[125] A. Ghosh, S. Mandal, P. K. Chattaraj, P. Banerjee, *Org. Lett.* **2016**, 18, 4940–4943.

[126] D. R. Boyd, R. Graham, *J. Chem. Soc. C* **1969**, 1, 2648.

[127] D. R. Boyd, R. Spratt, D. M. Jerina, *J. Chem. Soc. C* **1969**, 19, 2650–2654.

[128] E. Schmitz, R. Ohme, S. Schramm, H. Striegler, H.-U. Heyne, J. Rusche, *J. Prakt. Chem.* **1977**, 319, 195–200.

[129] A. Armstrong, R. S. Cooke, *Chem. Commun.* **2002**, 2, 904–905.

[130] A. Armstrong, L. H. Jones, J. D. Knight, R. D. Kelsey, *Org. Lett.* **2005**, 7, 713–716.

[131] S. Andreae, E. Schmitz, *Synthesis* **1991**, 1991, 327–341.

[132] P. C. Page, V. L. Murrell, C. Limousin, D. D. Laffan, D. Bethell, A. Slawin, T. A. Smith, *J. Org. Chem.* **2000**, 65, 4204–4207.

[133] S. Blanc, C. A. C. Bordogna, B. R. Buckley, M. R. J. Elsegood, P. C. B. Page, *Eur. J. Org. Chem.* **2010**, 2010, 882–889.

[134] F. A. Davis, R. T. Reddy, W. Han, P. J. Carroll, *J. Am. Chem. Soc.* **1992**, 114, 1428–1437.

[135] W. W. Zajac, T. R. Walters, M. G. Darcy, *J. Org. Chem.* **1988**, 53, 5856–5860.

[136] F. A. Davis, N. F. Abdul-Malik, S. B. Awad, M. E. Harakal, *Tetrahedron Lett.* **1981**, 22, 917–920.

[137] V. A. Petrov, G. Resnati, *Chem. Rev.* **1996**, 96, 1809–1824.

[138] V. A. Petrov, *Fluorinated Heterocyclic Compounds*, Wiley-VCH, **2009**.

[139] V. A. Petrov, D. D. DesMarteau, *J. Fluor. Chem.* **1996**, 77, 175–181.

[140] V. A. Petrov, D. D. DesMarteau, *J. Chem. Soc., Perkin Trans. 1* **1993**, 505–509.

[141] D. D. DesMarteau, V. A. Petrov, V. Montanari, M. Pregnolato, G. Resnati, *J. Org. Chem.* **1994**, 59, 2762–2765.

[142] C. Balsarini, B. Novo, G. Resnati, *J. Fluor. Chem.* **1996**, 80, 31–34.

[143] R. Bernardi, B. Novo, G. Resnati, *J. Chem. Soc., Perkin Trans.* **1996**, 2517–2521.

[144] A. Arnone, D. D. DesMarteau, B. Novo, V. A. Petrov, M. Pregnolato, G. Resnati, *J. Org. Chem.* **1996**, 61, 8805–8810.

[145] A. Arnone, S. Foletto, P. Metrangolo, M. Pregnolato, G. Resnati, *Org. Lett.* **1999**, 1, 281–284.

[146] D. D. DesMarteau, A. Donadelli, V. Montanari, V. A. Petrov, G. Resnati, *J. Am. Chem. Soc.* **1993**, 115, 4897–4898.

[147] W. Adam, R. Curci, J. O. Edwards, *Acc. Chem. Res.* **1989**, 22, 205–211.

[148] A. E. Sorochinsky, A. A. Petrenko, V. A. Soloshonok, G. Resnati, *Tetrahedron* **1997**, 53, 5995–6000.

[149] F. A. Davis, *J. Org. Chem.* **2006**, 71, 8993–9003.

[150] F. A. Davis, S. G. Lal, H. D. Durst, *J. Org. Chem.* **1988**, 53, 5004–5007.

[151] B. H. Brodsky, J. Du Bois, *J. Am. Chem. Soc.* **2005**, 127, 15391–15393.

[152] N. D. Litvinas, B. H. Brodsky, J. Du Bois, *Angew. Chem. Int. Ed.* **2009**, 48, 4513–4516.

[153] C. Flender, A. M. Adams, J. L. Roizen, E. McNeill, J. Du Bois, R. N. Zare, *Chem. Sci.* **2014**, 5, 3309–3314.

[154] F. A. Davis, *Tetrahedron* **2018**, 74, 3198–3214.

[155] W. H. Rastetter, W. R. Wagner, M. A. Findeis, *J. Org. Chem.* **1982**, 47, 419–422.

[156] Y. Gao, Y. Lam, *Adv. Synth. Catal.* **2008**, 350, 2937–2946.

[157] W. Susanto, Y. Lam, *Tetrahedron* **2011**, 67, 8353–8359.

[158] T. Prabhakar, J. Giaretta, R. Zulli, R. J. Rath, S. Farajikhah, S. Talebian, F. Dehghani, *Chem. Eng. J.* **2025**, 503, 158054.

[159] M. Ferré, R. Pleixats, M. Wong Chi Man, X. Cattoën, *Green Chem.* **2016**, 18, 881–922.

[160] Z.-Z. Zhang, Y. Zhang, H.-X. Duan, Z.-F. Deng, Y.-Q. Wang, *Chem. Commun.* **2020**, 56, 1553–1556.

[161] K. Ohsawa, M. Yoshida, T. Doi, *J. Org. Chem.* **2013**, 78, 3438–3444.

[162] V. Béreau, V. Jubéra, P. Arnaud, A. Kaiba, P. Guionneau, J.-P. Sutter, *Dalton Trans.* **2010**, 39, 2070–2077.

[163] D. Talukdar, S. Panda, R. Borah, D. Manna, *J. Phys. Chem. B* **2014**, 118, 7541–7553.

[164] K. A. Wayman, T. Sammakia, *Org. Lett.* **2003**, 5, 4105–4108.

[165] R. Krishnamurti, D. R. Bellew, G. K. S. Prakash, *J. Org. Chem.* **1991**, 56, 984–989.

[166] N. O. Ilchenko, D. V. Sudarikov, R. V. Rumyantcev, S. A. Rubtsova, A. V. Kutchin, *Russ. Chem. Bull.* **2024**, 73, 3593–3600.

[167] C. Wang, *Asian J. Org. Chem.* **2018**, 7, 509–521.

[168] M. B. Gawande, V. D. B. Bonifácio, R. Luque, P. S. Branco, R. S. Varma, *ChemSusChem* **2014**, 7, 24–44.

[169] G. Brahmachari, B. Banerjee, *Curr. Green Chem.* **2015**, 2, 274–305.

[170] C. Shi, C. Li, Y. Wang, J. Guo, S. Barry, Y. Zhang, N. Marmier, *Water* **2022**, 14, 2309.

[171] F. Cavani, J. H. Teles, *ChemSusChem* **2009**, 2, 508–534.

[172] K. C. Bhowmick, N. N. Joshi, *Tetrahedron: Asymmetry* **2006**, 17, 1901–1929.

[173] J. K. Cha, N.-S. Kim, *Chem. Rev.* **1995**, 95, 1761–1795.

[174] M. J. Rawling, N. C. O. Tomkinson, *Org. Biomol. Chem.* **2013**, 11, 1434–1440.

[175] W.-C. Chen, J.-R. Lin, M.-S. Liao, Y.-W. Wang, C.-M. Shu, *J. Therm. Anal. Calorim.* **2017**, 127, 1019–1026.

[176] P. Dupau, R. Epple, A. Thomas, V. Fokin, K. Sharpless, *Adv. Synth. Catal.* **2002**, 344, 421–433.

[177] T. Achard, S. Bellemin-Laponnaz, *Eur. J. Org. Chem.* **2021**, 2021, 877–896.

[178] T. V. Robinson, D. K. Taylor, E. R. T. Tiekink, *J. Org. Chem.* **2006**, 71, 7236–7244.

[179] D. Swern, *Chem. Rev.* **1949**, 45, 1–68.

[180] J. Brinksma, L. Schmieder, G. van Vliet, R. Boaron, R. Hage, D. E. de Vos, P. L. Alsters, B. L. Feringa, *Tetrahedron Lett.* **2002**, 43, 2619–2622.

[181] T. W.-S. Chow, Y. Liu, C.-M. Che, *Chem. Commun.* **2011**, 47, 11204–11206.

[182] B. Plietker, M. Niggemann, *Org. Biomol. Chem.* **2004**, 2, 2403–2407.

[183] T. K. M. Shing, E. K. W. Tam, V. W.-F. Tai, I. H. F. Chung, Q. Jiang, *Chem. Eur. J.* **1996**, 2, 50–57.

[184] P. Fan, S. Su, C. Wang, *ACS Catal.* **2018**, 8, 6820–6826.

[185] P. Fan, C. Wang, *Commun. Chem.* **2019**, 2, 104.

[186] Ł. Albrecht, H. Jiang, G. Dickmeiss, B. Gschwend, S. G. Hansen, K. A. Jørgensen, *J. Am. Chem. Soc.* **2010**, 132, 9188–9196.

[187] S. Rani, Y. D. Vankar, *Tetrahedron Lett.* **2003**, 44, 907–909.

[188] X. Wang, Y. R. Lee, *Tetrahedron Lett.* **2007**, 48, 6275–6280.

[189] T. Li, C. Li, *J. Agric. Food Chem.* **2013**, 61, 12522–12530.

[190] B. J. Deadman, S. Gian, V. E. Y. Lee, L. A. Adrio, K. Hellgardt, K. K. Hii, *Green Chem.* **2022**, 24, 5570–5578.

[191] M.-Z. Zhang, P. Wang, H.-Y. Liu, D. Wang, Y. Deng, Y.-H. Bai, F. Luo, W.-Y. Wu, T. Chen, *ChemSusChem* **2023**, 16, e202300583.

[192] P. Gogoi, S. D. Sharma, D. Konwar, *Lett. Org. Chem.* **2007**, 4, 249–252.

[193] C. Hampton, M. Simonetti, D. Leonori, *Angew. Chem. Int. Ed.* **2023**, 62, e202214508.

[194] Y. Masuda, D. Ikeshita, M. Murakami, *Helv. Chim. Acta* **2021**, 104, e2000228.

[195] M. Liu, T. Feng, Y. Wang, G. Kou, Q. Wang, Q. Wang, Y. Qiu, *Nat. Commun.* **2023**, 14, 6467.

[196] B. Gutmann, D. Cantillo, C. O. Kappe, *Angew. Chem. Int. Ed.* **2015**, 54, 6688–6728.

[197] J. Wu, R. Guillot, C. Kouklovsky, G. Vincent, *Adv. Synth. Catal.* **2020**, 362, 1712–1719.

[198] S. Da Chung, S. H. Park, S.-G. Lee, H. Kim, *Chem. Sci.* **2021**, 12, 5892–5897.

[199] S. Torii, P. Liu, N. Bhuvaneswari, C. Amatore, A. Jutand, *J. Org. Chem.* **1996**, 61, 3055–3060.

[200] X. M. Zhang, A. Archelas, R. Furstoss, *J. Org. Chem.* **1991**, 56, 3814–3817.

[201] Y. Xu, A. Li, X. Jia, Z. Li, *Green Chem.* **2011**, 13, 2452–2458.

[202] S. Wu, Y. Chen, Y. Xu, A. Li, Q. Xu, A. Glieder, Z. Li, *ACS Catal.* **2014**, 4, 409–420.

[203] B. R. Moser, S. C. Cermak, K. M. Doll, J. A. Kenar, B. K. Sharma, *J. Am. Oil Chem. Soc.* **2022**, 99, 801–842.

[204] C. Wang, L. Luo, H. Yamamoto, *Acc. Chem. Res.* **2016**, 49, 193–204.

[205] S. Meninno, A. Lattanzi, *Chem. Eur. J.* **2016**, 22, 3632–3642.

[206] M. Çelik, C. Alp, B. Coşkun, M. S. Gültekin, M. Balci, *Tetrahedron Lett.* **2006**, 47, 3659–3663.

[207] W. Zhong, S. Liu, J. Yang, X. Meng, Z. Li, *Org. Lett.* **2012**, 14, 3336–3339.

[208] W. Zhong, J. Yang, X. Meng, Z. Li, *J. Org. Chem.* **2011**, 76, 9997–10004.

[209] R. Bag, P. B. De, S. Pradhan, T. Punniyamurthy, *Eur. J. Org. Chem.* **2017**, 2017, 5424–5438.

[210] X.-F. Xia, S.-L. Zhu, Y.-N. Niu, D. Zhang, X. Liu, H. Wang, *Tetrahedron* **2016**, 72, 3068–3072.

[211] T. P. Hilditch, *J. Chem. Soc.* **1926**, 129, 1828–1836.

[212] W. C. Smit, J. Böeseken, *Recl. Trav. Chim. Pays-Bas* **1930**, 49, 675–685.

[213] D. Swern, G. N. Billen, T. W. Findley, J. T. Scanlan, *J. Am. Chem. Soc.* **1945**, 67, 1786–1789.

[214] Y. Usui, K. Sato, M. Tanaka, *Angew. Chem. Int. Ed.* **2003**, 42, 5623–5625.

[215] A. A. Rosatella, C. A. M. Afonso, *Adv. Synth. Catal.* **2011**, 353, 2920–2926.

[216] A. Hartung, M. A. Keane, A. Kraft, *J. Org. Chem.* **2007**, 72, 10235–10238.

[217] G. M. Keserü, M. Nógrádi, *Stud. Nat. Prod. Chem.* **1995**, 17, 357–394.

[218] P. Claeson, P. Tuchinda, V. Reutrakul, *J. Indian Chem. Soc.* **1994**, 71, 509–521.

[219] P. Claeson, P. Tuchinda, V. Reutrakul, in *Bioactive Natural Products*, ed. T. S. Taylor and M. Smith, Elsevier **2002**, pp. 881–908.

[220] S. Suzuki, T. Koeduka, A. Sugiyama, K. Yazaki, T. Umezawa, *Plant Biotechnol. J.* **2014**, 31, 465–482.

[221] P. Jirásek, *Synthesis of natural and non-natural diarylheptanoids and evaluation of their neuroprotective activity*, Universität Regensburg, **2015**.

[222] K. Konno, M. Miura, M. Toriyama, S. Motohashi, R. Sawamura, W. Watanabe, H. Yoshida, M. Kato, R. Yamamoto, K. Yasukawa, M. Kurokawa, *J. Nat. Med.* **2013**, 67, 773–781.

[223] S. Brand, D. Hölscher, A. Schierhorn, A. Svatos, J. Schröder, B. Schneider, *Planta Med.* **2006**, 224, 413–428.

[224] Y. Jahng, J. G. Park, *Molecules* **2018**, 23, 1–42.

[225] K. Sudarshan, S. Yarlagadda, S. Sengupta, *Chem. Asian J.* **2024**, 19, e202400380.

[226] T. Li, D.-B. Pan, Q.-Q. Pang, M. Zhou, X.-J. Yao, X.-S. Yao, H.-B. Li, Y. Yu, *RSC Adv.* **2021**, 11, 29376–29384.

[227] M. S. Ali, Y. Tezuka, S. Awale, A. H. Banskota, S. Kadota, *J. Nat. Prod.* **2001**, 64, 289–293.

[228] J.-M. Han, W. S. Lee, J.-R. Kim, J. Son, K.-H. Nam, S.-C. Choi, J.-S. Lim, T.-S. Jeong, *J. Agric. Food Chem.* **2007**, 55, 9457–9464.

[229] Y. Masuda, H. Kikuzaki, M. Hisamoto, N. Nakatani, *BioFactors* **2004**, 21, 293–296.

[230] Y. Yang, Q. Gong, W. Wang, Y.-L. Mao, X.-R. Wang, S. Yao, H.-Y. Zhang, C. Tang, Y. Ye, *J. Nat. Prod.* **2020**, 83, 3681–3688.

[231] H. Ohtsu, H. Itokawa, Z. Xiao, C.-Y. Su, C. C.-Y. Shih, T. Chiang, E. Chang, Y. Lee, S. Y. Chiu, C. Chang, K.-H. Lee, *Bioorg. Med. Chem.* **2003**, 11, 5083–5090.

[232] H. Lv, G. She, *Nat. Prod. Commun.* **2010**, 5, 1687–1708.

[233] M. S. Ali, A. H. Banskota, Y. Tezuka, I. Saiki, S. Kadota, *Biol. Pharm. Bull.* **2001**, 24, 525–528.

[234] N. Kaneda, A. D. Kinghorn, N. R. Farnsworth, P. Tuchinda, J. Udchachon, T. Santisuki and V. Reutrakul, *Phytochemistry* **1990**, 29, 3366–3368.

[235] Á. Alberti, E. Riethmüller, S. Béni, *J. Pharm. Biomed. Anal.* **2018**, 147, 13–34.

[236] H. Yang, S. H. Sung, J. Kim, Y. C. Kim, *Planta Med.* **2011**, 77, 841–845.

[237] A. T. Dinkova-Kostova, P. Talalay, *Mol. Nutr. Food Res.* **2008**, 52, 128–138.

[238] K. I. Priyadarsini, D. K. Maity, G. H. Naik, M. S. Kumar, M. K. Unnikrishnan, J. G. Satav, H. Mohan, *Radic. Biol. Med.* **2003**, 35, 475–484.

[239] K. Yasukawa, Y. Sun, S. Kitanaka, N. Tomizawa, M. Miura, S. Motohashi, *J. Nat. Med.* **2008**, 62, 374–378.

[240] X. L. Cheng, H. X. Li, J. Chen, P. Wu, J. H. Xue, Z. Y. Zhou, N. H. Xia, X. Y. Wei, *Nat. Prod. Bioprospect.* **2021**, 11, 63–72.

[241] S. Gamre, M. Tyagi, S. Chatterjee, B. S. Patro, S. Chattopadhyay, D. Goswami, *J. Nat. Prod.* **2021**, 84, 352–363.

[242] Z. Liu, M. M. Rafi, N. Zhu, K. Ryu, S. Sang, C.-T. Ho, R. T. Rosen, in *Food Factors in Health Promotion and Disease Prevention*, ed. F. Shahidi, C.-T. Ho, S. Watanabe and T. Osawa, American Chemical Society, Washington, DC **2003**, vol. 851, pp. 369–380.

[243] C. Vanucci-Bacqué, F. Bedos-Belval, *Bioorg. Med. Chem.* **2021**, 31, 115971.

[244] J. S. Yadav, E. Gyanchander, S. Bujaranipalli, S. Das, *Tetrahedron Lett.* **2015**, 56, 1360–1362.

[245] H. Hanawa, T. Hashimoto, K. Maruoka, *J. Am. Chem. Soc.* **2003**, 125, 1708–1709.

[246] H. Hanawa, D. Uraguchi, S. Konishi, T. Hashimoto, K. Maruoka, *Chem. Eur. J.* **2003**, 9, 4405–4413.

[247] V. VanRheenen, R. C. Kelly, D. Y. Cha, *Tetrahedron Lett.* **1976**, 17, 1973–1976.

[248] K. Venkatesham, S. Purushotham Reddy, B. Chinnababu, K. Suresh Babu, *Helv. Chim. Acta* **2015**, 98, 1307–1314.

[249] A. Bredenkamp, M. Wegener, S. Hummel, A. P. Häring, S. F. Kirsch, *Chem. Commun.* **2016**, 52, 1875–1878.

[250] A. Bredenkamp, Z.-B. Zhu, S. F. Kirsch, *Eur. J. Org. Chem.* **2016**, 2016, 252–254.

[251] F. Mittendorf, I.-E. Celik, S. F. Kirsch, *J. Org. Chem.* **2022**, 87, 14899–14908.

[252] F. Mittendorf, M. Quambusch, S. F. Kirsch, *Org. Biomol. Chem.* **2023**, 21, 4574–4577.

[253] I.-E. Celik, F. Mittendorf, A. Gómez-Suárez, S. F. Kirsch, *Tetrahedron Chem* **2024**, 9, 100065.

[254] L. Wang, K. Thai, M. Gravel, *Org. Lett.* **2009**, 11, 891–893.

[255] Y. Cheng, J. Rein, N. Le, S. Lin, *J. Am. Chem. Soc.* **2024**, 146, 31420–31432.

[256] A. Joosten, É. Lambert, J.-L. Vasse, J. Szymoniak, *Org. Lett.* **2010**, 12, 5128–5131.

[257] J. Zhang, V. V. Betkekar, K. Suzuki, K. Ohmori, *Synlett* **2024**, 35, 1458–1464.

[258] G. Li, Y. Huan, B. Yuan, J. Wang, Q. Jiang, Z. Lin, Z. Shen, H. Huang, *Eur. J. Med. Chem.* **2016**, 124, 103–116.

[259] H. N. L. Perumalla, T. Fujiwara, M. Okada, K. Asakubo, T. Okitsu, K. Kasama, H. Nambu, T. Yakura, *Chem. Pharm. Bull.* **2024**, 72, 75–79.

[260] T. K. Chakraborty, S. Ghosh, S. Jayaprakash, J. A. Sarma, V. Ravikanth, P. V. Diwan, R. Nagaraj, A. C. Kunwar, *J. Org. Chem.* **2000**, 65, 6441–6457.

[261] F. W. Kotch, V. Sidorov, Y.-F. Lam, K. J. Kayser, H. Li, M. S. Kaucher, J. T. Davis, *J. Am. Chem. Soc.* **2003**, 125, 15140–15150.

[262] S. Guyenne, E. I. León, A. Martín, I. Pérez-Martín, E. Suárez, *J. Org. Chem.* **2012**, 77, 7371–7391.

[263] W.-Y. Shi, Y.-N. Ding, N. Zheng, X.-Y. Gou, Z. Zhang, X. Chen, Y.-Y. Luan, Z.-J. Niu, Y.-M. Liang, *Chem. Commun.* **2021**, 57, 8945–8948.

[264] S. J. Gharpure, R. K. Patel, *Chem. Commun.* **2024**, 60, 12441–12444.

[265] A. Theodorou, C. G. Kokotos, *Green Chem.* **2017**, 19, 670–674.

[266] M. Rueping, V. B. Phapale, *Green Chem.* **2012**, 14, 55–57.

[267] A. Kamal, A. V. Subba Rao, M. V. P. S. Vishnuvardhan, T. Srinivas Reddy, K. Swapna, C. Bagul, N. V. Subba Reddy, V. Srinivasulu, *Org. Biomol. Chem.* **2015**, 13, 4879–4895.

[268] K. M. Rutledge, T. A. Hamlin, D. M. Baldisseri, F. M. Bickelhaupt, M. W. Peczuh, *Chem. Asian J.* **2017**, 12, 2623–2633.

[269] P.-S. Lai, J. A. Dubland, M. G. Sarwar, M. G. Chudzinski, M. S. Taylor, *Tetrahedron* **2011**, 67, 7586–7592.

[270] M. Pour, M. Spulák, V. Balsánek, J. Kunes, P. Kubanová, V. Buchta, *Bioorg. Med. Chem.* **2003**, 11, 2843–2866.

[271] R. J. Maza, J. Royes, J. J. Carbó, E. Fernández, *Chem. Commun.* **2020**, 56, 5973–5976.

[272] K. Fominova, T. Diachuk, D. Granat, T. Savchuk, V. Vilchynskyi, O. Svitlychnyi, V. Meliantsev, I. Kovalchuk, E. Litskan, V. V. Levterov, V. R. Badlo, R. I. Vaskevych, A. I. Vaskevych, A. V. Bolbut, V. V. Semeno, R. Iminov, K. Shvydenko, A. S. Kuznetsova, Y. V. Dmytriv, D. Vysochyn, V. Ripenko, A. A. Tolmachev, O. Pavlova, H. Kuznietsova, I. Pishel, P. Borysko, P. K. Mykhailiuk, *Chem. Sci.* **2021**, 12, 11294–11305.

[273] J. Hartung, S. Drees, M. Greb, P. Schmidt, I. Svoboda, H. Fuess, A. Murso, D. Stalke, *Eur. J. Org. Chem.* **2003**, 2003, 2388–2408.

[274] B. Zhou, V. G. Chandrashekhar, Z. Ma, C. Kreyenschulte, S. Bartling, H. Lund, M. Beller, R. V. Jagadeesh, *Angew. Chem. Int. Ed.* **2023**, 62, e202215699.

[275] A. P. Dieskau, B. Plietker, *Org. Lett.* **2011**, 13, 5544–5547.

[276] C. Dubiella, H. Cui, M. Gersch, A. J. Brouwer, S. A. Sieber, A. Krüger, R. M. J. Liskamp, M. Groll, *Angew. Chem. Int. Ed.* **2014**, 53, 11969–11973.

[277] A. Rezaeifard, M. Jafarpour, A. Farrokhi, S. Parvin, F. Feizpour, *RSC Adv.* **2016**, 6, 64640–64650.

[278] H. Xie, J. Lu, Y. Gui, L. Gao, Z. Song, *Synlett* **2017**, 28, 2453–2459.

[279] R. Ding, L. Lan, S. Li, Y. Liu, S. Yang, H. Tian, B. Sun, *Synthesis* **2018**, 50, 2555–2566.

[280] L. Shen, Q. Zheng, Y. Liu, J. Wu, Z. Lu, T. Tu, *Green Chem.* **2021**, 23, 5037–5042.

[281] V. Valerio, D. Petkova, C. Madelaine, N. Maulide, *Chem. Eur. J.* **2013**, 19, 2606–2610.

[282] X.-L. Xu, Z. Li, *Org. Lett.* **2019**, 21, 5078–5081.

[283] P. Thiruvengetam, D. K. Chand, *J. Org. Chem.* **2022**, 87, 4061–4077.

[284] Y. Tang, C. Shen, Q. Yao, X. Tian, B. Wang, K. Dong, *ChemCatChem* **2020**, 12, 5898–5902.

[285] T. Xu, S. Mal, M. van Gemmeren, *ACS Catal.* **2025**, 15, 2735–2741.

[286] Z. Li, W. Sun, X. Wang, L. Li, Y. Zhang, C. Li, *J. Am. Chem. Soc.* **2021**, 143, 3536–3543.

[287] J.-B. Zhu, E. M. Watson, J. Tang, E. Y.-X. Chen, *Science* **2018**, 360, 398–403.

[288] D. Prismawan, R. van der Vlag, H. Guo, F. J. Dekker, A. K. H. Hirsch, *Helv. Chim. Acta* **2019**, 102, e1900040.

[289] Y. Wang, G.-X. Li, G. Yang, G. He, G. Chen, *Chem. Sci.* **2016**, 7, 2679–2683.

[290] C. Callegari, C. Tedesco, A. Corbo, M. Prato, L. Malavasi, D. Ravelli, *Org. Lett.* **2025**, 27, 3667–3672.

[291] W. Li, T. Yang, N. Song, R. Li, J. Long, L. He, X. Zhang, H. Lv, *Chem. Sci.* **2022**, 13, 1808–1814.

[292] D. J. Kahl, K. M. Hutchings, E. M. Lisabeth, A. J. Haak, J. R. Leipprandt, T. Dexheimer, D. Khanna, P.-S. Tsou, P. L. Campbell, D. A. Fox, B. Wen, D. Sun, M. Bailie, R. R. Neubig, S. D. Larsen, *J. Med. Chem.* **2019**, 62, 4350–4369.

[293] C. B. Kelly, M. A. Mercadante, T. A. Hamlin, M. H. Fletcher, N. E. Leadbeater, *J. Org. Chem.* **2012**, 77, 8131–8141.

[294] Akanksha, D. Maiti, *Green Chem.* **2012**, 14, 2314–2320.

[295] Y. Li, H. Shi, *Chin. Chem. Lett.* **2024**, 35, 108650.

[296] J. Zhang, M. Jiang, C.-S. Wang, K. Guo, Q.-X. Li, C. Ma, S.-F. Ni, G.-Q. Chen, Y. Zong, H. Lu, L.-W. Xu, X. Shao, *Nat. Commun.* **2022**, 13, 7961.

[297] F. Schröder, R. Fettköther, U. Noldt, K. Dettner, W. A. König, W. Francke, *Liebigs Ann. Chem.* **1994**, 12, 1211–1218.

[298] Y.-A. Zhang, X. Gu, A. E. Wendlandt, *J. Am. Chem. Soc.* **2022**, 144, 599–605.

[299] T. Daiboun, M. A. Elalaoui, H. Thaler-Dao, C. Chavis, G. Maury, *Biocatalysis* **1993**, 7, 227–236.

[300] B. A. M. W. van den Broek, R. Becker, F. Kössl, M. M. E. Delville, P. J. Nieuwland, K. Koch, F. P. J. T. Rutjes, *ChemSusChem* **2012**, 5, 289–292.

[301] B. M. Bizzarri, A. Fanelli, L. Botta, C. Sadun, L. Gontrani, F. Ferella, M. Crucianelli, R. Saladino, *RSC Adv.* **2020**, 10, 17185–17194.

[302] L. He, H. S. Byun, R. Bittman, *J. Org. Chem.* **2000**, 65, 7618–7626.

[303] J.-L. Jiang, Z. Xiu, R. Hua, *Synth. Commun.* **2008**, 38, 232–238.

[304] S. Gao, W. Tang, M. Zhang, C. Wang, J. Xiao, *Synlett* **2016**, 27, 1748–1752.

[305] J. Huang, L. Ouyang, J. Li, J. Zheng, W. Yan, W. Wu, H. Jiang, *Org. Lett.* **2018**, 20, 5090–5093.

[306] H. Inada, M. Shibuya, Y. Yamamoto, *J. Org. Chem.* **2020**, 85, 11047–11059.

[307] R. Bag, T. Punniyamurthy, *ChemistrySelect* **2018**, 3, 6152–6155.

[308] A. Mandoli, D. Pini, M. Fiori, P. Salvadori, *Eur. J. Org. Chem.* **2005**, 2005, 1271–1282.

[309] E. P. Balskus, J. Méndez-Andino, R. M. Arbit, L. A. Paquette, *J. Org. Chem.* **2001**, 66, 6695–6704.

[310] E. M. Dangerfield, C. H. Plunkett, B. L. Stocker, M. S. M. Timmer, *Molecules* **2009**, 14, 5298–5307.

[311] D. Wang, W. A. Nugent, *J. Org. Chem.* **2007**, 72, 7307–7312.

[312] C.-H. Tan, A. B. Holmes, *Chem. Eur. J.* **2001**, 7, 1845–1854.

[313] G. Revelant, S. Dunand, S. Hesse, G. Kirsch, *Synthesis* **2011**, 2011, 2935–2940.

[314] N. J. Race, A. Faulkner, G. Fumagalli, T. Yamauchi, J. S. Scott, M. Rydén-Landergren, H. A. Sparkes, J. F. Bower, *Chem. Sci.* **2017**, 8, 1981–1985.